ANALYSIS OF THE CELL CYCLE REGULATED GOLGI DYNAMICS IN MAMMALIAN CELLS

by

Danming Tang

A dissertation submitted in partial fulfillment
of the requirements for degree of
Doctor of Philosophy
(Molecular Cellular and Developmental Biology)
in the University of Michigan
2013

Doctoral Committee:

Associate Professor Yanzhuang Wang, Chair
Professor Peter Arvans
Professor Kenneth M. Cadigan
Professor Steven E. Clark

2013

Dedication

This dissertation is dedicated to my parents and my grandparents.

Acknowledgements

I would like to express my gratitude to all the persons who have given me the possibility to complete this thesis. First I want to express my deepest appreciation to my thesis advisor, Dr. Yanzhuang Wang, whose patient instruction, stimulating suggestions and constant encouragement have accompanied me and pushed me forward in my six-year pre-doctoral research and study. Without his guidance and persistent help, this dissertation would not have been possible.

I also want to thank my thesis committee members, Dr. Peter Arvan, Dr. Kenneth M. Cadigan and Dr. Steven E. Clark, for their insightful suggestions and invaluable support to my research.

My former and current colleagues from the Dr. Yanzhuang Wang's lab have supported me in my research. I have been extremely fortunate to have their company. I would also like to acknowledge them for all their assistance, interest and valuable hints, especially Dr. Hebao Yuan who initiated this work and continuously gave me help whenever I needed. Also, special thanks to Dr. Yi Xiang for being great colleague as well as great friend.

I would like to particularly thank Dr. James Bardwell for granting me the opportunity to start my graduate study in his lab as a rotation student. And I really appreciate all the faculty and

staff members in the Department of Molecular, Cellular, and Development Biology, especially Mr. Gregg Sobocinski who has given me tremendous help on the microscopes to make my research possible, and Ms. Mary Carr who has been taking care of everything and made my life much easier. I also want to express my gratitude to all the collaborating research groups: Dr. Zhaohui Xu's lab, Dr. Frances M. Brodsky' lab and Dr. Franck Perez's lab. Without their suggestions and techniques, my research would not have developed as it has now.

Finally, I want to give my most sincere appreciations to my parents and grandparents, for their understanding, support and unconditional love. And special thanks to my dearest friends in Ann Arbor, who have been there for me always.

Chapter 1 is from a review prepared for Trends in Cell Biology, Danming Tang and Yanzhuang Wang: **Cell cycle regulation of Golgi membrane dynamics.** Danming Tang wrote the manuscript and Yanzhuang Wang revised it.

Chapter 2 is reprinted from the *Traffic*, 2010, Volume 11, Danming Tang, Hebao Yuan and Yanzhuang Wang: **The Role of GRASP65 in Golgi Cisternal Stacking and Cell Cycle Progression,** pages 827-842, Copyright (2010). Danming Tang and Yanzhuang Wang designed the experiments, Danming Tang and Dr. Hebao Yuan performed experiments in Figure 2.2, Danming Tang contributed to the rest of the experiments and wrote the paper.

Chapter 3 is reprinted from the *Biology Open*, 2012, Danming Tang, Hebao Yuan, Ole Vielemeyer, Franck Perez and Yanzhuang Wang: **Sequential phosphorylation of GRASP65 during mitotic Golgi disassembly,** advance online published, Copyright (2012). Danming Tang and Yanzhuang Wang designed the experiments, Danming Tang and Dr. Hebao Yuan performed experiments in Figure 3.1, Dr. Hebao Yuan performed the experiments in Figure 3.2, 3.3, 3.4A, B & D, and 3.S1. Danming Tang contributed to the rest of the experiments and wrote the paper.

Chapter 4 is reprinted from the *Nature Communications*, 2011, Danming Tang*, Yi Xiang*, Stefano De Renzis, Jochen Rink, Gen Zheng, Marino Zerial, and Yanzhuang Wang: **The ubiquitin ligase HACE1 regulates Golgi membrane dynamics during the cell cycle,** Copyright (2011). Dr. Yanzhuang Wang designed the research. Dr. Yi Xiang performed the experiments in Figure 4.4, 4.8, 4.S2I, 4.S3A. Dr. Stefano De Renzis performed the experiments in Figure 4.1 A, B & D. Dr. Gen Zheng performed the experiments in Figure 4.1E & G, 4.2 and 4.3. Danming Tang performed Figure 4.1F, 4.5, 4.7, 4.S2A-H & J, 4.S3 B & C. Dr. Yanzhuang Wang contributed to the rest data and wrote the paper. (*, equal contribution)

Chapter 5 is a manuscript in preparation by authors: Danming Tang, Hebao Yuan and Yanzhuang Wang: **Identification of GRASP65-interacting proteins in the cytosol that facilitate Golgi assembly,** Danming Tang and Dr. Yanzhuang Wang designed the research. Dr. Yanzhuang Wang and Dr. Hebao Yuan performed the experiment in Figure 5.1C, Dr. Yanzhuang Wang performed the experiments in Figure 5.S1 and 5.S2. Danming Tang contributed to the rest data and wrote the manuscript.

Chapter 6 is a manuscript prepared for the *Development Cell* by authors: Christopher Esk*, Danming Tang*, Lavanya Vasudevan, Yvette Schollmeier, Sophia Majeed, Amy Foraker, Bryant Chhun, Erin Adams, Bo Huang, Yanzhuang Wang[#], Frances M. Brodsky[#]: **Clathrin directly binds GRASP65 providing glue for Golgi ribbon integrity,** Laboratory experiments were performed by Christopher Esk, Danming Tang, Lavanya Vasudeven, Yvette Schollmeier, Sophia Majeed, Amy Foraker, Bryant Chhun and Erin Adams with equal and primary contributions from Christopher Esk and Danming Tang. Expression of full length CHC17 in insect cells was developed by Erin Adams and Yvette Schollmeier. STORM imaging was done in the laboratory of Bo Huang by Christopher Esk, Lavanya Vasudeven and Bryant Chhun. Data analysis was performed by Christopher Esk, Danming Tang, Bo Huang, Yanzhuang Wang and Frances Brodsky. The manuscript was written by Christopher Esk, Danming Tang, Yanzhuang Wang and Frances Brodsky, with input from Bo Huang. The contributions of the Brodsky and Wang laboratories were equal. Danming Tang performed experiments of Figure 6.1 C-E and 6.S1 (also included in Figure 5.4), 6.3 A-D (also included in Figure 5.6), Figure 6.4B (partially included in Figure 5.2) and 6.4 C-D, 6.5 A-C and 6.S3 (partially included in Figure 5.5), and 6.5 E-G. (*, equal contribution; [#], equal corresponding authors)

Table of contents

List of Figures

Chapter 1 . Introduction

The Golgi apparatus is a membranous organelle essential for intracellular protein and lipid trafficking and modification. In mammalian cells, the Golgi consists of dozens of stacks of 5-7 parallel-aligned flattened cisternae; Golgi stacks are highly concentrated in the pericentriolar region of the cell. In most cells, the enrichment of the Golgi stacks nearby the centrosome mediated by the microtubule minus end-directed motor protein dynein is likely required for lateral linking of the Golgi stacks into a ribbon, as treatment of cells by microtubule depolymerizing drugs disperses the Golgi ribbon into individual stacks. The Golgi structure is well maintained in a dynamic equilibrium between input and output of membranes from and to other organelles including the endoplasmic reticulum (ER), the endosome-lysosome system, and the plasma membrane [1].

The mitotic division of cells requires the duplication and partitioning of all cellular components. It is generally believed that the Golgi apparatus exists as an autonomous organelle and its division does not rely on other cellular organelles such as the ER [2, 3]. In mammalian cells, biogenesis of the Golgi during each cycle of cell division occurs through a unique disassembly and reassembly process. The Golgi is fragmented at the onset of mitosis, first with the stacks unlinked, which then undergo further unstacking and vesiculation, yielding thousands of vesicles that are distributed throughout the cytoplasm and equally into the two daughter cells.

In telophase, Golgi vesicles fuse to form new cisternae that are aligned as stacks. The Golgi stacks then accumulate in the pericentriolar region and form a ribbon in each daughter cell during cytokinesis. Thus mitotic Golgi disassembly could be divided into three steps: ribbon unlinking, cisternal unstacking and vesiculation. Conversely, post-mitotic Golgi reassembly includes membrane fusion/cisternae regrowth, cisternae stacking, and ribbon linking [4, 5]. Many factors are involved in the regulation of Golgi membrane dynamics during the cell cycle; these include Golgi matrix proteins, kinases and phosphatases, ubiquitin ligases and deubiquitinating enzymes, vesicle budding and fusion machineries, as well as actin and microtubule cytoskeleton. In this review we summarize recent findings on the mechanisms that regulate these three processes in mitotic Golgi disassembly and post-mitotic Golgi reassembly during the mammalian cell cycle, especially on Golgi stacking proteins in Golgi stack formation, ubiquitin in post-mitotic Golgi membrane fusion, and golgins and cytoskeleton in Golgi ribbon linking.

Golgi cisternal stacking and its regulation in the cell cycle

Golgi stacks are the basic structural and functional units of the Golgi in mammalian cells. Our current understanding of the mechanism of Golgi stacking largely benefits from an *in vitro* assay that reconstitutes the cell cycle regulated Golgi disassembly and reassembly process. Briefly, highly purified rat liver Golgi stacks [6] are incubated with mitotic cytosol to generate mitotic Golgi fragments (MGFs). After re-isolation, these MGFs reassemble into Golgi stacks upon incubation with interphase cytosol or purified cytosolic components. This provides a readily manipulatable biochemical system within which the sequence of morphological events can be precisely followed by quantitative electron microscopy (EM) or biochemical analysis [7,

8]. This approach has contributed to the discovery and characterization of many proteins that mediate Golgi membrane tethering, fusion, cisternal stacking, and regulation [4, 9-11].

The role of GRASP65 and GRASP55 in Golgi cisternal stacking

The mechanism and biological significance of Golgi stacking in protein trafficking and processing remain as interesting and significant questions to be answered in the field. So far the only proteins that are shown to directly participate in Golgi stacking are the Golgi reassembly stacking proteins (GRASPs), which include GRASP65 and GRASP55 in mammalian cells (Figure 1.1A). GRASP65 was first identified as a peripheral Golgi protein that is accessible to N-ethylmaleimide (NEM) only when the Golgi stacks are disassembled, and NEM treatment of the Golgi membranes abolished Golgi cisternae re-stacking in the *in vitro* reassembly assay described above. GRASP65 localizes to the *cis*-Golgi; its homologue GRASP55 was subsequently discovered based on sequence similarity that stacks the *medial*-to-*trans* cisternae [12]. Several lines of evidence support the idea that GRASPs are involved in Golgi stacking. Antibodies against GRASP65 or GRASP55 inhibited the stacking of newly formed cisternae in the *in vitro* assay [12, 13], whereas microinjection of anti-GRASP65 antibodies into mitotic cells inhibited subsequent Golgi stack formation in the daughter cells [14]. Furthermore, depletion of GRASP65 or GRASP55 in mammalian cells by RNA interference (RNAi) reduced the number of cisternae per stack [15-17]. Since GRASP65 and GRASP55 localize to the *cis*- and *medial*-to-*trans* Golgi, respectively [12], the reduced cisternae number by knocking down each individual GRASP protein was possibly due to losing either the *cis* or the *medial*-to-*trans* cisternae from the Golgi stacks. Simultaneous depletion of both GRASPs resulted in complete disassembly of the Golgi stacks [16], suggesting that they play complementary roles in the formation of the

polarized stacked structure of the Golgi [4, 16]. GRASPs are peripheral membrane proteins that form stable homodimers, and dimers from adjacent cisternae oligomerize in *trans* through their N-terminal GRASP domains to zip the cisternae into stacks. The oligomerization state of GRASPs is regulated by mitotic phosphorylation at the C-terminal Serine/Proline-Rich (SPR) domain discussed below (Figure 1.1) [4, 16, 18].

Cell cycle regulation of GRASP65 and GRASP55 in Golgi stacking

The Golgi apparatus undergoes cisternae unstacking and restacking during the cell cycle [14, 16, 17]. This process depends on the mitotic phosphorylation and post-mitotic dephosphorylation of the GRASP proteins. The phosphorylation of GRASP65 on multiple sites in the SPR domain by cdc2 (cdk1) and polo-like kinase 1 (Plk1) during mitosis changes its conformation, leads to GRASP65 de-oligomerization and thereby allows the Golgi cisternae to separate [18]. After mitosis, GRASP65 is de-phosphorylated by the phosphatase PP2A, reforms *trans*-oligomers and stacks Golgi cisternae [7]. GRASP55 is regulated in a similar way [16]; it is phosphorylated by MEK1/ERK during mitosis and is dephosphorylated by a phosphatase yet to be identified [16]. When phospho-deficient mutants of GRASP65 or GRASP55 are expressed in cells, mitotic Golgi fragmentation is at least partially inhibited [17, 18]. Conversely, expression of their phosphomimetic mutants, or inhibition of their dephosphorylation, accelerates mitotic Golgi disassembly and reduces Golgi reassembly [16].

GRASP65 has multiple phosphorylation sites localized to the C-terminal SPR domain that are phosphorylated by cdc2 during mitosis [19, 20]. It is recently shown that these sites are sequentially phosphorylated and dephosphorylated during the cell cycle; and the phosphorylation

of a Threonine 220/Threonine 224 site, which is physically close to the GRASP domain at the amino acid level, is likely the most important in regulating Golgi unstacking [20-23]. Besides the many phosphorylation sites in the SPR domain, Serine 189 in the N-terminal GRASP domain has been identified as a plk1 site in both GRASP65 and GRASP55. Phosphorylation of this site also interrupts GRASP oligomerization and is required for mitotic Golgi disassembly [24, 25]. Since expressing the GRASP domain including S189 inhibits Golgi fragmentation [16, 17], it is possible that S189 phosphorylation alone may not be sufficient to regulate GRASP oligomerization. Alternatively, phosphorylation of the SPR domain by cdc2 may be a prerequisite of S189 phosphorylation by plk1, as it has been shown that phosphorylation by cdc2 is required for docking plk1 onto GRASP65 [19].

It is worth noting that GRASPs have multiple functions. Their roles in Golgi ribbon formation will be discussed in the later sections in this review. Other functions, including unconventional secretion and cell cycle regulation have been discussed elsewhere [22, 23]. GRASPs are also involved in vesicle mediated Golgi transport. Inhibition of GRASP65 function by microinjecting GRASP65 antibodies into the cell accelerated protein trafficking, possibly because unstacked Golgi cisternae have more surface area to generate vesicles [26]. During mitosis, Golgi unstacking by GRASP phosphorylation facilitates the vesiculation of Golgi membranes, as discussed below.

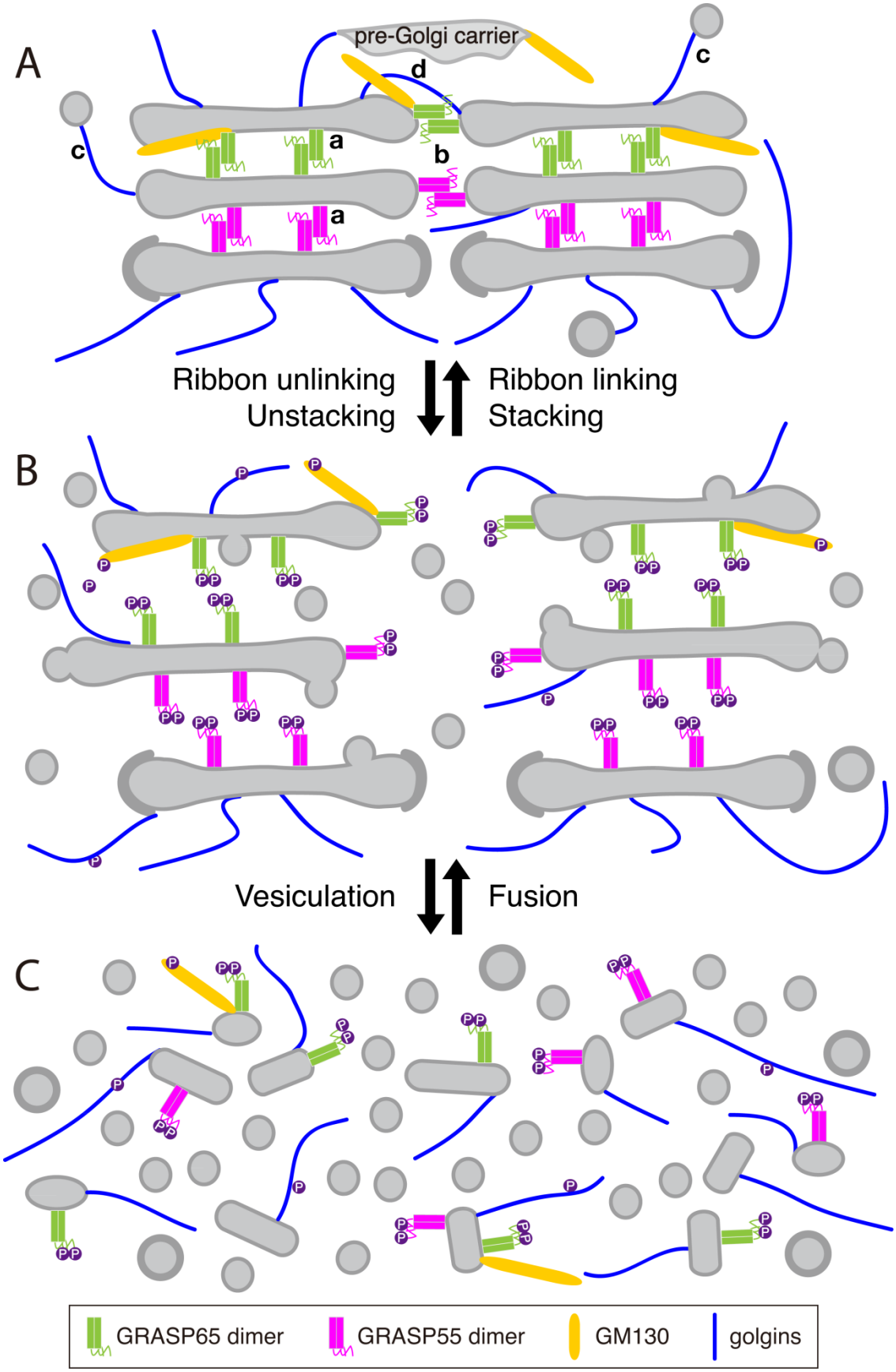
A
pre-Golgi carrier
d
c
c
a
b
a
Ribbon unlinking
Unstacking
Ribbon linking
Stacking
B
Vesiculation
Fusion
C
GRASP65 dimer
GRASP55 dimer
GM130
golgins

Figure 1.1. GRASPs and golgins in Golgi stacking and ribbon linking during the cell cycle.
(A) GRASP65 (locates to *cis*-Golgi) and GRASP55 (locates to *medial*-to-*trans*-Golgi) homodimers on adjacent membranes form *trans*-oligomerizers, bring the membrane closer to each other to (a) form stacks when GRASPs localize between the cisternae, and to (b) form a ribbon when GRASPs are at the rims of the Golgi stacks. In addition to GRASPs, golgins are also required for the maintenance of Golgi ribbon integrity by either (c) tethering vesicles/transport carriers to Golgi membranes, such as GM130, or by (d) tethering membranes from neighboring stacks, as GMAP210. **(B)** During mitosis, GRASPs and GM130 are phosphorylated by mitotic kinases, which disrupts their oligomerizations and allows ribbon unlinking and cisternae unstacking. **(C)** The resulted single cisternae by unstacking undergo continuous vesicle budding to further disassemble Golgi membranes into vesicles and tubular structures. In cells, Golgi ribbon unlinking occurs in G2 phase, while Golgi unstacking and vesiculation take place in prophase and prometaphase. The reverse processes, Golgi membrane fusion, stacking and ribbon linking, occur in telophase and cytokinesis.

Golgi cisternae vesiculation and regeneration during the cell cycle

During interphase, COPI vesicles are generated from one Golgi subcompartment and fuse with another for intra-Golgi and Golgi-to-ER trafficking [27]. During mitosis, the Golgi membranes disassemble via continuous COPI vesicle budding while fusion is inhibited. In post-mitotic Golgi reassembly, those COPI vesicles fuse to generate new cisternae (Figure 1.1). This vesiculation and cisternae regeneration process is mediated by vesicle budding and fusion machineries, which are modulated by the vesicle tethers.

Golgi vesiculation during mitosis

During prophase and prometaphase, Golgi cisternae undergo extensive COPI-dependent vesiculation [28, 29]. Treatment of unstacked Golgi membranes (induced by kinase treatment) with purified Arf1 and coatomer is sufficient to transform the Golgi cisternal membrane into vesicles *in vitro* [7], suggesting that Arf1 and coatomer are sufficient to trigger Golgi membrane vesiculation. Not all of the Golgi membranes are turned into vesicles during mitosis; some remain as tubulovesicular structures. These membranes contain Golgi matrix proteins including GRASPs and golgins and may serve as templates in late mitosis for the formation of new Golgi apparatus in the daughter cells [30, 31], but the underlying mechanism remains elusive.

Post-mitotic Golgi membrane fusion

Post-mitotic Golgi membrane fusion requires tethering proteins like p115, giantin and GM130, soluble NSF attachment protein (SNAP) receptors (SNAREs), and two AAA ATPases, N-ethylmaleimide sensitive fusion protein (NSF) and valosin-containing protein p97 [VCP] with their adaptors (Figure 1.2) [32]. NSF and its adaptors α/γ-SNAPs catalyze the disassembly of *cis*-SNARE complex after membrane fusion therefore allows a new round of fusion to take place. In interphase, this process is required for both ER-to-Golgi and intra-Golgi transport (Figure 1.2A). In post-mitotic Golgi reassembly, two steps of NSF function are required for post-mitotic Golgi reassembly. At the onset of mitosis when the Golgi is vesiculated, NSF drives SNARE dissociation by hydrolyzing ATP, similar to its function in interphase. At the second step in late mitosis, NSF catalyzes the complex formation between GATE-16 and the v-SNARE GS28. The binding with GATE-16 precludes GS28 from binding its cognate t-SNARE syntaxin-5. This process appears to be important for post-mitotic Golgi membrane fusion and is independent of ATP hydrolysis (Figure 1.2C) [32].

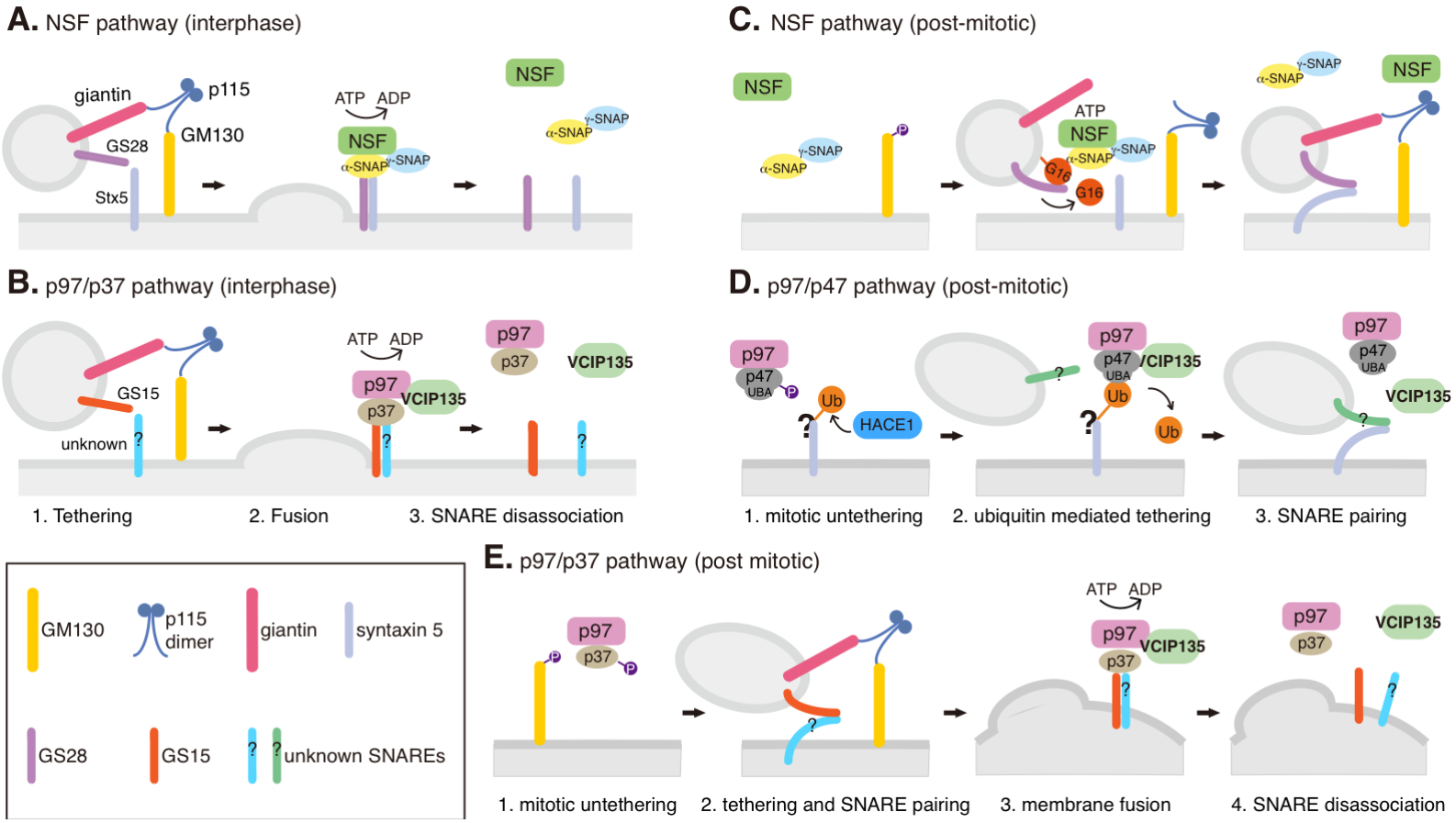

Figure 1.2. NSF and p97 pathways in interphase Golgi membrane fusion and post-mitotic Golgi reassembly
(A-B) Interphase Golgi membrane fusion mediated by NSF (A) and p97/p37 (B). Vesicles or Golgi membranes are tethered by the p115/GM130 complex, which facilitates SNARE-mediated fusion. The SNARE complexes are disassociated by NSF or p97 by ATP hydrolysis to allow next round vesicle fusion. **(C-D)** Ubiquitin involved post-mitotic Golgi fusion by NSF (C) and p97/p47 (D). During mitosis, GM130 phosphorylation interrupts its interaction with p115 and facilitates Golgi vesiculation. After mitosis, ubiquitination operates as a general mechanism for Golgi cisternae regrowth. In the NSF pathway (C), GATE-16, a ubiquitin-like protein, recruits NSF onto the membranes. NSF then catalyzes GATE-16 to form a complex with GS28 and inhibits GS28-syntaxin 5 interaction in an ATP-hydrolysis independent manner. GATE-16 is released from the membrane by an unknown mechanism to allow SNARE complex assembly and membrane fusion. In the p97/p47 pathway (D), HACE1 attaches ubiquitin onto unknown substrates on the Golgi membranes during mitosis; ubiquitination of these Golgi proteins may inhibit vesicle fusion. In late mitosis, the ubiquitin bound to a Golgi protein interacts with the UBA domain of p47 and recruits the p97/p47/VCIP135 complex onto Golgi vesicles. VCIP135 removes ubiquitin from Golgi proteins and allows p97/p47 to fuse the Golgi fragments into new cisternae. How p97/p47 regulates SNARE pairing and membrane fusion in this process is still unclear. **(E)** Ubiquitin is not involved in post-mitotic Golgi fusion by p97/p37. During mitosis, p37 is phosphorylated and thus membrane fusion is inhibited. After mitosis, dephosphorylation of p37 allows membrane fusion similar to that in interphase (B). In this pathway, SNARE complex is disassembled by p97 ATP hydrolysis, while the p97/p37 complex is disassembled by VCIP135.

The other AAA ATPase p97, with its adaptor p47, promotes post-mitotic cisternae regrowth but not interphase trafficking [33]. Unlike NSF, p97/47-mediated post-mitotic Golgi reassembly requires neither p115 tethering nor GS28; however uses syntaxin 5 as a shared receptor. Therefore, it is proposed that NSF pathway mediates heterotypic fusion between vesicles and Golgi remnants, while p97 pathway mediates homotypic fusion between Golgi remnants (Figure 1.2D) [32]. Another p97 adaptor, p37 is involved in both post-mitotic reassembly and interphase maintenance of the Golgi complex. The p97/p37 pathway for Golgi reassembly requires p115 and GS15 but not syntaxin 5, suggesting a mechanism different from either the NSF pathway or the p97/p47 pathway (Figure 1.2B&E) [34].

The role of ubiquitin in post-mitotic Golgi membrane fusion

One exciting finding in cell cycle regulated Golgi dynamics concerns the involvement of ubiquitin in post-mitotic membrane fusion [32]. The first evidence that indicates the role of ubiquitin in post-mitotic Golgi fusion came from the domain analysis of p47. p47 contains a ubiquitin-associated (UBA) domain that binds mono-ubiquitin; inhibition of p47-ubiquitin interaction suppresses p97/p47-mediated Golgi membrane fusion [35]. Mono-ubiquitination of Golgi proteins occurs during mitotic Golgi disassembly and is required subsequently at the end of mitosis for targeting p97/p47 complex onto the Golgi remnants for reassembly [36, 37]. This process does not involve the proteasomes [36]. Both the ubiquitin ligase and the deubiquitinating enzyme (DUB) have been recently discovered. The ubiquitin E3 ligase was identified as HACE1 (the HECT domain and ankyrin repeat containing E3 ubiquitin protein ligase 1) [37], a HECT (Homologous to the E6-AP Carboxyl Terminus) domain-containing ubiquitin ligase that is down

regulated in a variety of tumors [38]. And VCIP135 (valosin-containing protein p97/p47 complex-interacting protein, p135) was identified as the deubiquitinating enzyme (DUB). VCIP135 forms a quaternary complex with syntaxin 5 and the p97/p47 complex via a ubiquitin fold domain and its enzymatic activity is required for post-mitotic Golgi membrane fusion [36]. Furthermore, VCIP135 interacts with WAC, which enhances the DUB activity of VCIP135. Depletion of WAC by RNAi in cells resulted in extreme Golgi vesiculation and VCIP135 mis-localization from the Golgi [39]. These results indicate a cycle of ubiquitination and deubiquitination in p97/p47-mediated Golgi dynamics.

The ubiquitin moieties on these substrates, added by HACE1 during mitosis, likely serve as receptors for the p97/p47/VCIP135 complex at the end of mitosis to carry on fusion reactions after the removal of the ubiquitin tags by VCIP135 (Figure 1.2D) [36, 37]. It has been proposed that during mitosis when the Golgi membranes are disassembled, HACE1 attaches monoubiquitin onto a Golgi membrane protein(s), which subsequently recruits the p97/p47 complex onto the Golgi fragments through the UBA domain of p47. The deubiquitinase VCIP135, which is associated with the p97/p47 complex, removes the ubiquitin moiety and thus allows p97/p47 to fuse the membranes after mitosis (Figure 1.2D) [37]. The underlying mechanism, however, remains largely unknown. For example, it has not been determined whether p97/p47-mediated membrane fusion requires cognate SNARE pairing and whether p97 drives SNARE disassociation by hydrolyzing ATP. In addition, since the substrates of HACE1 and VCIP135 on the Golgi membranes are still unidentified, it is not clear whether membrane association of the p97/p47 complex depends on the level of ubiquitin on the Golgi membranes and whether ubiquitination of Golgi membrane proteins is the cause of shutting down membrane

trafficking during mammalian cell division. Unlike p47, p37 lacks a ubiquitin-binding domain that interacts with ubiquitin, thus the p97/p37 pathway does not need ubiquitin and WAC. However, the p97/p37 pathway requires VCIP135 for disassociating the p37-GS15 complex, although its deubiquitinating activity is not required (Figure 1.2E) [34, 39], suggesting that VCIP135 has a ubiquitin-independent role in regulating SNARE pairing.

The other AAA ATPase, NSF, although does not interact with ubiquitin as the p97/p47 complex, requires a ubiquitin like protein GATE-16 to drive the post-mitotic cisternal regrowth [32]. GATE-16 recruits NSF/SNAPs complex onto vesicles through direct interaction with NSF. NSF then catalyzes GATE-16 binding to the Golgi v-SNARE GS28, which blocks the interaction between GS28 and syntaxin-5 and thus negatively regulates their pairing [40]. Releasing GATE-16 allows SNARE pairing and subsequent membrane fusion. In this way, GATE-16 serves as a receptor for the NSF/SNAPs complex, like ubiquitin for the p97/p47 complex, with the membrane association and dissociation of GATE-16 possibly through a lipidation/de-lipidation cycle [32], which requires further confirmation. So far it has not been shown whether GATE-16 can be covalently linked to proteins in a similar way as ubiquitin. In addition, NSF does not hydrolyze ATP to disassemble SNARE complexes during post-mitotic membrane fusion. Instead, it catalyzes GATE-16 to interact with GS28 to negatively regulate SNARE pairing. How this results in membrane fusion remains as a mystery. Nevertheless, these observations suggest that ubiquitination operates as a general mechanism for Golgi cisternae regrowth after mitosis (Figure 1.2C&D).

Cell cycle regulation of golgins in vesicle tethering

Golgins are long coiled-coil proteins that play key roles in vesicle tethering, trafficking and Golgi ribbon formation (Box 1). In interphase, vesicles are tethered to the Golgi membranes by golgins before SNARE-mediated fusion [41]. Some golgins are phosphorylated during mitosis, which disrupts their tethering function and facilitates mitotic Golgi disassembly. For example, GM130, p115 and giantin form a complex that captures COPI vesicles to the *cis*-Golgi in interphase cells [42]. During mitosis, phosphorylation of GM130 on Serine 25 by cdc2 prevents p115 binding, while subsequent dephosphorylation of GM130 by PP2A after mitosis resumes its interaction with p115 and restores NSF and p97/p37 mediated fusion. Another golgin, golgin-84, which tethers vesicle for intra-Golgi trafficking, may be regulated similarly to GM130 in the cell cycle [11, 43, 44]. Besides their function in tethering vesicles, many golgins are required for maintaining Golgi ribbon integrity, as discussed in the next section.

Golgi ribbon formation and cell cycle regulation

Unlinking of the Golgi ribbon at the onset of mitosis is likely to be important for partitioning the Golgi membranes into the two daughters [4] and for mitotic progression [45]. Golgi ribbon unlinking occurs in late G2 phase, prior to Golgi cisternal unstacking and vesiculation that start in prophase [46]. So far the exact mechanism for Golgi ribbon linking is not well understood, but involves a number of proteins including the GRASP proteins, several golgins, CtBP/BARS, as well as the microtubule and actin cytoskeleton [4, 47, 48].

Cell cycle regulation of GRASP65 and GRASP55 in Golgi ribbon linking

In addition to Golgi cisternal stacking, GRASP65 and GRASP55 also link the Golgi stacks laterally into a ribbon (Figure 1.1A). Depletion of either GRASP65 or GRASP55 causes Golgi

ribbon breakdown in the cell [16, 49-51]. It has been proposed that GRASP *trans*-oligomers also exist at the rims of Golgi stacks for stack tethering, which is also regulated by phosphorylation and dephosphorylation during the cell cycle [24, 46, 50, 51]. In late G2 phase, MEK and ERK kinases are activated and phosphorylate GRASP55, which promotes Golgi unlinking [46]. GRASP65, on the other hand, is phosphorylated at Serine 277 and Serine 376 by cdc2 and Serine 189 by plk in late G2 phase, correlating to Golgi ribbon disassembly [19, 20, 24]. Expressing a phospho-deficient mutant of GRASP55 inhibited Golgi disassembly in G2 phase [46]; whereas expression of phospho-mimic mutant of GRASP65 or GRASP55 leads to Golgi fragmentation in interphase cells [24, 51]. As in cisternae stacking, GRASPs must be dephosphorylated at the end of mitosis to allow Golgi ribbon to reform (Figure 1.1).

CtBP/BARS in Golgi ribbon unlinking in G2 phase

CtBP/BARS is a protein that plays a dual role in gene transcription and Golgi membrane fission. In addition to its function in helping vesicle fission in interphase Golgi transport, CtBP/BARS is also required for Golgi ribbon unlinking at late G2 phase, earlier than the mitotic vesiculation of Golgi membranes. In cells that CtBP/BARS is depleted or inhibited by microinjected antibodies, the Golgi remains connected during mitosis and cell mitotic progression is arrested [52, 53]. However, how CtBP/BARS coordinates with GRASPs and golgins in regulating Golgi ribbon linking in the cell cycle remains elusive.

Golgins in Golgi ribbon formation

Golgins are long coiled-coil proteins that are associated with the cytoplasmic face of Golgi membranes either by a C-terminal transmembrane domain or through interaction with small

GTPases (Rabs, Arf and Arls). Many golgins have multiple Rab binding sites, which may facilitate capturing membranes bearing specific Rabs and excluding other cellular organelles like ribosomes from the Golgi region [54]. Based on their locations, golgins can be simply divided into *cis*-golgins, golgins on the rim of the stacks and *trans*-golgins [1, 55, 56].

Well-characterized *cis*-golgins include GM130, GMAP210 and golgin-160. GM130 targets to the Golgi membranes through its interaction with GRASP65 and other adaptors such as Rab1, mediates ER-to-Golgi transport and the formation of *cis*-Golgi cisternae. When GM130 is depleted Golgi, ribbon breaks down [57]. GMAP210 contains an N-terminal ALPS motif that forms an amphipathic α-helical structure and interacts with the curved membrane structures (e.g. the Golgi rims and vesicles), and a C-terminal GRAB domain that can be recruited to the Golgi cisternae flat surface through interaction with Arf1 GTPase. The C-terminus can also bind to γ-tubulin in the centrosome [58-61]. GMAP210 is required for maintaining Golgi ribbon integrity, possibly by pulling one Golgi stack to a neighboring stack, and by directing Golgi stacks to the centrosome [58-61]. The ALPS motif of GMAP210 may also be required to tether vesicles to the Golgi for ER-to-Golgi transportation [62]. The third *cis*-golgin, golgin-160, is the Golgi receptor for dynein, which is required for the localization of the Golgi membranes in the pericentriolar region and ribbon formation [63].

Three golgins that localize to the rim through the whole stack, giantin, golgin-84 and CASP, have transmembrane domains at their C-terminus required for membrane anchoring. Giantin is involved in anterograde whereas golgin-84 and CASP play a role in retrograde trafficking through the Golgi stack [1].

Trans-golgins include the GRIP domain golgins GCC88, GCC185, golgin-97 and golgin-245 (also known as p230 or tGolgin-1). These four golgins all contain C-terminal GRIP domains that dimerize and simultaneously interact with two small GTPases [55]. Localization of golgin-97 and golgin-245 to the *trans*-Golgi is mediated by Arl1-GTP, whereas the recruitment of GCC88 and GCC185 is still controversial [64]. GCC88 and GCC185 localize to different domains of the TGN and mediate different retrograde transport pathways from endosome to the TGN [65]. GCC185 was also shown to recruit microtubule +end binding proteins CLASPs to the TGN, which is required for Golgi-derived microtubule formation and Golgi ribbon integrity [66]. ARL4A, an Arf/Arl family protein, is shown to interact with GCC185 and regulate GCC185-mediated recruitment of CLASPs [67].

Golgins are also ideal candidates in Golgi ribbon formation due to their long rod shape. The best example is perhaps GM130, a golgin that interacts with GRASP65. Knockdown of GM130 causes Golgi ribbon unlinking, similar to GRASP65 depletion [57]. Since the gaps between the stacks in the ribbon are relatively larger and more heterogeneous (10s to 100s nm) compared to those between the cisternae in the stack, it is reasonable to speculate the long coiled-coil proteins like GM130 as better candidates for stack tethering. Another possible mechanism for GRASP65 and GM130 in Golgi ribbon formation depends on their vesicle tethering function, as continuous membrane input from the ER to the Golgi is required to maintain Golgi ribbon integrity. A similar hypothesis applies to GRASP55 and its interacting protein golgin-45 as well as several other golgins [1, 4].

In addition to GM130, depletion of many other golgins including p115, GMAP210, golgin-160, giantin, golgin-84, GCC185 and golgin-245 by RNAi, or impairing golgin-97 function by microinjection of inhibitory antibodies, all lead to Golgi fragmentation [1]. Since most of these proteins function in membrane tethering, their function in maintaining Golgi integrity may relies on membrane trafficking. Alternatively, some golgins including GM130, p115, golgin-160, GMAP210 and GCC185 interact with microtubules, which regulate the centralization and lateral linking of the Golgi stacks (see below and in Box 2). A third mechanism, suggested by the *cis*-Golgi golgin GMAP210, is to directly link membranes from adjacent stacks. In addition to its interaction with γ-tubulin, GMAP210 binds the *cis*-Golgi by interacting with Arf1 via its C-terminal GRAB domain and highly curved membranes (vesicles or the rim of a neighboring stack) by its N-terminal ALPS motif, therefore directs homotypic fusion of *cis*-cisternae between two stacks (Figure 1.1A) [61]. Despite the findings about golgins in maintaining Golgi integrity in interphase, how they are regulated during the cell cycle is largely unknown.

The role of microtubule organization in Golgi positioning and ribbon linking during the cell cycle

Assembly of Golgi ribbon in the cell center requires an intact microtubule network with microtubule arrays shooting from the microtubule organization centers (MTOCs) (including the centrosome and the Golgi membranes) to the cell periphery (Box 2). The microtubule minus end-directed motor, the dynein/dynactin complex, brings Golgi membranes and ER-derived vesicles to the cell center [68]. During mitosis, microtubules are reorganized into a mitotic spindle and the Golgi disassembles. The derived vesicles disassociate from the spindle microtubules, while some Golgi remnants remain associated with the spindle, undergo ordered partitioning and may

serve as Golgi templates in the reassembly [69]. In telophase, Golgi ministacks form by membrane fusion and stacking in a microtubule-independent manner. Subsequently, microtubules generated from both the Golgi ministacks and the centrosome direct Golgi stacks moving towards each other and to the cell center for new ribbon assembly (Figure 1.3) [70].

The role of microtubule cytoskeleton in Golgi ribbon formation is highlighted by a recent finding that a *cis*-Golgi protein golgin-160 recruits dynein to the Golgi by direct interaction. Depletion of golgin-160 abolished ER-to-Golgi trafficking and caused Golgi ribbon unlinking, similar to the effect caused by nocodazole treatment. Golgin-160 is recruited to the *cis*-Golgi by interacting with Arf1 GTPase while its seventh coiled-coil domain cc7 binds to dynein [63]. During mitosis, golgin-160 disassociates from Golgi membranes through an unknown mechanism, which allows the Golgi to disperse.

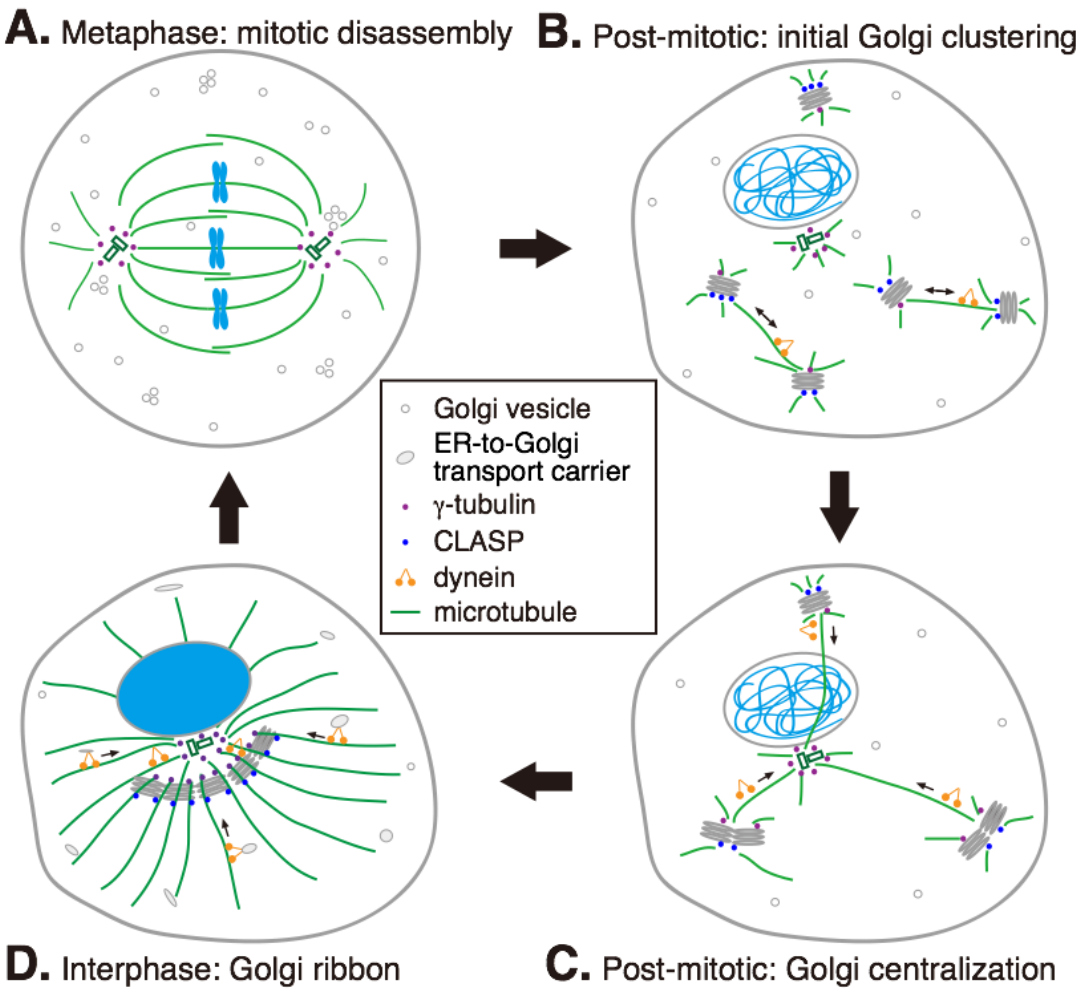

Figure 1.3 Microtubules cytoskeleton in post-mitotic Golgi ribbon formation
(A) Golgi disassembly in mitosis. During mitosis, centrosome-derived microtubules are assembled into a mitotic spindle while Golgi-derived microtubules are depolymerized. Golgi membranes are disassembled into vesicles and mitotic Golgi clusters, the latter of which are partially associated with spindle microtubules. **(B)** Golgi clustering in telophase. At mitotic exit, Golgi ministacks start to form. In the initial stage, ministacks move by dynein motor proteins towards each other along Golgi derived microtubules that are stabilized by CLASP. **(C)** Golgi ribbon formation in later telophase and cytokinesis. After the initial Golgi clustering directed by Golgi-derived microtubules Golgi clusters are captured by centrosome-derived microtubules and carried by dynein to the minus end of microtubules. The high concentration of Golgi membrane in the cell center allows further membrane fusion and ribbon formation. **(D)** Maintenance of the Golgi ribbon in interphase. Golgi is positioned surrounding the centrosome, with *cis*-golgins (GMAP210 or AKAP450/GM130) associate with microtubules derived from centrosomal γ-tubulin. Golgi-associated γ-tubulin also nucleates microtubules on the *cis*-Golgi. These microtubules are elongated through the *trans*-Golgi where they are stabilized by CLASP (through interaction with *trans*-golgin GCC185) towards the cell periphery. Dynein is required for maintaining Golgi ribbon in the pericentriolar region and for the directional movement of newly formed pre-Golgi transport carriers from cell periphery to the Golgi ribbon. *Cis*-golgin golgin-160 is the dynein receptor on Golgi apparatus.

Golgi-derived microtubules and microtubule-regulated Golgi reassembly

Golgi reassembly depends on microtubules. Conversely, Golgi serves as an unconventional MTOC and regulates microtubule organization. Several recent studies have demonstrated the formation of Golgi-derived microtubules and their roles in Golgi assembly and maintenance [66, 70-72]. Microtubules require γ-tubulin complexes to initiate the growth. Two *cis*-golgins, GM130 (through AKAP450) [72] and GMAP210 [73, 74], anchor γ-tubulin complexes to the *cis*-side of the Golgi complex. Golgi-derived microtubules need to be stabilized by CLASPs (CLASP1/2) that are tethered to *trans*-Golgi membranes through *trans*-golgin GCC185 [66, 67]. In addition, CAP350 and Hook3 may be involved in microtubule stabilization on the Golgi [75, 76].

Golgi-derived microtubules concert with centrosome-derived microtubules in Golgi reassembly at mitotic exit and in the assay after nocodazole washout. The reassembly of the Golgi ribbon from cell periphery includes two stages. First, Golgi ministacks generated by simple vesicle fusion and stacking undergo initial clustering at the cell periphery, which is referred as the Golgi stage. At this stage, the Golgi clusters stay far away from centrosome and spindle, but linked by peripheral microtubules derived from the Golgi. During this stage of Golgi reassembly, the size of each Golgi particle is doubled and total number of Golgi particles reduced. Depleting CLASP from the cell abolishes Golgi-derived microtubule formation and the initial clustering of Golgi ministacks. In the second stage, Golgi clusters move towards the cell center along centrosome-derived radial microtubule arrays to complete Golgi ribbon assembly. This stage is called centrosome stage. Without the Golgi-derived microtubules by CLASP depletion, the Golgi ministacks can still be relocated to the cell center by centrosome-derived

microtubules, but remain more fragmented [70]. On the other hand, when centrosome-derived microtubules were disrupted by laser ablation of the centrosome, a large portion of the Golgi clusters can still move towards each other and finally to the cell center [77]. However, some small fragments are blocked by the nucleus and remain uncaptured in the absence of centrosomal microtubules. Interestingly, once the Golgi is presented in the cell center, Golgi-derived microtubules are sufficient to support Golgi integrity, and the centrosome becomes dispensable [77]. Both stages of Golgi assembly require the function of dynein [70, 77]. This is consistent with the fact that when the Golgi anchor of dynein, golgin-160, is depleted, Golgi fragments into ministacks throughout the cell [63].

Actin filaments in Golgi biogenesis

In addition to microtubules, actin filaments are also involved in Golgi trafficking and structure maintenance but the underlying mechanism remains largely unknown. Impairing actin dynamics by treating cells with either actin depolymerizing or stabilizing drugs both give a compact morphology of the Golgi [78]. Actin polymerization facilitates membrane deformation to drive vesicle formation, fission and fusion, and short-range movement [79]. Not much is known about the function of actin in Golgi dynamics in mitosis. The only indication came from the study in *Drosophila* S2 cells, in which Golgi stacks are duplicated and exist as pairs before cell division. At late G2 phase, depolymerization of actin filaments induces scission of the paired-Golgi and the number of total Golgi stacks in the cell doubles. This process is mediated by inactivation of the actin nucleation promoting factors WAVE/Scar/Abi [80]. These paired Golgi stacks have been observed in human cells, however whether Golgi pairing and unpairing is also regulated by the same mechanism in mammalian cells is yet to be determined [80].

Concluding remarks

Golgi inheritance during cell division is a dynamic process that requires the cooperation of many factors including Golgi matrix proteins, membrane tethers, vesicle budding and fusion machineries, cytoskeletons, as well as kinases and phosphatases that transmit signals onto the Golgi membranes. During the cell cycle, these factors coordinately regulate mitotic ribbon unlinking, cisternae unstacking and membrane vesiculation; and post-mitotic cisternae growth, cisternae stacking and ribbon formation. Although much progress has been made in elucidating the mechanisms of Golgi membrane dynamics during the cell cycle, a number of questions remain to be addressed. First, the GRASP proteins are certainly important for Golgi structure formation, but whether they are involved in Golgi stacking, ribbon linking or both is still under debate. Second, although ubiquitin is required for post-mitotic Golgi membrane fusion, how ubiquitin and GATE-16 promote p97/p47- and NSF-mediated membrane fusion, what are the ubiquitinated substrates in the p97/p47 pathway and how GATE-16 is added onto or removed from the Golgi membranes, remain unknown. Third, whether the two functions of golgins, membrane tethering and Golgi ribbon linking, are coupled, and how they coordinate with the reorganization of the microtubule cytoskeleton during the cell cycle, require further exploration. Fourth, actin filaments play important roles not only in regulating Golgi transport but also in Golgi morphology maintenance. However, the mechanism is largely unknown. Finally, Golgi defects have been observed in several diseases such as cancer, neurodegeneration and viral infection [81, 82]. These defects may affect the trafficking, sorting and modification of a large number of proteins and cause global effects to the cell surface that compromise a variety of

cellular functions. Defining the cause of the Golgi defects at the molecular level may provide insight into the pathogenesis of the related diseases.

Chapter 2 . The role of GRASP65 in Golgi cisternal stacking and cell cycle progression

Abstract

In vitro assays identified the Golgi peripheral protein GRASP65 as a Golgi stacking factor that links adjacent Golgi cisternae by forming mitotically regulated trans-oligomers. These conclusions, however, require further confirmation in the cell. In this study, we demonstrated that the first 112 amino acids at the N-terminus (including the first PDZ domain, PDZ1) of the protein are sufficient for oligomerization. Systematic electron microscopic analysis showed that expression of non-regulatable GRASP65 mutants in HeLa cells enhanced Golgi stacking in interphase and inhibited Golgi fragmentation during mitosis. Depletion of GRASP65 by small interference RNA (siRNA) reduced the number of cisternae in the Golgi stacks; this reduction was rescued by expressing exogenous GRASP65. Further experiments revealed that inhibition of mitotic Golgi disassembly by expressing non-regulatable GRASP65 mutants did not affect equal partitioning of the Golgi membranes into the daughter cells. However, it delayed mitotic entry and suppressed cell growth; this effect was diminished by dispersing the Golgi apparatus with Brefeldin A treatment prior to mitosis, suggesting that Golgi disassembly at the onset of mitosis plays a role in cell cycle progression.

Introduction

The Golgi apparatus is the central conduit for protein trafficking, processing and secretion in almost all eukaryotic cells. In interphase mammalian cells, the Golgi apparatus consists of stacks of parallel aligned flattened membrane cisternae, which are further linked laterally by tubules to form a ribbon-like structure [83]. During mitosis, the Golgi apparatus undergoes extensive disassembly; the generated vesicles are equally partitioned into the two daughter cells where these membranes are reassembled into new Golgi stacks [84]. *In vitro* assays that reconstitute the cell cycle-regulated Golgi disassembly and reassembly processes demonstrated that mitotic Golgi disassembly consists of two reactions: Golgi unstacking mediated by phosphorylation of Golgi structural proteins and vesiculation mediated by COPI vesicle formation; while post-mitotic Golgi reassembly requires vesicle fusion for single cisterna formation and stacking of the newly formed cisternae [7]. The molecular mechanism of Golgi stacking remains unclear. Accumulating evidence suggests that stack formation requires the Golgi reassembly stacking protein GRASP65. GRASP65 was first identified as a Golgi peripheral protein that is accessible to the alkylating reagent *N-ethylmaleimide* (NEM) only when the Golgi stacks were disassembled [13]. Further experiments showed that adding GRASP65 antibodies to the *in vitro* Golgi reassembly assay inhibited stacking of newly formed Golgi cisternae [13]. Consistently, microinjection of GRASP65 antibodies into mitotic cells inhibited subsequent Golgi stack formation in the daughter cells [14].

Biochemical experiments revealed a possible mechanism for GRASP65 in Golgi stacking. GRASP65 forms homodimers that further oligomerize in *trans* to hold the adjacent Golgi membranes into stacks. Oligomerization is mitotically regulated. During mitosis, GRASP65 is phosphorylated by two mitotic kinases, cdc2 and polo-like kinase (plk), which leads to

GRASP65 de-oligomerization and thus Golgi unstacking [14, 18]. Oligomerization of GRASP65 is mediated by the N-terminal GRASP domain, while its phosphorylation occurs at the C-terminal SPR (serine/proline rich) domain [18]. Further studies showed that, when targeted to the outer membranes of mitochondria, GRASP65 is capable of tethering mitochondria into clusters [85]. Finally, expression of a caspase-resistant form of GRASP65 partially prevented Golgi fragmentation in apoptotic cells [86]. GRASP65 is concentrated in the *cis* Golgi membranes, while its homolog, GRASP55, is primarily localized to the *medial-trans* cisternae [12]. These studies provided evidence that GRASP65 is both necessary and sufficient to hold the *cis* Golgi membranes into stacks, while GRASP55 may stack the *medial-trans* cisternae in a similar manner [16, 87]. During mitosis, phosphorylation of the GRASP proteins allows unstacking of the Golgi cisternae, which may facilitate COPI vesicle formation and fragmentation of the Golgi membranes [8, 16, 26, 28]. Subsequent dephosphorylation of GRASP and other Golgi structural proteins is required for post-mitotic Golgi reassembly [8, 9].

However, the hypothesis that Golgi stacking is the primary role of GRASP65 has recently been challenged based on studies of GRASP65 homologs in other species [88, 89] and knockdown experiments of mammalian GRASP65 [15, 49]. In Drosophila, knockdown of the sole GRASP protein, dGRASP, and its interaction protein GM130, resulted in at least partial disassembly of the Golgi stacks into single cisternae and vesicles in S2 cells [89]. In mammalian cells, depletion of GRASP65 using small interference RNA (siRNA) led to either Golgi ribbon unlinking [49] or an arrest in cell division accompanied by irregular mitotic spindle formation and cell death, with the number of cisternae in the stacks decreased [15]. Obviously, the siRNA technique has limitations (such as incomplete knockdown and off-target effects); simple

knockdown experiments [15, 49] and the experiments using forced ectopic targeting of GRASP65 [85] may not be able to exclude the possibility of side effects. In addition, the roles (e.g. stacking, ribbon linking and cell cycle control) of GRASP65 in the cell may be related to each other. Therefore, a re-evaluation of GRASP65 functions *in vivo* is necessary and important.

The exact role of mitotic Golgi disassembly is so far unknown, but it is thought to facilitate equal partitioning of the Golgi membranes into the daughter cells [9, 10]. In addition, Golgi ribbon unlinking at late G2 phase may function as a new check point for cell cycle progression into mitosis, as inhibition of Golgi ribbon cleavage at the onset of mitosis by blocking the activity of the Golgi fission protein BARS [45] or MEK1 kinase [46] delayed mitotic entry of the cells. This delay was rescued when the cells were treated with Brefeldin A (BFA), a fungi product that disassembles the Golgi apparatus, prior to mitosis [46, 90]. Interestingly, interrupting GRASP65 function by microinjection of either a C-terminal fragment of GRASP65 or antibodies to this fragment into normal rat kidney cells (NRK) prevented cell entry into mitosis [90]. Further studies showed that phosphorylation of GRASP65 on serine 277 plays an important role in cell cycle regulation, as a peptide containing this site, but not its serine to alanine (S277A) mutant, delayed mitotic entry when microinjected into NRK cells [91]. The underlying mechanism for GRASP65 in cell cycle control is so far unclear. One possibility is through its regulation on mitotic kinases. Since GRASP65 is a substrate of cdc2 and plk, manipulation of GRASP65 level may affect the localization and activity of these kinases in cell cycle progression, as suggested by a previous study [19]. Alternatively, physical disruption of the Golgi structure mediated in part by GRASP65 phosphorylation and thus de-oligomerization may be required for the separation of the duplicated centrosomes for spindle formation and mitotic

progression [21]. If this is the case, inhibition of GRASP65 phosphorylation may delay Golgi disassembly at the onset of mitosis and thus interrupt cell cycle progression.

In this study, we have applied biochemical and cell biology approaches to study the function of GRASP65 in mammalian cells. We established stable cell lines in which endogenous GRASP65 was depleted by siRNA and exogenous wild-type GRSAP65 or its phosphorylation defective mutants was expressed under an inducible promoter. This allowed us to determine the role of GRASP65 in Golgi stacking by systematic EM analysis. Our results support that GRASP65 stacks Golgi cisternal membranes. In addition, we found that exogenous expression of the PDZ1 region, which is necessary and sufficient for Golgi targeting and promotion of cisternal stacking but lacks the entire phosphorylation domain, delays mitotic progression, indicating that Golgi disassembly, instead of GRASP65 phosphorylation itself, is important for the regulation of mitotic progression. Our study provides evidence and a molecular mechanism demonstrating that GRASP65 directly functions as a Golgi stacking factor and that mitotic Golgi disassembly is linked to cell cycle progression.

Results

The N-terminal 112 amino acids (PDZ1) of GRASP65 are sufficient for dimerization and oligomerization

Previous results showed that GRASP65 forms both dimers and oligomers [14] and subsequent studies revealed that the N-terminal GRASP domain (aa1-201) is both necessary and sufficient for dimerization and oligomerization [18]. Since the GRASP domain has two PDZ-containing domains, PDZ1 (aa1-112) and PDZ2 (aa113-201; Figure 2.1A), we first tested whether PDZ1 or PDZ2 is sufficient to mediate GRASP65 oligomerization using an established co-purification assay [14, 18]. Recombinant MBP (Maltose Binding Protein)- and GST (glutathione S-transferase)-tagged PDZ1 and PDZ2 were expressed in bacteria and purified separately, then mixed and incubated. Protein complexes were re-isolated using amylose beads or glutathione beads and the co-purified proteins were determined by Western blotting. As shown in Figure 2.1B, only MBP-PDZ1 and GST-PDZ1 co-purified, regardless of the beads that were used (Figure 2.1B, lane 3). However, MBP-PDZ1 was not able to interact with GST-PDZ2 (Figure 2.1B, lane 6), nor MBP-PDZ2 with GST-PDZ1 or GST-PDZ2 (Figure 2.1C, lanes 3 and 6). The results suggest that PDZ1 interacts with itself to form oligomers, while PDZ2 is not sufficient for oligomerization.

We then analyzed PDZ1 oligomerization by non-denaturing electrophoresis. As shown in Figure 2.1D, GST-PDZ1 exhibited four bands on the gel, as indicated by arrows (lane 2). The lowest band of 82 kDa was about twice the size of the estimated molecular weight of monomeric GST-PDZ1 (41 kDa); the upper bands exhibited molecular weights of 185, 307 and 424 kDa. These results suggest that PDZ1 exists as dimers and higher order oligomers, consistent with the

oligomeric properties of GRASP65 shown in previous studies [14, 18]. GST-PDZ2 (Figure 2.1D, lane 3), however, exhibited only one band of 64 kDa on the gel, which was about twice the molecular weight of GST-PDZ2 (33 kDa), indicating that PDZ2 forms dimers but not oligomers. All these bands were excised from the gel and further confirmed by denaturing electrophoresis and Western blotting. As GST itself forms homodimers [92], this result was confirmed using His-tagged PDZ1 and PDZ2 (not shown). We also analyzed PDZ1 dimerization and oligomerization using other biochemical techniques. In a sedimentation gradient (Figure 2.1E), MBP-tagged PDZ1 was concentrated in two groups of fractions, dimers in fraction 4-7 and oligomers in heavier fractions including 13-14; in gel filtration (Figure 2.1F), His-tagged PDZ1 was eluted as two peaks, one sharp peak of 48 kDa (dimer) and another broad one of 116-980 kDa (6-48mer). Since PDZ1 was the smallest fragment that is capable of oligomerization, it was further characterized in the following experiments.

We employed a well established bead aggregation assay [14] to test whether PDZ1 is sufficient to link adjacent surfaces. When incubated with bovine serum albumin (BSA), a significant amount (19.7 ± 1.1%) of the Dynal beads coated with His-tagged PDZ1 formed aggregates, similar to those coated with full length GRASP65 (23.1 ± 1.7%). In contrast, only 6.7 ± 0.6% of the beads coated with BSA formed aggregates under the same condition (Figure 2.1 I-J). Incubation with interphase cytosol (IC) greatly enhanced the aggregation of Dynal beads coated with PDZ1; 80.2 ± 3.2% of the beads were in aggregates, similar to those coated with full length GRASP65 (81.0 ± 1.7%; Figure 2.1, M vs. K; N). In addition, an excess amount of His-PDZ1, when added into the reaction, inhibited the aggregation of beads coated with full length GRASP65 (Figure 2.1, L and N). In agreement with our results, a recent study showed that

PDZ1, when expressed and targeted to the outer membrane of mitochondria, linked mitochondria to form clusters [85]. Taken together, these results demonstrate that PDZ1 of GRASP65 is both necessary and sufficient to hold surfaces together through oligomerization.

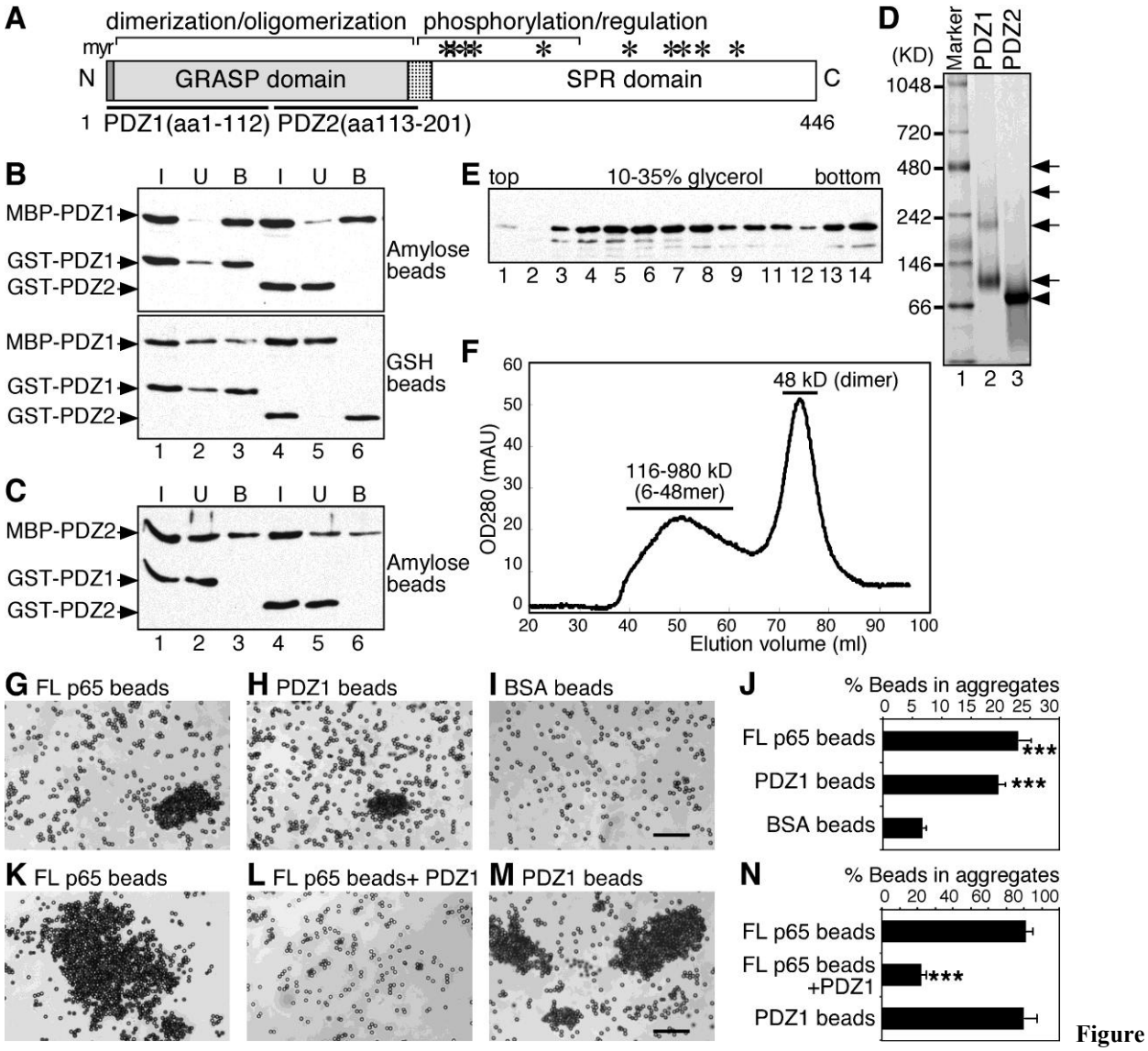

Figure 2.1. The N-terminal half of the GRASP domain (PDZ1) is sufficient to form dimers and oligomers.
(A) Domain structure of GRASP65. Indicated are the N-terminal GRASP domain with myristoylated N-terminal glycine (myr), and the C-terminal Serine/Proline Rich (SPR) domain with phosphorylation sites (*). The GRASP domain contains two PDZ subdomains, PDZ1 (aa1-112) and PDZ2 (aa113-201). **(B)** PDZ1 is sufficient to form oligomers as shown by a co-purification assay. Separately purified recombinant MBP-tagged PDZ1 was mixed and incubated with GST-tagged PDZ1 or PDZ2. The protein complexes were isolated using either amylose or glutathione (GSH) beads, as indicated. Equal proportions of the input (I), unbound (U) or bound (B) fractions were analyzed by immunoblotting for GRASP65. Note that PDZ1 co-purified with itself (lane 3), but not with PDZ2 (lane 6). **(C)** PDZ2 does not form oligomers. As in B but using MBP-PDZ2 as the bait. Note that PDZ2 did not co-purify with PDZ1 (lane 3) or itself (lane 6). **(D)** Analysis of oligomerization of PDZ1 and PDZ2 by non-denaturing gels. GST-tagged PDZ1 and PDZ2 were incubated at 37 ℃ and analyzed by non-denaturing electrophoresis and stained with Coomassie Blue. Molecular weight standards are indicated on the left. Note that PDZ1 formed dimers and

oligomers (arrows), while PDZ2 formed dimers (arrowhead) only. **(E)** Analysis of PDZ1 oligomerization by velocity gradient. Purified recombinant MBP-tagged PDZ1 was sedimented in 10-35% glycerol gradients. Shown is the Western blot for GRASP65 in each fraction. PDZ1 is found in both the upper (4-7; dimers) and deep fractions (13-14; higher-order structures). **(F)** Gel filtration analysis of PDZ1. Purified His-tagged PDZ1 was analyzed by gel filtration using a Sephacryl S-300 column. The protein was separated into two peaks: a broad peak of 116-980 kDa (6-48mer) and a sharp peak of 48 kDa (dimer). Sizes were calculated according to the calibration with a gel filtration molecular weight standard (Sigma). **(G-I)** Bead aggregation assay showing that PDZ1 is sufficient to form oligomers. Beads coated with His-tagged full length (FL) GRASP65 (G), PDZ1 (H) or bovine serum albumin (BSA, I) were incubated with BSA at 37℃ for 60 min. After incubation, the beads were placed on glass slides and random fields were photographed. A representative image of each condition is shown. Bar, 50 μm. Note that full-length and PDZ1-coated beads formed aggregates. **(J)** Quantitation of the percentage of beads in aggregates in G-I from 3 independent experiments. ***, $p<0.001$, compared to BSA-coated beads. **(K-M)** Bead aggregation assay showing that soluble PDZ1 inhibits oligomerization of full length GRASP65. Beads coated with His-tagged full length (FL) GRASP65 (K-L) or PDZ1 (M) were incubated with interphase cytosol at 37℃ for 60 min. In L, purified recombinant PDZ1 was added into the reaction. After incubation, the beads were placed on glass slides and random fields were photographed. A representative image of each condition is shown. Bar, 50 μm. Note that PDZ1 can inhibit the aggregation of GRASP65-coated beads. **(N)** Quantitation of the percentage of beads in aggregates in K-M. Results in J and N expressed as the mean ± SEM from 3 sets of independent experiments. ***, $p<0.001$, compared with full length GRASP65-coated beads in the absence of PDZ1 added to the reaction.

Expression of non-regulatable GRASP65 mutants enhances Golgi stacking in interphase cells

To test the function of GRASP65 in the cell, we expressed the wild type protein or its mutants using a retroviral *tet*-inducible mammalian expression system (*tet*-on) [16, 93]. The coding sequence was integrated into the genome but the exogenous protein is not expressed unless induced by doxycycline. This is particularly important, as continuous over-expression of GRASP65 or its mutants may affect cell growth [15]. Establishment of stable cell lines expressing the exogenous protein in an inducible manner also allowed a systematic analysis by electron microscopy (EM). The expression level of the exogenous proteins was well controlled, thus nonspecific effects caused by protein over-expression was not a concern in our study. Five lines of HeLa cells were generated that express: 1) GFP (enhanced green fluorescent protein), and GFP-tagged 2) wild type (WT) GRASP65, 3) non-phosphorylatable GRASP65 mutant, mG, with 7 phosphorylation sites mutated to alanines (S216A/S217A/T222A/T224A/S277A/S367A/S376A) [18, 94], 4) the GRASP domain (aa1-201), and 5) PDZ1 (aa1-112) of rat GRASP65. The last three mutants form oligomers, but their oligomerization cannot be regulated through phosphorylation [18], and thus they are termed as

non-regulatable mutants. The GRASP domain has been examined previously [18] and was used as a positive control in this study. Other constructs, such as PDZ2 (Figure 2.1) and the SPR-domain [18], do not form oligomers and thus were not examined in this experiment. The cytoplasmic soluble mutant (G2A) of the protein was originally included in this study but did not show significant effect on the Golgi structure [18] and thus was not further characterized. The exogenous proteins were well expressed when induced by doxycycline, as shown by Western blot analysis (Figure 2.2L). Fluorescence microscopy (Figure 2.2, A-E) showed that the expressed GRASP65 WT-GFP, mG-GFP and GRASP domain-GFP localized to the Golgi in interphase cells, indicated by co-localization with the Golgi marker GM130 (Figure 2.2, B-D); while PDZ1-GFP (Figure 2.2E) was partially Golgi-localized and GFP (Figure 2.2A) was found in the nucleus and cytosol. Expression of GRASP65 and its mutants did not significantly affect the overall Golgi organization at the light microscopic level when using GM130 (Figure 2.2, A-E), α-mannosidase II and Gos28 (not shown) as Golgi markers.

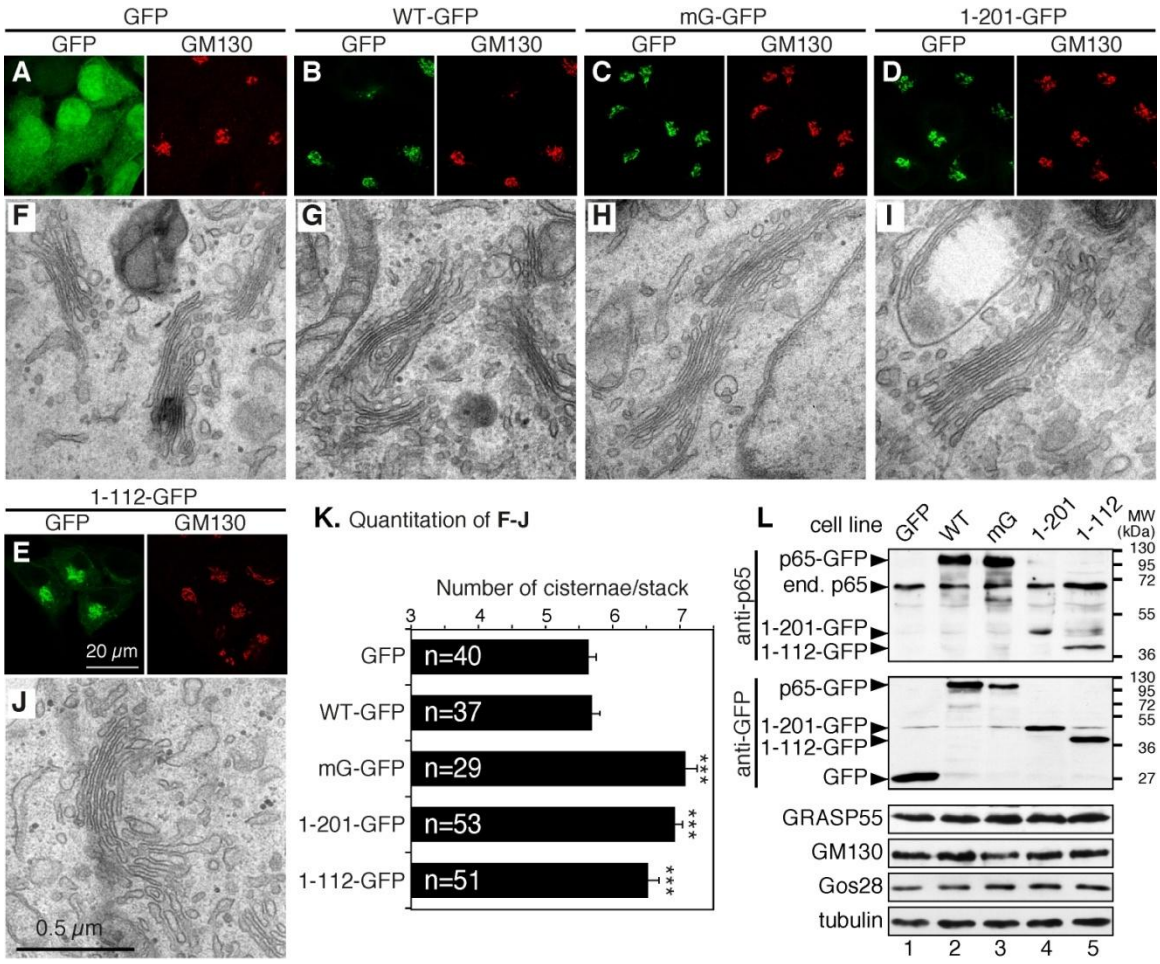

Figure 2.2. Expression of non-regulatable GRASP65 mutants enhances Golgi stacking in interphase cells. **(A-E)** Confocal images of interphase HeLa cells stably expressing indicated GRASP65 constructs using an (*tet*-on) inducible retroviral expression system. Cells were treated with 1 μg/ml doxycycline for 72 h, fixed and stained for GM130. **(F-J)** Representative EM images of interphase cells expressing indicated GRASP65 constructs. Bar, 0.5 μm. Note that the number of cisternae in the Golgi stacks were increased in cells expressing the mG mutant (H), the GRASP domain (aa1-201, I) and PDZ1 (aa1-112, J) compared to cells expressing GFP (F) and wild type GRASP65 (G). **(K)** Quantitation of F-J. Results expressed as the mean ± SEM. The number of stacks quantified for each cell line was indicated. Statistical significance was assessed by comparison to the GFP cell line. ***, *p<0.001*. Bar charts indicating the actual frequency of each value of cisternal numbers are shown in Figure 2.S1. **(L)** Western blot images of cells described in A-E. Cells were lysed in SDS buffer followed by Western blotting for GFP and other indicated proteins. 'End. p65', endogenous GRASP65.

When analyzed under the electron microscopy (EM), cells expressing non-regulatable GRASP65 showed improved cisternal alignment in the Golgi stacks in comparison to cells expressing GFP or wild type GRASP65 (Figure 2.2, F-J; 2.S1). The number of cisternae per stack significantly increased in mG (7.1 ± 0.2), GRASP domain (6.9 ± 0.1) or PDZ1 (6.5 ± 0.2) expressing cells compared to control GFP expressing cells (5.6 ± 0.1), but not in cells expressing

wild type GRASP65 (5.7 ± 0.1; Figure 2.2K). Further analysis of the EM micrographs showed that most Golgi stacks in cells expressing the non-regulatable GRASP65 mutants contained 7-8 cisternae, a significant increase from 5-6 cisternae per stack in cells expressing GFP or wild type GRASP65 (Figure 2.S1). These results provided direct evidence that GRASP65 plays a critical role in Golgi stacking *in vivo*. In addition, since wild type GRASP65 did not enhance stacking as its non-regulatable mutants, it suggests that phosphorylation of GRASP65 may regulate stacking in interphase, which may be important for Golgi remodeling under certain conditions such as cell migration in wound healing [21].

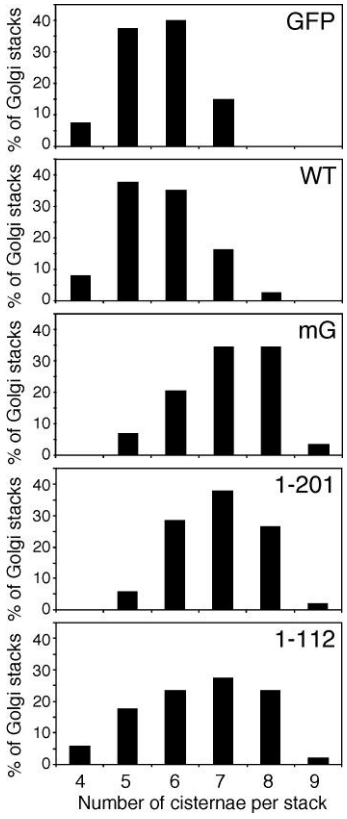

Figure 2.S1. Expression of non-regulatable GRASP65 mutants enhances Golgi stacking in interphase cells.
Bar charts of Figure 2.2K indicating the actual frequency of each value of number of cisternae per stack in HeLa cells expressing GFP or indicated GFP-tagged GRASP65 constructs. Note that expression of non-regulatable GRASP65 mutants, but not the wild type protein, increased the number of cisternae in the stacks.

Expression of non-regulatable GRASP65 mutants inhibits mitotic Golgi disassembly

Previous reports demonstrated that GRASP65 phosphorylation at the onset of mitosis is required for Golgi membrane unstacking, which facilitates subsequent vesiculation of the

membranes [7, 14]. Consistently, expression of the GRASP domain of GRASP65 inhibited Golgi fragmentation in mitosis [18], suggesting that the expressed non-regulatable GRASP65 mutants may inhibit mitotic Golgi disassembly as they remain as oligomers during mitosis. We therefore examined mitotic Golgi fragmentation in the cell lines described above. After 72 h doxycycline induction, cells were fixed, stained for DNA to select metaphase cells and GM130 to reveal the Golgi membranes. As shown in Figure 2.3, the Golgi membranes were extensively fragmented in metaphase cells expressing GFP or GRASP65-GFP. However, in cells expressing either the GRASP65 mG mutant, the GRASP domain, or PDZ1, the Golgi were observed as large dots, or mitotic Golgi clusters, indicated by the Golgi marker GM130. Quantitation of the images showed that a significant higher amount of the Golgi membranes remained as clusters in cells expressing non-regulatable GRASP65 mutants compared to that in cells expressing GFP or wild-type GRASP65-GFP (Figure 2.3F). The exogenous GRASP65 mG-GFP and the GRASP domain-GFP co-localized with the endogenous GM130 on the mitotic Golgi clusters, suggesting that the reduced Golgi disassembly was caused by the expressed exogenous proteins. Although the PDZ1 was only partially localized to the Golgi, it inhibited Golgi fragmentation to the same extent as the mG mutant or the GRASP domain (Figure 2.3).

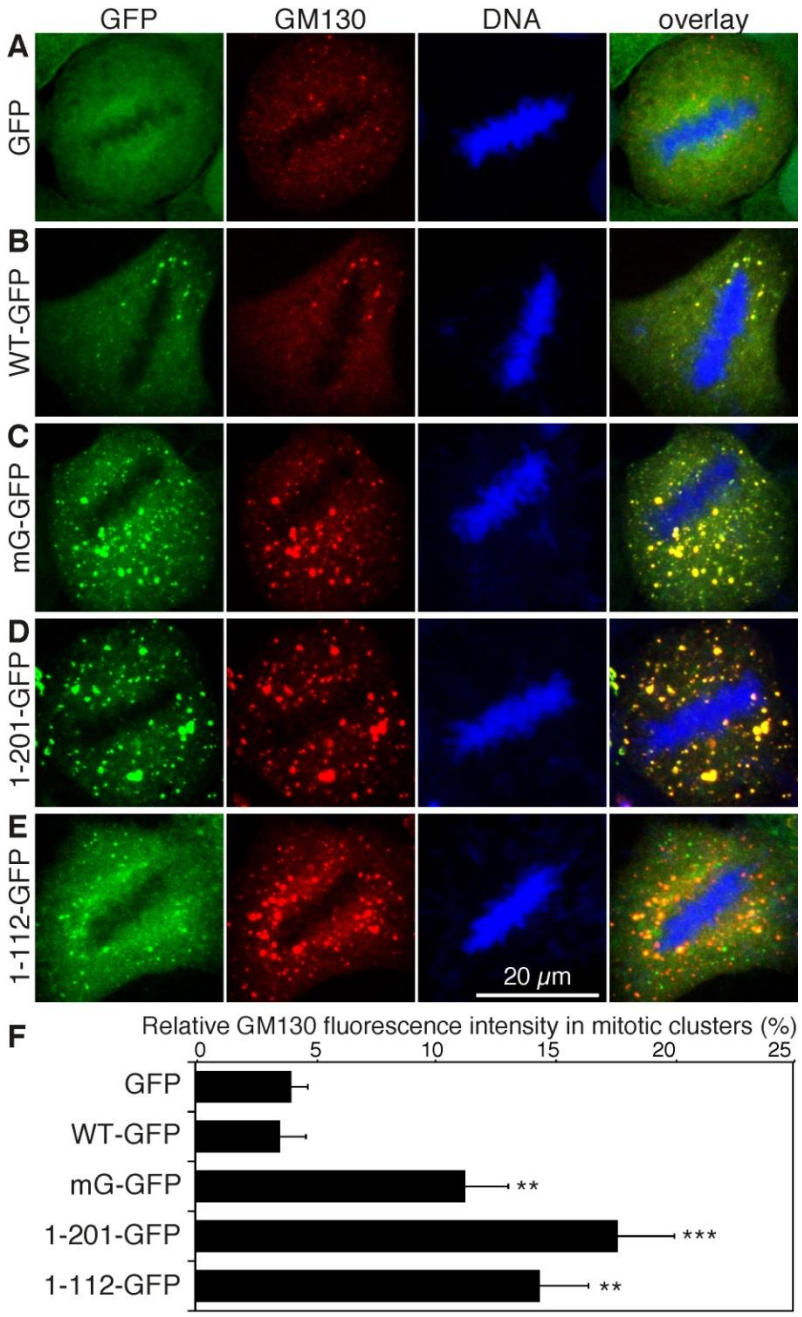

Figure 2.3. Expression of non-regulatable GRASP65 mutants inhibits mitotic Golgi disassembly at the light microscopy level.

(A-E) Confocal images of mitotic HeLa cells stably expressing the indicated GRASP65 proteins. Cells were induced by doxycycline for 72 hrs and fixed, and stained for DNA and GM130. Note that cells expressing the mG mutant (C), the GRASP domain (aa1-201, D) and PDZ1 (aa1-112, E) had more mitotic clusters compared to those expressing GFP (A) and wild type GRASP65 (B). Scale bar, 20 μm. **(F)** Relative distribution (%) of the Golgi membranes in mitotic Golgi clusters in the indicated cell lines. The fluorescence intensity of GM130 was quantified using the ImageJ software for the total fluorescent intensity and a threshold was used to filter the fluorescence in Golgi haze to quantify the fluorescent intensity in mitotic Golgi clusters. The average percentage of fluorescent intensity in Golgi clusters (mean ± SEM) from 10 cells in each cell line is shown. Statistical significance was assessed by comparison to the GFP cell line. **, $p<0.005$; ***, $p<0.001$.

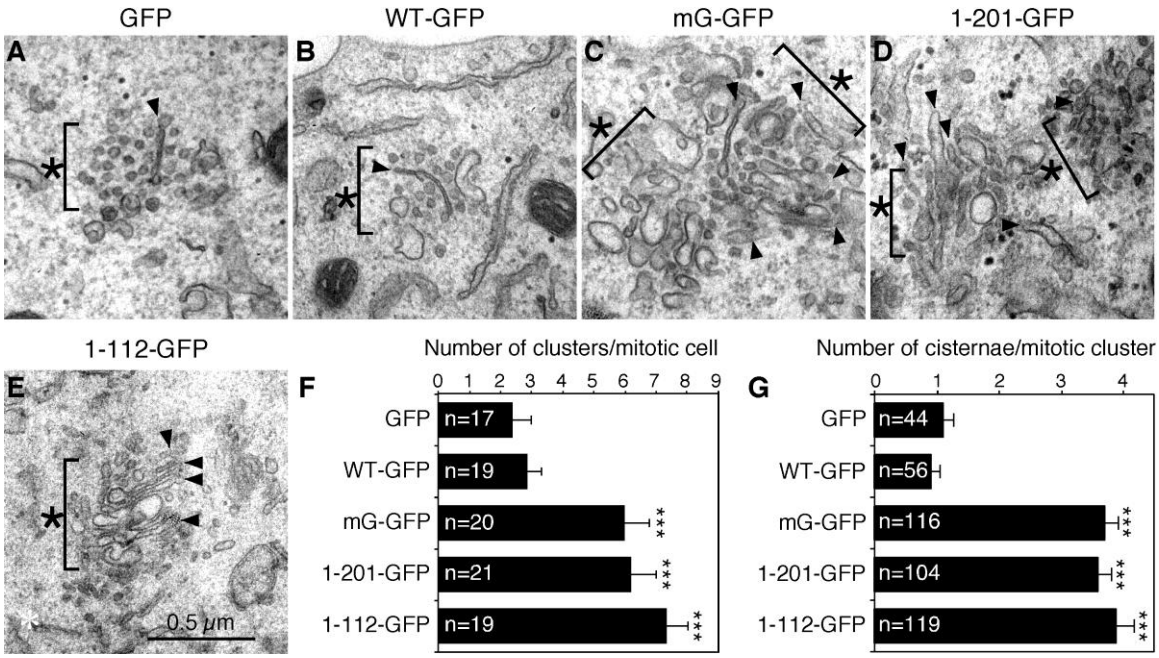

Figure 2.4. Expression of non-regulatable GRASP65 mutants inhibits mitotic Golgi disassembly when examined by EM.
(A-E) Representative EM images of Golgi clusters (asterisks) in mitotic cells expressing indicated GRASP65 constructs. Mitotic cells were collected by shake-off of cells released from a double-thymidine block and processed for EM. Bar, 0.5 μm. Note that the mitotic Golgi clusters were larger and more compact in cells expressing the mG mutant (C), the GRASP domain (D) and PDZ1 (E), with an increased number of remaining Golgi cisternal structures (arrowheads) in the clusters. **(F-G)** Quantitation results of A-E to determine the number of mitotic clusters per mitotic cell profile (F) and the number of cisternae per mitotic cluster (G). Only cells with condensed chromosomes but no detectable nuclear envelope were counted. The number of cells (F) and clusters (G) quantified for each cell line was indicated and results expressed as the mean ± SEM. Statistical significance was assessed by comparison to the GFP cell line. ***, $p<0.001$.

We then examined these cells under the EM. Mitotic HeLa cells were collected by shake-off after double thymidine block and release. Unlike mitotic cells expressing GFP or wild type GRASP65 in which the Golgi complex was extensively disassembled and diffused, considerable amounts of Golgi membranes remained as Golgi clusters in cells expressing non-regulatable GRASP65 mutants (Figure 2.4, C-F, asterisks). These clusters consisted of short cisternae (arrowheads), tubular structures or even ministacks that were surrounded by vesicles. Quantitation of the EM images showed that the number of mitotic clusters per mitotic cell profile (with condensed chromosomes but no nuclear envelope) was significantly increased in cells expressing mG (6.0 ± 0.8), the GRASP domain (6.2 ± 0.8) or PDZ1 (7.3 ± 0.7) compared to cells

expressing GFP (2.4 ± 0.6) or wild type GRASP65 (2.8 ± 0.4; Figure 2.4F). The mitotic clusters in cells expressing the non-regulatable mutants were also larger in size and more compact. In addition, each mitotic Golgi cluster contained more remaining Golgi cisternae in cells expressing mG (3.7 ± 0.2), the GRASP domain (3.6 ± 0.2) and PDZ1 (3.9 ± 0.3) compared to those expressing GFP (1.1 ± 0.2) and wild type GRASP65 (0.9 ± 0.2; Figure 2.4G). These results suggest that expression of the non-regulatable GRASP65 mutants inhibited the disassembly of Golgi membranes during mitosis.

Depletion of GRASP65 reduced the number of cisternae per Golgi stack, which was rescued by expressing exogenous GRASP65

If GRASP65 plays a direct role in Golgi stacking, depletion of GRASP65 would reduce the number of cisternae in the stack. Indeed, it has been reported that knockdown of GRASP65 reduced the number of cisternae per stack from 6 to 3 [15]. However, in another report, GRASP65 depletion in the same cell line using identical siRNA oligos led to Golgi ribbon unlinking [49]. It is not clear whether the discrepancy was caused by different knockdown efficiencies between the two groups, off-target effects of the siRNA, or a limitation of the methods employed to analyze the effects. Therefore we have re-evaluated the possible phenotypes in cells in which GRASP65 was efficiently depleted by both immunofluorescence microscopy and EM. Both Western blotting (Figure 2.5O) and immunofluorescence microscopy (Figure 2.5B) showed that endogenous GRASP65 was efficiently depleted (94.1 ± 2.9% depletion, quantified from Western blot results) 96 h after transfection with GRASP65 siRNA oligos. At the fluorescence microscopy level, no obvious change in the Golgi morphology was detected (Figure 2.5, B vs. A). However, when analyzed under the EM, the number of cisternae

per Golgi stack in GRASP65-depleted cells (4.0 ± 0.1) was significantly reduced compared to cells transfected with control siRNA (5.9 ± 0.2; Figure 2.5, I vs. H; 2.5Q; 2.S2A), in agreement with a previous report [15]. As GRASP65 is concentrated to the *cis* Golgi [12], this result indicates that GRASP65 is essential for stacking the *cis* Golgi membranes.

To ensure that the observed effect was specific for GRASP65 depletion, we expressed exogenous rat GRASP65 in cells in which the endogenous GRASP65 was knocked down. We took advantage of the HeLa cell lines described above that stably express rat GRASP65 or its mutant in an inducible system. These cells were first transfected with siRNA targeted to human but not rat GRASP65; 24 h after transfection, doxycycline was added into the tissue culture medium followed by an additional 72 h incubation to induce the expression of exogenous GRASP65 proteins. As shown by the Western blot results (Figure 2.5P), 95.4 ± 0.6% of the endogenous GRASP65 was depleted in the GFP cell line, while the exogenous GFP or GFP-tagged GRASP65 and its mutants were well expressed. At the fluorescence microscopy level using GM130 (Figure 2.5) and Gos28 (not shown) as Golgi markers, the overall Golgi structure did not exhibit any obvious differences between GFP- and GRASP65-expressing cells in which the endogenous GRASP65 was depleted (Figure 2.5, D vs. C). When examined under the EM, cells expressing GRASP65-GFP had an increased number of cisternae per stack (5.7 ± 0.1) compared to those expressing GFP (4.0 ± 0.1; Figure 2.5R; 2.S2B). A similar result was obtained in cells expressing GFP-tagged mG (5.7 ± 0.1), the GRASP domain (5.8 ± 0.1), or PDZ1 (5.6 ± 0.1; Figure 2.5R; 2.S2B). These results showed that the reduction of Golgi stacking in cells transfected with GRASP65 siRNA oligos was a direct consequence of GRASP65 depletion.

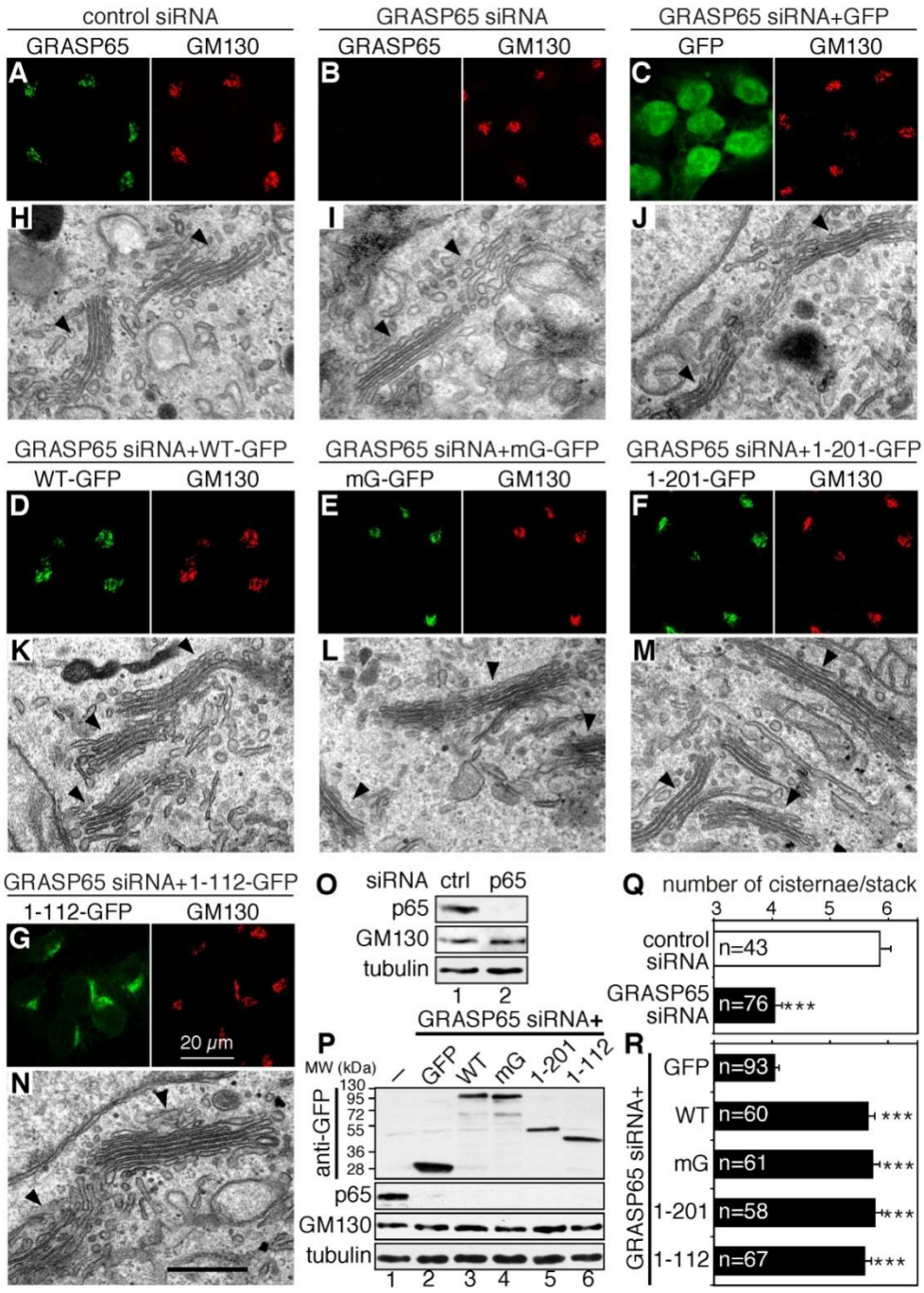

Figure 2.5. Depletion of GRASP65 reduces the number of cisternae per stack, which can be rescued by expression of exogenous GRASP65.

(A-B) Confocal fluorescence images of GRASP65 knockdown cells. HeLa cells transfected with indicated siRNA oligos were fixed and immunostained for GRASP65 and GM130. **(C-G)** Confocal fluorescence images of HeLa cells in which endogenous GRASP65 was replaced by exogenous GRASP65 or its mutants. HeLa cells expressing indicated proteins were transfected with siRNA oligos for human GRASP65. Doxycycline was added 24 h after transfection. Cells were fixed 96 h after transfection and immunostained for GM130. **(H-N)** Representative EM micrographs of cells described in A-G. Arrowheads indicate Golgi stacks. Note that the number of cisternae per stack was reduced in GRASP65 depleted cells (I), which was restored by expression of rat GRASP65 or its mutants (K-N), but not by GFP (J). **(O)** Immunoblots of HeLa cells described in A-B. The knockdown efficiency of

GRASP65 was 94.1% ± 2.9%. **(P)** Immunoblots of HeLa cells described in C-G, in which endogenous GRASP65 was replaced by rat GRASP65 or its mutant. Lane 1, control cells with neither GRASP65 depleted nor exogenous protein expressed; lane 2-6, cells with GRASP65 knocked down and indicated exogenous protein expressed. The knockdown efficiency for GRASP65 was 95.4 ± 0.6% for the GFP cell line and was similar in other cell lines, while GM130 expression level was not significantly affected. **(Q)** Quantitation of the EM images in H-I in one representative experiment from 3 sets of independent experiments. Only stacks with 3 or more cisternae were counted. The numbers of Golgi stacks quantified were indicated. Results expressed as the mean ± SEM. Note that GRASP65 depletion reduced the average number of cisternae per stack. ***, *p<0.001*. **(R)** Quantitation of the EM images in J-N. Note the increase of cisternal number per stack by expression of GRASP65 and its mutants in GRASP65 knockdown cells. Statistical significance was assessed by comparison to the GFP cell line. ***, *p < 0.001*. Bar charts indicating the actual frequency of each value of Golgi cisternae are shown in Figure 2.S2.

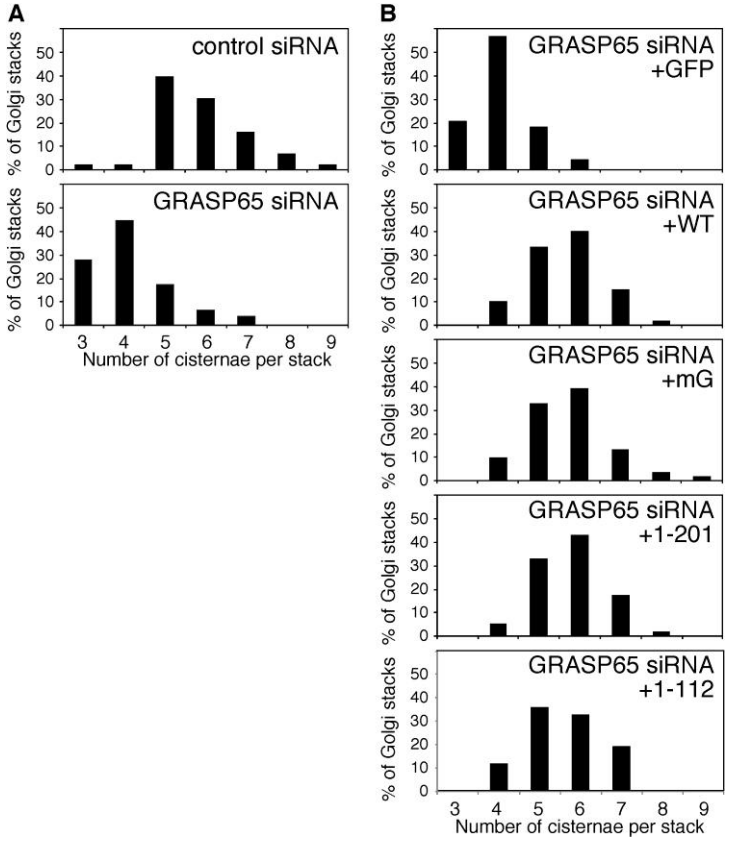

Figure 2.S2. Knockdown of GRASP65 reduces the number of cisternae per stack, which can be rescued by expression of exogenous GRASP65.
(A) Bar charts of Figure 2.5Q showing the actual frequency of Golgi cisternal numbers in the stacks in HeLa cells transfected with control or GRASP65 siRNA. Note the shift of the bars to lower numbers when GRASP65 was depleted (lower panel) compared to the control siRNA transfected cells (upper panel). **(B)** Bar charts of Figure 2.5R showing the actual frequency of Golgi cisternal numbers in the stacks in HeLa cells in which endogenous GRASP65 was replaced by GFP, rat GRASP65 or its mutants, as indicated. Note that expression of GRASP65 and its mutant increased the number of cisternae in the stacks compared to the GFP cell line.

Expression of GRASP65 mutants does not affect equal distribution of Golgi membranes into the daughter cells during cell division

Golgi disassembly during mitosis in mammalian cells is generally thought to facilitate its equal partitioning into the two daughter cells [9, 95]. However, it has also been suggested that mitotic Golgi clusters may undergo ordered inheritance [96]. Therefore it is necessary to evaluate whether inhibition of mitotic Golgi disassembly affects Golgi partitioning. We took advantage of the cell lines expressing non-phosphorylatable GRASP65 mutants in which mitotic Golgi disassembly is inhibited (Figure 2.3) and quantified the amount of the Golgi membranes in the two daughter cells using GM130 as the marker. At least 10 pairs of daughter cells in cytokinesis in each cell line were observed under confocal microscopy and the fluorescence intensity in each daughter cell was quantified (Figure 2.6). No statistical difference in GM130 distribution in the two daughter cells was detected between the cell lines examined. This result demonstrated that although mitotic Golgi fragmentation is inhibited in the cells that express GRASP65 mutants, Golgi partitioning into the two daughter cells is as accurate as control GFP-expressing cells. Similar results were obtained using other Golgi markers such as Gos28 (not shown). Consistent with this observation, it has been shown that inhibition of mitotic Golgi fragmentation by microinjection of a non-phosphorylatable p47 mutant did not affect equal distribution of Golgi membranes into the daughter cells [97]. These results imply that either partial disassembly of the Golgi in mitosis (e.g. fragmentation of the Golgi ribbon into stack) is sufficient for its equal partitioning into the daughter cells, in which case an ordered partitioning mechanism may be involved, or the primary role of mitotic Golgi disassembly is not for equal Golgi membrane distribution.

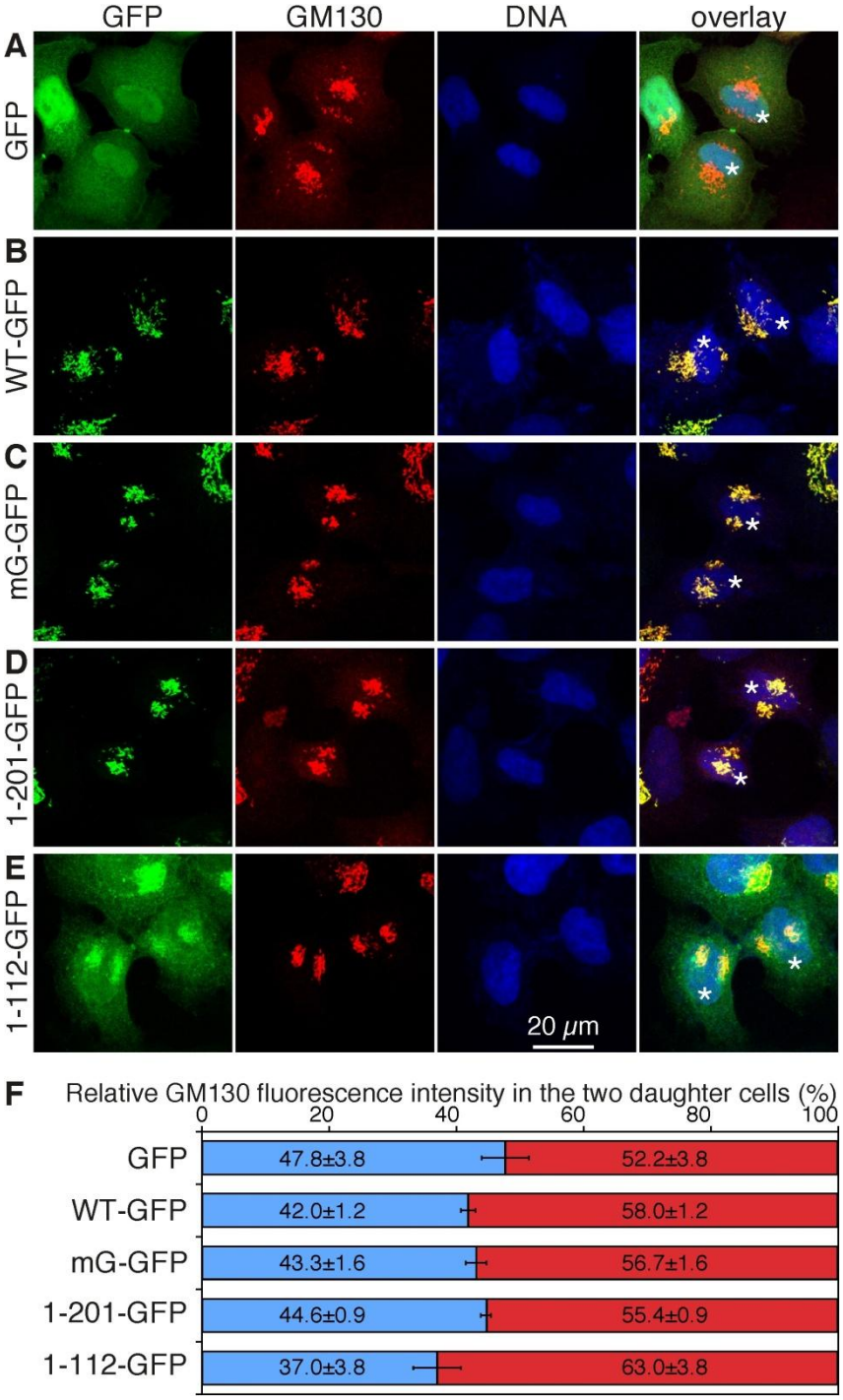

Figure 2.6. Expression of non-regulatable GRASP65 mutants does not significantly affect Golgi membrane distribution into the two daughter cells.

(A-E) Confocal images of indicated HeLa cell lines in cytokinesis. Cells were induced by doxycycline for 72 hrs and fixed, stained for DNA and GM130. Asterisks indicate the two daughter cells. Scale bar, 20 μm. **(F)** Relative distribution of the Golgi membranes in the two daughter cells using GM130 as a marker. The fluorescence intensity of GM130 in 10 pairs of daughter cells in each cell line was quantified using the NIH ImageJ software. The average (mean ± SEM) intensity in the daughter cells with relatively lower intensity compared to their pairs is shown in blue, and the average intensity in the cells with relatively higher GM130 signal is shown in red. The distribution of GM130 in the two daughter cells is statistically insignificant between all the cell lines ($p>0.05$).

Inhibition of mitotic Golgi disassembly delays cell cycle progression

Previous reports suggested that the Golgi structure (and/or its mitotic disassembly) plays a role in cell cycle control [46, 53]. Since expression of the non-regulatable GRASP65 mutants inhibited mitotic Golgi fragmentation, these cell lines provided us with excellent tools to determine the relationship between mitotic Golgi fragmentation and cell cycle progression. To evaluate whether inhibition of mitotic Golgi fragmentation affects mitotic entry, cells expressing GFP or GFP-tagged GRASP65 constructs (induced by doxycycline) were synchronized to G1/S phase by double thymidine block and the mitotic index of each cell line was determined over time after thymidine release. As shown in Figure 2.7A, the mitotic index of the GFP-expressing cells peaked at 7 h after thymidine release. Cells expressing wild type GRASP65 showed a similar cohort of mitotic index, demonstrating that expression of wild type GRASP65 protein did not affect mitotic entry. However, when the mG mutant, the GRASP domain or PDZ1 was expressed, the peak mitotic index was delayed for 1 - 2 h, suggesting that inhibition of mitotic Golgi fragmentation delayed cell cycle progression, which is consistent with previous reports [46, 53].

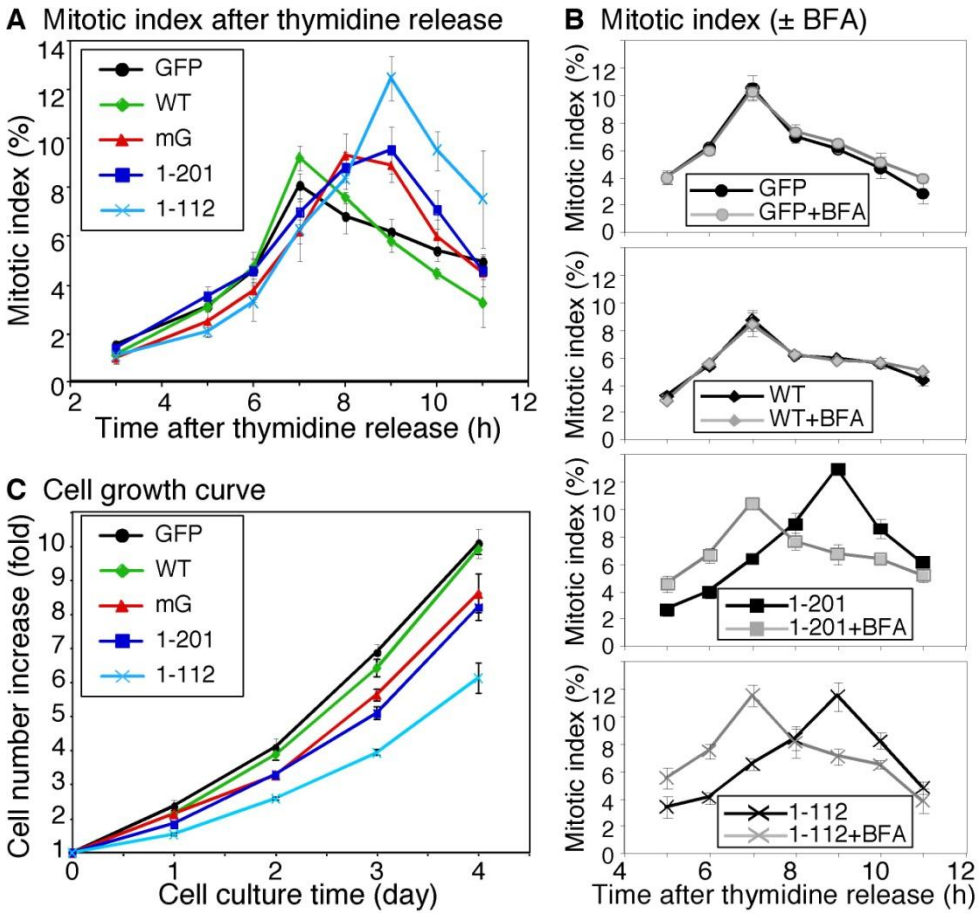

Figure 2.7. Inhibition of mitotic Golgi fragmentation by expression of non-regulatable GRASP65 mutants delays mitotic entry and inhibits cell proliferation.
(A) Inhibition of mitotic Golgi fragmentation delayed cell cycle progression. The percentage of cells in mitosis (mitotic index) at the indicated time points of release from double thymidine block was determined for cells expressing GFP or GRASP65 constructs as indicated. Note that the cells expressing GFP or wild type GRASP65 passed through mitosis in a cohort that peaks at 7 h. This peak was significantly delayed in the cells expressing the mG mutant, the GRASP domain or PDZ1 of GRASP65. **(B)** Brefeldin A (BFA)-induced Golgi disruption in cells expressing non-regulatable GRASP65 mutants rescued mitotic progression. As in (A), except that 5 μg/ml BFA was added to the tissue culture medium 4 h after the release from the double thymidine block. Note that the BFA treatment suppressed the mitotic delay in cells expressing the GRASP domain or PDZ1. **(C)** Expression of non-regulatable mutants of GRASP65 reduced the cell growth rate. The cell number of each cell line was measured by staining the cells with crystal violet at indicated time points and normalized with the cell number at the starting point. Note that expression of the mG mutant, the GRASP domain or PDZ1 reduced the cell growth rate compared to expression of GFP or wild type GRASP65.

The fact that disrupting GRASP65 function by expression or microinjection of a C-terminal fragment of the protein leads to a delay in cell mitotic entry has been described previously [90, 91]; however, the mechanism remains unknown. One possible mechanism is that GRASP65 regulates the function of mitotic kinases cdc2 and plk and therefore delays mitosis progression. It

has been shown that expression of the wild type GRASP65 C-terminal SPR domain but not the phosphorylation defective mutant caused a delay in cell cycle progression [19]. However, the non-regulatable GRASP65 mutants used in our study were not substrates of the mitotic kinases, since the phosphorylation sites were either mutated or deleted. In addition, these proteins are localized on the Golgi when expressed in the cell, which is different from the cytosolic SPR domain used in previous studies [19, 90]. Expression of these constructs also showed no effect on the expression level and localization of cdc2, cyclin B1 and plk in the cell (not shown). Therefore, it is unlikely that the delay in mitotic entry observed in this study occurred through inhibition or modulation of the mitotic kinases.

Another possible explanation for the cell cycle progression delay is that Golgi disassembly is required for mitotic entry, as suggested by previous reports [21, 90]. In this model, GRASP65 has no direct role in cell cycle control, but inhibition of mitotic Golgi fragmentation by interrupting GRASP65 function may delay mitotic entry. If this is the case, physical disruption of the Golgi by BFA before mitosis [46] may abolish the mitotic delay caused by the expression of non-regulatable GRASP65 mutants. To test this possibility, we added BFA into the tissue culture medium 4 h after final release from the double thymidine block and measured the mitotic index at later time points. As shown in Figure 2.7B, BFA treatment abrogated the 2 h mitotic delay caused by expression of the GRASP domain or PDZ1. In contrast, disruption of the Golgi structure by BFA treatment did not affect mitotic entry of cells expressing GFP or wild type GRASP65-GFP. This result indicated that the cell cycle delay caused by expression of non-regulatable GRASP65 mutants was through inhibition of Golgi disassembly at the onset of mitosis.

Next, we examined the growth of cells that express non-regulatable GRASP65 mutants. Equal numbers of cells were plated into 24-well plates. After two days of doxycycline induction to express the exogenous proteins, the number of cells was measured over time using crystal violet, a DNA-binding dye. As shown in Figure 2.7C, the increase of the cell number was reduced in cells expressing the mG mutant, the GRASP domain or PDZ1 compared to those expressing GFP or GRASP65 wild type protein at all time points examined. The effect was most significant on day 3, with $p < 0.01$ when comparing cells expressing mG, the GRASP domain or PDZ1 with those expressing GFP (Figure 2.7C). It became less significant on day 4, possibly because the cells were confluent on the dish. The effect was observed only when the exogenous proteins were induced, but not in the absence of doxycycline. These results suggest that inhibition of mitotic Golgi disassembly delays cell cycle progression and slows down cell growth. To summarize, our study demonstrate that oligomerization of GRASP65 through its N-terminal 112 amino acids is essential for Golgi stacking in tissue culture cells, and inhibition of mitotic Golgi disassembly by expressing GRASP65 mutants delays cell cycle progression.

Discussion

In this study we have examined the role of GRASP65 in Golgi stacking using a combination of biochemical approaches, an inducible expression system, the siRNA technique and systematic EM analysis. We first showed that its first PDZ domain oligomerizes with itself, which is sufficient to hold surfaces together. Our results further demonstrated that expression of non-regulatable GRASP65 mutants enhances Golgi stacking and inhibits Golgi fragmentation in mitotic cells. GRASP65 is required for full stacking as GRASP65-depletion reduces the number of cisternae in the stack; this effect can be rescued by expression of exogenous GRASP65. Furthermore, using non-regulatable GRASP65 as a tool, we showed that inhibition of Golgi fragmentation at the onset of mitosis does not significantly affect the accuracy of Golgi inheritance, but it delays mitotic entry and slows down cell growth, supporting a model in which Golgi fragmentation is needed for proper cell cycle progression. Our results revealed the mechanism for GRASP65 as a Golgi stacking factor, which holds the adjacent cisternal membranes by forming *trans*-oligomers through the N-terminal PDZ1 domain. Although GRASP65 does not seem to play a direct role in cell cycle control, physical disruption of the Golgi is required for mitotic entry.

GRASP65 has multiple functions that are possibly carried out by different domains. The first PDZ domain interacts with itself and plays a significant role in Golgi stacking. The second PDZ domain interacts with GM130, a protein that plays a role in protein trafficking [98-101]. Therefore, GRASP65 may also coordinate with GM130 through the second PDZ domain and function in membrane trafficking [102]. The C-terminal SPR-domain contains all the phosphorylations sites and thus is important for mitotic regulation of GRASP65 oligomerization and Golgi disassembly [18]. In addition, different phosphorylation sites may be regulated by

different pathway. Mutants that affect one function but not the others may serve as useful tools to further dissect the functions of the GRASP65 as well as the biological significance of Golgi stacking in mammalian cells.

One interesting observation concerns PDZ1 targeting to the Golgi membranes. GRASP65 is myristoylated, which serves as the anchor to the Golgi membranes. Deletion of this myristoylation site by mutating the N-terminal glycine to alanine (G2A) led to the loss of Golgi membrane targeting and thus the protein became cytosolic [18, 103]. GRASP65 function requires correct Golgi localization, as the G2A mutant of the protein did not exhibit significant effect on Golgi stacking in our study [18]. GRASP65 and GM130 form a stable complex, which is directly targeted to the Golgi membranes right after their biosynthesis. It was originally proposed that GRASP65 targets GM130 to the Golgi membranes, as it contains a membrane anchor [103, 104]. However, GM130 is found on the Golgi membranes in GRASP65-depleted cells (Figure 2.5), consistent with a previous observation [49]. Furthermore, PDZ1 (aa1-112, tagged with GFP), which lacks the GM130 binding site, was largely concentrated on the Golgi (Figure 2.2E). Interestingly, the Golgi localization of PDZ1 did not depend on (the oligomerization with) the endogenous GRASP65, as it was found enriched on the Golgi membranes in cells in which the endogenous GRASP65 was depleted (Figure 2.5G). In general, one myristoylation modification may not be sufficient to target the protein to certain membranes. However, as GRAS65 forms oligomers, multiple myristic acid moieties on the protein complex may be sufficient for Golgi membrane localization. In this case, the interaction with GM130 may enhance and specify the Golgi targeting of GRASP65, but may not be absolutely required for its Golgi localization.

Another interesting observation concerns the different effects caused by expression of GRASP65 wild type protein versus its non-regulatable mutants. Expressing the non-regulatable GRASP65 mutants enhanced Golgi stacking during interphase and inhibited Golgi fragmentation during mitosis, while expression of wild type GRASP65 had little, if any, effect. These results suggest that GRASP65 may be regulated during both mitosis and interphase, consistent with the report that GRASP65 is phosphorylated by the MAP kinase ERK on S277 when the Golgi structure is remodeled for cell migration in a wound healing assay [21]. From an evolutionary point of view, it is not known what controls the number of cisternae in each stack. For example, the budding yeast *Saccharomyces cerevisiae* has a GRASP65 homolog but lacks stacked Golgi under normal conditions; while in mammalian cells, the number of cisternae per stack is highly conserved in different cell types, at least in the cell lines and tissues that we have examined. In this study, the number of cisternae per stack (7.1 ± 0.2) in cells expressing the non-phosphorylatable GRASP65 was significantly increased compared to that of 5.6 ± 0.1 in control cells expressing GFP (Figure 2.2K), while depletion of the endogenous GRASP65 reduced the number to 4.0 ± 0.1, suggesting that studies on GRASP65 and its homolog protein, GRASP55 [16], may shed light on the molecular control of the cisterna number in the Golgi stacks. Future EM analysis will determine the identity of the additional cisternae in cells expressing GRASP65 mutants and the lost cisternae in GRASP65-depleted cells.

Although GRASP65 was originally discovered as a Golgi stacking factor and many studies support this idea, it has also been shown that GRASP65 depletion in HeLa cells led to Golgi ribbon unlinking [49]. However, as knockdown of GRASP65 affects the integrity of the Golgi

stacks, it is possible that Golgi ribbon unlinking in GRASP65-depleted cells was caused, at least in part, by disassembly of the Golgi stacks. In all the conditions examined in this study, we observed by both light and electron microscopy that the Golgi membranes were concentrated in the perinuclear region and thus we were unable to obtain evidence that GRASP65-depletion leads to scattered Golgi as previously reported [49], even though the number of cisternae in the stacks was reduced (Figure 2.5), which is consistent with a different report [15]. In addition, the observed phenotype was rescued by expression of rat GRASP65, which validated the specificity of the effect. A recent report showed that GRASP65, when targeted to the outer membrane of the mitochondria, caused mitochondria clustering [85]. This result was used to support the role of GRASP65 in Golgi ribbon formation. However, it can also be interpreted as evidence for Golgi stacking, since it indicates oligomerization of the protein. In general, a protein involved in Golgi ribbon linking should localize (and possibly concentrate) on the Golgi rims where Golgi ribbon linking occurs, as suggested by the Golgi ribbon linking protein GMAP210 [61]. However, GRASP65 was discovered as a Golgi membrane protein that is accessible to the alkylating reagent, NEM, only when the Golgi membranes were disassembled by mitotic cytosol [13], suggesting that the protein is not concentrated on the rims of the Golgi cisternae. Instead, immuno-EM showed that GRASP65 is distributed on the body of the Golgi cisternae [12]. Therefore it is more likely that GRASP65 is primarily involved in Golgi stacking. Indeed, results from the expression and knockdown experiments in this study provided strong evidence that GRASP65 is directly involved in Golgi stacking. Whether GRASP65 plays a direct role in Golgi ribbon linking requires further investigation.

Golgi disassembly is related to cell cycle progression, as inhibition of Golgi fragmentation at the onset of mitosis delays mitotic entry [46, 53, 90]. So far it is unclear what role GRASP65 plays in cell cycle control, nor the biological significance of mitotic Golgi disassembly. It has been suggested that Golgi dispersal during mitosis may aid in equal partitioning of Golgi into the new daughter cells [10]. In our study, the inhibition of Golgi fragmentation during mitosis by expression of the non-regulatable mutants of GRASP65 did not lead to an unequal distribution of the Golgi membranes (Figure 2.6), suggesting that extensive Golgi fragmentation may not be required for accurate Golgi inheritance.

An alternative possible role for mitotic Golgi disassembly is to allow the separation of the duplicated centrosomes for mitotic spindle formation, as an intact Golgi complex may physically block centrosome separation during prometaphase. Consistent with this speculation, our results showed that inhibition of Golgi fragmentation by expression of non-regulatable GRASP65 mutants delayed mitotic entry, while disruption of the Golgi by BFA treatment diminished this effect. Previous studies demonstrated that microinjecting recombinant GRASP65 or its antibodies, or expressing its C-terminal fragment, caused a delay in mitotic entry [90, 91], possibly through modulation of the related mitotic kinases [19]. In contrast to the previous studies, expression of Golgi-localized non-regulatable GRASP65 does not affect mitotic kinase expression or subcellular localization, since these constructs are not substrates of the mitotic kinases. Therefore, our results suggest that the observed mitotic delay may occur through inhibition of mitotic Golgi disassembly, which is generally regulated through GRASP65 phosphorylation and de-oligomerization. Furthermore, the mitotic index of cells expressing non-regulatable mutants of GRASP65 exhibited broader peaks. This may be because there are more

mitotic cells when the mutants were expressed, or these cells require a longer period to complete mitosis. In the latter case, an extended time period required for complete Golgi disassembly may contribute largely to the delay in cell cycle progression. Alternatively, the cells may need a longer time period to equally distribute the mitotic clusters (than completely disassembled Golgi vesicles) into the two daughter cells. In summary, our results demonstrate that GRASP65 stacks Golgi cisternae by oligomerization through its N-terminal PDZ1 domain. The disassembly of GRASP65 *trans*-oligomers caused by phosphorylation is essential for Golgi unstacking and fragmentation, which in turn regulates the cell cycle progression and cell growth. Future directions include determination of the effects caused by the expression of GRASP65 with single point mutation of the phosphorylation sites (e.g. S277), the dynamic of mitotic Golgi disassembly and post-mitotic Golgi reassembly in cells expressing GRASP65 mutants, the signaling pathways that regulate Golgi membrane dynamics during the cell cycle, and especially the effect of Golgi stacking/unstacking on protein trafficking, modifications and secretion.

Materials and Methods

Reagents

All reagents were from Sigma Co., Roche or Calbiochem, unless otherwise stated. The following antibodies were used: monoclonal antibodies against Gos28 and GM130 (Transduction Laboratories), and α-tubulin (K. Gull); polyclonal antibodies against green fluorescence protein (GFP, J. Seemann), GM130 (N73, J. Seemann), human GRASP65 (J. Seemann), rat GRASP65 [18], and human GRASP55 (Proteintech Group, Inc.).

Preparation of GRASP65 fusion proteins

GRASP65 cDNAs [13, 14, 18] were cloned into pMAL-c2X (New England Biolabs), pGEX (GE Healthcare), or pET30a (Novagen) vectors by PCR or restriction digestion and confirmed by DNA sequencing. GRASP65 point mutations were introduced using the QuikChange mutagenesis kit (Stratagene) and confirmed by DNA sequencing. Proteins were expressed in BL21-CodonPlus(DE3)RILP bacteria and purified on amylose (New England Biolabs), nickel (Qiagen), or glutathione-Sepharose (GE Healthcare) beads.

GRASP65 dimerization and oligomerization

To test the oligomerization of GRASP65 fragments, separately expressed and purified MBP-tagged or GST-tagged GRASP65 fragments were mixed and incubated in the presence of an ATP-regenerating system (10 mM creatine phosphate, 0.1 mM ATP, 20 μg/ml creatine kinase, 20 μg/ml cytochalasin B) at 37 ºC for 1 h. The protein complex was isolated using glutathione or amylose beads and analyzed by Western blotting.

For sedimentation analysis, purified MBP tagged PDZ1 (120 μg) was incubated at 37ºC for 1 h in gradient buffer (25 mM Hepes-KOH, pH7.4, 150 mM KCl, 5 mM $MgCl_2$, 1 mM DTT) in a final volume of 150 μl. Top-loaded glycerol gradients (10-35% w/v) were centrifuged for 4 h at 55,000 rpm (260,000 g) in a VTI65.1 rotor and portions of the 1 ml fractions were analyzed by Western blotting.

For non-denaturing electrophoresis, purified GST-tagged PDZ1 or PDZ2 domain was incubated with KHM buffer (20 mM Hepes-KOH, pH 7.4, 0.2 M sucrose, 60 mM KCl, 5 mM Mg(OAc)2, 2 mM ATP, 1 mM GTP, 1 mM glutathione with protease inhibitors) at 37ºC for 1 h, mixed with non-denaturing sample buffer and loaded onto a 4-12% NuPAGE Novex Bis-Tris mini gel (Invitrogen) [16, 105]. After electrophoresis, the gel was stained with Coomassie Blue. Major bands were excised from the gel and further analyzed by denaturing electrophoresis and Western blotting.

For gel filtration, His-tagged PDZ1 was incubated with an ATP regeneration system at 37ºC with KHM buffer for 1 h and analyzed by a Sephacryl-S300 column. 2 ml fractions were collected at a flow rate of 0.5 ml/min. Proteins in the peak fractions were confirmed by Western blotting.

Bead aggregation assay was performed as previously described [14, 18]. Briefly, His-tagged recombinant GRASP65 full-length and PDZ1 were subjected to centrifugation at 15,000 rpm for 30 min in a tabletop centrifuge at 4ºC. The proteins in the supernatant were then cross-linked to M500 magnetic beads (Dynal Biotech). The beads were incubated for 60 min at 37˚C

with either bovine serum albumin (BSA), or interphase cytosol prepared from HeLa S3 cells [14], in KHM buffer to allow the aggregation. In some experiments, an excess amount (0.5 μg/μl) of purified His-PDZ1 was included in the reaction. For quantitation of the beads, 15 random phase contrast digital images of each reaction were captured with a 20x lens and a Spot Slider2 Camera (Diagnostic Instruments). Images were analyzed with the MATLAB7.4 software to determine the surface area of objects, which was used to calculate the number of beads in the clusters. Aggregates were defined as those with ≥ 6 beads. For large aggregates, only visible surface beads were counted; therefore, the number of beads in these aggregates was underestimated. Results were expressed as the mean ± SEM from 3 independent experiments; statistical significance was assessed by Student's t-test.

Cell culture, siRNA, and establishment of stable cell lines

HeLa cells were transfected with Stealth siRNA oligos (Invitrogen) prepared according to the reported sequence for human GRASP65 (5'-CCTGAAGGCACTACTGAAAGCCAAT-3') [15] using lipofectamine RNAiMAX (Invitrogen) following the manufacturer's instructions. Control non-specific siRNA oligos were purchased from Ambion. Assays were performed 96 h after transfection. The knockdown efficiency of endogenous GRASP65 was analyzed using the ImageJ software from Western blotting results and normalized with tubulin as a loading control.

To establish stable cell lines, rtTAm2 HeLa cells were infected with retroviral particles encoding indicated exogenous genes cloned in the pRevTRE2 vector. Wild type rat GRASP65, the mG mutant in which seven phosphorylation sites were mutated to alanines (S216A/S217A/T220A/T224A/S277A/S367A/S376A) [18] and the GRASP domain (aa1-201)

were first cloned into pEGFP-N2 vector via the EcoRI and ApaI sites. GFP (enhanced green fluorescent protein), GRASP65-GFP, GRASP65 mG-GFP and GRASP domain-GFP cDNA were then excised by HindIII and NotI and re-ligated into the pRevTRE2 vector. For GRASP65 PDZ1 (aa1-112)-GFP, GFP cDNA was first cloned into the pRevTRE2 vector through the HindIII and NotI sites. The PDZ1 coding sequence was inserted in frame into the BamHI and HindIII sites at the N-terminus of GFP. Procedures for viral preparation, infection and cell selection were previously described [93]. GFP positive cells were enriched by flow cytometry. The expression of exogenous proteins was induced with 1 μg/ml doxycycline for 72 h. For the gene replacement experiment, GRASP65- or GFP-cell lines were transfected with GRASP65 siRNA for 24 h followed by induction with doxycycline for 72 h.

Microscopy and quantitation

Immunofluorescence microscopy and collection of mitotic cells were previously reported [28]. Pictures were taken with a Leica SP5 confocal laser-scanning microscope using a 100x oil lens. For metaphase cells, images were captured using fixed parameters with 0.3 μm intervals at the Z-axis and then processed for maximum-value projection. Images were analyzed using the NIH ImageJ software, and a threshold was introduced to exclude cytoplasmic staining and the Golgi haze [34]. All pixels above this threshold value were counted as Golgi remnants and summed up as the fluorescence intensity in Golgi clusters. The percentage of fluorescence intensity in Golgi clusters was calculated versus total fluorescence intensity in the cell above background. Cells in cytokinesis were defined as two daughter cells linked with a thin connection (contractile ring); chromosomes are concentrated in the center of each daughter cell although the DNA may not de-condensed; the Golgi has started to reform but the process has not

completed. Fluorescence intensity for indicated Golgi proteins in each daughter cell (above the background of the image) was measured; the percentage of the Golgi membrane inherited by one daughter cell was calculated against the total fluorescence intensity of the cell pair. More than 10 cells or cell pairs were quantified for each cell line in each experiment. The average (mean ± SEM) percentage of fluorescence intensity in the daughter cells with relative lower fluorescence level compared to their pairs was calculated and presented in Figure 2.6F.

For EM analysis, Golgi stacks and clusters were identified using morphological criteria and quantified using standard stereological techniques [18]. For interphase cells, the profiles had to contain a nuclear profile with an intact nuclear envelope; only the obvious stacked structures with 3 or more cisternae were counted. For mitotic cells, the profile had to contain one or more profiles of condensed chromosomes and lack a nuclear envelope; very often multiple condensed chromosomes were aligned in the center of the cell. A low magnification (normally 1600x) image and serial images of higher magnification (normally 11,000x) were taken to cover the entire cell. About 20 cells were quantified. To quantify the cisternae number in each mitotic Golgi cluster, a cisterna was defined as a membrane-bound structure in the Golgi cluster whose length is at least 4 times its width, normally 20-30 nm in width and longer than 150 nm [106].

Mitotic index and growth rate analysis

The mitotic index analysis of cells after double thymidine block and release was performed as previously described [46]. Briefly, cells of about 40% confluence were incubated in growth medium with 2 mM thymidine for 24 h, then washed with phosphate-buffered saline (PBS) and incubated with growth medium for 14 h. Cells were then maintained in growth medium with

thymidine for an additional 20 h before the final release. At different time points after release, cells were assayed for mitotic index by tallying the number of cells displaying clear mitotic (rounded perimeter, discernible mitotic plate) and interphase characteristics using an inverted microscope and a 20x phase contrast objective [46]. About 300 cells were counted at each time point within 5 min. For the stable cell lines, 1 μg/ml doxycycline was added at the starting time of the first thymidine block. In some experiments, 5 μg/ml Brefeldin A (BFA) from a 5 mg/ml stock, or an equal volume of ethanol, was added 4 h after the final thymidine release to disperse the Golgi structure. The experiment was repeated at least 3 times and the results were expressed as the mean ± SEM.

To analyze the growth rate of the stable cell lines, 5,000 cells were added into each well of 24-well plates and incubated in growth medium with 1 μg/ml doxycycline to induce the expression of the exogenous proteins. Two days later, cell numbers were measured every 24 h for 4 days by crystal violet staining [107]. Briefly, cells were washed with pre-warmed PBS, fixed in 4% formaldehyde for 30 min and stained with 0.5% crystal violet (in 30% methanol) for 15 min. After extensively washing with H_2O, DNA bound dye was extracted with 1 ml 10% acetic acid and measured for OD at 590 nm. The cell numbers at different days were normalized to the cell number from the first measurement. The results were shown as the mean ± SEM, n = 3.

Acknoledgement

We thank Joachim Seemann and Graham Warren for antibodies and cDNA constructs, Blanche Schwappach for the retroviral vector and the rtTA HeLa cell line, Hana Popelkova for technical help with gel filtration, Majan Varedi and Xiaoxia Lin for developing the Matlab program to quantify beads in aggregates, Yi Xiang and other members of the Wang Lab for suggestions and reagents.

This work was supported by the Pardee Cancer Research Foundation, the National Institute of Health (GM087364), American Cancer Society (RGS-09-278-01-CSM), a University of Michigan Rackham Faculty Research Grant, the NIH-funded Michigan Alzheimer's Disease Research Center (P50 AG08761) and an anonymous donation to Y. Wang. The authors declare no conflicts of interest.

Abbreviations

BSA, bovine serum albumin; GFP, enhanced green fluorescent protein; EM, electron microscopy; GRASP65, Golgi reassembly stacking protein of 65 kDa; IC, interphase cytosol; NEM, N-ethylmaleimide; NRK, normal rat kidney cells; PBS, phosphate-buffered saline; plk, polo-like kinase; siRNA, small interference RNA.

Chapter 3 . Sequential phosphorylation of GRASP65 orchestrates mitotic Golgi disassembly

Abstract

GRASP65 phosphorylation during mitosis and dephosphorylation after mitosis are required for Golgi disassembly and reassembly during the cell cycle. At least eight phosphorylation sites on GRASP65 have been identified, but whether they are modified in a coordinated fashion during mitosis is so far unknown. In this study, we raised phospho-specific antibodies that recognize phosphorylated T220/T224, S277 and S376 residues of GRASP65, respectively. Biochemical analysis showed that cdc2 phosphorylates all the three sites, while plk1 enhances the phosphorylation. Microscopic studies using these antibodies for double and triple labeling demonstrate sequential phosphorylation and dephosphorylation during the cell cycle. S277 and S376 are phosphorylated from late G2 phase through metaphase until telophase when the new Golgi is reassembled. T220/224 is not modified until prophase, but is highly modified from prometaphase to anaphase. In metaphase, phospho-T220/224 signal localizes on both Golgi haze and mitotic Golgi clusters that represent dispersed Golgi vesicles and Golgi remnants, respectively; while phospho-S277 and S376 labeling is more concentrated on mitotic Golgi clusters. Expression of a phosphorylation-resistant GRASP65 mutant T220A/T224A inhibited mitotic Golgi fragmentation to a much larger extent than the expression of the S277A and S376A mutants. In cytokinesis, T220/224 dephosphorylation occurs prior to that of S277, but after S376.

This study provides evidence that GRASP65 is sequentially phosphorylated and dephosphorylated during mitosis at different sites to orchestrate Golgi disassembly and reassembly during cell division with phosphorylation of the T220/224 site being most critical in the process.

Introduction

In mammalian cells, the Golgi apparatus consists of over a hundred stacks of parallel-aligned membrane cisternae, which are further laterally linked to form a Golgi ribbon [83]. This complex structure undergoes dramatic morphological changes during the cell cycle. In early mitosis, the Golgi is disassembled into vesicles that can be observed as Golgi haze, and into tubulovesicular structures that are seen as mitotic Golgi clusters observed by fluorescence microscopy. In telophase, these fragments are evenly distributed into the two daughter cells where they are reassembled into a new Golgi apparatus each. The exact details of how the Golgi structure is maintained and how their assembly and disassembly is orchestrated are not well understood. One key element is a protein network called the "Golgi matrix" [108], which is comprised of golgins, GRASP proteins and other Golgi structural proteins. The two GRASP proteins, GRASP65 and GRASP55, were first identified as Golgi stacking factors in an *in vitro* system that reconstitutes mitotic Golgi disassembly and post-mitotic Golgi reassembly [12, 13]. Later research demonstrated that these proteins are involved in additional functions, including Golgi ribbon linking, cell cycle progression, trafficking, and unconventional secretion [15, 49-51, 89, 102, 109-111].

At the molecular level, it has been shown that each GRASP protein forms *trans*-oligomers through the PDZ domains at each respective N-terminus. This oligomerization possibly mediates tethering of the cisternae into stacks as well as linking of Golgi stacks into a ribbon [14, 16, 18, 49, 85, 112]. Whether the oligomerization of the GRASP proteins is also helping to regulate protein trafficking and unconventional secretion remains unknown. Oligomerization of the GRASP proteins is believed to be regulated by phosphorylation [4, 22]. GRASP65 is known to

be the major target of mitotic kinases on the Golgi membranes [14]. The protein is phosphorylated by cdc2 (also called cdk1) and polo-like kinase 1 (plk1) during mitosis [7, 19, 113, 114]. GRASP55, on the other hand, is phosphorylated by the MAP kinase ERK2 [16, 115]. Phosphorylation of GRASP65 and GRASP55 causes their de-oligomerization and thus disrupts Golgi cisternal stacking and Golgi ribbon linking [14, 16, 22, 51]. This subsequently allows Golgi membrane vesiculation that yields a large number of vesicles dispersed throughout the cell.

At the end of mitosis, GRASP65 is dephosphorylated by the protein phosphatase PP2A, which leads to the reformation of GRASP65 *trans*-oligomers [7]. Golgi fragments then fuse in a coordinated fashion to form new cisternae, which are subsequently tethered into stacks and ultimately the Golgi ribbon [4, 9, 22]. It has been shown that the expression of a phospho-deficient GRASP65 mutant (mG), in which 5 serine residues (S216, S217, S277, S367 and S376) and 2 threonine moieties (T220 and T224) were mutated to alanines, inhibited Golgi fragmentation during mitosis in the cell [17]. This strongly suggests that GRASP65 phosphorylation plays an important role in regulating Golgi architecture throughout cell division. GRASP65 can also be phosphorylated on residue S277 in interphase cells, particularly upon growth factor stimulation, which mediates the remodeling of the Golgi to facilitate membrane trafficking in migrating cells [21, 91]. Many features of this Golgi remodeling process during interphase are similar to that seen during mitosis, although architectural changes happen to a much lesser degree. Finally, the residue S367 is also found to be phosphorylated during interphase condition in an *in vitro* phosphorylation assay [19]. It is not clear whether activation of this site is, like S277, involved in Golgi remodeling in interphase cells.

One of the previously used phospho-deficient mutant of GRASP65, mG, contains seven known/putative phosphorylation sites [17]. Expression of this mutant inhibited Golgi fragmentation during mitosis, suggesting that the phosphorylation of at least one of these sites is necessary for Golgi disassembly during mitosis. Several lines of evidence suggest that each site may be phosphorylated in a distinct fashion to help carry out different functions. For example, several distinct phospho-peptides were generated when GRASP65 was treated with either cdc2 or plk1 followed by trypsinization and 2D gel analysis [113], indicating that cdc2 and plk1 modify different residues on GRASP65. In another *in vitro* phosphorylation assay using recombinant GRASP65, seven phosphorylation sites were identified by mass spectrometry, Six of the seven sites were also present in the mG mutant; an additional site, S400, was identified. In this analysis four sites were shown to be phosphorylated by cdc2. Modification of GRASP65 by cdc2 recruits plk1 binding and allows plk1 to phosphorylate the protein [19]. Yet another phosphorylation site, S189, was identified as a plk1 target [116]. Its activation disrupts GRASP65 oligomers [117]. Whether the different phosphorylation sites present in GRASP65 are modified simultaneously or sequentially at the onset of mitosis, and whether they are equally important for mitotic Golgi fragmentation, remain poorly understood.

In this study we utilized five GRASP65 phospho-specific antibodies that target three different phosphorylation sites. We show that the three sites are phosphorylated and dephosphorylated sequentially during the process of cell division. In early mitosis, S277 and S376 are phosphorylated in late G2 phase, while phosphorylation of T220/T224 by cdc2 begins in prophase. During mitosis, phosphorylation of T220/T224 is most critical for mitotic Golgi

disassembly, as expression of the T220A/T224A mutant of GRASP65 inhibited mitotic Golgi fragmentation to a much greater extent than that expression of either S277A or S376A mutants. In late mitosis during cytokinesis, S376 is dephosphorylated, prior to T220/T224, while S277 remains phosphorylated even in late cytokinesis. Our study demonstrated that GRASP65 is sequentially phosphorylated and dephosphorylated at different sites during the cell cycle, which allows regulated mitotic Golgi disassembly and reassembly.

Results

Development and characterization of phospho-specific antibodies that recognize various GRASP65 phosphorylation sites in rodent cells

To better understand the role of GRASP65 phosphorylation in mitotic Golgi disassembly, we raised and subsequently characterized phospho-specific antibodies against different phosphorylation sites. We prepared phosphorylated GRASP65 by treatment of recombinant wild type (WT) His-tagged rat GRASP65 full-length protein with mitotic cytosol. In a first approach this phospho-protein was used to immunize mice. One resulting monoclonal mouse antibody, LX108, was found to recognize only phosphorylated GRASP65 but not its non-phosphorylated form. In a second approach we generated three single chain monoclonal phospho-specific antibodies (scFv antibodies), R3G3, R3F2 and RB7 using an *in vitro* approach [94] (Table S1). To determine the precise epitope of each phospho-specific antibody on GRASP65, purified recombinant WT GRASP65 and 10 different phosphorylation-resistant mutants (Figure 3.1A) were incubated with either mitotic (Figure 3.1, B-C) or interphase (Figure 3.1,D-E) cytosol followed by Western blot analysis using these phospho-antibodies. If mutation of a particular site lead to a weakening of the signal of a particular antibody, despite treatment with mitotic cytosol, it was assumed that a conformation created by phosphorylation of the non-mutated site was specifically recognized by the antibody. As shown in Figure 3.1, LX108 recognized GRASP65 only after treatment with mitotic but not interphase cytosol. Among the mutants treated with mitotic cytosol, LX108 recognized phosphorylated mB, mC, mF and mJ mutants, but not mA, mD, mE, mG, mH and mI. Modification of S216/S217 and T220/T224 abolished the signal (mA, mD, mE and mG in Figure 3.1B); while mutation of T220/T224 but not S216/S217 also abrogated it (mH and mI in Figure 3.1C). The only common site that was altered in all mutant

constructs affecting the immunoreactivity of LX108 was T220/T224, strongly suggesting that LX108 specifically recognizes this site after phosphorylation. Using the same approach, we showed that both R3F2 and RB7 scFv antibodies specifically recognize the mitotically phosphorylated S376 epitope [94] while the scFv antibody R3G3 recognizes phospho-S277, which is phosphorylated in both interphase and mitosis, with a weaker signal after interphase cytosol treatment (Figure 3.1), consistent with the previous reports that S277 is phosphorylated during interphase [21, 91].

To determine whether these phospho-specific antibodies recognize GRASP65 in cells, we performed Western blot analysis of HeLa cells stably expressing either wild type (WT) rat GRASP65-GFP, mG-GFP, or simply GFP. A monoclonal antibody, 7E10, which recognizes rat GRASP65 regardless of its phosphorylation state, was used as a control. During interphase, WT GRASP65-GFP (but not the mG mutant) was recognized by R3G3 but not by LX108 or R3F2 (Figure 3.2, A-D). During mitosis, WT GRASP65-GFP was recognized by all three phospho-antibodies (Figure 3.2E). These results suggest that the phospho-antibodies are able to recognize phospho-rat-GRASP65 *in vivo*, and also indicate that those antibodies do not recognize the endogenous human GRASP65 in HeLa cells even after phosphorylation. This was confirmed by immunofluorescence microscopy. Rat GRASP65-GFP was recognized by LX108 in mitotic but not interphase cells (Figure 3.3, A vs. B), validating that LX108 is a phospho-specific antibody for rat GRASP65. LX108 also recognized endogenous GRASP65 in mitotic NRK cells of rat origin (Figure 3.3C & 3.S1). Similar results were reported for R3G3, R3F2 and RB7 [94]. Furthermore, all phospho-specific antibodies, LX108, R3G3, R3F2 (Figure 3.3, D-I) and RB7 (not shown), detected WT but not the mG mutant of rat GRASP65 in mitotic cells.

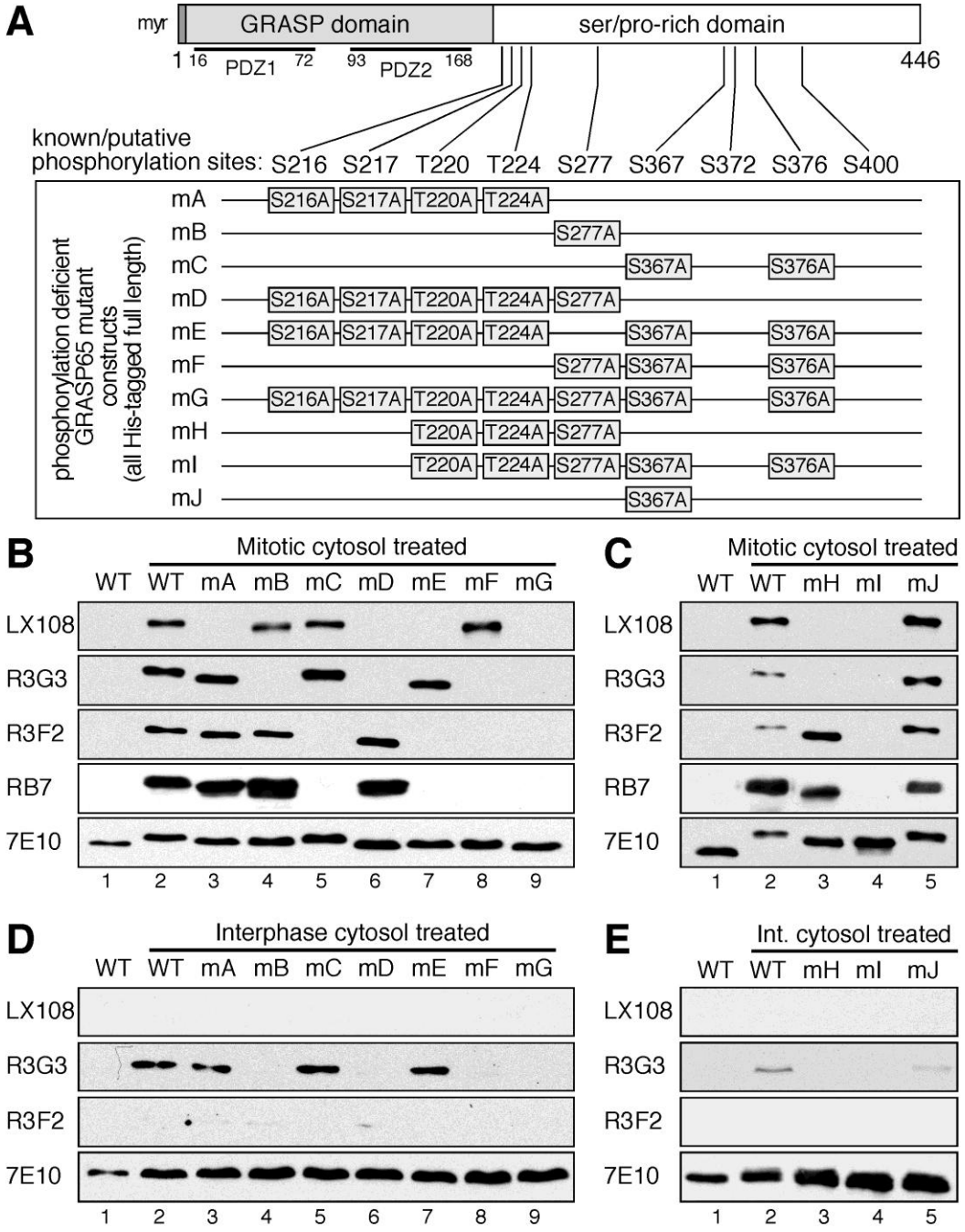

Figure 3.1. Determination of the phosphorylation sites on GRASP65 that the phospho-specific antibodies recognize.

(A) Schematic illustration of known and putative phosphorylation sites on GRASP65 and its mutants in which indicated phosphorylation sites were mutated to alanines. **(B-E)** Purified His-tagged full-length wild type GRASP65 or its phosphorylation deficient mutants were incubated with either buffer alone (first lane in each blot) or with cytosol from either mitotic cells (panels B and C), or interphase cells (panels D and E) as indicated. Equal amounts of protein were analyzed by Western blots. Five anti-GRASP65 antibodies (see Table S1) were used, 7E10 being a non-phospho specific anti-GRASP65 antibody. LX108 (a mouse monoclonal antibody) failed to recognize any constructs where T220/T224 is mutated or when proteins were incubated with interphase cytosol. R3G3 (scFv recombinant antibody) did not bind mutants of S277; R3F2 and RB7 (two different scFv antibodies) both fail to bind mutated S376. In each case, loss of signal for a given mutant indicated that at least one of the mutated phospho-

residues must be phosphorylated in the wild type protein for antibody binding. Thus LX108 recognizes phosphorylated T220/T224, R3G3 specifically binds pS277, while R3F2 and RB7 bind pS376.

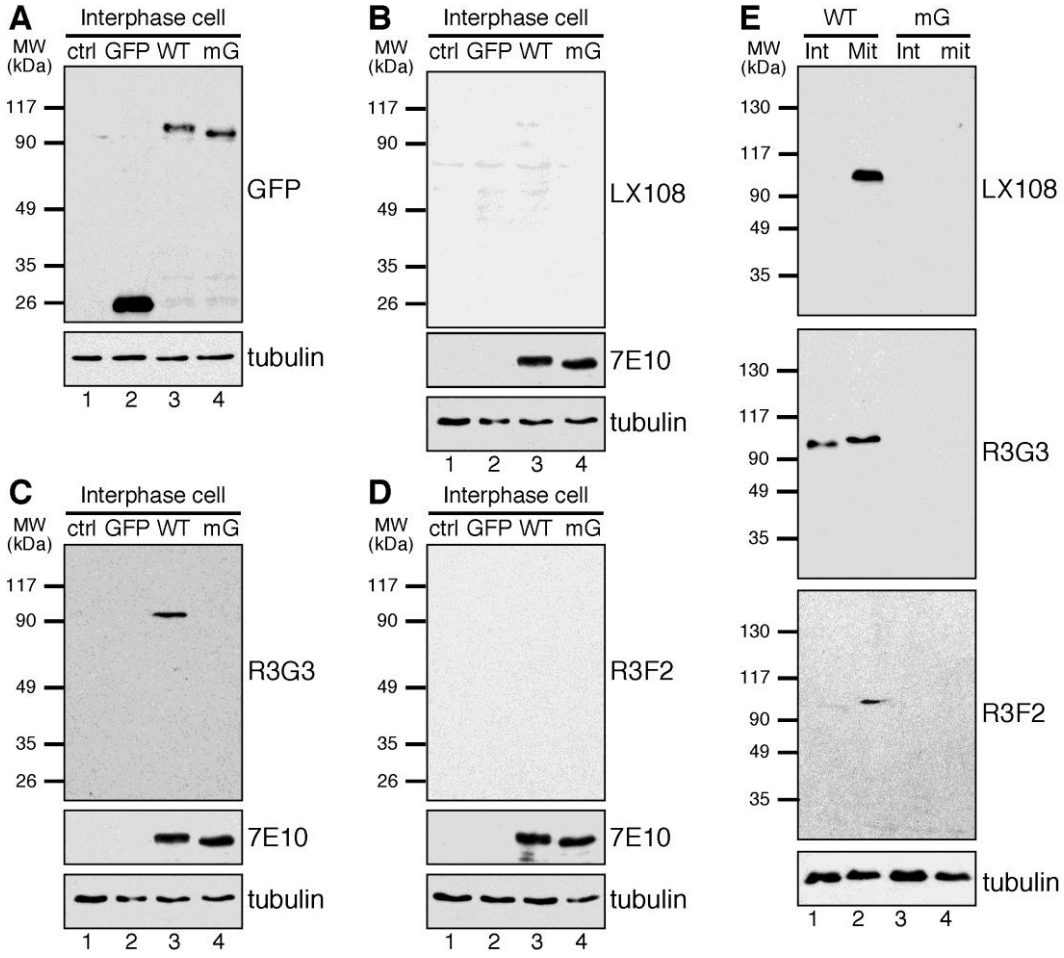

Figure 3.2. LX108, R3G3 and R3F2 recognize mitotically phosphorylated GRASP65 in cell lysate by Western blot.

(A-D) HeLa cells (lane 1 in each blot), or HeLa cells stably expressing GFP, GFP-tagged rat wild type (WT) GRASP65, or the mG mutant with all 7 phosphorylation sites mutated to alanines (see Figure 3.1A for details) (lanes 2-4 in each blot) were analyzed by Western blot using the indicated antibodies. Only S277 (detected by R3G3) is phosphorylated in interphase cells but at a relatively lower level than in mitosis (C). **(E)** Non synchronized interphase (Int) or nocodazole-blocked, synchronized mitotic (Mit) HeLa cells expressing WT or mG GRASP65-GFP were analyzed by Western blot, LX108 and R3F2 were able to detect the phospho-protein in WT transfected synchronized cells (lane 2 each blot).

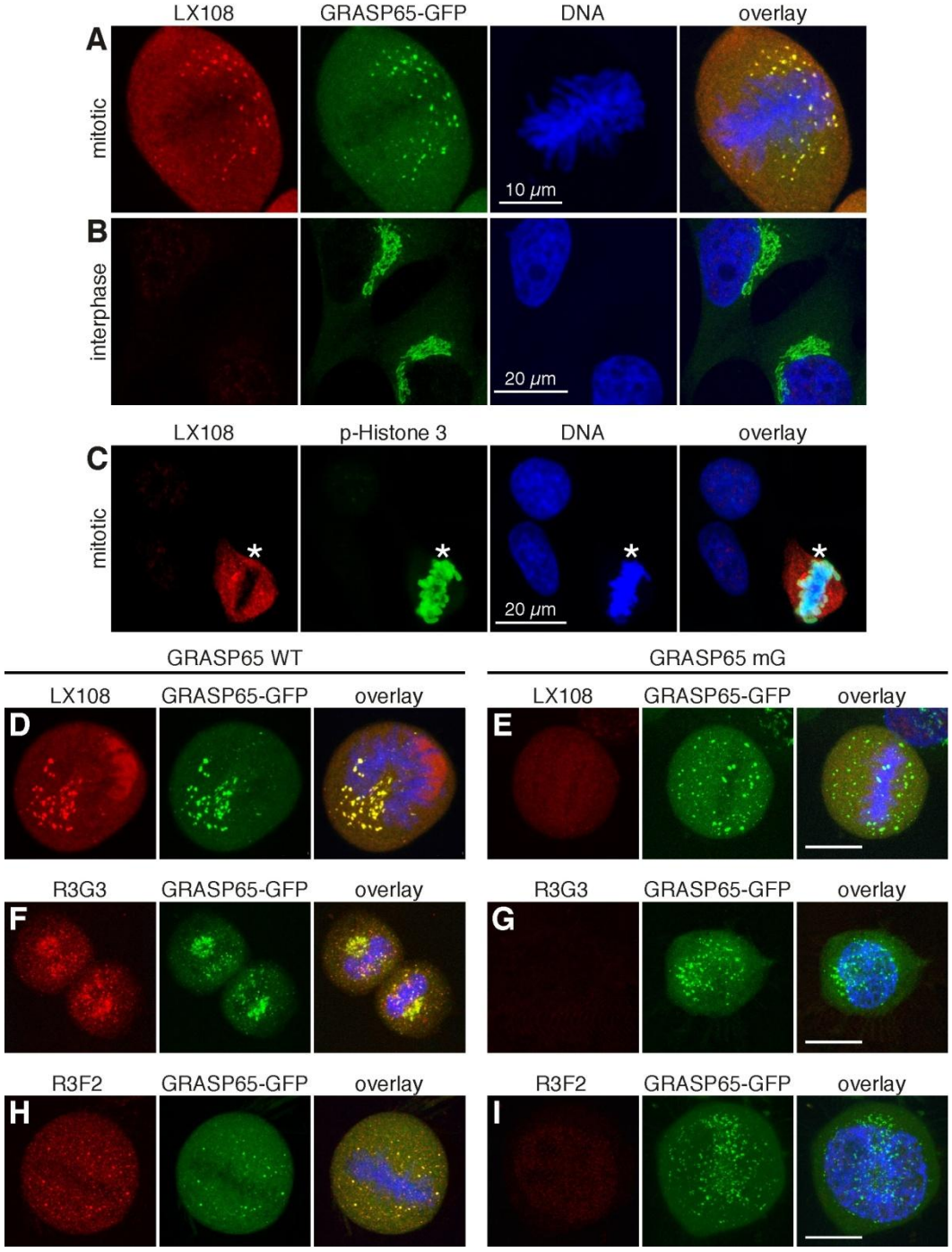

Figure 3.3. The phospho-specific antibodies LX108, R3G3, R3F2 and RB7 recognize WT GRASP65 but not its phosphorylation deficient mG mutant in mitotic cells.
(A-B) Mitotic (prometaphase, A) or interphase (B) HeLa cells stably expressing WT GRASP65-GFP were stained by LX108 (red), GFP (green), and DNA (blue). Note the LX108 signal in mitotic but not interphase cells. **(C)** Rat origin NRK cells were stained by LX108 (red), phospho-Histone H3 (p-Histone H3, green) and DNA (blue). Asterisks indicate mitotic cells. **(D-I)** Immunofluorescence images of mitotic HeLa cells expressing WT GRASP65-GFP (D, F, and H) or its phosphorylation mutant mG (E, G, and I) were stained with LX108 (T220/T224, D-E), R3G3 (S277, F-G), or R3F2 (S376, H-I) antibodies. GFP epifluorescence is shown in green. Scale bar, 10 μm.

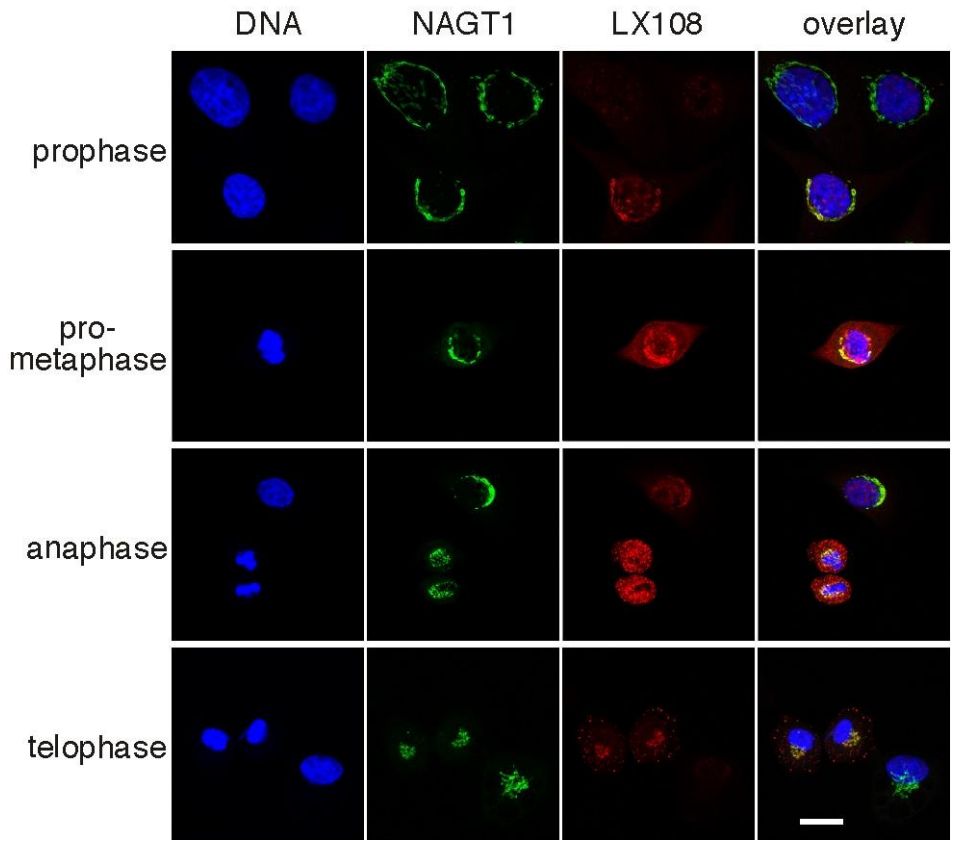

Figure 3.S1. The monoclonal antibody LX108 recognizes the endogenous GRASP65 in mitotic NRK cells. Normal rat kidney (NRK) cells stably expressing N-acetylglucosamine transferase I (NAGT1) of indicated cell cycle phases were immunostained with LX108 and Hoechst (DNA). Scale bar in all panels, 10 μm.

The T220/T224 site is phosphorylated by cdc2

Previous work has shown that GRASP65 is phosphorylated by cdc2 and plk1 during mitosis and by the MAP kinase ERK2 in interphase [19, 91, 113]. To identify the kinase(s) responsible for phosphorylation of GRASP65 at different sites of the protein, we treated purified rat liver Golgi membranes with mitotic cytosol, or with recombinant cdc2, plk1 or a combination of both kinases at various concentrations (Figure 3.4A-B). Phosphorylation of GRASP65 was then analyzed by Western blot using LX108 and 7E10. 7E10 recognizes GRASP65 regardless of its phosphorylation, though phospho-GRASP65 can be detected by a mobility shift of the protein. Treatment with cdc2 alone caused GRASP65 phosphorylation as indicated by the band

shift on the 7E10 blot and by the immunoreactivity to LX108. The addition of plk1 increased the phosphorylation state in a dose dependent manner (Figure 3.4B, lanes 3-7 and 9). Incubation with plk1 alone induced slow migration of GRASP65 compared to non-treated GRASP65 on the 7E10 blot; but the shifted band was not recognized by LX108 (Figure 3.4A-B, lane 8). These results suggest that GRASP65 is phosphorylated on T220/T224 by cdc2. Plk1 enhances cdc2 activity on this site; and plk1 may, in addition, phosphorylate other sites on GRASP65.

We next confirmed these results in cells. HeLa cells transfected with a GRASP65-GFP plasmid were synchronized to mitosis by 18 h nocodazole treatment and further treated with different kinase inhibitors. As shown in Figure 3.4C, treatment of the mitotic cells with the general kinase inhibitor staurosporine totally abolished GRASP65 phosphorylation on T220/T224 on the LX108 blot. The cdc2 inhibitor, roscovitine, largely reduced T220/T224 phosphorylation, but the plk1 inhibitor BI2536 and MEK inhibitor U0126 had no detectable effect on inhibition of T220/T224 phosphorylation. This indicates again that T220/T224 is phosphorylated by cdc2 during mitosis.

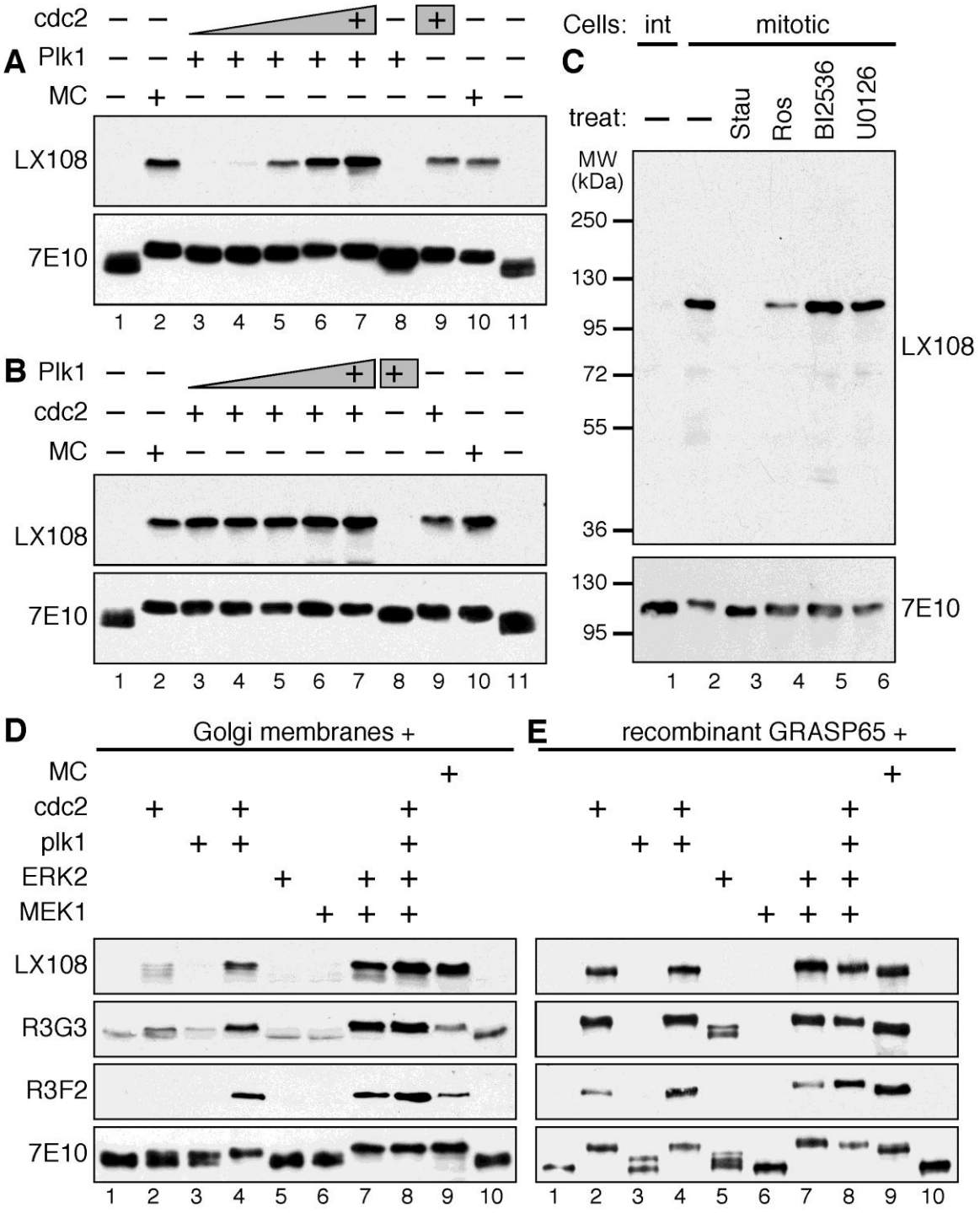

Figure 3.4. The LX108 recognition site, T220/T224, is phosphorylated by cdc2.
(A) Purified rat live Golgi membranes (20 µg each reaction) were incubated with buffer (lanes 1 and 11), 500 µg mitotic cell cytosol (MC, lanes 2 and 10), or 30 µg plk1 (lanes 3-8) in the presence of increasing amount of cdc2 (lanes 3-7, 0.3, 0.9, 3, 9, and 30 µg, respectively; lane 9, 30 µg). Proteins were solubilized in SDS buffer and analyzed by Western blot for GRASP65 using the LX108 and 7E10 antibodies. Note that LX108 immuno-reactivity is detected only when the membranes were treated with MC or cdc2 (in a dose dependent manner), but not with plk1. **(B)** As in A. but with increasing amount of plk1 (lanes 3-8, 0.3, 0.9, 3, 9, 30, and 30 µg, respectively) and 30

μg cdc2 (lanes 3-7, 9). Note that plk1 alone does not cause GRASP65 phosphorylation, but adding plk1 increases cdc2 activity towards GRASP65 (lanes 3-7 vs. 8).
Interphase (int) or mitotic (mit) HeLa cells stably expressing WT GRASP65-GFP were treated with staurosporine (Stau, a general kinase inhibitor), Roscovitine (Ros, a cdk-specific inhibitor), BI2536 (a plk1 inhibitor) or U0126 (a MAPK inhibitor), lysed and analyzed by Western blot for indicated antibodies. Binding is abolished with the general kinas inhibitor (Stau) and reduced with the cdk-specific inhibitor (Ros). **(D-E)** Purified rat liver Golgi membranes (D) or recombinant wild type His-GRASP65 full length protein (E) were treated with indicated combinations of kinases and analyzed by Western blot for GRASP65 using the indicated antibodies. 20 μg Golgi membranes or 50 ng recombinant GRASP65 per lane were loaded and Western blot performed using LX108, R3G3 and R3F2; while 5 μg/lane Golgi membranes or 10 ng/lane recombinant His-GRASP65 was used when 7E10 was used for Western blot. Note that cdc2 phosphorylated all three sites during mitosis, while plk1 enhances the activity.

To determine the enzymes that phosphorylate residues S277 and S376, we treated purified Golgi membranes or recombinant GRASP65 with different combinations of kinases, as indicated in Figure 3.4D-E. When analyzing Golgi membranes, cdc2 alone phosphorylated both T220/T224 and S277, as indicated by LX108 and R3G3 signals, correspondingly, though only at a relatively low level (Figure 3.4D, lane 2). However, a combination of cdc2 and plk1 phosphorylated all three sites to a much larger degree than either enzyme alone (Figure 3.4D, lane 4), suggesting that plk1 enhances GRASP65 phosphorylation on Golgi membranes. The S277 site was phosphorylated by ERK2 at a low level (Figure 3.4D, lane 5). Adding active MEK1, an activator of ERK2, significantly enhanced S277 phosphorylation. Strong activation of ERK2 also led to phosphorylation of all other sites (Figure 3.4D, lane 7). When purified recombinant GRASP65 protein was used in the phosphorylation assay, T220/224, S277 and S376 were all phosphorylated by cdc2 but not plk1, although a combination of both kinases increased the phosphorylation level (Figure 3.4E, lane 2-4). S277 was phosphorylated by ERK2, and the activity was enhanced by adding constitutively active MEK1 (Figure 3.4E, lane 5 vs. 7). A combination of MEK1 with ERK2 could phosphorylate all the three sites. However, since ERK2 is relatively low during mitosis [118], these results may only be found *in vitro* with high

level of ERK2 activity. In conclusion, cdc2 can phosphorylate all three sites during mitosis, while plk1 enhances the activity of cdc2.

The phosphorylation cycle of each site on GRASP65 during cell division

To analyze at what point each site on GRASP65 is phosphorylated and dephosphorylated during the cell cycle, we next examined NRK cells progressing through mitosis using immunofluorescence microscopy. Cells were co-stained with one of the GRASP65 phospho-specific antibodies (LX108, R3G3 or R3F2), with an antibody to phospho-Histone H3 (p-Histone H3), and for DNA to clearly identify the cell cycle phases. Histone H3 phosphorylation, which starts late in G2 phase and remains present until anaphase, was nicely visualized with p-Histone H3 (see Figure 3.5). All three phospho-specific GRASP65 antibodies stained the Golgi at some point during mitosis, but the exact timing of appearance of the signal was different for each of them. The LX108 (T220/T224) signal started to appear in prophase, when the Golgi fragmentation was already discernible in light microscopy, and lasted until telophase, albeit with a much reduced signal at this point (Figure 3.5A). The R3G3 (S277) signal was weakly detected in interphase cells, consistent with previous reports that S277 is activated in interphase by ERK2 in addition to its mitotic phosphorylation by cdc2 [19, 91]. The R3G3 signal became clearly visible already in late G2 phase and remained strong until telophase (Figure 3.5B). In fact, the enhanced R3G3 signal appeared earlier and lasted longer throughout mitosis when compared with that of the other phospho-specific antibodies. R3F2 (S376) had a weak signal during late G2 phase, became stronger from prophase and was reduced at telophase (Figure 3.5C). Quantitation of the fluorescence images confirmed these results (Figure 3.S2A and B). Overall, these results suggest that GRASP65 phosphorylation on different sites occurs sequentially.

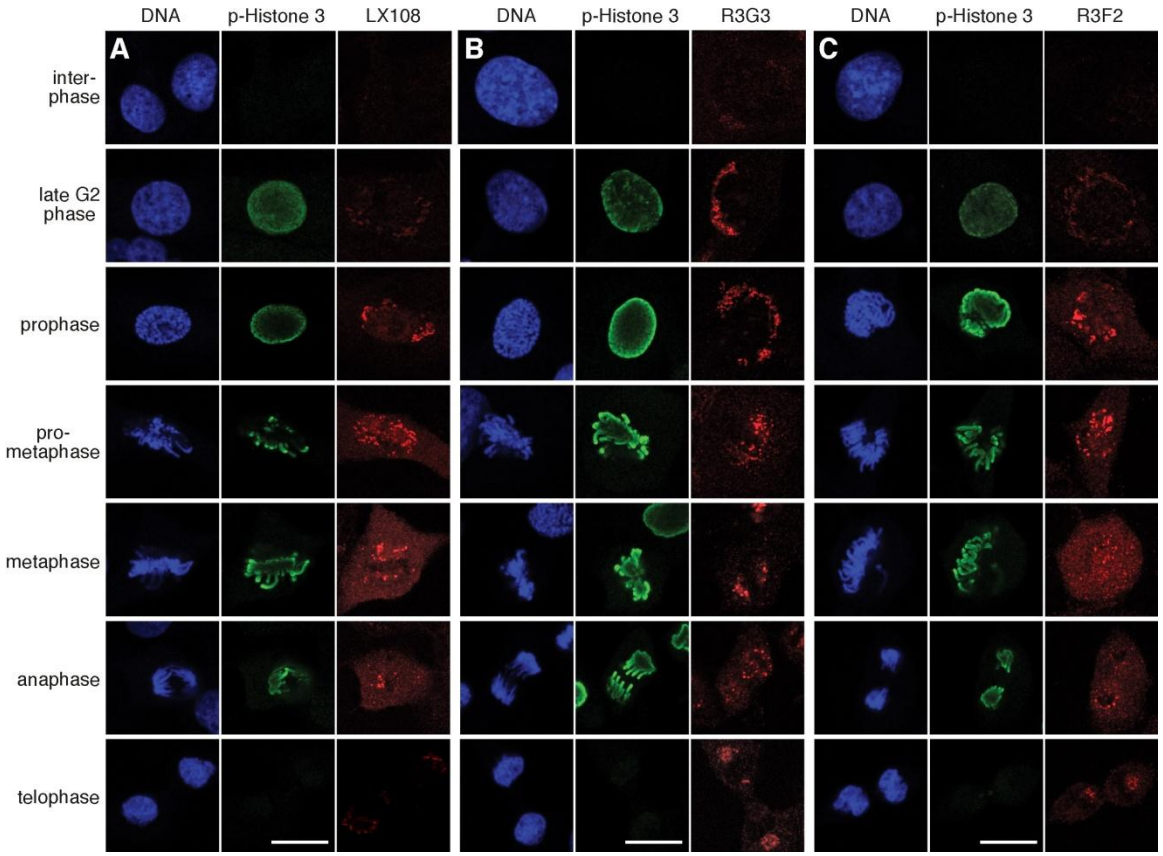

Figure 3.5. Phosphorylation of GRASP65 at three different sites during cell cycle progression.
NRK cells of indicated cell cycle phases were stained for DNA, phosphorylated Histone H3 (Ser10) and GRASP65 with LX108 (T220/T224, A), R3G3 (S277, B), or R3F2 (S376, C) antibodies. Note that in late G2 phase, the staining of R3G3 was much stronger than in interphase and than that of the other two antibodies. Scale bar in all panels, 10 μm.

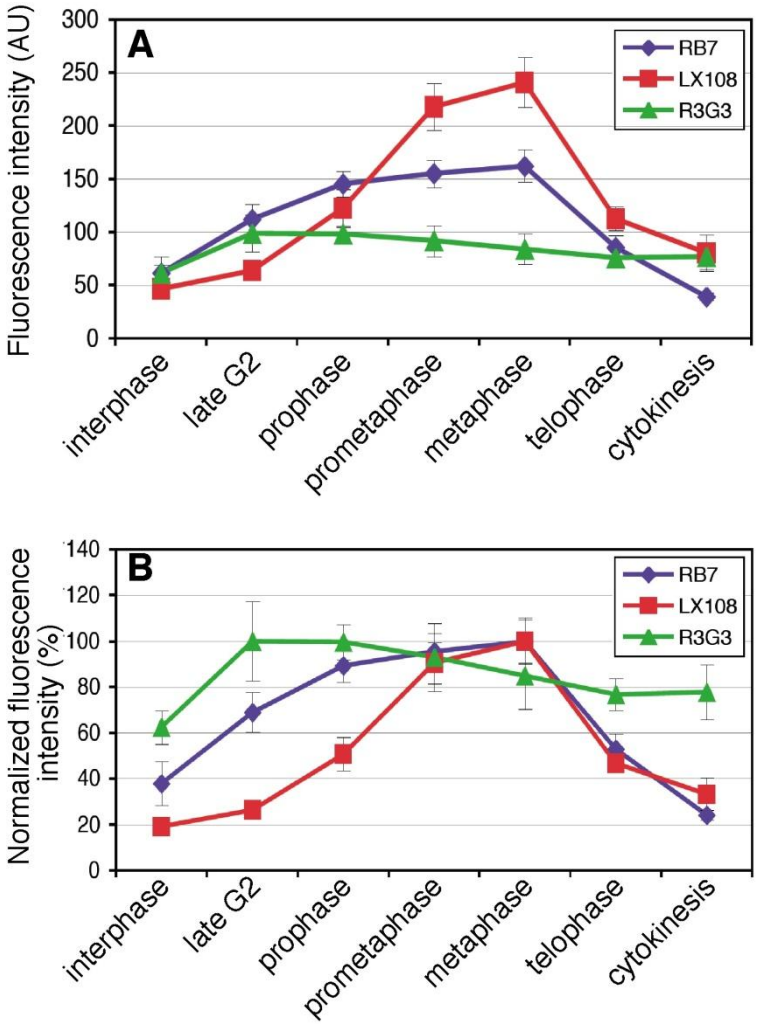

Figure 3.S2. Quantification of total cellular fluorescence intensity of indicated phospho-antibodies throughout the cell cycle.
(A) Total fluorescence intensity of the three phospho-specific antibodies at different cell cycle stages. Values plotted as mean ± SEM. (B) As in A, but maximum intensity of each individual antibody in the cell cycle normalized to 100%.

Sequential phosphorylation and dephosphorylation of GRASP65 during the cell cycle

To confirm our observation that GRASP65 is phosphorylated and dephosphorylated sequentially at the three studied sites while cells progress through mitosis, we performed double staining of NRK cells with LX108 (T220/T224), and one of the two scFv antibodies, R3G3 (S277) or RB7 (S376). Furthermore, in order to better study the chronology of S277 and S376 phosphorylation during the cell cycle, we obtained an anti-phospho-S277 rabbit polyclonal

antibody from Dr. Nobuhiro Nakamura [91], here referred to as pS277. This collection of antibodies allowed us to study the dynamics of phosphorylation and dephosphorylation of all three phosphorylation sites in pairs using LX108 vs. R3G3, LX108 vs. RB7, and pS277 vs. RB7, at different stages of the cell cycle (Figure 3.6 and 3.S2). In late G2 phase, S277 was the first residue to be mitotically phosphorylated as indicated by the enhanced R3G3 and pS277 signals. No LX108 signal was detected during this phase, while RB7 showed a weak signal. In early prophase, R3G3 and pS277 signals remained strong, sometimes even increased slightly. At the same time RB7 signal increased significantly and LX108 signal started to appear. During late prophase, LX108 signal became more intense. In prometaphase, LX108 signal reached its highest level, while the fluorescence intensity of the other antibodies remained unchanged. Quantification and graphic depiction of the observed distinct differences in fluorescence intensity for each antibody over time is graphically depicted in Figure 3.S2. In summary, these results strongly suggest that during early mitosis GRASP65 is first phosphorylated on residue S277, followed by modification of the S376 residue, and eventually activation of T220/T224. Upon careful analysis of the fluorescence images we observed that from late prophase to telophase, the R3G3-, pS277- and RB7-signals (indicating phosphorylation of S277 and S376) were largely localized on the Golgi clusters (the Golgi remnants during mitosis) while the LX108-signal (phosphorylated T220/224) appeared in a more dispersed fashion, likely representing the Golgi haze (e.g. dispersed mitotic Golgi vesicles and tubules). Since GRASP65 is a membrane-associated protein that does not detach from the membranes during mitosis [13], and since LX108 antibody staining has little if any background in interphase cells (Figure 3.3B), the more homogeneous signal of LX108 likely marks dispersed mitotic Golgi vesicles and tubules at a size below the resolution of light microscopy.

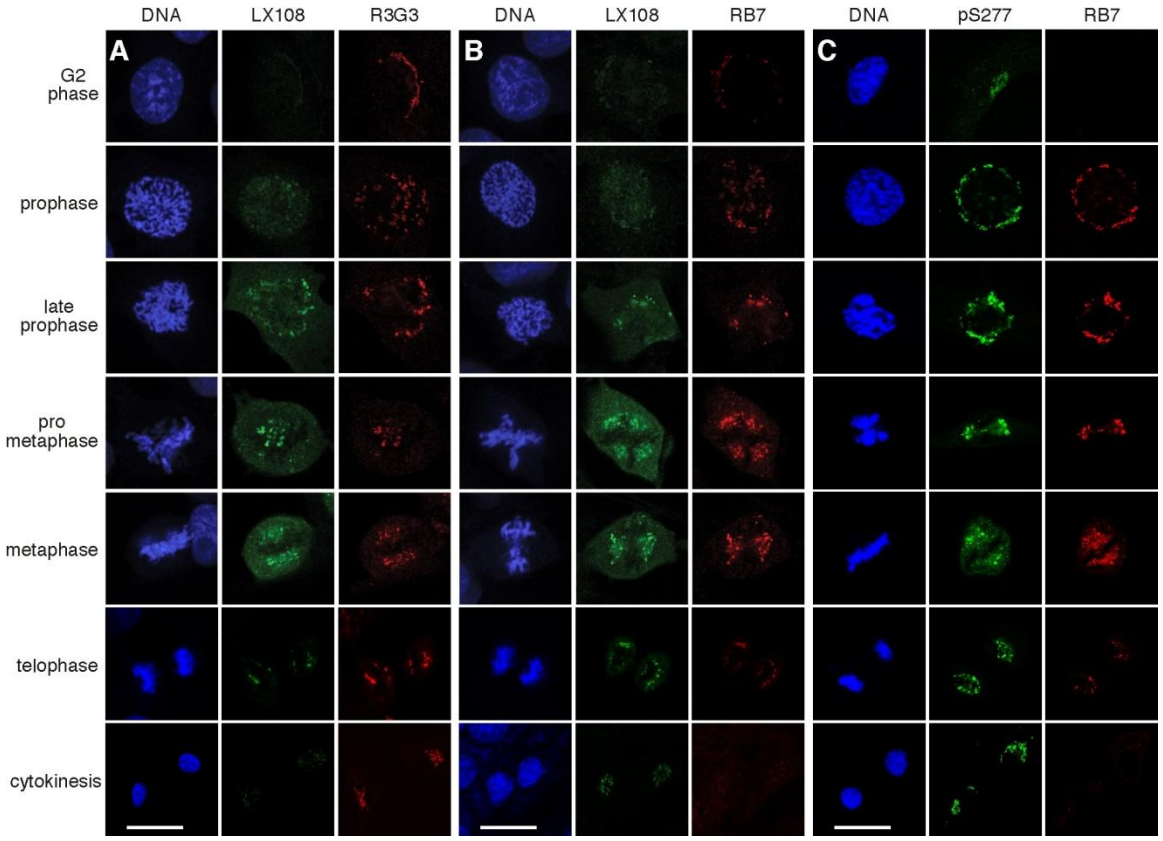

Figure 3.6. Different phosphorylation sites of GRASP65 are phosphorylated during mitosis and dephosphorylated in telophase at distinct times.
NRK cells of indicated cell cycle phases were double stained by the following antibodies: A. LX108 (T220/T224) and R3G3 (S277); B. LX108 and RB7 (S376); and C. a polyclonal antibody pS277 that recognized phosphorylated S277 and RB7. Cell cycle stage was determined by the morphology of the DNA. Note that the signals for R3G3 and RB7 were detected earlier than that of LX108, indicating that the three recognized sites are activated sequentially during mitosis. The intensity of the LX108 signal correlated with the extent of Golgi fragmentation, suggesting that T220/T224 phosphorylation is critical for mitotic Golgi disassembly. Scale bar in all panels, 10 μm.

Dephosphorylation also appeared to be sequential (Figure 3.6 and 3.S2). In telophase, both LX108 and RB7 signals became reduced significantly, while the signals for R3G3 and pS277 remained strong. During cytokinesis, no more RB7 signal was discernible, while a faint LX108-signal remained. R3G3 and pS277 staining was reduced but remained relatively strong. These results indicate that dephosphorylation at the end of mitosis is a coordinated process similar to that seen for phosphorylation at the onset of cell division. The S376 residue is inactivated first, followed by T220/T224, and eventually S277 partial dephosphorylation.

Phosphorylation of T220/T224 is critical for Golgi vesiculation

LX108 preferentially stained Golgi vesicles, while R3G3, pS277 and RB7 signals, respectively, were stronger on the mitotic Golgi clusters (Figure 3.5, 3.6 and 3.S2). For a better overall characterization we examined the Golgi morphology using an antibody that recognizes the total GRASP65 pool regardless of its phosphorylation state and then evaluated the phosphorylation of the protein at different sites. We performed triple labeling of NRK cells with LX108, R3G3 or RB7, and "Mary". Mary is a rabbit polyclonal antibody that recognizes rat GRASP65 in both its phosphorylated and non-phosphorylated forms [17, 18]. Our observation that phosphorylation of T220/224 is more critical for complete Golgi disassembly during mitosis than activation of other sites (see above) was verified. As shown in Figure 3.7, the T220/T224 residues began to be modified in prophase, at the time when the Golgi apparatus started to disassemble; R3G3 and RB7 signals were already easily discernible. In the ensuing prometaphase, T220/T224 phosphorylation reached a higher level; at this stage the Golgi apparatus was already significantly fragmented. In metaphase, T220/T224 was highly phosphorylated; Golgi disassembly was completed. Toward the end of mitosis, during telophase, RB7 but not LX108 signal significantly decreased, Golgi reassembly was initiated. Finally during cytokinesis, T220/T224 was dephosphorylated and Golgi reassembly was completed. These results suggest a correlation between T220/T224 dephosphorylation and complete Golgi reassembly.

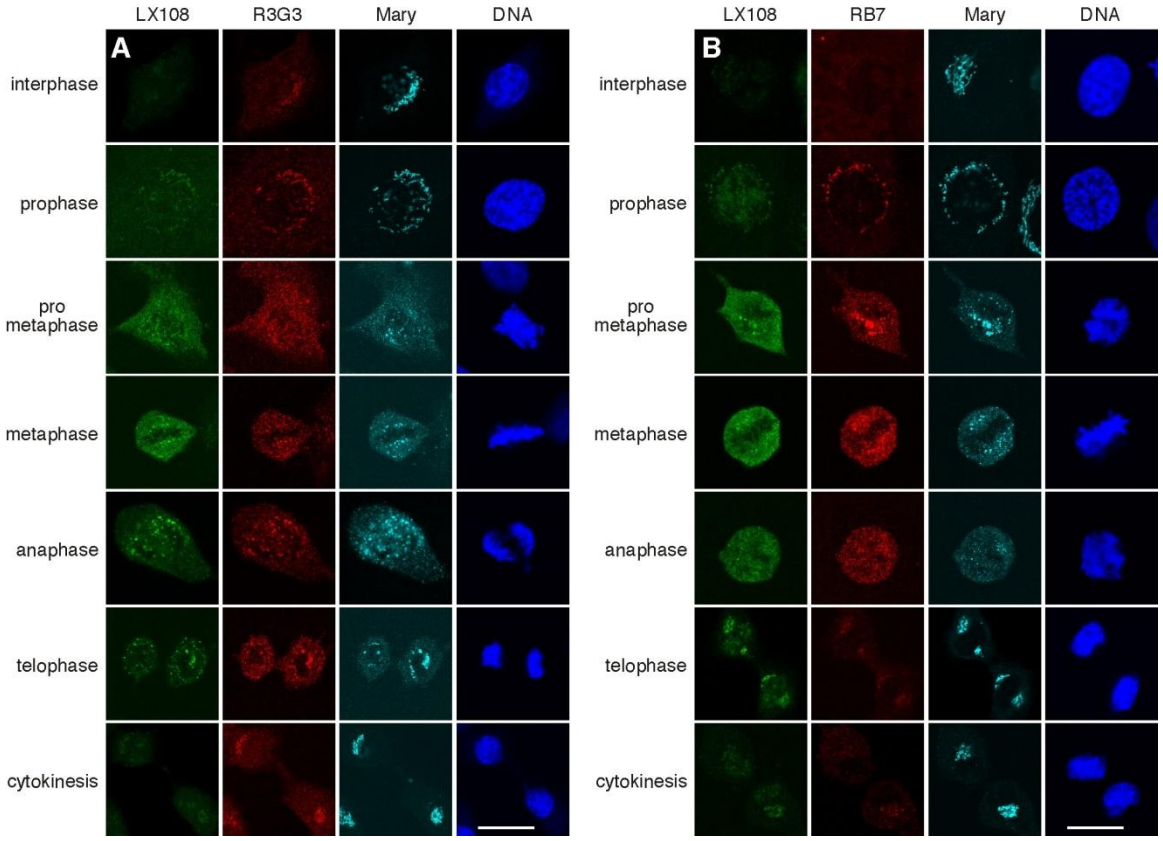

Figure 3.7. Sequential phosphorylation and dephosphorylation of GRASP65 orchestrates mitotic Golgi disassembly and post-mitotic reassembly.
NRK cells of indicated cell cycle phases were triple labeled by LX108 (T220/T224), R3G3 (S277) and Mary (total GRASP65 regardless of the phosphorylation state) in panel A; and by LX108, RB7 (S376) and Mary in panel B. Cell cycle stage was determined by the morphology of the DNA. Note that the intensity of LX108 signal correlates with the progress of Golgi disassembly. Scale bar in all panels, 10 μm.

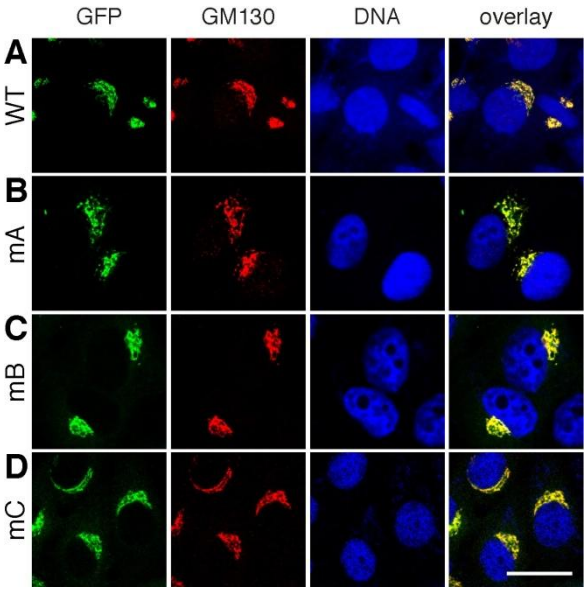

Figure 3.S3. The phospho-deficient mutants of GRASP65 are targeted to the Golgi in interphase cells.
Interphase cells expressing WT, the mA, mB or mC mutants of GRASP65-GFP were stained for GM130 and DNA overlaid with the GFP signals. Note that the expressed proteins colocalized with GM130. Scale bar in all panels, 20 μm.

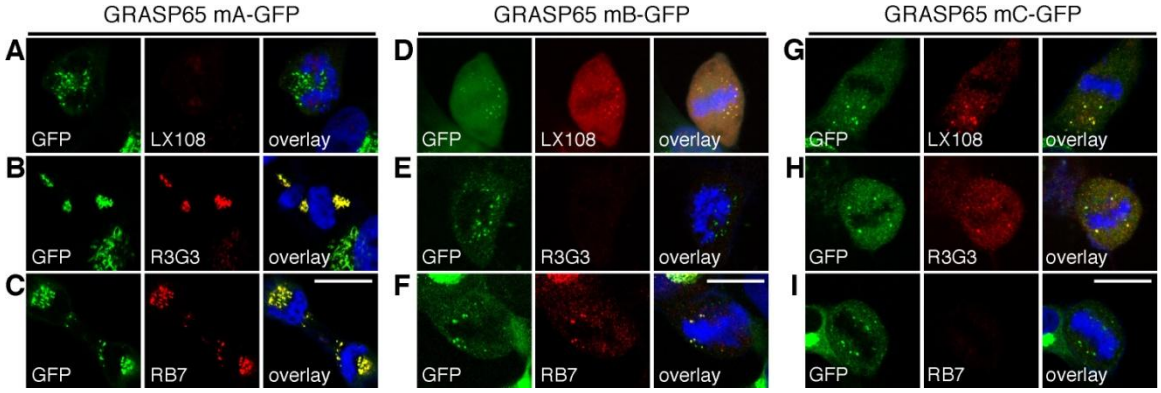

Figure 3.S4. The GRASP65 phospho-deficient mutants are not recognized by the relevant phospho-specific antibodies in immunofluorescence.
Mitotic HeLa cells expressing the mA (A-C), mB (D-F) or mC (G-I) mutants of rat GRASP65-GFP were stained with LX108 (T220/T224), R3G3 (S277) or RB7 (S376) antibodies. Note that the signal is markedly reduced when the antibody's specific recognition residue is mutated (mA for LX108, mB for R3G3 and mC for RB7). Scale bar in all panels, 10 μm.

To provide further evidence for the critical role of T220/T224 phosphorylation in Golgi vesiculation, we established HeLa cell lines stably expressing GFP-tagged GRASP65 mutants mA (S216A/S217A/T220A/T224A), mB (S277A), and mC (S367A/S376A), respectively, under a tet-inducible promoter [16, 17]. All proteins correctly localize to the Golgi apparatus (Figure 3.S3) and none of the mutants are recognized by their corresponding phospho-specific antibodies as expected (Figure 3.S4). To determine the effects caused by these mutant proteins on the Golgi architecture, we analyzed these cells using fluorescence microscopy. Metaphase cells expressing WT GRASP65-GFP or the mA, mB, mC mutants were immunostained with GM130. As shown in Figure 3.8A, the Golgi membranes were extensively fragmented in cells expressing wild type GRASP65-GFP. Expression of mB-GFP or mC-GFP mutants had only a minor if any effect (Figure 3.8C-D). However, in cells expressing the mA-GFP mutant (Figure 3.8B), the Golgi was observed as large punctae, or mitotic Golgi clusters, similar to what we previously reported with

cells expressing the GRASP65 mG mutant [17, 18]. Quantification of the fluorescence images showed that in mitotic mA-GFP expressing cells, 21.34 ± 3.00% of total GM130 fluorescent signal in the cell was found on mitotic Golgi clusters. This was significant higher than the percentage seen in WT GRASP65-expressing cells (4.36 ± 0.77%), suggesting that mA expression reduced mitotic Golgi disassembly. The intensity of the GM130 signal on mitotic Golgi clusters was not significantly affected by the expression of mB-GFP and mC-GFP mutants, leading to 2.91 ± 0.62% and 5.43 ± 1.20% of the total GM130 signal on the clusters, respectively (Figure 3.8E), suggesting that phosphorylation at other sites is less important for this process.

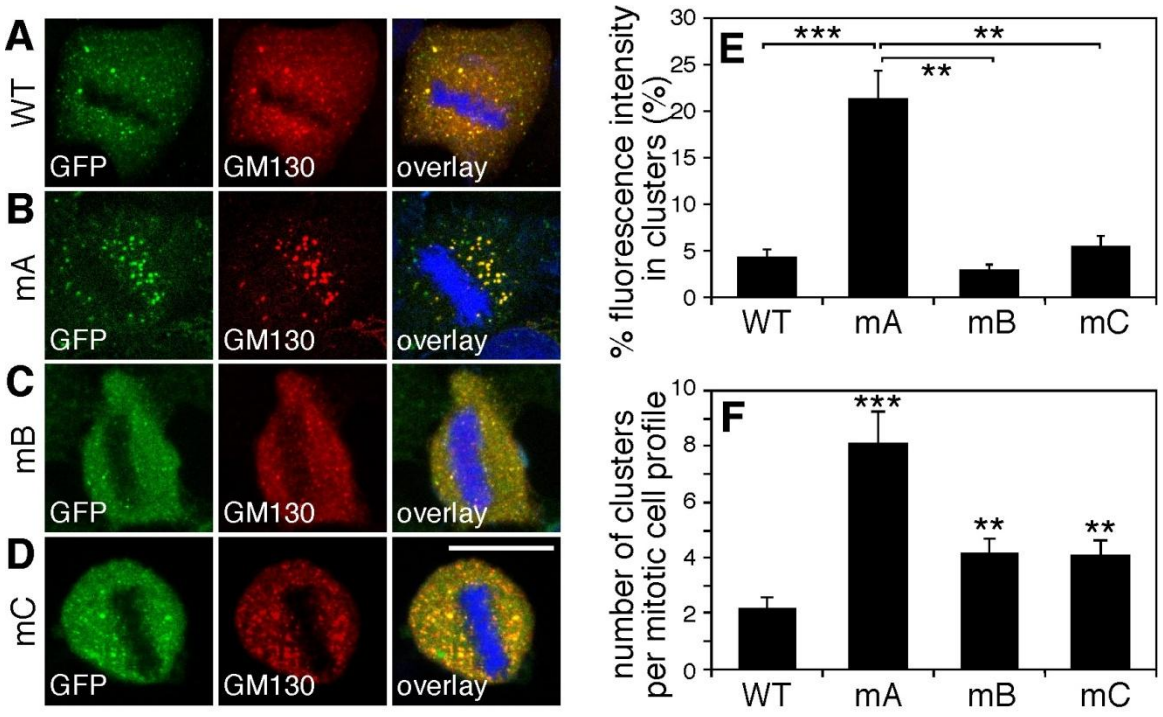

Figure 3.8. Mutation of the phosphorylation sites especially of the residue T220/T224 inhibits mitotic Golgi fragmentation.
(A-D) Expression of the mA mutant of GRASP65 inhibits Golgi fragmentation in mitosis. Cells expressing indicated GFP-tagged GRASP65 mutants were stained for GM130 and DNA. Metaphase cells were selected. Note the large remaining clusters, likely representing Golgi structures in the mA-expressing cell line. Scale bar in all panels, 10 μm. (E) Quantification of fluorescence intensity of GM130 on mitotic Golgi clusters as compared to whole-cell fluorescence. The percentage was expressed as the mean ± SEM. Statistical significance was assessed by student's t-test between the indicated pairs. **, $p < 0.01$; ***, $p < 0.001$. (F) Quantification of EM images counting the number of remaining mitotic Golgi clusters per mitotic cell in cells expressing either GRASP65 WT or mutants

as indicated. The number of observed mitotic Golgi clusters per cell was expressed as the mean ± SEM. Statistical significance was assessed by comparison to the cell line expressing WT GRASP65. **, $p < 0.01$; ***, $p < 0.001$.

Finally, analysis by electron microscopy showed that mA-GFP expressing cells contained significantly greater amounts of large membranes that remained as clusters of vesicles, short cisternae and tubular structures (Figure 3.S5). Quantification of the EM images showed that the number of mitotic Golgi clusters per mitotic cell in cells expressing the mA mutant (8.1 ± 1.1) was significantly higher than in cells expressing WT GRASP65 (2.2 ± 0.4). In contrast, the number of mitotic Golgi clusters per cell was only mildly increased in mB and mC expressing cells (4.2 ± 0.5 or 4.1 ± 0.5 respectively), significantly lower than that in the mA expressing cells ($p<0.01$) (Figure 3.8F). These results confirmed that T220/T224 is the key regulation site for Golgi vesiculation during mitosis.

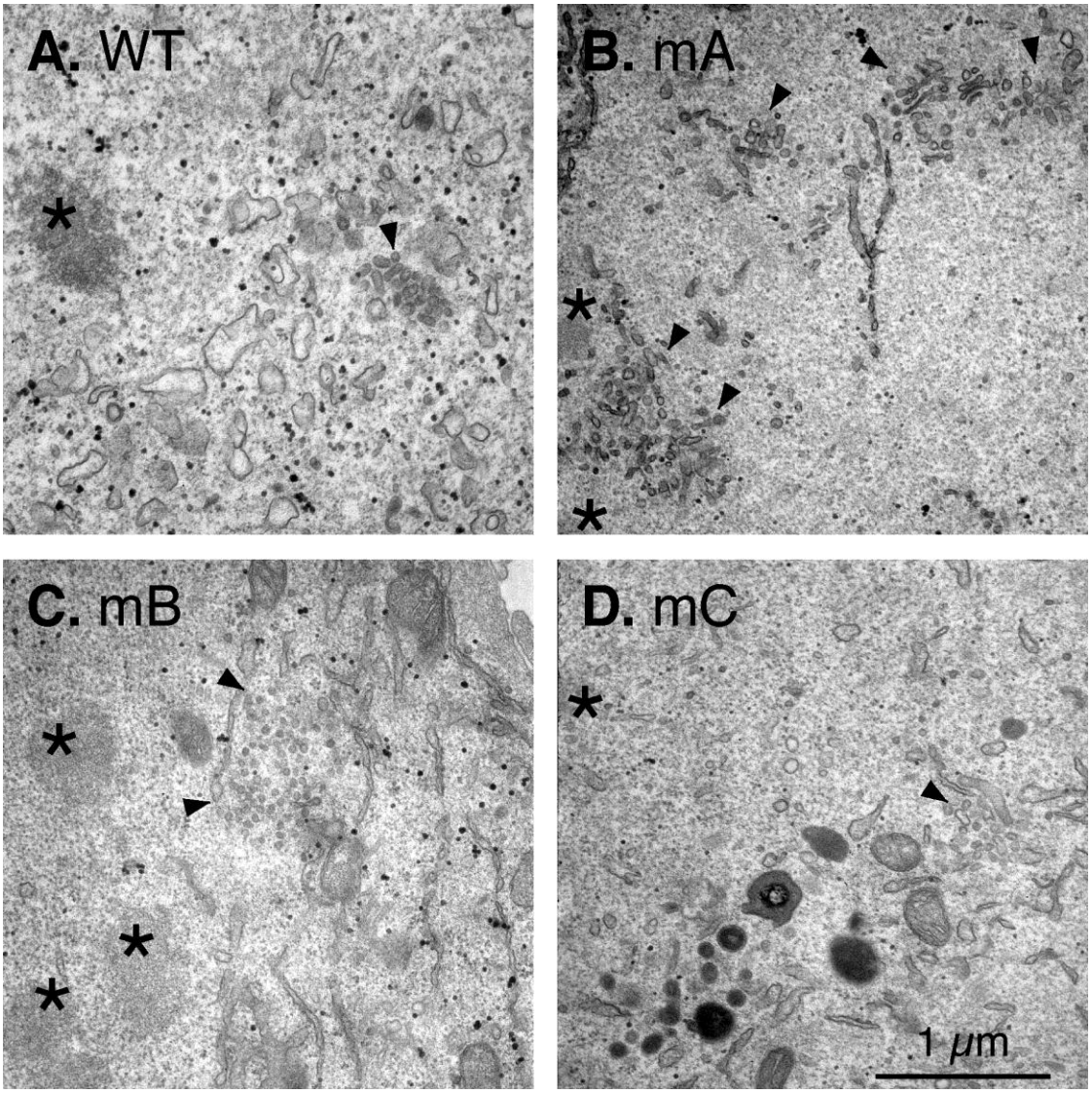

Figure 3.S5. Expression of the mA mutant of GRASP65 inhibits Golgi fragmentation during mitosis.
Electron microscopy images of mitotic cells expressing indicated GRASP65 WT (A), mA (B), mB (C) and mC (D) constructs. Arrowheads indicate mitotic Golgi clusters; while asterisks mark condensed chromosomes. Note the larger number of remaining Golgi clusters in panel B.

Discussion

In this study we generated and utilized phospho-specific antibodies, and dissected GRASP65 phosphorylation in the cell cycle in more detail by determining the biological significance of modification of each of the sites. The particular importance of T220/T224 phosphorylation for mitotic Golgi fragmentation was shown using the phospho-specific antibody LX108. Using this and four other GRASP65 phospho-specific antibodies, we were able to follow the temporal sequence of phosphorylation of three sites, T220/T224, S277 and S376, throughout cell cycle progression. These phosphorylation sites had been predicted in previous studies according to the amino acid sequence [18] and some had been confirmed by analysis of *in vitro* phosphorylated recombinant GRASP65 by mass spectrometry [19]. In this study, we confirmed their phosphorylation in single cells. In combination with an *in vitro* phosphorylation assay, these antibodies also allowed us to determine the mitotic kinases responsible for each site. Furthermore, kinase inhibitors were used as a complementary approach to ensure specificity of our findings. We confirmed that cdc2 phosphorylates the T220/T224 residues required for Golgi disassembly during mitosis. Our *in vitro* phosphorylation assay using recombinant GRASP65 protein also suggested that S277 and S376 are phosphorylated by cdc2 during mitosis.

The fact that we were able to use phospho-specific antibodies against GRASP65 residues from different species (human, rabbit and mouse) was particularly important. It allowed us to perform double or triple labeling for immunofluorescence microscopy and thus to determine the sequence of phosphorylation on each site in the same cell and with exact knowledge of the stage of the cell cycle by monitoring DNA morphological changes and phosphorylation of Histone H3. Analyses could also be performed looking at Golgi morphology changes by co-staining cells

with an antibody that recognized GRASP65 regardless of its phosphorylation state. Two major observations were made. First, GRASP65 is not phosphorylated at the T220/T224 site until prophase i.e. until after the beginning of Golgi disassembly. In contrast, residues S277 and S376 are phosphorylated in late G2 phase, a time when Histone H3 is phosphorylated but the Golgi is not yet significantly fragmented. Eventually GRASP65 is highly phosphorylated at the T220/T224 site from prophase to anaphase, at the time when the Golgi is severely fragmented. Secondly we observed that the phospho-GRASP65 pool, modified on T220/T224 localizes onto the Golgi vesicles. In NRK cells, from prometaphase to anaphase, the Golgi apparatus disassembles into thousands of vesicles distributed throughout the cytosol that were observed as "Golgi haze" under the fluorescence microscopy. Some parts of the Golgi membranes, however, remain as tubulovesicular remnants or "mitotic Golgi clusters" that appear to be more concentrated near the spindle poles [30, 69]. Unlike the phospho-S277 or phospho-S376 signal that was mainly observed on the Golgi clusters, the LX108 signal for phospho-T220/T224 appeared on both Golgi clusters and Golgi haze. Furthermore, expressing the mA, i.e. T220A/T224A, mutant in HeLa cells inhibited Golgi vesiculation during mitosis, while mB or mC mutants had a much smaller effect. These results suggest that phosphorylation of T220/T224 is the key site needed for mitotic Golgi fragmentation. Previous studies have shown that GRASP65 exerts its function through oligomerization. This is mediated by the GRASP-domain but is regulated by phosphorylation at the C-terminus [14, 18]. Of all the characterized phosphorylation sites, the T220/T224 residue is in closest proximity to the GRASP domain, and we speculate that it thus is likely the most important for regulating GRASP65 oligomerization.

The residue S277 is phosphorylated in mitosis (from late G2 phase to cytokinesis) as well as in interphase when cells are stimulated by EGF, although by different kinases [21, 91] and to a lesser degree (Figure 3.5B). Phosphorylation of S277 during interphase is directed by the MEK/ERK pathway. Mitotic phosphorylation of GRASP65 has been shown to regulate its oligomeric state and thereby Golgi cisternal stacking and ribbon linking [4, 9, 22, 23]. In interphase cells, partial phosphorylation of GRASP65 is required for dynamic Golgi remodeling in migrating cells [21]. Phosphorylation of S277 by MAP kinase partially de-oligomerizes GRASP65 complexes, accompanied by partial disassembly of the Golgi apparatus, thus allowing the organelle to reorganize and migrate towards the leading edge of the cell. Unlike what is observed in mitotic cells, massive Golgi vesiculation has not been observed in migrating cells suggesting that the phosphorylation of S277 is required for continuous reorganization of the Golgi during interphase, but that their modification may not be enough for a complete organelle disassembly during mitosis. Instead, complete collapse of the ribbon requires phosphorylation of T220/T224. Expressing the S277A (mB) or S367A/S376A (mC) mutant somewhat raised the number of Golgi clusters in mitotic cells compared to expressing the WT protein (Figure 3.8F). This indicates that S277 phosphorylation facilitates Golgi fragmentation, but not to the same dramatic extent as activation of T220/T224. GRASP65 phosphorylation at different sites leads to different effects and thus serves different functions. This elaborate phosphorylation system allows the cell and its organelle to adapt to different situations and at the same time to effectively divide the single Golgi apparatus to its two daughter cells during cell division.

At the end of mitosis, S376 is the first of the three studied residues to be dephosphorylated, followed by T220/T224, and eventually S277, the latter remaining partially phosphorylated until

interphase. It is likely that S277 is constitutively phosphorylated because of the need of the Golgi apparatus to undergo constant remodeling in interphase cells [119]. The role of S376 phosphorylation is least well understood to date. In addition to the three phosphorylation sites characterized in this study, GRASP65 is also modified by kinases on S189, S216, S217 and S367 at least *in vitro* [19, 116]. Characterization of these sites and their relationships may provide further insight in understanding the function of GRASP65 and Golgi biogenesis during cell division.

Materials and methods

Reagents

All reagents were purchased from Sigma-Aldrich, Roche or Calbiochem, unless otherwise stated. The following antibodies were used: monoclonal antibodies against GM130 (Transduction Laboratories) and α-tubulin (Developmental Studies Hybridoma Bank University of Iowa); polyclonal antibodies against GFP [37], GRASP65 called "Mary" [14] and phospho-Histone H3 (Upstate Biotechnology). The monoclonal phospho-specific antibody LX108 was generated by immunizing mice with recombinant WT His-GRASP65 full-length protein treated with mitotic cytosol; antibodies were collected from the medium of cultured hybridoma and subsequently enriched by protein G sepharose. The human single chain (scFv) monoclonal antibodies against phosphorylated GRASP65 (R3G3, R3F2 and RB7) were described previously [94]. A mouse monoclonal antibody against rat GRASP65, called 7E10, was generously provided by Dr. Graham Warren (Max F. Perutz Laboratories, Austria); a rabbit polyclonal antibody for GRASP65 phosphorylated at S277 (pS277) was generously provided by Dr. Nobuhiro Nakamura (Kyoto Sangyo University, Japan). Secondary antibodies for indirect immunofluorescence and immunoblotting were purchased from Jackson Laboratories and Invitrogen.

Preparation of GRASP65 recombinant proteins

The rat GRASP65 cDNA was cloned into the pQE9 (Qiagen) vector; correct insertion was confirmed by DNA sequencing. GRASP65 point mutations mA - mJ were introduced using the QuikChange mutagenesis kit (Stratagene) and changes were confirmed by DNA sequencing.

Proteins were expressed in BL21-CodonPlus(DE3)RILP bacteria and purified on Ni-NTA agarose (Qiagen).

Characterization of phospho-specific antibodies by Western blot

For epitope mapping, the purified His-tagged GRASP65 full-length protein and various phosphorylation deficient mutants (potential phosphorylation sites mutated to alanines) were incubated with interphase cytosol or mitotic cytosol (buffers were used as negative control) at 37ºC for 1 h and purified with Ni-NTA beads. Bound proteins were analyzed by SDS-PAGE and Western blot using antibodies as indicated.

To determine the specificity of GRASP65 phospho-specific antibodies, HeLa cell lines stably expressing wild type rat GRASP65 or its phosphorylation deficient mutants as indicated were either synchronized with 100 ng/ml nocodazole for 20 h or incubated without synchronization. Subsequently, cells were collected, lysed and analyzed by SDS-PAGE and Western blot with antibodies as indicated.

In vitro and in vivo GRASP65 phosphorylation assay

Recombinant GRASP65 proteins or purified rat liver Golgi membranes (RLG) [120] were incubated with mitotic cytosol [8] or with different combinations of kinases [14]. Typically, 20 µg RLG (or 50 ng recombinant GRASP65) were treated with 500 µg HeLa cytosol, or equivalent activity of kinases, in MEB buffer (50 mM Tris-HCl, pH7.4, 0.2 M sucrose, 50 mM KCl, 20 mM β-glycerophosphate, 15 mM EGTA, 10 mM MgCl2, 2 mM ATP, 1 mM GTP, 1 mM glutathione,

and protease inhibitors) at 37ºC for 60 min. The samples were subsequently analyzed by Western blot [28, 121].

To identify the kinases that phosphorylate GRASP65 *in vivo*, HeLa cells stably expressing wild type rat GRASP65-GFP were first incubated with 100 ng/ml nocodazole for 18 h. Cells were then treated with one of the following chemicals: 1) a general kinase inhibitor staurosporine (at 2 μM) for 30 min [122], 2) a cdk inhibitor roscovitine (at 40 μM) for 2 h [123], 3) a plk1 inhibitor BI2536 (at 0.1 μM) for 2 h [124, 125], and 4) a MAPK inhibitor U0126 (at 20 μM) for 2 h [115, 126]. Cells were subsequently lysed and GRASP65-GFP was immunoprecipitated using an anti-GFP antibody. The phosphorylation of rat GRASP65-GFP was revealed via Western-blot using the indicated phospho-specific GRASP65 antibodies.

Cell lines and microscopy

To establish stable cell lines expressing various rat GRASP65 constructs, rtTAm2 HeLa cells were infected with retroviral particles encoding indicated exogenous genes cloned in the pRevTRE2 vector. Wild type rat GRASP65 and the related mA, mB, mC and mG mutants were first cloned into the pEGFP-N2 vector via the EcoRI and ApaI sites. cDNA encoding GFP (enhanced green fluorescent protein) alone, or GRASP65-GFP, mA-GFP, mB-GFP, or mG-GFP were then excised by Hind III and NotI and religated into the pRevTRE2 vector. Viral preparation, infection and cell selection were performed as previously described [16, 17]. GFP-positive cells were enriched by flow cytometry. The expression of exogenous proteins was induced with 1 μg/ml doxycycline.

Immunofluorescence microscopy was performed as previously reported [17]. To enrich mitotic cells, NRK cells, or HeLa cell lines expressing rat GRASP65-GFP, were first synchronized with 2 mM thymidine for 24 h and then incubated in regular growth medium without thymidine for 8 h prior to fixation. Images were obtained with a Leica SP5 confocal laser scanning microscope using a 100x oil objective. For metaphase cells, images were captured using fixed parameters with 0.3 μm intervals at the z-axis and then processed for maximum value projection. For triple labeling of phosphorylated GRASP65 in mitotic NRK cells, three secondary antibodies, goat-anti-mouse IgG-FITC, donkey-anti-human IgG-Cy3 and goat-anti-rabbit IgG-Cy5 were used to stain LX108, R3G3 or RB7, and Mary, respectively.

Quantification of immunofluorescence intensity

Whole-cell fluorescence intensity, generated by the respective phospho-antibody at different cell cycle stages, was quantified using the NIH ImageJ software. For better comparison of the relative changes between the three antibodies, the maximum total cellular intensity of each antibody detected throughout the cell cycle was normalized to 100%. The cell cycle stages were defined based on the chromosome shape, Golgi structure and phospho-Histone H3 staining. Late G2 phase cell were distinguished from interphase cells based on phospho-Histone H3 staining. Cells in cytokinesis were identified as cell pairs, which were not fully separated and had relatively intact nuclei and Golgi structure.

To determine the proportion of fluorescence signal attributed to specific recognition of Golgi clusters, mitotic cells expressing various GRASP65 constructs as indicated were additionally immunostained for GM130. Whole-cell fluorescence intensity was quantified using

the NIH ImageJ software and using an adjacent cell free region as background. The light intensity on mitotic Golgi clusters (larger bright dots on fluorescence images) was quantified using the Analyze Particle function of ImageJ. The percentage of the total fluorescence intensity emitted from mitotic Golgi clusters was then calculated.

Electron microscopy

EM analysis was performed as described previously [17], mitotic Golgi clusters were identified using morphological criteria and quantified by standard stereological techniques [18]. For a cell to be considered mitotic, the profile had to contain one or more condensed chromosomes and lack a nuclear envelope. Often multiple condensed chromosomes were aligned in the center of the cell. A low magnification (normally 1,600×) image and serial images of higher magnification (normally 11,000×) were taken to cover the entire cell. At least 15 cells were examined and quantified for each cell line.

Acknowledgements

We thank Nobuhiro Nakamura and Graham Warren for antibodies, Yi Xiang and other members of the Wang Lab for suggestions and reagents. This work was supported by the National Institute of Health (GM087364) and American Cancer Society (RGS-09-278-01-CSM) to Y. Wang. D. Tang was supported by the Rackham Predoctoral Fellowship from the University Michigan. The authors declare no conflicts of interest.

Abbreviations

BSA, bovine serum albumin; GFP, enhanced green fluorescent protein; EM, electron microscopy; GRASP65, Golgi reassembly stacking protein of 65 kDa; IC, interphase cytosol; NEM, *N-ethylmaleimide*; NRK, normal rat kidney cells; PBS, phosphate-buffered saline; plk1, polo-like kinase 1; scFv, single-chain variable fragment; siRNA, small interference RNA.

Chapter 4 . The ubiquitin ligase HACE1 regulates Golgi membrane dynamics during the cell cycle

Abstract

Partitioning of the Golgi membrane into daughter cells during mammalian cell division occurs through a unique disassembly and reassembly process that is regulated by ubiquitination. However, the identity of the ubiquitin ligase is unknown. Here we show that the Homologous to the E6-AP Carboxyl Terminus (HECT) domain containing ubiquitin ligase HACE1 is targeted to the Golgi membrane through interactions with Rab proteins. The ubiquitin ligase activity of HACE1 in mitotic Golgi disassembly is required for subsequent postmitotic Golgi membrane fusion. Depletion of HACE1 using small interfering RNAs or expression of an inactive HACE1 mutant protein in cells impaired postmitotic Golgi membrane fusion. The identification of HACE1 as a Golgi-localized ubiquitin ligase provides evidence that ubiquitin has a critical role in Golgi biogenesis during the cell cycle.

Introduction

Mitosis requires the duplication and even partitioning of all cellular components into the daughter cells. In mammalian cells, inheritance of the Golgi apparatus during cell division occurs through a unique disassembly and reassembly process [9, 10]. The Golgi is fragmented at the onset of mitosis to disperse the stacks, which then undergo further vesiculation. This yields thousands of vesicles that are distributed throughout the cytoplasm [127]. Studies using a cell free assay that reconstitutes mitotic Golgi fragmentation [7, 8, 128, 129] showed that mitotic Golgi disassembly involves two processes: cisternal unstacking and membrane vesiculation. Unstacking is mediated by mitotic kinases that phosphorylate the Golgi stacking proteins GRASP65 and GRASP55 [14, 16-18]. In interphase cells, GRASP proteins form oligomers that hold the membranes in stacks. During mitosis, phosphorylation of GRASPs leads to de-oligomerization of the proteins and cisternal unstacking. Vesiculation of the unstacked cisternae occurs through continuous formation of COPI vesicles, which is mediated by the small GTPase ARF1 (ADP-ribosylation factor 1) and the coatomer complex [28]. Phosphorylation of Golgi tethering proteins, such as GM130, disrupts membrane fusion, and continuous COPI vesicle budding without fusion results in vesiculation of the Golgi membranes during mitosis [130]. During telophase, Golgi vesicles are distributed equally between daughter cells, where they are assembled into stacks and ribbons. Post-mitotic Golgi reassembly is mediated by membrane fusion to form single cisternae and by cisternal stacking. Post-mitotic Golgi membrane fusion is mediated by two AAA (ATPases Associated with various cellular Activities) ATPases, N-ethylmaleimide-sensitive factor (NSF) and p97 (also referred to as valosin-containing protein, VCP, or Cdc48 in yeast), which work together with their adaptor proteins [131-136]. Golgi

membrane restacking is mediated by dephosphorylation and subsequent re-oligomerization of Golgi stacking proteins [7, 9, 14, 16-18, 36].

Several converging lines of evidence have suggested that monoubiquitination plays an essential role in the regulation of post-mitotic Golgi membrane fusion. First, monoubiquitination occurs during mitotic Golgi disassembly and is required for subsequent Golgi reassembly [35]. Second, the p97/p47 complex binds to monoubiquitin through the UBA domain of the adaptor protein p47. Inhibition of the p47-ubiquitin interaction suppresses p97-mediated Golgi membrane fusion [35]. Third, VCIP135, a cofactor of the p97/p47 complex, is a deubiquitinating enzyme whose activity is required for post-mitotic Golgi reassembly [36]. Finally, proteasome activity is not involved in either Golgi disassembly or reassembly [36]. These data suggest that cycles of addition and removal of ubiquitin to and from substrates is necessary for Golgi reassembly. The role of ubiquitination in Golgi membrane fusion is likely not restricted to the p97/p47 complex, as it has been shown that another required ATPase, NSF, binds to GATE-16, a ubiquitin-like protein [40, 137]. These results suggest that ubiquitination may operate as a general mechanism to regulate Golgi membrane dynamics during the cell cycle. Both NSF- and p97-mediated Golgi reassembly require syntaxin 5, but these two pathways contribute non-additively to cisternal regrowth [132]. This suggests that they may have distinct roles in post-mitotic Golgi membrane fusion, but the coordination between the two pathways has not been elucidated.

Further understanding of the underlying mechanism of ubiquitin in the regulation of Golgi membrane dynamics during cell division requires identification of the ubiquitin ligase on the

Golgi membranes. Here, we show that HACE1, a HECT domain (Homologous to the E6-AP Carboxyl Terminus)-containing ubiquitin ligase, is involved in this process. HACE1 is recruited to the Golgi membrane via interaction with Rab1, and regulates Golgi membrane fusion both *in vitro* and *in vivo*. The identification of HACE1 as a Golgi-localized ubiquitin ligase provides further evidence that ubiquitin plays a critical role in Golgi biogenesis during the cell cycle.

Results

Identification of HACE1 as a Rab interacting protein

Rab proteins have been shown to be important for membrane organization [138]. In an effort to identify Rab-interacting proteins using an affinity chromatography-based proteomic approach [139], we identified HACE1, which binds specifically to the GTP-bound state of Rab4 (Figure 4.1A). The HACE1 cDNA was cloned from a human cDNA library. It consisted of 909 amino acids and migrated at 100 kDa on an SDS-PAGE gel. HACE1 contains six ankyrin repeats and a HECT domain [140], a defining feature of one family of ubiquitin E3 ligases. Using a thioester bond formation assay containing ubiquitin, an E1 activating enzyme, the E2 conjugating enzyme UbcH7 and recombinant HACE1, we demonstrated that wild-type (WT) HACE1 is capable of catalyzing the formation of thioester bonds, but the inactive C876A (CA) mutant is not (Figure 4.1B). This result is consistent with previous reports that HACE1 functions as an active ubiquitin ligase [38, 140].

When examined by fluorescence microscopy, both Rab4 and HACE1 were concentrated in the perinuclear region, which appeared to be the Golgi apparatus (Figure 4.1C). In addition to the Golgi, Rab4, but not HACE1, was also found on endosomal membranes that were irregularly shaped and dispersed throughout the cytosol (Figure 4.1C). Because HACE1 binds to Rab4, which is only partially localized to the Golgi, we examined whether HACE1 also interacts with other Rabs, including those localized on the Golgi, using a well-established Rab pull-down assay [11, 139]. Immobilized GST-tagged Rab proteins were incubated with purified recombinant HACE1 in the presence of GDP or GTPγS and the presence of HACE1 in the bound fraction was detected by Western blot. As shown in Figure 4.1D-E, HACE1 bound to Rab1, Rab4 and Rab11

in a GTP-dependent manner, but not to Rab2, 5, 6 and 7 irrespective of the nucleotide used. To confirm the interaction, we tested HACE1 binding to the GDP- (Rab1S25N, Rab4S22N and Rab11S25N) and GTP-restricted (Rab1Q67L, Rab4Q67L and Rab11Q70L) mutants of Rab1, 4 and 11. As shown in Figure 4.1F, HACE1 bound to the wild-type and QL-forms of all three Rabs but not their inactive mutants. Using HeLa cell lysate, we further showed that endogenous HACE1 bound to Rab1-GTP in a similar pattern as p115, a protein known to interact with Rab1. A strong interaction was also observed for Rab11, but no interactions were detected for Rab5 or Rab6 (Figure 4.1G). These results demonstrate that HACE1 interacts with Rab1, Rab4 and Rab11 in a GTP-dependent manner.

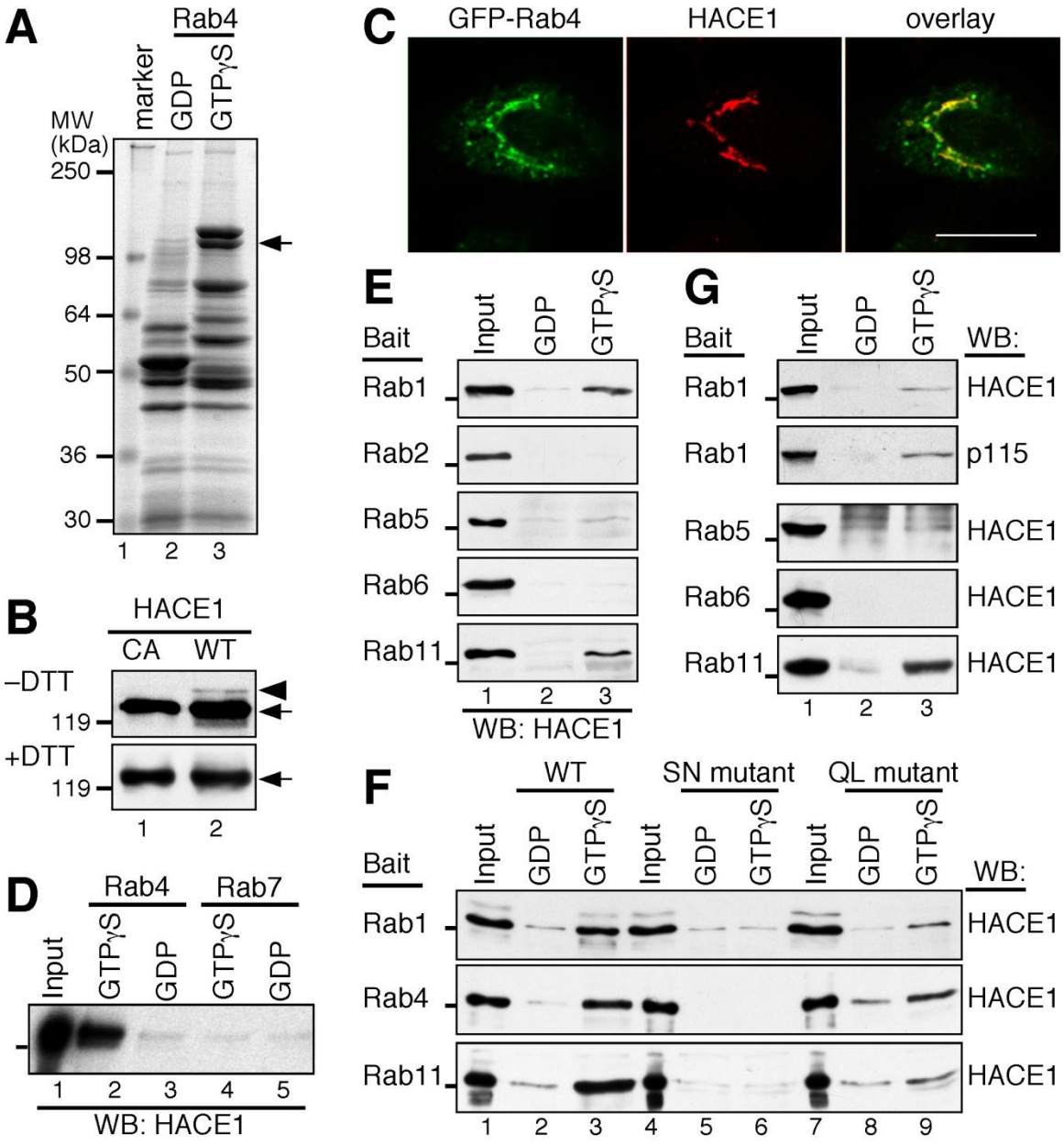

Figure 4.1. HACE1 binds to Golgi-associated Rab proteins.
(A) HACE1 binds Rab4–GTP. Immobilized GST-tagged Rab4 was incubated with bovine brain cytosol in the presence of GDP or GTPγS. After washing, the bound proteins were eluted and analysed by SDS–PAGE and coomassie blue staining. Specific bands in the GTPγS lane were excised and identified by mass spectrometry. The arrow indicates HACE1. **(B)** HACE1 exhibits ubiquitin ligase activity *in vitro*. A thioester bond formation assay was performed using the C876A (CA) point mutant and WT recombinant HACE1 protein, ubiquitin, E1-activating enzyme and the E2-conjugating enzyme UbcH7. Following incubation, the reactions were mixed with SDS buffer ± DTT and boiling. HACE1 was detected by western blot. The arrows indicate HACE1 and the arrowhead indicates Ub-HACE1. Note that the Ub-HACE1 band was observed in the absence of DTT with WT HACE1. **(C)** HACE1 colocalizes with Rab4 in the perinuclear region. Immunofluorescence images of A431 cells expressing GFP–Rab4 (in green) and stained for HACE1 (in red). Note that HACE1 colocalizes with Rab4 in the perinuclear region, while additional Rab4 signal is found in the cytoplasm. Scale bar, 20 μm. **(D)** HACE1 directly binds Rab4–GTP but not Rab7. Immobilized GST-tagged Rab4 and Rab7 were incubated with purified recombinant HACE1 in the presence of GDP or GTPγS. After washing, HACE1 was detected by western blot for HACE1. Input, 5%. **(E)** Recombinant

HACE1 binds Rab1 and 11 but not Rab2, 5 and 6. Input, 5%. **(F)** HACE1 interacts with Rabs in a nucleotide-dependent manner. Same as in (E) but with the WT Rab1, 4 and 11 (WT, lanes 1–3), and their 'GDP' (SN mutant, lanes 4–6) and 'GTP' (QL mutant, lanes 7–9) locked forms. Input, 5%. **(G)** Endogenous HACE1 binds Golgi-associated Rabs. As in (D) but using HeLa cell lysates instead of purified HACE1 protein. Input, 10%. Lines on the left of the blots in (D–G) indicate the molecular weight marker of 95 kDa.

HACE1 is associated with Golgi membranes

HACE1 lacks a transmembrane domain and has been shown to be associated, at least in part, with the endoplasmic reticulum (ER) in NIH3T3 cells [140]. NIH3T3 cells are not often used in studies of Golgi proteins partially because of their relatively small size. Considering the interactions of HACE1 with Rab1, Rab4 and Rab11, which are at least partially localized to Golgi membranes [8, 11, 17, 141, 142], we determined whether HACE1 localizes to the Golgi during interphase in normal rat kidney (NRK) cells. A fraction of HACE1 co-localized with GRASP65, a Golgi marker, and the rest of the protein appeared to be cytosolic (Figure 4.2A), similar to the results observed in A431 cells (Figure 4.1C). Both the Golgi and cytosolic signals were diminished by the addition of recombinant HACE1 protein to displace the antibodies (Figure 4.2B, anti-HACE1+peptide), suggesting that the antibody had high specificity.

We then treated the cells with chemicals known to affect the Golgi structure. Nocodazole treatment leads to fragmentation of the Golgi ribbon. After nocodazole treatment, HACE1 colocalized with the Golgi remnants indicated by GM130 (Figure 4.2C). Brefeldin A (BFA) treatment leads to Golgi membrane fusion with the ER. In the presence of BFA, Golgi remnants, marked by GRASP65, were dispersed throughout the cell along with HACE1 (Figure 4.2D). After BFA was washed out, HACE1 accumulated in perinuclear regions where the Golgi membranes were concentrated (Figure 4.2E). Finally, in mitotic cells with fragmented Golgi

membranes, HACE1 associated with mitotic Golgi clusters, as determined by the presence of GM130 (Figure 4.2F).

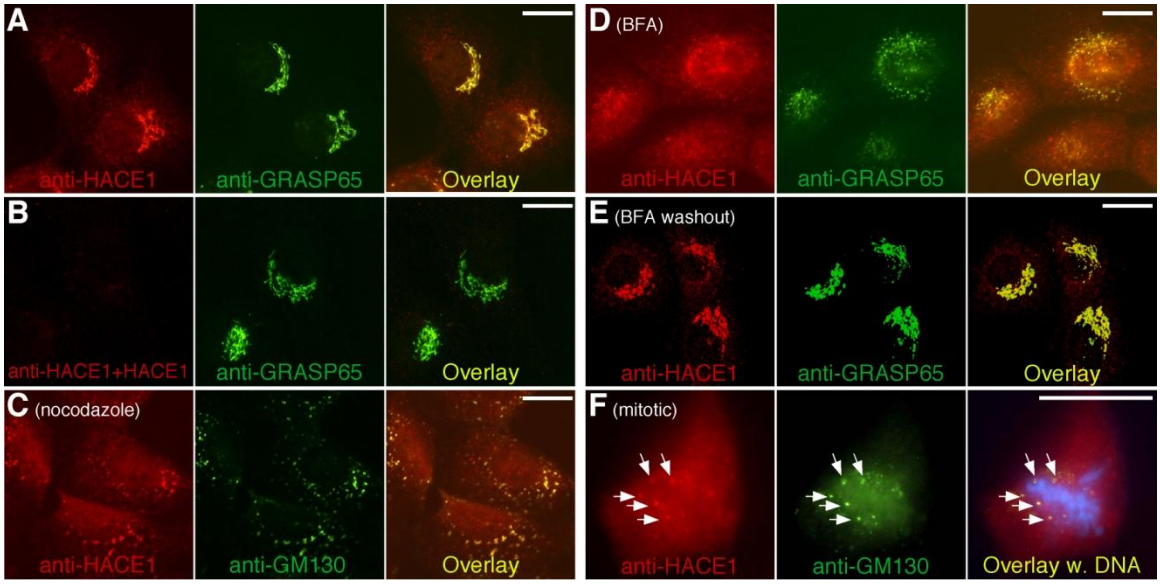

Figure 4.2. HACE1 is concentrated on the Golgi apparatus.
(A) HACE1 is concentrated on the Golgi in interphase cells. NRK cells were immunostained with an affinity-purified polyclonal antibody to HACE1 (left panel, in red) and a monoclonal antibody to GRASP65 (middle panel, in green). **(B)** The HACE1 antibodies are specific. Same as in (A), except the HACE1 antibodies were pre-incubated with purified HACE1 recombinant protein to quench the antibodies. Note that the HACE1 fluorescence was displaced by the recombinant HACE1. **(C)** HACE1 is associated with Golgi fragments after nocodazole treatment. NRK cells were treated with 0.5 μg/ml nocodazole for 2 h and stained for HACE1 and GM130. **(D)** Brefeldin A (BFA) treatment leads to the dispersal of HACE1 in the cell. NRK cells were treated with 5 μg/ml BFA for 2 h and analysed as in (A). **(E)** BFA washout. After the removal of BFA, cells were further incubated in growth media for 2 h and stained for HACE1 and GRASP65. **(F)** HACE1 is partially associated with the Golgi fragments in prometaphase cells. Prometaphase NRK cells stained for HACE1 (red), GM130 (green) and DNA (blue). Note that HACE1 is localized on the mitotic Golgi fragments (indicated by arrows). Scale bars in all panels, 10 μm.

Further microscopic analysis indicated that HACE1 co-localized well with the *cis*-Golgi markers GRASP65, and GM130 (Figure 4.2) and with GalNac-T2-GFP (N-acetylgalactosaminyltransferase 2), a Golgi enzyme localized throughout the Golgi stack (Figure 4.S1) [143]. HACE1 also co-localized with the *medial* and *trans* Golgi markers α-mannosidase II (ManII) [144] and syntaxin 6 [145], though to a lesser extent compared to the *cis*-Golgi markers. In addition, it showed partial co-localization with the ER-Golgi intermediate compartment marker ERGIC53[146] in the perinuclear region where Golgi membranes were

concentrated. Co-localization of HACE1 with *cis*-Golgi markers, compared to other Golgi compartment markers, was more evident when the Golgi apparatus was fragmented by nocodazole treatment (Figure 4.2C, 4.S1).

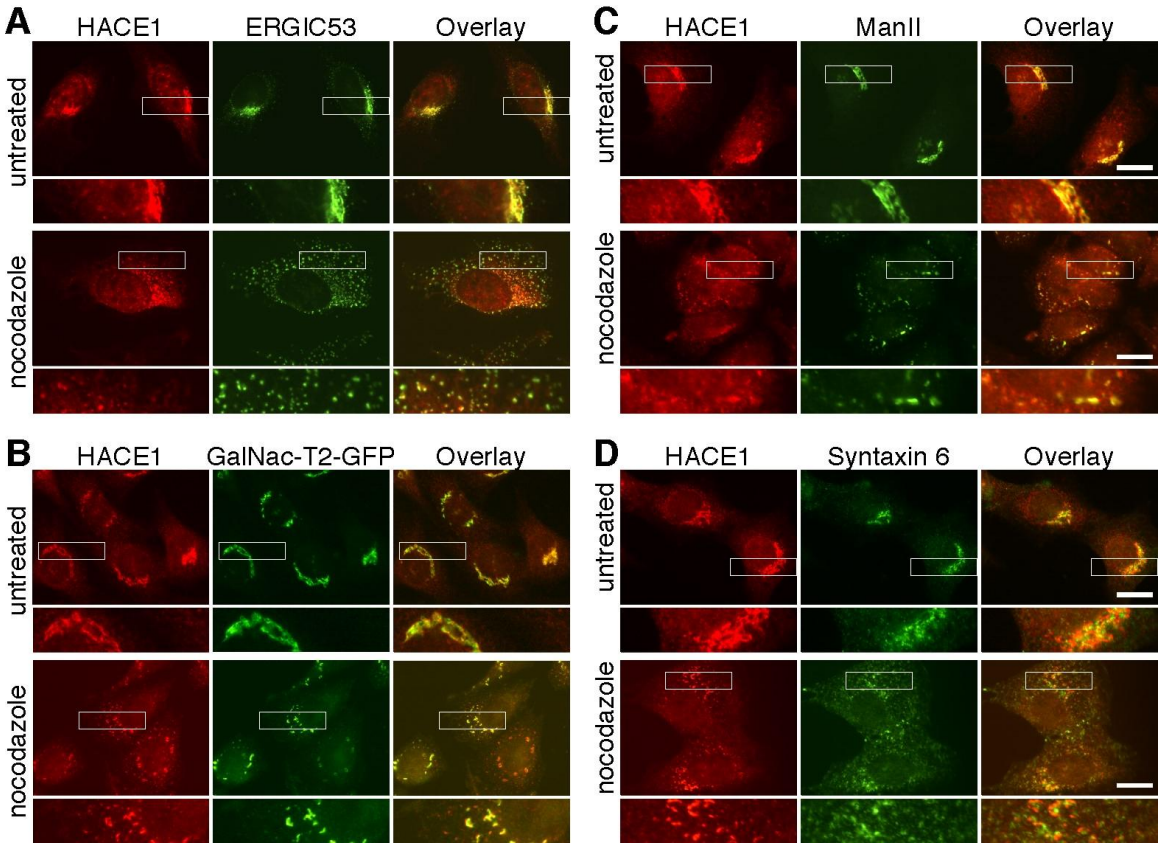

Figure 4.S1. HACE1 co-localizes with *cis*-Golgi markers.
(A) Co-localization of HACE1 with ERGIC53, an endoplasmic reticulum-Golgi intermediate compartment (ERGIC) marker. Untreated (upper panels) and nocodazole-treated (lower panels) NRK cells were immunostained with an affinity-purified HACE1 polyclonal antibody (left panels, in red) and a monoclonal ERGIC53 antibody (middle panel, in green). The overlay is shown on the right. Lower panels are enlarged images of the boxed regions. **(B)** Co-localization of HACE1 with GFP-tagged N-acetylgalactosaminyltransferase 2 (GalNAc-T2-EGFP). Same as in A but with the EGFP signal from stably expressed GalNac-T2-EGFP. **(C)** Co-localization of HACE1 with mannosidase II (ManII), an enzyme localized in the *medial*-Golgi. **(D)** Co-localization of HACE1 with syntaxin 6, a *trans*-Golgi-localized SNARE protein. Scale bars in all panels: 10 μm.

Biochemical analysis also confirmed the association of HACE1 with Golgi membranes. Western blot of cell lysate prepared from unsynchronized interphase NRK cells and nocodazole blocked mitotic cells detected one major band of ~100 kDa (Figure 4.3A). When subcellular

membrane organelles were separated using equilibrium sucrose gradients, the distribution of HACE1 was similar to the Golgi markers GM130, GRASP65, syntaxin 5 and Gos28 but was different from the ER markers Sec61 and protein disulfide isomerase (PDI) (Figure 4.3B). Taken together, these results show that HACE1 is associated with Golgi membranes.

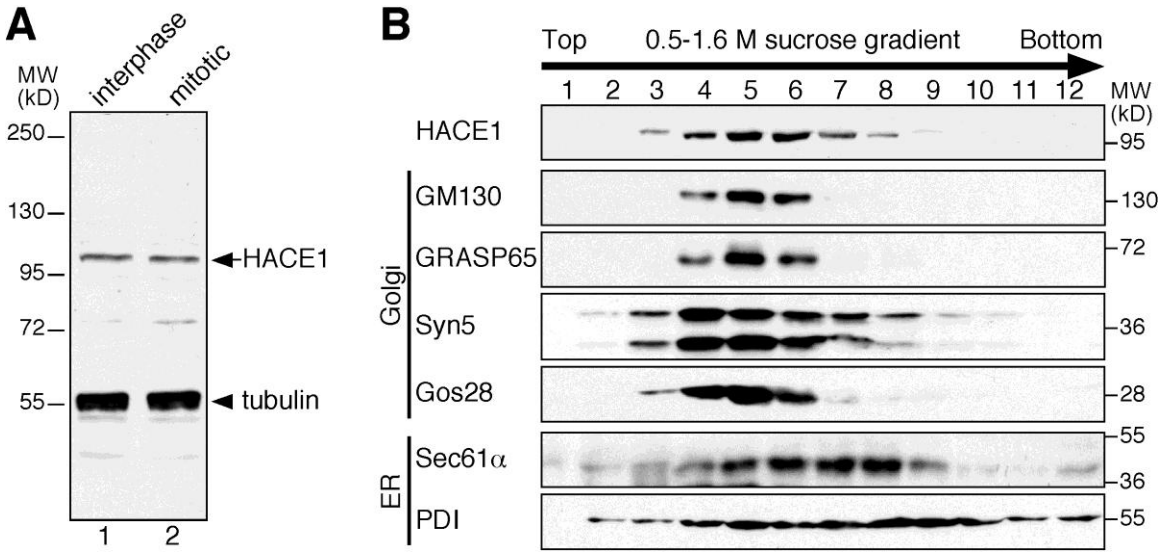

Figure 4.3. HACE1 is a ubiquitin ligase bound to Golgi membranes.
(A) The affinity-purified HACE1 antibody recognizes one major band in NRK cells. Western blot of non-synchronized interphase and nocodazole-treated mitotic NRK cell lysates for HACE1 and tubulin. **(B)** HACE1 colocalizes with the Golgi in sucrose gradients. Post nuclear supernatant (PNS) from interphase NRK cells was fractionated by equilibrium centrifugation on a sucrose gradient (0.5–1.6 M). Membranes from each fraction were pelleted and equal volumes were analysed by western blot for the indicated proteins. Golgi membranes were enriched in fraction 5 (with about 0.8 M sucrose), while ER membranes are more widely distributed and concentrated in heavier fractions.

HACE1 is targeted to the Golgi membrane by Rab1

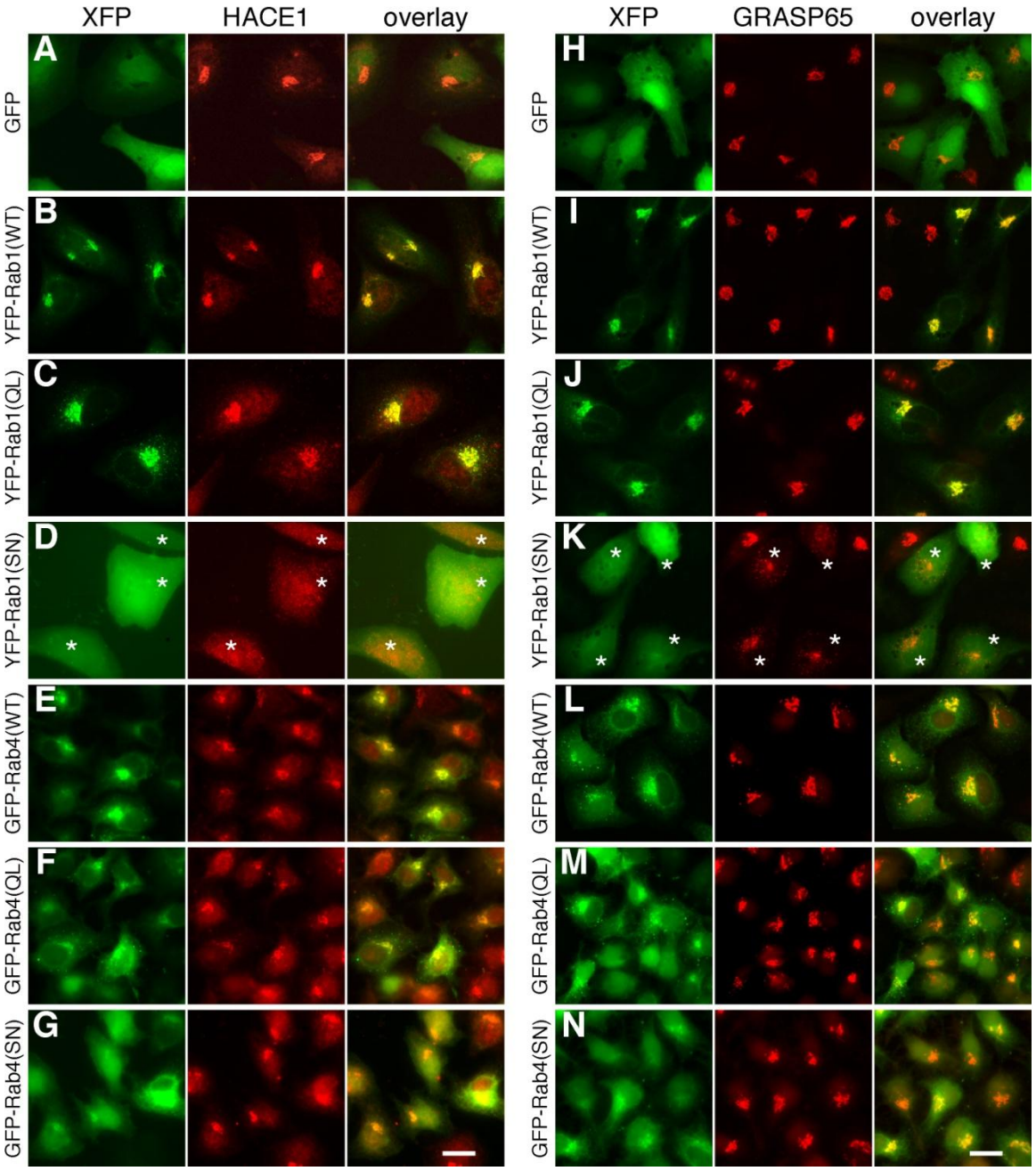

Figure 4.4. Expression of an inactive Rab1 mutant interrupts HACE1 localization and Golgi structure.
HeLa cells expressing GFP (A and H), YFP-Rab1 wild-type or mutant constructs (B-D, I-K), GFP-Rab4 wild-type or mutant constructs (E-G, L-N) as indicated were immunostained for HACE1 (A-G) or GRASP65 (H-N). The overlays with the YFP or GFP signals (in green) are shown on the right. Asterisks indicate cells expressing the Rab1 (SN) mutant, which have HACE1 dispersed from the Golgi membranes (D) and fragmented Golgi (K). Scale bars in all panels: 20 μm.

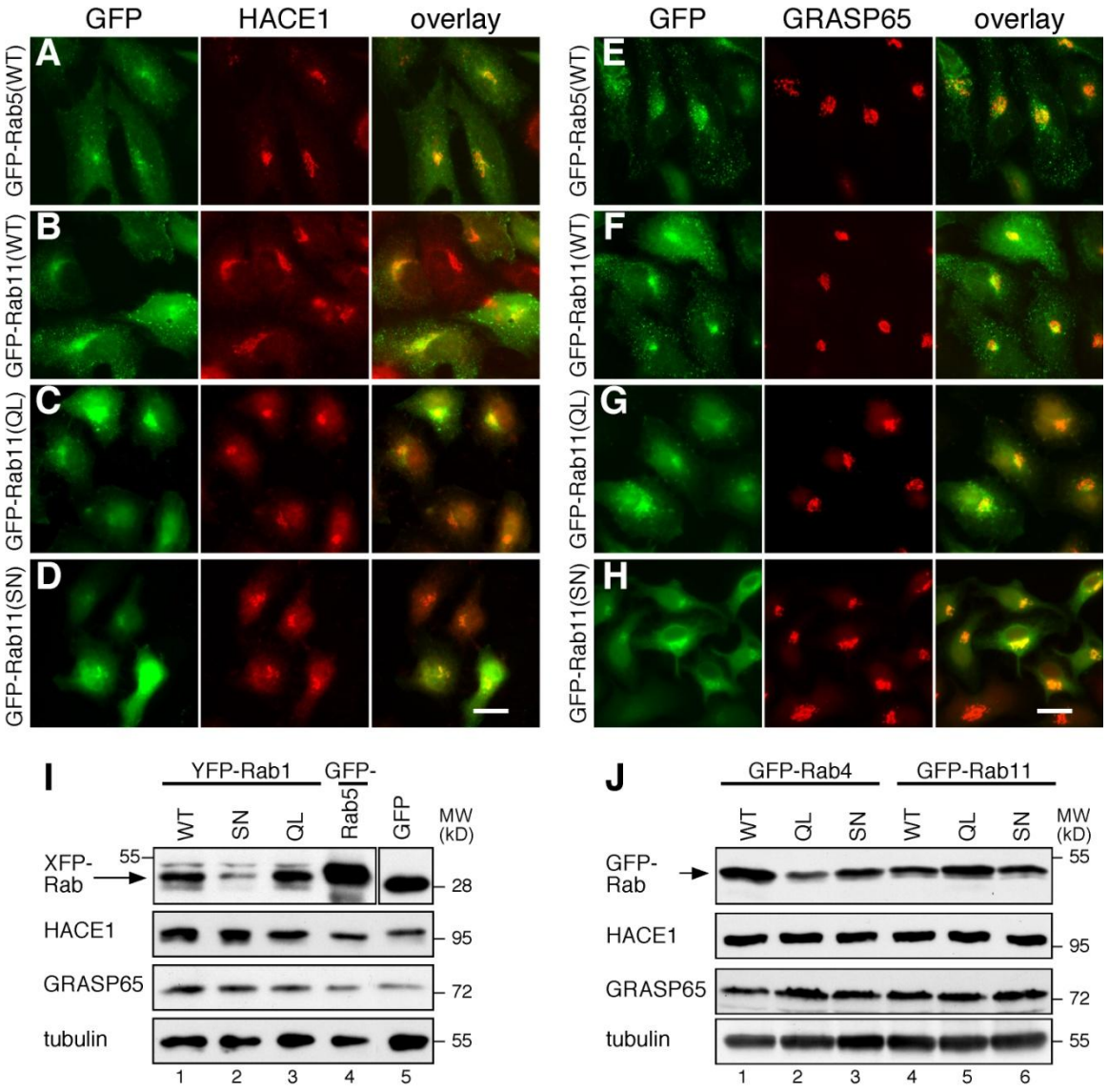

Figure 4.S2. Expression of Rab5 and Rab11 does affect HACE1 Golgi localization and Golgi organization. **(A-H)** HeLa cells expressing the indicated Rab constructs (GFP-Rab5, GFP-Rab11 and mutants) were immunostained for HACE1 (A-D) or GRASP65 (E-H). Scale bars in all panels: 20 μm. **(I-J)** Western blots of cells described in Figure 4.3 and Figure 4.S4A-H. Cells were lysed in SDS buffer followed by Western blot to detect indicated proteins. The split of the GFP blot (lane 5 in I) from the same gel was due to the different sizes of GFP and GFP-Rab.

If Rabs target HACE1 to the Golgi, inhibition of Rab activity may affect HACE1 Golgi localization. We therefore used wild-type and mutant Rabs to test this hypothesis. Expression of wild-type Rabs did not affect HACE1 Golgi localization or Golgi structure (Figure 4.4, 4.S2). In addition, wild-type Rab1, Rab4 and Rab11, but not Rab5, were partially concentrated on Golgi

membranes (Figure 4.1C, 4.4, 4.S2). Expression of the active Rab1 Q67L mutant had no effect on HACE1 localization or Golgi morphology. In contrast, expression of the S25N mutant at a relatively low level (Figure 4.S2I, lane 2 vs. other lanes) disrupted HACE1 Golgi localization (Figure 4.4D). Furthermore, expression of the Rab1 S25N mutant also caused Golgi fragmentation (Figure 4.4K), which is consistent with previous reports [147] and suggests that HACE1 may serve as a Rab1 effector required for Golgi integrity. Expression of Rab4, Rab11 and their mutants had no effect on HACE1 Golgi localization or the Golgi organization (Figure 4.4, 4.S2). Taken together, our data suggest that the interaction of HACE1 with Rab1 is important for HACE1 Golgi localization and function.

HACE1 is required for post-mitotic Golgi membrane fusion

To test the role of HACE1 in the formation of Golgi structure, we expressed myc-tagged wild-type (WT) and mutant HACE1 in HeLa cells and examined Golgi morphology. Deletion of the HECT domain (aa 1-553 lacking the HECT domain, designated HACE1 ΔC) or mutation of cysteine 876 to analine (the CA mutant, Figure 4.5A) abolished the ubiquitin ligase activity [38]. The exogenously expressed proteins were partially localized on the Golgi examined by fluorescence microscopy (Figure 4.5B). Expression of the WT HACE1 did not affect the integrity of the Golgi structure. However, expression of the CA or the ΔC mutant led to Golgi fragmentation; with 33.4 ± 1.4% and 49.8 ± 0.1% of the cells had fragmented Golgi, respectively, which was significantly higher than cells transfected with WT HACE1 (9.6 ± 1.0%) or with the vector alone (8.9 ± 0.1%) (Figure 4.5). These results suggest that HACE1 ubiquitin ligase activity is involved in maintaining Golgi integrity.

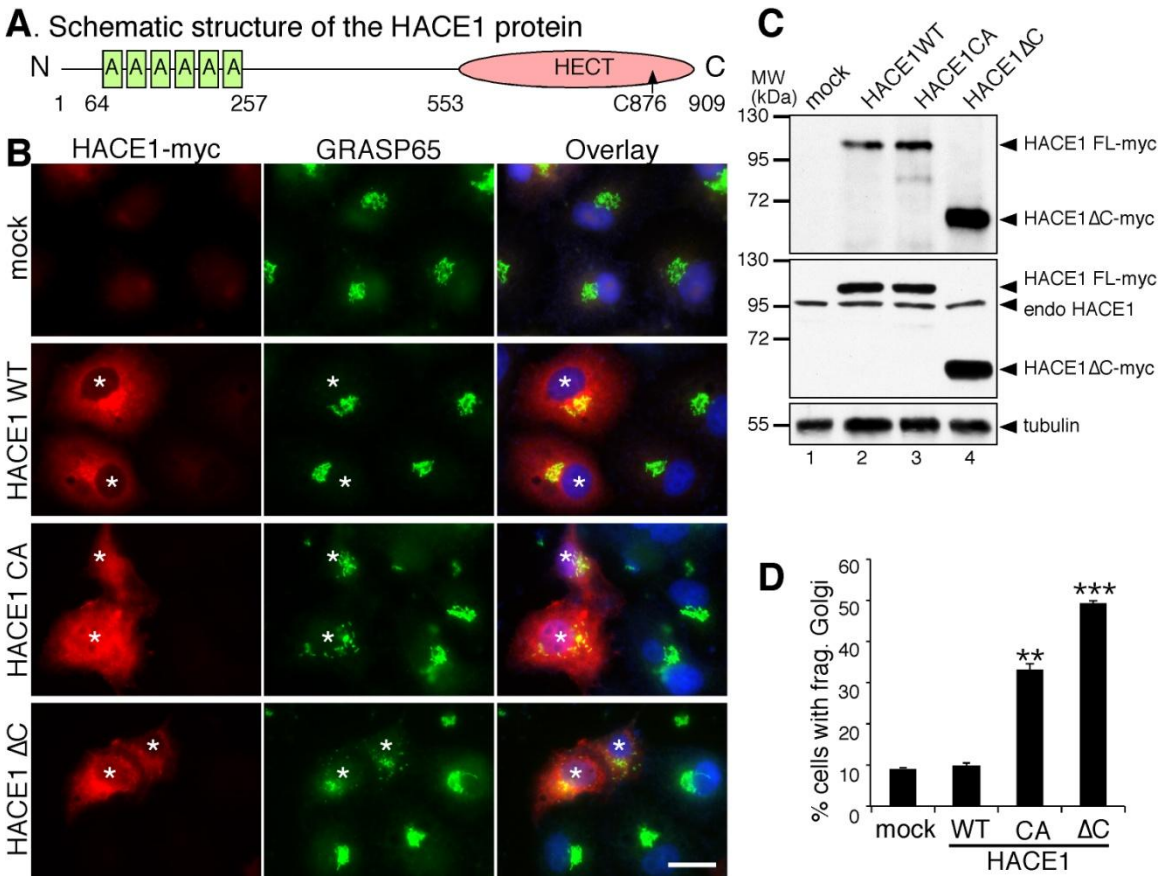

Figure 4.5. Expression of HACE1 mutants leads to Golgi fragmentation.
(A) Schematic structure of HACE1. It contains six ankyrin repeats at the Nterminus and a HECT domain at the C terminus. Cysteine 876 has been shown to be essential for the ubiquitin ligase activity. A construct with the HECT domain deleted (ΔC, amino acids 1–553) was used in this study. **(B)** HeLa cells expressing myc-tagged WT HACE1 protein, the inactive C876A (CA) mutant and the ΔC mutant. Mock transfection with the empty vector. Asterisks indicate transfected cells. Note that expression of the CA and ΔC mutants leads to Golgi fragmentation. Scale bar, 20 μm. **(C)** Western blots illustrating that the correct proteins were expressed. Endo HACE1 refers to endogenous HACE1. **(D)** Quantification of Golgi fragmentation in 300 myc-tagged HACE1-expressing cells for each set of experiments. Shown are representative results (mean ± s.e.m.) from three independent experiments. Statistical significance was assessed by comparison to the mock transfection. *P*-value was determined by Student's *t*-test; $^{**}P < 0.005$; $^{***}P < 0.001$.

Previous experiments have suggested that ubiquitin plays a role in p97/p47-mediated post-mitotic Golgi membrane fusion [35, 36], it is possible that HACE1 functions in the same ubiquitination-deubiquitination pathway. Therefore, we used the standard Golgi disassembly and reassembly assay [8] to test the role of HACE1 in regulation of Golgi membrane dynamics. We first treated purified Golgi membranes with mitotic cytosol to induce membrane fragmentation.

These mitotic Golgi fragments were further treated with interphase cytosol. After incubation, membranes were examined by electron microscopy (EM) and the percentage of membranes in cisternae was quantified [11, 36]. To manipulate HACE1 activity, we added affinity purified anti-HACE1 antibodies, or purified wild-type HACE1 or C876A mutant proteins into either the disassembly or the reassembly reactions. As shown in Figure 4.6, manipulation of HACE1 activity in the Golgi membrane disassembly reaction alone (Figure 4.6A) or in the reassembly alone (Figure 4.6B) had no effect.

Our previous results have demonstrated that ubiquitination occurs during Golgi disassembly and is required for subsequent reassembly [36]; therefore, HACE1 may function in disassembly, which impacts subsequent Golgi reassembly. To test this idea, we first treated purified Golgi membranes with mitotic cytosol in the presence of either HACE1 recombinant protein or HACE1 antibodies and used the resulting Golgi fragments for reassembly. The addition of anti-HACE1 antibodies or the inactive HACE1 C876A mutant protein inhibited subsequent Golgi membrane reassembly. In contrast, the addition of wild-type HACE1 protein enhanced the subsequent Golgi membrane reassembly (Figure 4.6C). These results suggest that the HACE1 ubiquitin ligase activity in mitotic Golgi membrane disassembly is required for subsequent post-mitotic Golgi membrane reassembly.

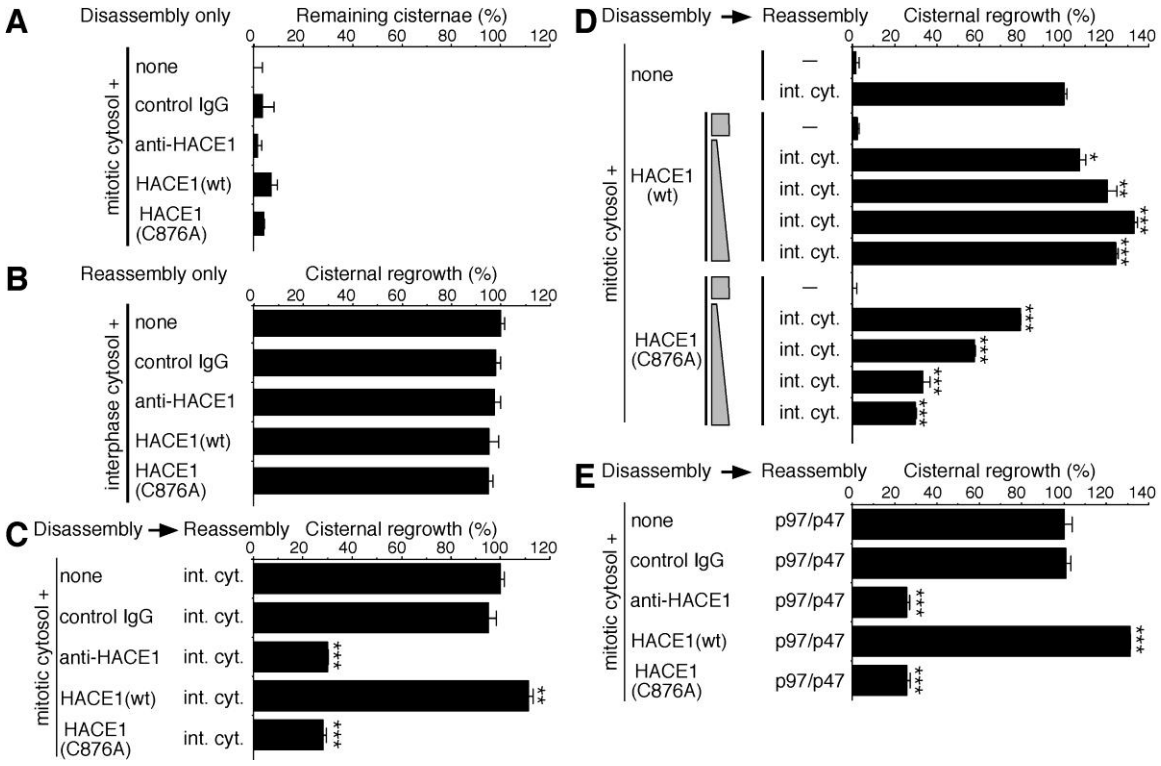

Figure 4.6. HACE1 regulates p97/p47-mediated post-mitotic Golgi membrane reassembly *in vitro*.
(A-B) HACE1 in mitotic Golgi disassembly or post-mitotic reassembly. Purified rat Golgi were treated with mitotic cytosol (mit. cyt.), then with interphase cytosol. Control rabbit IgG, affinity purified anti-HACE1 antibodies or purified proteins of wild-type HACE1 or the C876A mutant were added into the disassembly (A) or reassembly (B) reactions, as indicated. Membranes were processed for EM, and the results were quantified to estimate the percentage of cisternal membranes. Mitotic Golgi fragments (none, 23.6 ± 1.1% membranes in cisternae) were normalized to 0%. Reassembly in interphase cytosol without any additional components (none, 57.1 ± 0.5% membranes in cisternae) was normalized to 100%. **(C)** HACE1 ubiquitin ligase activity in mitotic Golgi disassembly is required for subsequent post-mitotic Golgi membrane reassembly. Golgi membranes were fragmented by mitotic cytosol in the presence of the indicated reagents and incubated with interphase cytosol (int. cyt.). **(D)** HACE1 ligase activity levels correlate with the efficiency of post-mitotic Golgi membrane assembly in a dose-dependent manner. Same as in (C) except with a serial increasing amount (0.1 – 1 μM) of purified wild-type HACE1 or C876A mutant included in the reassembly reactions. 0% represents mitotic Golgi fragments treated with mitotic cytosol and then fixed (24.1 ± 0.6% membranes in cisternae), and 100% represents membranes reassembled in interphase cytosol (58.5 ± 0.5% membranes in cisternae). **(E)** HACE1 affects p97/p47-mediated membrane fusion. Same as in (D), except that mitotic Golgi membranes were subsequently incubated with the purified p97/p47 proteins instead of interphase cytosol. 0% represents mitotic Golgi fragments treated with mitotic cytosol and then fixed (26.5 ± 0.1% membranes in cisternae), and 100% represents membranes reassembled with p97/47 (53.6 ± 1.1% membranes in cisternae). The results represent the mean of three independent experiments ± SEM. P-value was determined by Student's t-test; *, $p<0.05$; **, $p<0.005$; ***, $p<0.001$.

To ensure that the observed effects resulted from the addition of HACE1, we titrated different amounts of HACE1 recombinant protein into the disassembly reaction and used the membranes for subsequent reassembly. Higher concentrations of the WT HACE1 protein

increased the stimulatory effects, whereas increasing the amount of HACE1 C876A mutant increased the inhibitory effects (Figure 4.6D). These results show that HACE1 ligase activity levels are correlated with the efficiency of post-mitotic Golgi membrane assembly in a dose-dependent manner.

We then used the defined Golgi disassembly and reassembly assay [8] to determine whether HACE1 functions through p97/p47-mediated membrane fusion. Similar to the experiments described above, HACE1 antibodies and purified proteins were added to the disassembly reactions, and the generated mitotic Golgi membranes were subsequently incubated with purified p97/p47 proteins. As shown in Figure 4.6E, the addition of anti-HACE1 antibodies or the purified HACE1 C876A mutant protein inhibited Golgi membrane reassembly, in contrast with the stimulatory effect of the WT protein. Because the experimental conditions were optimized for Golgi membrane fusion, the increased reassembly efficiency caused by the addition of wild-type HACE1 strengthened the conclusion that HACE1 is involved in the regulation of Golgi membrane dynamics. Taken together, these results strongly suggest that HACE1 ubiquitin ligase activity in mitotic Golgi disassembly is required for p97/p47-mediated post-mitotic Golgi membrane reassembly *in vitro*.

HACE1 regulates Golgi membrane fusion in cells

To determine whether HACE1 is needed for Golgi integrity *in vivo*, we reduced cellular HACE1 level using small interfering RNAs (siRNA) (Figure 4.7A-B). Four pairs of RNA oligos were tested, and the most efficient pair was selected. HACE1 mRNA levels determined by real-time PCR (RT-PCR) were reduced by 66.8 ± 4.8% and 74.1 ± 4.3% 2 days and 4 days after

transfection, respectively (Figure 4.7C). At the protein level, there was a 62.0 ± 4.8% reduction 4 days after transfection (Figure 4.7D). These results indicate that endogenous HACE1 is a relatively stable protein. Indeed, when cells were treated with the protein synthesis inhibitor cycloheximide (CHX) for 24 hours, HACE1 protein levels were not significantly affected; in contrast, the same treatment caused a noticeable reduction of GRASP65 (Figure 4.S3A). To confirm the specificity of our siRNA oligos, HeLa cells were transiently transfected with a HACE1-myc cDNA and HACE1 or control siRNA oligos. HACE1-myc was expressed well when co-transfected with the control siRNA but not with the HACE1 siRNA (Figure 4.S3B). These results confirmed that the siRNA used to deplete the HACE1 mRNA and protein is specific and, to some degree, effective.

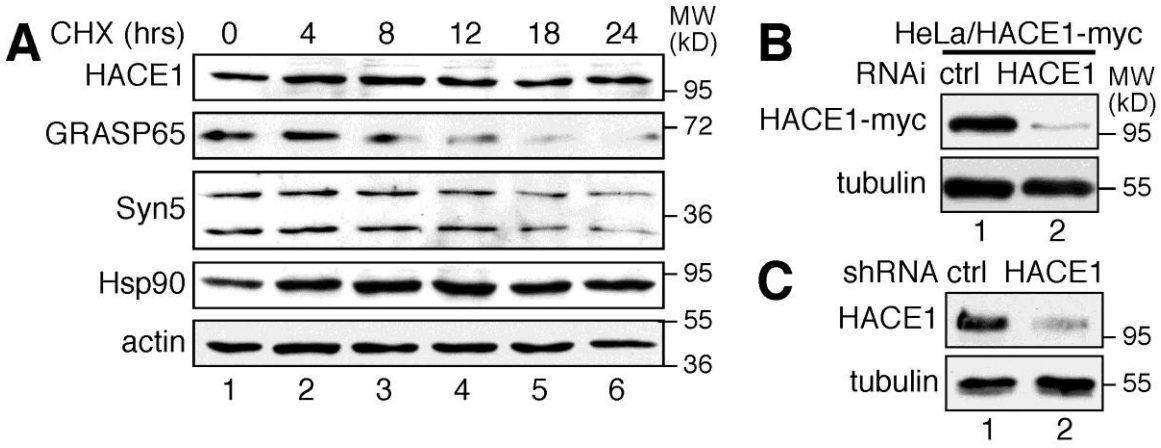

Figure 4.S3. HACE1 depletion in cells.
(A) HACE1 protein levels do not significantly decrease 24 h after cycloheximide (CHX) treatment. NRK cells were incubated in growth media with 20 μg/ml CHX for the indicated time periods (0-24 hours). Cells were lysed in SDS buffer and analyzed for the indicated proteins by Western blot. Note that HACE1 levels remained relatively unchanged 24 h after treatment, while GRASP65 levels reduced. **(B)** Exogenous HACE1 is readily depleted by siRNA treatment. HeLa cells were treated with HACE1 or control siRNA oligos for 3 days followed by transient transfection with a HACE1-myc cDNA. Cells were lysed, and HACE1 and tubulin were detected by Western blot. Note that HACE1-myc expression was reduced in the presence of HACE1 siRNA (lane 2). **(C)** Depletion of HACE1 by lentiviral infection. HeLa cells were infected by control or HACE1 shRNA lentiviral particles followed by Western blot for HACE1 and tubulin.

We then analyzed the Golgi morphology in HACE1-depleted cells. These cells had reduced signal for HACE1 when analyzed by fluorescence microscopy (Figure 4.7A-B). Depletion of

HACE1 led to Golgi fragmentation using GM130 (Figure 4.7 B vs. A), GRASP65 or syntaxin 5 (data not shown) as Golgi markers; 83.0 ± 0.9% of the HACE1-depleted cells exhibited Golgi fragmentation, a significant increase compared to control siRNA transfected cells (4.8 ± 0.2%, Figure 4.7E). Since *in vitro* experiments indicate that HACE1 is involved in post-mitotic Golgi reassembly, we monitored the reformation of Golgi ribbon in control or HACE1-depleted cells using time-lapse microscopy. We infected HeLa cells by lentivirus packaged either an empty vector or a vector encoding HACE1 shRNA and generated stable cells. The knockdown efficiency of the HACE1 protein in these cells was similar to HACE1 siRNA transfection, as assessed by Western blot (Figure 4.S3C). Control cells or HACE1 shRNA-expressing cells were then co-transfected with cDNAs encoding ManII-mCherry to label the Golgi membranes and Histone H2B-GFP to visualize the morphology of the chromosomes in the cells. Metaphase cells with aligned chromosomes were then analyzed by time-lapse microscopy for post-mitotic Golgi formation. The frame right before chromosome separation (the onset of anaphase) was set to 0 time point. Golgi reassembly was completed within 80 ± 5 min in control siRNA treated cells; while in HACE1 knockdown cells, the Golgi remained fragmented 180 min after mitosis (Figure 4.7F-G, Supplementary Movies 4.1-4.2). These results demonstrate that HACE1 depletion impairs post-mitotic Golgi reassembly.

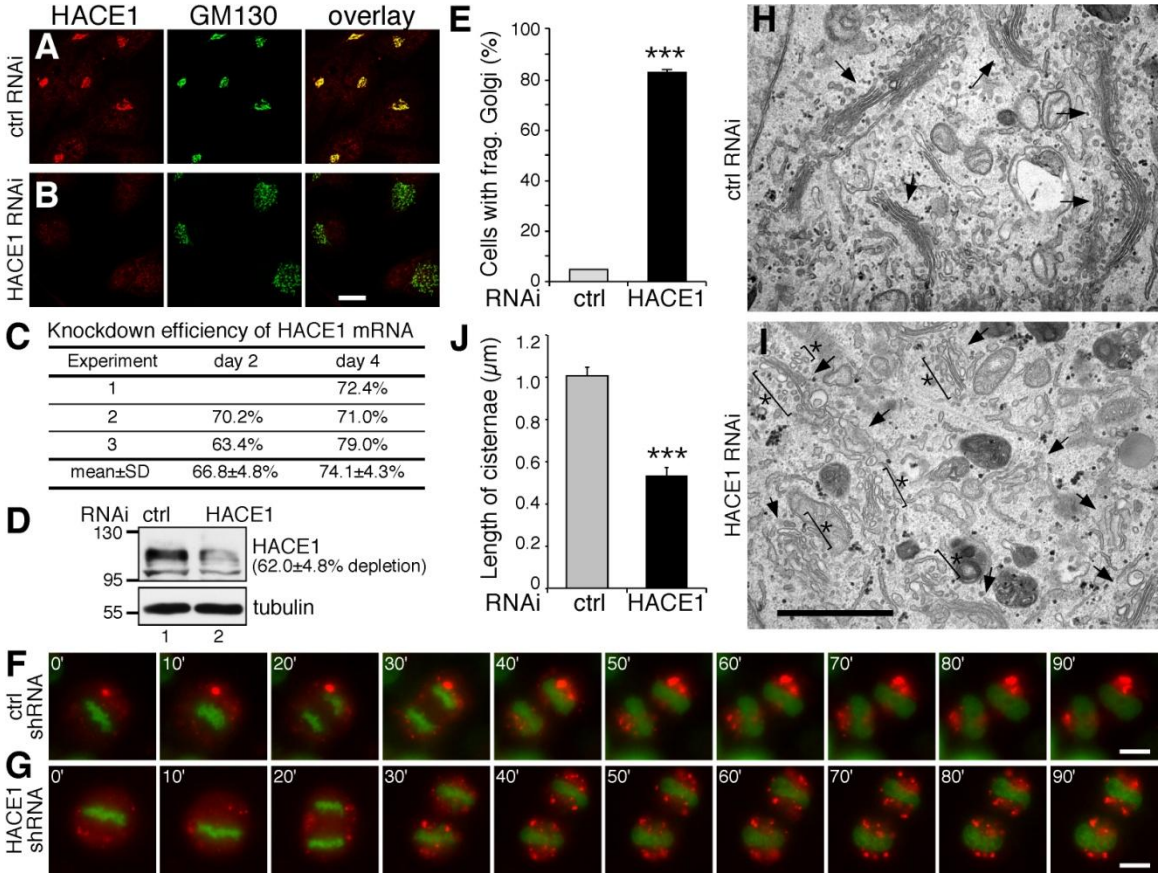

Figure 4.7. Depletion of HACE1 leads to Golgi fragmentation.
(A-B) Confocal fluorescence images of HACE1 knockdown cells. HeLa cells transfected with the indicated siRNA oligos were fixed and stained for HACE1 and GM130. Scale bars in all panels: 20 μm. **(C)** Knockdown efficiency of HACE1 mRNA on days 2 and 4 quantified by RT-PCR. The results presented are the percent reduction in the HACE1 mRNA in HACE1 knockdown cells compared to cells treated in parallel with a control siRNA. **(D)** Immunoblots of HeLa cells described in (A-B). The knockdown efficiency of HACE1 protein was 62.0% ± 4.8% from three independent experiments. **(E)** Quantitation of the fluorescence images in A-B from three independent experiments. Shown is the percentage of cells with fragmented Golgi, and 300 cells were counted for each experiment. The results expressed are the means ± SEM. **(F-G)** HACE1 depletion delays post-mitotic Golgi formation. HeLa cells were infected by control lentivirus (F) or lentivirus that expresses HACE1 shRNA (G). Cells were then co-transfected with cDNAs for Histone H2B-GFP (in green) and Man II-mCherry (in red) followed by time-lapse microscopy in 10 min intervals over 3 h (see Supplementary Movies S1-2). Metaphase cells with aligned chromosomes were set to 0 time point. Scale bar, 10 μm. **(H-I)** Representative EM micrographs of the cells described in A-B. The arrowheads indicate Golgi stacks, and asterisks indicate fragmented cisternal membranes. Scale bar, 1 μm. Note that the Golgi ribbon in HACE1-depleted cells is disorganized, and the cisternae are shorter compared to control siRNA-treated cells. **(J)** Quantitation of the EM images in F-G from three independent experiments. Note that cisternal length is reduced by HACE1 depletion. Statistical significance was assessed by comparison to the control siRNA-treated cells. ***, $p < 0.001$.

We then examined the Golgi structure more closely by EM. Control siRNA transfected cells showed well-organized stacks, which often aligned in parallel to form a ribbon. In contrast, HACE1-depleted cells had fragmented Golgi. The Golgi membranes were disorganized and the

cisternae were relatively short, while a large part of the membranes were vesiculated, and small stacks or single cisterna were dispersed throughout the cells and did not form a ribbon (Figure 4.7, I vs. H). The average cisternal length was reduced from 1.01 ± 0.04 μm in control siRNA transfected cells to 0.53 ± 0.04 μm in HACE1-depleted cells (Figure 4.7J). These results suggest that HACE1 depletion reduces membrane fusion activity, which may subsequently impair Golgi ribbon linking observed as fragmented Golgi under the light microscope (Figure 4.5B, D; 4.7B, E and G).

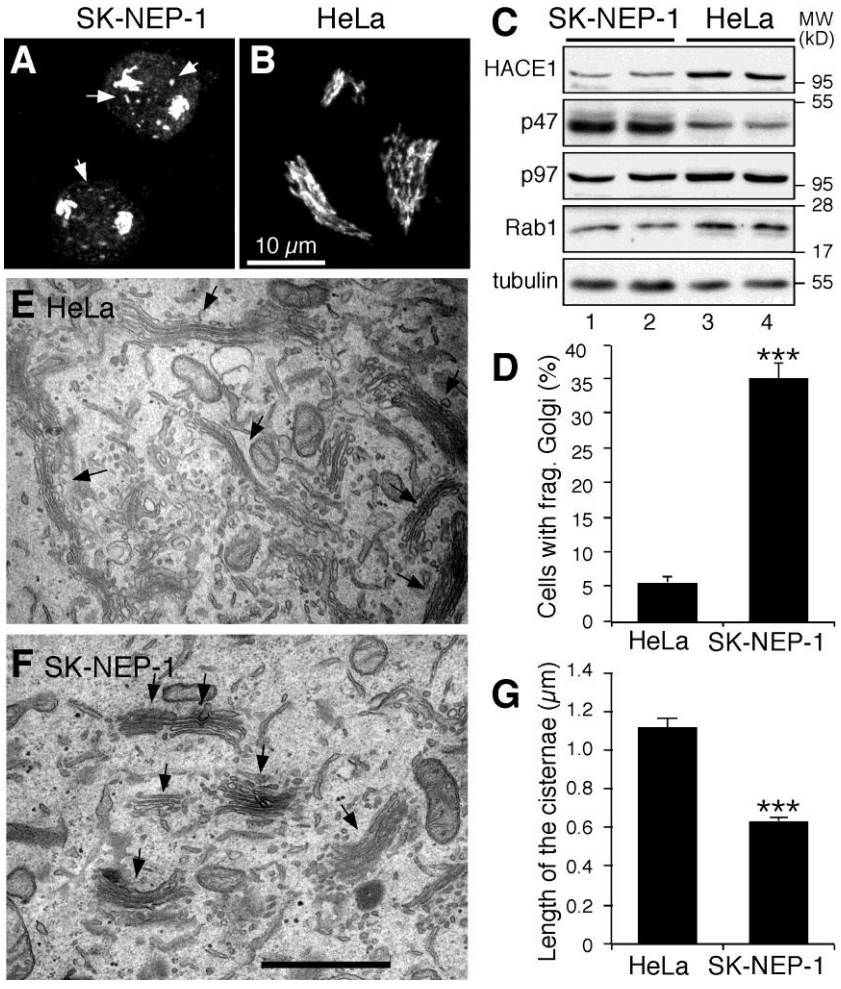

Figure 4.8. The Golgi apparatus is fragmented in SK-NEP-1 cells that have reduced HACE1 expression.
(A-B) Representative fluorescence images of SK-NEP-1 cells showing that the Golgi indicated by GRASP65 is fragmented compared with HeLa cells. Arrows indicate isolated Golgi fragments. Scale bar, 10 μm. **(C)** HACE1 expression is reduced in SK-NEP-1 cells. Western blot detecting HACE1, tubulin, p97 and p47 in HeLa cells and SK-NEP-1 cell lysates. **(D)** Quantification of the number of HeLa and SK-NEP-1 cells containing fragmented Golgi.

(E-F) EM images of (E) HeLa and (F) SK-NEP-1 cells. Scale bar, 1 μm. Note that SK-NEP-1 cells have isolated stacks with relatively short cisternae. **(G)** Quantification of the EM images in (E-F) from three independent experiments. The average length of the cisternae in HeLa cells was 1.12 ± 0.05 μm (mean ± s.e.m.), while in SK-NEP-1 cells it was 0.63 ± 0.02 μm. *P*-value was determined by Student's *t*-test; ***$P < 0.001$.

It has been previously observed that the SK-NEP-1 cell line expresses relatively low level of HACE1 protein [140]; therefore, we examined the Golgi morphology in these cells in comparison with HeLa cells (Figure 4.8A-B). Indeed, HACE1 protein level in this cell line was 30.9 ± 3.1% compared to HeLa cells as determined by Western blots (Figure 4.8C). The expression levels of HACE1 were similar in several cell lines, such as HeLa, A431 and NRK cells (data not shown). When analyzed by fluorescence microscopy, a large number of SK-NEP-1 cells showed fragmented Golgi. Compared to HeLa cells (Figure 4.8B) and several other cell lines in which the Golgi membranes were well organized into a perinuclear ribbon-like structure, the Golgi membranes in SK-NEP-1 cells were disconnected, not localized to the perinuclear region and dispersed throughout the cell. Fragmented Golgi structures were observed in 34.9 ± 2.2% of the SK-NEP-1 cells compared to 5.6 ± 1.0% in HeLa cells (Figure 4.8A, D), suggesting that these cells had a possible Golgi membrane fusion defect.

The SK-NEP-1 cells were then analyzed by EM in parallel with HeLa cells. HeLa cells contained well-organized stacks that often aligned into a ribbon-like structure (Figure 4.8E), whereas in SK-NEP-1 cells the Golgi structure was less well organized. The cisternae were often not aligned into stacks, and the stacks were often more dispersed. More importantly, cisternae were shorter compared to those in HeLa cells. The average length of the SK-NEP-1 cisternae was 0.63 ± 0.02 μm, a significant reduction compared to that (1.12 ± 0.05 μm) found in HeLa cells (Figure 4.8G). Cisternal length was similar in several cell lines tested, including HeLa,

NRK and CHO cells (data not shown). These results agree with the HACE1 knockdown experiment, suggesting that HACE1 regulates Golgi membrane fusion. Taken together, these results demonstrate that HACE1 plays a critical role in Golgi biogenesis during the cell cycle.

Discussion

We have identified the ubiquitin ligase HACE1 that interacts with Rab1 and is targeted to the Golgi membrane. Its activity in mitotic Golgi disassembly is required for subsequent post-mitotic Golgi reassembly mediated by the p97/p47 complex. Depletion of HACE1, or expression of inactive HACE1 mutants, reduced the length of cisternae in the stacks and affected the overall Golgi structure. HACE1 depletion had stronger effect on the Golgi structure than the expression of inactive HACE1; this is likely due to three possible reasons. First, the mutants of HACE1 may not function as strong dominant negative mutants to inhibit the endogenous HACE1. Second, the effect of the exogenous protein may be concentration dependent and the expression level in the cells is heterogeneous. Third, HACE1 exhibits its activity during mitotic Golgi disassembly, which is required for the subsequent Golgi reassembly. Therefore, the effect on the Golgi morphology may require one or more cycles of cell division. The cells transfected with siRNA were examined 96 hours after transfection, whereas the cells expressing the mutant proteins were examined about 16 h after transfection. Most of the siRNA transfected cells should have gone through at least one cell cycle, whereas the percentage of mutant HACE1-expressing cells that went through mitosis was much lower. Nevertheless, these findings provided evidence that HACE1 is a key regulator of Golgi membrane dynamics during the cell cycle. The tight interaction between HACE1 and Rab1 also suggests that HACE1 is an effector of Rab1 GTPases. The expression of Rab1 inactive mutant caused dissociation of HACE1 from the Golgi membranes and Golgi fragmentation, suggesting that Rab1 plays a critical role for HACE1 function on the Golgi membranes. This result is consistent with the requirement of a functional Rab1 for Golgi structure and function [147].

HACE1 was previously identified as a critical tumor suppressor involved in multiple cancers, such as sporadic Wilms' tumor [38, 140, 148]. The mechanism by which HACE1 depletion leads to cancer formation, however, remains elusive. One attractive hypothesis is that the role of HACE1 in cell proliferation is related to its role in regulating Golgi biogenesis during the cell cycle. The Golgi is the central machinery for protein modification, processing, trafficking and secretion. Defects in the Golgi structure and function may directly affect cell growth and proliferation. Golgi defects may also impair the accuracy of protein glycosylation, including cell adhesion molecules on cell surface, which may lead to metastasis. Indeed, abnormal Golgi division has been observed in cancer cells [149], and defects in protein processing and secretion have been related to cancer cell metastasis [150-152].

The mechanism by which ubiquitination and deubiquitination regulate Golgi dynamics remains elusive. It has been shown that the activity of the VCIP135 deubiquitinating enzyme is required for post-mitotic Golgi membrane fusion [36]. Therefore, it is likely that at least one Golgi membrane protein is ubiquitinated by HACE1 at the onset of mitosis when the Golgi undergoes mitotic fragmentation. Monoubiquitination does not result in the degradation of the substrate; instead, it recruits the p97/p47 complex to the Golgi membrane through interaction between the p47 UBA domain and ubiquitin [35, 36]. Subsequently, the p97/p47 complex recruits VCIP135 to the membrane. When the ubiquitin is removed from the substrate(s) by VCIP135, the membranes are subjected to p97/p47-mediated fusion. Consistently, our *in vivo* and *in vitro* experiments demonstrate that the lack of HACE1 activity reduces Golgi membrane fusion and results in short cisternae, possibly because of the reduced recruitment of the p97/p47 complex to the membranes. The reduced cisternal length in the stacks resulted from HACE1-

depletion also suggests that membrane fusion mediated by NSF, another machinery in post-mitotic Golgi membrane fusion, cannot compensate the loss of p97 (and ubiquitin)-mediated membrane fusion activity. Consistent with this, it has been shown that NSF- and p97-mediated Golgi reassembly pathways contribute non-additively to cisternal regrowth [132], but the coordination between two pathways has not been fully elucidated.

Our results suggest a mechanism by which ubiquitination functions as a signal that regulates Golgi reassembly after cell division. The key question for understanding the mechanism requires the identification of the ubiquitinated substrate(s), which will help determine whether the lack of Golgi membrane fusion activity during mitosis is due to ubiquitination of Golgi membrane proteins. It is tempting to speculate that the target in this pathway is part of the membrane fusion machinery that includes SNAREs and SNARE interacting proteins as well as the key Golgi structural proteins such as Golgins and GRASP proteins. Further experiments are necessary to identify these substrates on the Golgi membrane and to determine how HACE1 activity is regulated during the cell cycle.

Materials and Methods

Reagents

All reagents were purchased from Sigma-Aldrich, Roche or Calbiochem, unless otherwise stated. The following antibodies were used: monoclonal antibodies against ERGIC53 (P. Arvan), Gos28 and GM130 (Transduction Laboratories), myc (D. Sheff), syntaxin 6 (BD Biosciences) and α-tubulin (Developmental Studies Hybridoma Bank University of Iowa); polyclonal antibodies against PDI (P. Arvan), GFP [16], GM130 [17], rat GRASP55 [16], GRASP65 [14], α-mannosidase II (G. Warren), p47 and p97 [36], Rab1A, , Rab6 and Rab11 [121], sec61α (Upstate). The HACE1 antibody was generated in rabbits using recombinant GST-HACE1 (aa 1-548) as the immunogen and subsequently affinity purified; it was used at 1:1000 dilution for Western blot and 1:100 for fluorescence microscopy. The GalNAc-T2-GFP cDNA was a gift from G. Warren. Secondary antibodies were from Jackson Lab and Invitrogen. The GST-Rab1a (WT, Q67L and S25N) and GST-Rab2 cDNA constructs were kindly provided by Dr. Graham Warren. The GST-Rab5, GST-Rab6 and GST-Rab11 plasmids were a gift from Dr. Suzanne Pfeffer. GFP-tagged Rab4 (WT, Q67L and S22N) constructs were from Dr. Stephen Ferguson. GFP-Rab11 (WT, Q70L and S25N) constructs were from Dr. David Sheff.

HACE1 identification and Rab interaction

To purify Rab4 effectors, GST-Rab4 was expressed in 20 L of DH5α cells and bound to 2 ml of glutathione beads (GE Healthcare). The sample was equally divided into two tubes and incubated with nucleotide-exchange buffer (NE buffer; 20 mM Hepes-KOH, pH 7.5, 100 mM NaCl, 10 mM EDTA, 5 mM $MgCl_2$ and 1 mM DTT), containing 1 mM GTPγS in one tube and 1 mM GDP in the other, for 20 min at room temperature with rotation. This step was repeated

three times. GST-Rab4 bound to beads was then stabilized with nucleotide-stabilization buffer (NS buffer; 20 mM Hepes-KOH, pH 7.5, 100 mM NaCl, 5 mM $MgCl_2$ and 1 mM DTT) in the presence of 1 mM GTPγS or GDP for 20 min at room temperature with rotation. Beads were then incubated with 50 ml of bovine brain cytosol (20 mg/ml) [139] for 2 h at 4°C. After incubation, the beads were washed with 10 column volumes of NS buffer with 10 μM GTPγS or GDP; 10 volumes of NS buffer containing 250 mM NaCl and 10 μM GTPγS or GDP and 1 volume of 20 mM Hepes-KOH, pH 7.5, 250 mM NaCl and 1 mM DTT. To elute the bound proteins, the beads were incubated with 1.5 column volumes of elution buffer (20 mM Hepes-KOH, pH 7.5, 1.5 M NaCl, 20 mM EDTA, 1 mM DTT and 5 mM GDP) for 20 min at room temperature with rotation. Eluted proteins were analyzed by SDS-PAGE and coomassie blue staining. The bands in the GTPγS lane were excised and analyzed by mass spectrometry. The generated peptide sequences were used to search NCBI EST database.

HACE1 cloning

The ILTSLAEVA peptide identified by mass spectrometry was found in a HACE1 EST clone (NCBI accession no. AI130909). This EST clone was sequenced, and the translated sequence contained three other peptides identified by mass spectrometry: VLEHLSQQE, QNEDLR and DTAQILLLR. The full-length HACE1 cDNA clone was isolated by screening the SUPERSCRIPT HeLa cDNA library (Life Technologies) using a primer derived from the 5' end of this EST sequence. The *HACE1* coding sequence was amplified by PCR using primers that contained EcoRI and BamHI sites at the 5'- or 3'-ends and inserted into pcDNA3.1/myc-His(-)A (Invitrogen) for mammalian expression or and a EcoRI and XhoI fragment into pGEX-6p-1 (GE Healthcare) for expression in *E. coli*. The C876A mutation was introduced using the

QuikChange mutagenesis kit (Stratagene). The HACE1 ΔC construct was generated by inserting an EcoRI/BamHI fragment (aa 1-553) into pCDNA3.1 or an EcoRI/SalI fragment (aa 1-548) into pGEX-6p-1 for antigen preparation. All of the constructs were confirmed by DNA sequencing.

Preparation of HACE1 fusion proteins

GST-HACE1 proteins were expressed in BL21 (DE3) Gold bacteria and purified on glutathione Sepharose beads (GE Healthcare). For the HACE1-Rab interaction assay, the HACE1 protein on glutathione Sepharose beads was cleaved from the tag by PreScission protease, and the supernatant was further incubated with glutathione beads to remove GST-tagged proteins. Untagged HACE1 protein in the supernatant was used to assay binding to Rab proteins.

Thioester bond formation assay

To test whether HACE1 is an active ubiquitin ligase, 60 nM recombinant human ubiquitin activating enzyme E1 (Biomol International), 200 nM recombinant human UbcH7 (Biomol International) [140], 19 μM biotinylated ubiquitin and 600 nM recombinant GST-tagged WT or mutant HACE1 were mixed in 40 μl reactions in reaction buffer that contained 20 mM Tris-HCl, pH 7.4, 50 mM KCl, 5 mM $MgCl_2$, 2 mM ATP, 0.2 M sucrose and protease inhibitors (Roche). Reactions were incubated at 30°C for 60 min and mixed with SDS-PAGE sample buffer with or without DTT followed by detection of HACE1 by Western blot.

Pull-down assay for HACE1-Rab interactions

The interactions between HACE1 and Rab were determined by a pull-down assay following a previously established procedure [11]. For each reaction, GST-tagged Rabs were expressed in BL21 (DE3) bacteria with 125 ml of LB media. The GST-Rabs were immobilized on 25 μl of glutathione beads (bed volume) in a 1.5 ml Eppendorf tube. The beads were washed with 1 ml of NE buffer containing 10 μM GDP or GTPγS and incubated two times with NE buffer containing 1 mM GDP or GTPγS at RT for 30 min. The beads were then washed with 1 ml of NS buffer containing 10 μM GDP or GTPγS and incubated with NS buffer containing 1 mM GDP or GTPγS at room temperature for 30 min.

Five micrograms of HACE1 protein (without a tag) prepared above was incubated with the GDP or GTPγS charged beads in 150 μl of cytosol buffer (20 mM Hepes-KOH pH 7.4, 250 mM NaCl, 5 mM $MgCl_2$, 1 mM DTT, 1% Triton X-100 and protease inhibitors) containing 1 mM GDP or GTPγS at 4ºC for 2 h. The beads were washed three times with cytosol buffer containing 10 μM GDP or GTPγS at 4ºC for 10 min. To elute the bound proteins, the beads were incubated with 12.5 μl of elution buffer (20 mM Hepes-KOH, pH 7.4, 1.5 M NaCl, 20 mM EDTA, 1 mM DTT, 1% Triton X-100 and protease inhibitor cocktail) for 10 min at room temperature. Elution was repeated three times, and the elutions were pooled. Equal volumes were analyzed by Western blot.

To test the interaction between endogenous HACE1 and Rabs, cell lysates were prepared as previously described [28]. Briefly, cells were grown in 10 X 15 cm dishes to 80% confluency, washed with PBS three times, and harvested with 3 ml of homogenization buffer (20 mM Hepes-KOH, pH 7.4, 100 mM NaCl, 5 mM $MgCl_2$, 1 mM DTT and protease inhibitor cocktail). Cells

were cracked with a ball bearing homogenizer to reach 75-80% breakage determined by Trypan blue exclusion. The homogenate was centrifuged for 10 min at 1000 *g* and 4˚C. The post-nuclear supernatant (PNS) was supplemented with 1% Triton X-100 and rotated at 4˚C for 30 min. Solubilized proteins were exchanged into cytosol buffer (20 mM Hepes-KOH pH 7.4, 100 mM NaCl, 5 mM $MgCl_2$, 1 mM DTT, 1% Triton X-100 and protease inhibitors) using the BIO-RAD Econo-Pac® 10DG column following the manufacturer's instructions. Five milligrams of cell lysate was incubated with GDP or GTPγS charged beads in 800 µl of cytosol buffer containing 1 mM GDP or GTPγS at 4ºC overnight. The beads were washed three times with cytosol buffer containing 10 µM GDP or GTPγS at 4ºC for 10 min and once with cytosol buffer containing 250 mM NaCl and eluted with 80 µl of elution buffer for 20 min at RT and subjected to Western blot analysis.

Cell culture

HeLa and NRK cells were routinely cultured in DMEM supplemented with 7.5% fetal calf serum, 2 mM L-glutamine, penicillin (100 U/ml), and streptomycin (100 µg/ml). SK-NEP-1 cells were cultured in McCoy's medium with 15% FCS. For nocodazole treatment, cells were treated with 0.5 µg/ml nocodazole for 2 hours followed by fluorescence microscopy. For BFA treatment and washout, cells were treated with 5 µg/ml BFA for 2 hours, washed twice with PBS and further incubated in growth media for 2 hours. siRNA oligos were designed using the Invitrogen BLOCK-iT™ RNAi Designer software according to the human HACE1 sequence (sense: UAU AGC GCU GAU GUC AAC A(TT), antisense: UGU UGA CAU CAG CGC UAU A(TT)). In a previous report [38], three pairs of RNA oligos from Invitrogen were used to deplete HACE1. These oligos were less effective at knocking down HACE1 than our newly designed oligos.

HeLa and HEK 293T cells were transfected using Lipofectamine RNAiMAX (Invitrogen) following the manufacturer's instructions. Control transfections were performed simultaneously using non-specific siRNA oligos purchased from Ambion. Assays were performed 96 h after transfection unless otherwise stated. Depletion efficiency of endogenous HACE1 was quantified from the Western blot results using the NIH ImageJ software and normalized to tubulin levels. To construct HACE1 knockdown stable cell lines, HeLa cells were infected by MISSION HACE1 shRNA lentiviral particles (Sigma, product # SHCLNV-NM_020771, contains 5 shRNA lentiviral clones) and transduced cells were selected by the addition of 1 μg/ml puromycin into the culture medium. Among the 5 HACE1 shRNA lentiviral clones, clone TRCN0000003414 gave the best knockdown efficiency examined by Western blots (Figure 4.S3C). Lentivirus packaged with the pLentilox3.7-GFP vector was obtained from the University of Michigan Vector Core and used as a control. For expression of exogenous HACE1, HeLa cells were transfected with the indicated HACE1 constructs using Lipofectamine 2000 (Invitrogen).

RT-PCR

mRNA was purified from a 6-cm dish of HeLa cells using RNeasy columns (QIAGEN Inc.). First-strand cDNA was synthesized using Superscript III RT (Invitrogen) and utilized for semi-quantitative real-time PCR using IQ SYBR Green Supermix (Bio-Rad). A Bio-Rad IQ iCycler was used to measure the expression levels of transcripts. The HACE1 mRNA level was normalized to glyceraldehyde 3-phosphate dehydrogenase (GAPDH). Intron-spanning primers are designed using the "Primer 3" software. The following primer sequences were used for HACE1: forward primer: GCTCTTGCAGGGAGACAGGA, reverse primer:

AGTCATTCCCGGAGGCATCT. The GAPDH primers were provided by Dr. Haoxing Xu [153].

Subcellular fractionation and equilibrium gradients

NRK cells at 80% confluency were scraped and resuspended in 800 µl of homogenization buffer (0.25 M sucrose, 1 mM EDTA, 1 mM Mg acetate, 10 mM Hepes-KOH, pH 7.2 and protease inhibitors). Cells were cracked with a ball-bearing homogenizer to a breakage of 75-80%. The homogenate was centrifuged for 10 min at 1000 *g*, 4°C. The postnuclear supernatant (PNS) was removed and subjected to ultracentrifugation in a TLA55 rotor at 120,000 *g* for 60 min. The supernatant (cytosol) was removed, and the membranes in the pellet were resuspended in homogenization buffer. Equal volumes of the PNS, cytosol and membrane fractions were analyzed by SDS-PAGE and Western blot. The PNS was also fractionated on a sucrose gradient as previously described [7, 8, 28].

Microscopy, quantitation and statistical analyses

Immunofluorescence microscopy and the electron microscopy are performed as described [8, 18],[11], collection of mitotic cells were previously reported [28]. For SK-NEP-1 cells, cells were grown on collagen coated glass plate for 24h and processed for immunofluorescence. For antibody displacement, diluted HACE1 antibodies were pre-incubated with 50 µg/ml recombinant HACE1 for 1 h before incubation with the cells. Pictures were taken with a Leica SP5 laser-scanning confocal microscope using a 100X oil lens or a Zeiss Observer Z1 epifluorescence microscope with a 63X oil lens. In interphase cells, fragmented Golgi was defined as scattered dots that were not connected in the perinuclear region. Although some Golgi

membranes were concentrated near the nucleus in SK-NEP-1 cells, multiple miniGolgi (isolated dots detected by fluorescence microscopy) were observed to be dissociated from the major Golgi apparatus. These cells were categorized as containing fragmented Golgi. To quantify the percentage of cells with fragmented Golgi, more than 300 cells transfected with control or HACE1 siRNAs, or with wild type or mutant HACE1 cDNA constructs, were counted, and the results are presented as mean ± SEM (n=3).

For live cell imaging, cells infected with control or HACE1 shRNA lentivirus were co-transfected with cDNAs for ManII-mCherry and H2B-GFP (Addgene) for 16 h. Mitotic cells were analyzed by time-lapse microscopy with 10 min intervals using a Zeiss Axio Observer Z1 epifluorescence microscope with a 63X oil lens and an AxioCam CCD camera using the AV Rel4.8 software (Zeiss). Temperature (37ºC), humidity and CO2 concentration (5%) were maintained using a Tokai Hit Stage Top Incubator (Tokai Hit) during recording.

Electron microscopy

For EM analysis, Golgi stacks and clusters were identified using morphological criteria and quantified using standard stereological techniques [8, 18]. Interphase cells were defined as profiles that contained an intact nuclear envelope. Only stacked structures containing three or more cisternae were measured for cisternal length. Golgi stack images were captured at 11000x magnification to obtain a better view of the stacks. The longest cisterna was measured as the cisternal length of a Golgi stack using the ruler tool in the Photoshop CS3 software or the line tools in ImageJ, both of which gave essentially identical results. At least 20 cells were quantified

in each experiment, and the results represent at least three independent experiments. Statistical significance was assessed by Student's *t*-test.

Golgi disassembly and reassembly assay and quantitation

Golgi membranes were purified from rat liver [154]. Interphase (IC) and mitotic (MC) cytosols were prepared from HeLa S3 cells [129]. His-tagged p47 was expressed in bacteria and purified using nickel beads [35]. p97 was prepared using a bacterial expression system or purified from rat liver cytosol by gel filtration [35, 134]. The Golgi disassembly assay was performed as described previously [7]. Briefly, purified Golgi membranes (20 μg) were mixed with 2 mg of mitotic cytosol, 1 mM GTP and an ATP-regenerating system (10 mM creatine phosphate, 1 mM ATP, 20 μg/ml creatine kinase and 20 ng/ml cytochalasin B) in MEB buffer (50 mM Tris-HCl, pH 7.4, 0.2 M sucrose, 50 mM KCl, 20 mM β-glycerophosphate, 15 mM EGTA, 10 mM $MgCl_2$, 2 mM ATP, 1 mM GTP, 1 mM glutathione and protease inhibitors) in a final volume of 200 μl. In some reactions, 1 μM or an increasing amount (0.1-1 μM) of wild-type or mutant HACE1 recombinant proteins or 10 ng/μl anti-HACE1 antibodies were added into the disassembly assay as indicated. After incubation for 60 min at 37°C, mitotic Golgi fragments (MGF) were isolated and soluble proteins were removed by centrifugation (135,000 *g* for 30 min in a TLA55 rotor) through a 0.4 M sucrose cushion in KHM buffer (20 mM Hepes-KOH, pH 7.0, 0.2 M sucrose, 60 mM KCl, 5 mM $Mg(OAc)_2$, 2 mM ATP, 1 mM GTP, 1 mM glutathione and protease inhibitors) onto a 6-μl 2 M sucrose cushion. The membranes were resuspended in KHM buffer and were either fixed and processed for EM [7, 14, 28] or used in reassembly reactions. For Golgi reassembly, 20 μg of Golgi fragments were resuspended in KHM buffer, mixed with either 400 μg IC or 100 ng/μl p97 and 25 ng/μl p47 in KHM buffer in

the presence of an ATP regeneration system in a final volume of 30 µl and incubated at 37°C for 60 min. The membranes were pelleted by centrifugation, and processed for EM.

For EM analysis, the percentage of membranes in cisternae or in vesicles was determined by the intersection method [14, 128]. Cisternae were defined as long membrane profiles with a length greater than four times their width, and the latter did not exceed 60 nm. Normal cisternae ranged from 20-30 nm in width and were longer than 200 nm. Stacks were defined as two or more cisternae that were separated by no more than 15 nm and overlapped in parallel by more than 50% of their length. All experiments were repeated at least 3 times; statistical significance was assessed by Student's *t*-test.

Acknowledgements

We thank Stephen Ferguson, Suzanne Pfeffer, David Sheff and Graham Warren for Rab constructs, David Sheff for the Rab antibodies, Peter Arvan and Jaemin Lee for the ERGIC and PDI antibodies, Poul Sorensen for the SK-NEP-1 cells, Xiping Cheng and Haoxing Xu for help with RT-PCR, Youjian Chi, Feng Cui, Honghao Zhang and Xiaoyan Zhang for ideas and technical support, and other members of the Wang Lab for suggestions and reagents. We are grateful to Hemmo Meyer for providing us with purified p97 and p47 proteins and Graham Warren for ideas and support pertaining to this project.

This work was supported by the National Institutes of Health (GM087364) and the American Cancer Society (RGS-09-278-01-CSM) to Y. Wang.

Abbreviations

ARF1, ADP-ribosylation factor 1; BFA, Brefeldin A; BSA, bovine serum albumin; EM, electron microscopy; ER, endoplasmic reticulum; ERGIC, endoplasmic reticulum-Golgi intermediate compartment; GalNAc-T2, N-acetylgalactosaminyltransferase 2; GFP, enhanced green fluorescent protein; GRASP65, Golgi reassembly stacking protein of 65 kDa; HACE1, HECT domain and ankyrin repeat-containing E3 ubiquitin protein ligase 1; HECT, Homologous to the E6-AP Carboxyl Terminus; IC, interphase cytosol; Man II, α-mannosidase II; MC, mitotic cytosol; NEM, *N-ethylmaleimide*; NRK, normal rat kidney cells; NSF, N-*ethylmaleimide*-sensitive factor; PBS, phosphate-buffered saline; PDI, protein disulfide isomerase; plk, polo-like kinase; siRNA, small interference RNA; SNARE, SNAP (soluble NSF attachment protein) receptor.

Chapter 5 . Identification of GRASP65-interacting proteins in the cytosol that facilitate Golgi assembly

Abstract

The Golgi peripheral protein GRASP65 was identified as a Golgi stacking factor that links adjacent Golgi cisternae by forming mitotically regulated *trans*-oligomers. Later, GRASP65 was also found required for Golgi ribbon connectivity. Biochemical experiments indicate that GRASP65 function is regulated by proteins in the cytosol. In this study, we have applied biochemical approaches to identify GRASP65-interacting proteins. HeLa cell cytosol was subjected to fractionations using standard biochemical methods followed by affinity chromatography. Proteins that bind to GRASP65 were identified by mass spectrometry and further characterized. Among the identified proteins, clathrin heavy chain, MENA, SHIP2 and Dja1 were confirmed for their interaction with GRASP65 and recruitment to the Golgi membranes. Depletion of these GRASP65-interacting proteins by small interference RNA (siRNA) from HeLa cells resulted in Golgi fragmentation. Interphase cytosol with GRASP65-interacting proteins depleted or inhibited had a reduced activity to enhance GRASP65 oligomerization in a GRASP65-coated aggregation assay, and to promote Golgi reformation in an *in vitro* Golgi reassembly assay. Our study has identified potential cytosolic factors that play essential roles in Golgi formation.

Introduction

In mammalian cells, the Golgi apparatus displays a unique ribbon-like structure which occupies the cell center and locates adjacent to the centrosome. The Golgi consists of dozens of stacked Golgi cisternae, which are aligned parallel to each other tightly. Golgi stacks are further connected laterally into a ribbon [155]. During cell division, the Golgi apparatus is equally partitioned into the two daughter cells through a unique disassembly and reassembly process. At the onset of mitosis, the Golgi complex undergoes ribbon unlinking, cisternae unstacking and membrane vesiculation, yielding thousands of vesicles that are dispersed throughout the cytoplasm and partitioned into the two daughter cells. During telophase and cytokinesis, the Golgi is reassembled by vesicle fusion to generate new cisternae, cisternae restacking and ribbon linking [4, 5]. During Golgi disassembly and reassembly, one of the Golgi matrix proteins, GRASP65 (Golgi ReAssembly Stacking Protein, 65kD), has been demonstrated to play significant roles in Golgi cisternal stacking and ribbon linkage [13, 14, 17, 18].

GRASP65, together with its homolog GRASP55, are the only two proteins that have been shown to direct participate in Golgi cisternae stacking [12, 13]. GRASP65 localizes to the *cis*-Golgi while GRASP55 localizes to the *medial*/*trans*-Golgi [12]. Depletion of either GRASP65 or GRASP55 reduced the number of Golgi cisternae in Golgi stacks, possibly due to losing the *cis*- or the *medial*/*trans*-Golgi cisternae respectively. Simultaneously depleting both GRASPs led to complete disassembly of the Golgi stacks [15-17]. GRASPs from adjacent Golgi cisternae form *trans*-oligomers therefore zip the cisternae into a stack [14, 16, 17]. During mitosis, GRASPs are phosphorylated by mitotic kinases. The phosphorylation of GRASPs inhibits their oligomerization and leads to cisternae separation [14, 16, 17]. After mitosis, GRASPs are

dephosphorylated by phosphatases, which allows the reformation of GRASP trans-oligomers and restacking of Golgi cisternae [7, 14, 16-18].

GRASP65 and GRASP55 are also involved in Golgi ribbon formation. Depletion of either GRASP causes Golgi ribbon break down [49-51]. It has been suggested that GRASPs link Golgi stacks into a ribbon through forming *trans*-oligomers from the rim of neighboring Golgi stacks, similarly to their mechanism in cisternae stacking. However, since the gaps between Golgi stacks in the ribbon are always larger and relatively more heterogeneous (10s to 100s nm) compared to the gaps between Golgi cisternae in the stack (11nm, [156]), it is also possible that GRASPs tethers Golgi stacks via the bridging of some GRASP- interacting proteins. For example, golgins that mediate membrane tethering by their long coiled-coil rod domain are ideal candidates [55]. A good example is GM130, a golgin that interacts with GRASP65 [103]. Depletion of GM130 from the cells leads to Golgi fragmentation, similarly to the effect of GRASP65 knock down, suggesting that GRASP65 may tether Golgi stacks through GM130 [57].

In this study, we have applied biochemical approaches to identify GRASP65-interacting proteins by affinity chromatography and mass spectrometry. Among the identified proteins, clathrin heavy chain (CHC) [157, 158], mammalian enabled homologue (MENA) [159], SH2-containing inositol phosphatase 2 (SHIP2, also known as INPPL1, inositol polyphosphate phosphatase-like 1) [160, 161] and heat shock protein DnaJA1 (Dja1) [162] were confirmed for their interaction with GRASP65 and recruitment to the Golgi membranes. Depletion of these GRASP65-interacting proteins by small interference RNA (siRNA) from HeLa cells led to Golgi fragmentation. These proteins were required to enhance GRASP65 oligomerization in a

GRASP65-coated bead aggregation assay and facilitate Golgi reassembly in an *in vitro* Golgi reassembly assay. Therefore, our study has identified cytosolic GRASP65-interacting proteins that play essential roles in Golgi ribbon formation.

Result

Identification of GRASP65-interacting proteins in the cytosol

In our previous work, Dynal M-500 magnetic beads that were coated with purified GRASP65 were used as a model system to mimic the tethering of Golgi membrane mediated by GRASP65 oligomerization [14, 17, 18]. When GRASP65 coated beads were incubated with either interphase cytosol or buffer containing some BSA, the beads were able to form aggregates, suggesting that GRASP65 oligomerization acts to link neighboring surface together. It is worth to note, that the aggregation was more dramatic when the beads were incubated with interphase cytosol, suggesting that interphase cytosol contains components that facilitate GRASP65 oligomerization [14]. In this study, we first confirmed this previous finding. Aggregation efficiency of GRASP65-coated beads after incubation with interphase cytosol vs. equal concentration of BSA was first determined. As shown in Figure 5.1A, purified HeLa cytosol significantly enhanced the aggregation efficiency of GRASP65 coated beads (92.7 ± 3.5%) compared to buffer containing BSA (34.2 ± 2.8%) (Figure 5.1B), consistent with our previous report [14]. To further confirm that interphase cytosol contains GRASP65 oligomerization enhancing factors, GRASP65 coupled beads that were dispersed by mitotic kinases treatment were incubated with either purified PP2A which dephosphorylates GRASP65 or interphase cytosol. When the aggregates of GRASP65 beads were treated with mitotic kinases cdc2 and plk1, phosphorylation and de-oligomerization of GRASP65 disassemble the bead aggregates into single beads. Dephosphorylation of GRASP65 by subsequent PP2A treatment allowed GRASP65 beads to tether as clusters, which, however, were much smaller compared to the ones formed with subsequent interphase cytosol treatment (Figure 5.S1A). This result further

confirmed the existence of interphase cytosolic components that facilitate GRASP65 oligomerization.

To determine the biochemical property of these factors, we treated the interphase cytosol with high salt, heat and protease. All these treatments abolished the activity of interphase cytosol to enhance GRASP65-coated beads aggregation, suggesting that the cytosolic factors are proteins in nature (Figure 5.S1B). Furthermore, experiments using a variety of nucleotides or their analogues showed that these factors require ATP but not ATP hydrolysis for their activity (Figure 5.S1C). We then tried to enrich the GRASP65-oligomerization-enhancing factors from interphase cytosol by sequential ammonium sulfate precipitation followed with a glycerol velocity gradient. Enrichment of these factors was followed by GRASP65 bead aggregation. As shown in Figure 5.S2, the factors were enriched in 10-20% and 20-30% ammonium sulfate precipitants (Figure 5.S2A). When the 15-30% ammonium sulfate precipitants of cytosol were further fractionated by the velocity gradient, the enhancing factors were enriched in the 9^{th} fraction out of 12 fractions from top to the bottom of the gradient. This result suggested that the factors that enhance GRASP65 oligomerization form big protein complexes of approximately 1000 kDa (Figure 5.S2B).

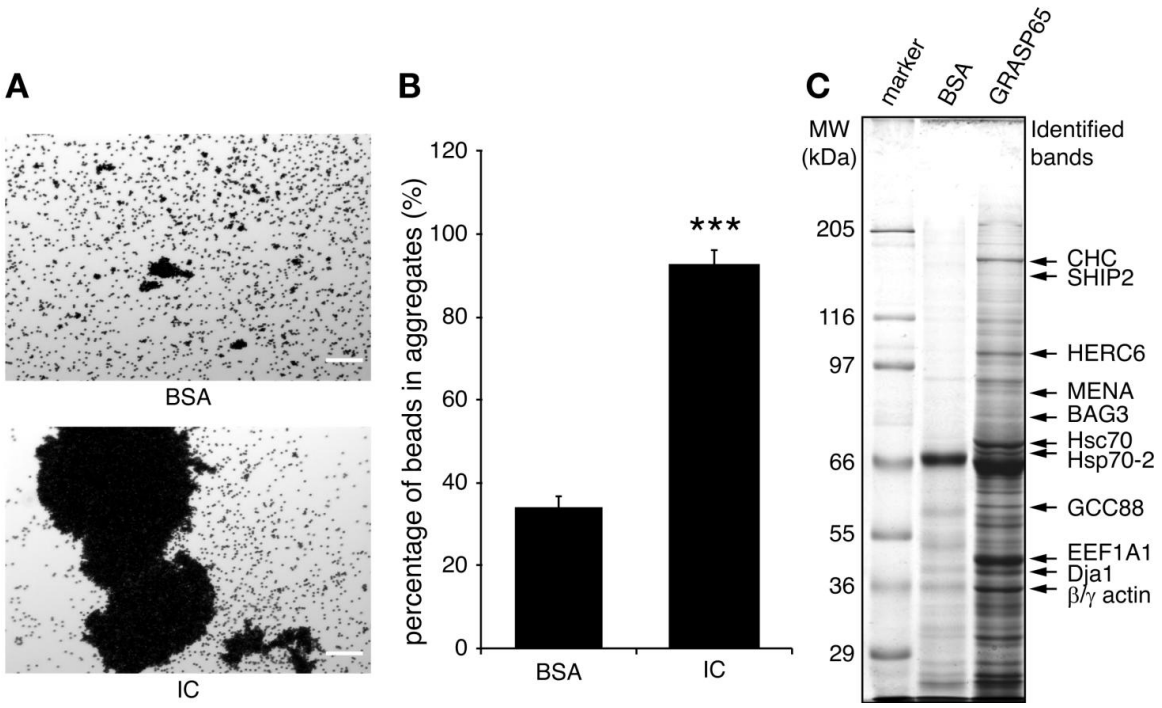

Figure 5.1. Identification of cytosolic factors that enhance GRASP65 oligomerization.
(A) GRASP65 pre-coupled Dynal M-500 beads were incubated with either buffer containing BSA or HeLa interphase cytosol (IC). After incubation, the beads were placed on glass slides and random fields were photographed. A representative image of each condition is shown. Scale bar, 100 μm. Note that interphase cytosol greatly enhanced GRASP65 beads to form large aggregates. **(B)** Quantification of the percentage of GRASP65 coupled beads in aggregation after incubated with BSA and interphase cytosol. P-value was determined by Student's t-test; ***, $p<0.001$. **(C)** Affinity purification of GRAS65-interacting proteins. Interphase cytosol fractionated by 15-30% ammonium sulfate precipitation was incubated with either BSA or His-GRASP65 coupled beads, the bound proteins were analyzed by SDS-PAGE and coomassie blue staining. Arrows indicate the bands that were excised and determined by mass spectrometry.

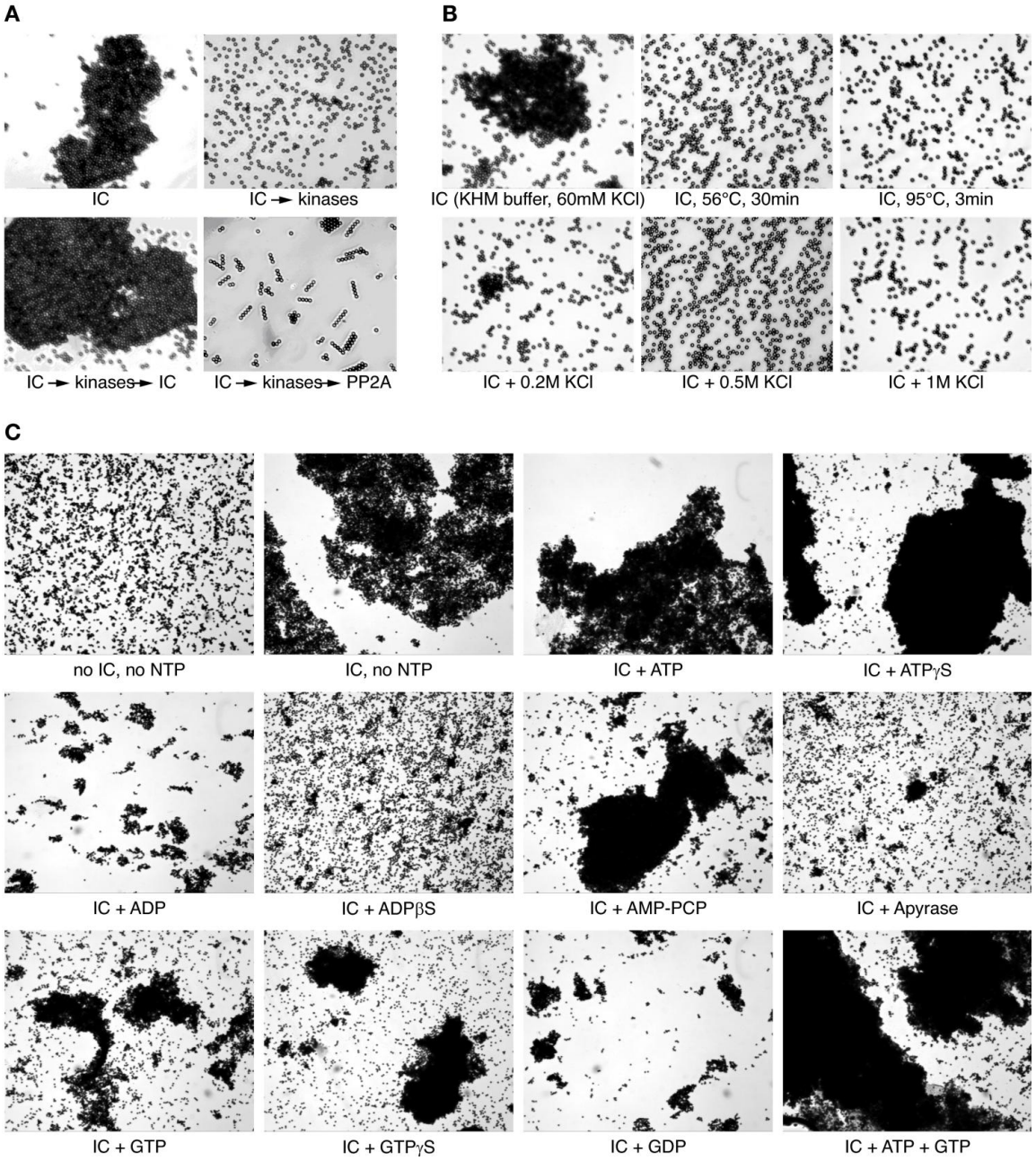

Figure 5.S1. Biochemical properties of the cytosolic factors that enhance GRASP65 oligomerization.
(A) GRASP65 coupled beads incubated with interphase cytosol (IC), then isolated and treated with kinases (IC→kinases), and further treated with either interphase cytosol (IC→kinases→IC) or PP2A (IC→kinases→PP2A) **(B)** GRASP65 coupled beads incubated with interphase cytosol that was treated with indicated conditions. **(C)** GRASP65 coupled beads incubated under indicated conditions, with or without interphase cytosol, plus ATP or GTP or their analogs.

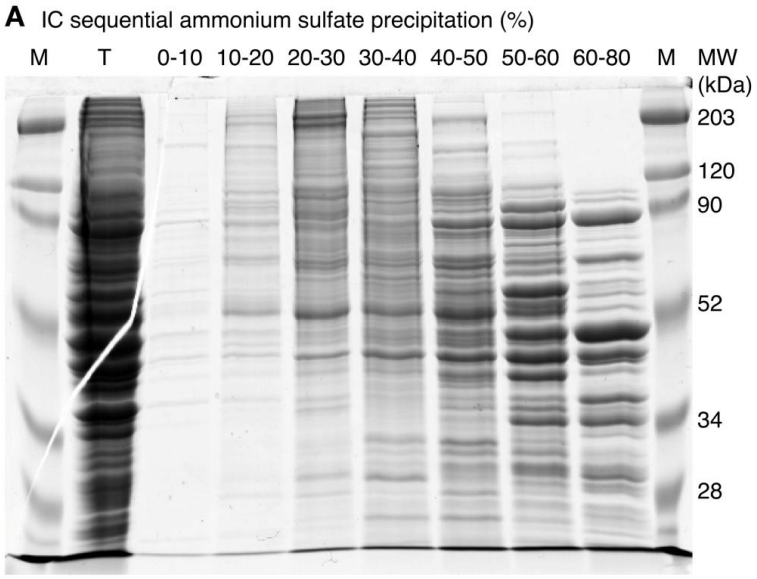

%ASP	Activity
Total	++++
0-10	+
10-20	+++
20-30	++++
30-40	++
40-50	+
50-60	+/-
60-80	-

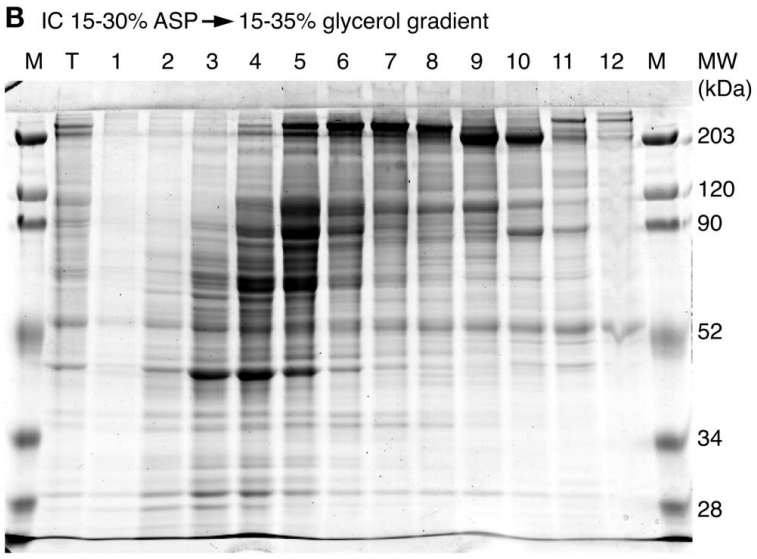

Fraction	Activity
Total	+++
1	+
2	+
3	+/-
4	+/-
5	+/-
6	+++
7	++
8	++
9	++++
10	++
11	+
12	+

Figure 5.S2. Enrichment of cytosolic proteins that enhance GRASP65 beads aggregation.
(A) Proteins from interphase cytosol were fractionated by sequential ammonium sulfate precipitation. Proteins that precipitated at indicated ammonium sulfate cut were dissolved and dialyzed into KHM buffer, analyzed by SDS-PAGE and coomassie blue staining (left panel) and tested for activity in GRASP65 bead aggregation assay (right panel). **(B)** Cytosolic protein that were precipitated at 15-30% ammonium sulfate cut were dissolved and dialyzed then further separated by a 15-35% glycerol gradient. The gradient was then fractionated from top to the bottom into 12 fractions. The proteins in each fraction were analyzed by SDS-PAGE PAGE and coomassie blue staining (left panel) and tested for activity in GRASP65 bead aggregation assay (right panel).

To identify these cytosolic proteins that enhance GRASP65 beads aggregation, proteins enriched from HeLa cell cytosol by 15-30% ammonium sulfate cut was subjected to affinity chromatography and mass spectrometry. The ammonium sulfate precipitants of cytosol was

collected, dissolved, dialyzed and then incubated with GRASP65 or BSA cross-linked cyanogens bromide (CNBr) beads. After extensive washing, the bound proteins were analyzed by SDS-PAGE and coomassie blue staining. A number of protein bands that specifically bound to GRASP65 but not to BSA were excised and analyzed by mass spectrometry (Figure 5.1C).

Table 5.S1. Proteins identified from affinity chromatography of GRASP65

1	Clathrin heavy chain	190KD	a	
2	Matrin-3	93KD	f	
3	SHIP2 (INPPL1)	139KD	a	c
4	SFPQ (splicing factor, proline and glutamine-rich)	76KD	f	
5	RAVER1	70KD	f	
6	UBASH3A (ubiquitin-associated and SH3 domain-containing protein A)	76KD	e	
7	HERC6	112KD	a	e
8	MENA (ENAH, enabled homolog)	89KD	d	
9	BAG3	62KD	b	
10	ALS2 (Alsin)	88KD	b	
11	Hsc70 (HSPA8)	71KD	a	b
12	Hsp70-2 (HSPA2)	72KD	b	
13	poly(rC) binding protein	40KD	f	
14	RING finger protein C14orf4	84KD	e	
15	APPBP1 (Amyloid beta precursor protein binding protein 1)	61KD	e	
16	Pyruvate kinase	59KD		
17	DCLK2 (serine/threonine-protein kinase)	85KD		
18	GCC1 (GRIP and coiled-coil domain containing protein, GCC88)	88KD	c	
19	EEF1A1 (Elongation factor 1-alpha)	48KD	d	
20	Dja1 (DNAJA1)	46KD	a	b
21	ACTB, ACTG	42KD	d	
22	CTBP2 (C-terminal binding protein 2)	47KD	f	
23	HNRPA (heterogeneous nuclear ribonucleoprotein A)	34KD	f	

Categories of identified proteins: **(a)** clathrin associated; **(b)** chaperone; **(c)** membrane trafficking related; **(d)** actin associated; **(e)** ubiquitin enzymes; **(f)** DNA interacting proteins.

As listed in Table 5.S1, twenty-three proteins were identified, which can be categorized into 6 groups: 1) clathrin heave chain and its associated proteins, 2) protein chaperones ; 3) membrane trafficking related proteins; 4) actin associated proteins; 5) ubiquitin conjugating enzymes; and 6) DNA binding proteins. To further select possible candidates, we performed *in vitro* binding assay to test the interaction of each candidate with GRASP65, as well as depleting each candidate by RNAi from HeLa cells to examine their effect on the Golgi structure. Those candidates that have high affinity with GRASP65 and caused Golgi morphological change upon depletion were further characterized (see below and Table 5.S2), including clathrin heavy chain (CHC) [157, 158], a J-domain heat shock protein Dja1 [162], actin nucleation promoting factor MENA [159], and inositol 5-phoaphatase SHIP2 [160, 161].

Table 5.S2. Characters of identified GRASP65-interacting candidate proteins

Protein Name	Interaction with GRASP65 (in vitro)	Effect upon knock down	Localization on Golgi
Clathrin heavy chain	+++++	Golgi fragmentation	Lots of
SHIP2 (INPPL1)	++	Golgi fragmentation	some
HERC6	+++	No effect	some
MENA (ENAH)	++	Golgi fragmentation	Lots of
BAG3	-	No effect	some
Hsc70	+/-	Golgi fragmentaion	little
Hsp70-2	+/-	No effect	little
GCC88	N/A	N/A	Lots of
EEF1A1 or 2	+/-	Golgi fragmentation	little
DjA1 (DNAJA1)	+++++	Golgi fragmentation	little
β/γ-actin	+/-	Golgi fragmentation	Lots of

CHC, Dja1, MENA and SHIP2 interact with GRASP65 in vitro

We first confirmed the interactions between the candidates and GRASP65 by affinity chromatography. Interphase cytosolic proteins that were enriched by a 15-30% ammonium sulfate precipitation were incubated with either BSA or GRASP65 immobilized CNBr beads. After washing, the bound proteins were analyzed by western blotting. As shown in Figure 5.2A, CHC, Dja1, MENA and SHIP2 all interact with GRASP65 but not BSA. In contrast, Hsc70, which was found in the pull-down and identified by mass spec (Figure 5.1C), did not demonstrate a strong interaction with GRASP65, suggesting its binding with GRASP65 shown in the mass spectrometry result was either trivial or non-specific.

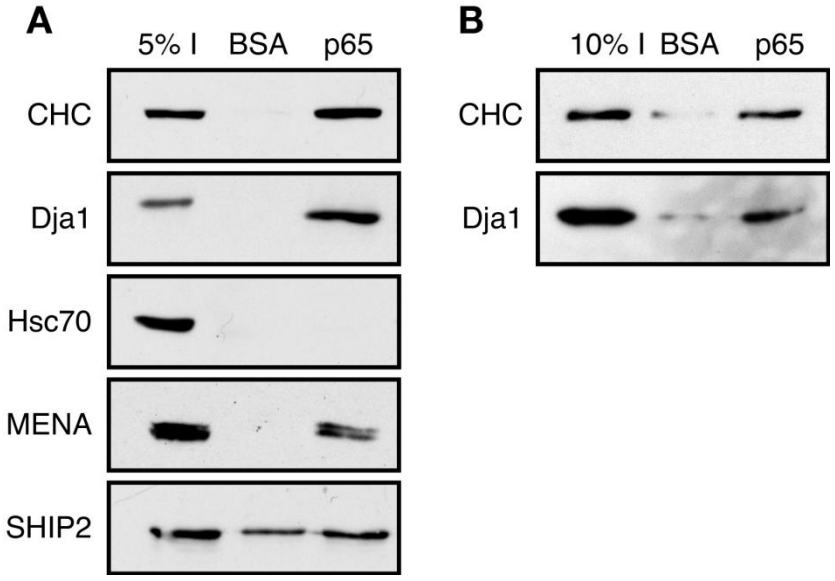

Figure 5.2. GRASP65 interacts with CHC, Dja1, MENA and SHIP2.
(A) GRASP65 interacts with CHC, Dja1, MENA and SHIP2 in the interphase cytosol. BSA or His-GRASP65 coupled CNBr beads were incubated with interphase cytosol fractionated by 15-30% ammonium sulfate precipitation. After extensive washing, bound proteins were analyzed by SDS-PAGE and probed for indicated proteins. **(B)** Purified full length clathrin or His-Dja1 was incubated with BSA or MBP-GRASP65 coupled CNBr beads which were pre-blocked by BSA. Indicated proteins were detected from the bound fraction.

Next we examined whether the interaction between the candidates and GRASP65 is direct by using purified recombinant proteins. Instead of proteins that were precipitated from the cytosol, purified recombinant CHC or His-tagged Dja1 proteins were tested in GRASP65 affinity chromatography. As Figure 5.2B shows, CHC and Dja1 directly binds GRASP65 but not BSA.

CHC, Dja1, MENA and SHIP2 are recruited to the Golgi membranes

Among the four candidates we tested, only CHC is known as a protein locates on the Golgi complex. CHC is enriched on the trans-Golgi network (TGN), and is required for TGN to endosomal/lysosomal transport which is mediated by clathrin coated vesicles [48]. In collaboration with Dr. Frances Brodsky lab and Dr. Bo Huang lab, we also found that CHC colocalized with GM130 on the *cis*-Golgi using STORM microscopy (shown in Chapter 6, Figure 6.4). We then examined whether Dja1, MENA and SHIP2 also localize on the Golgi complex in HeLa cells. By immunostaining, we found that a fraction of MENA and SHIP2 colocalized with GRASP65 on the Golgi, while the rest appeared to be cytosolic (Figure 5.3A). Exogenously expressed GFP-tagged MENA or SHIP2 also partially localized on the Golgi apparatus (Figure 5.3B). However, GFP-Dja1 was not enriched on the Golgi. Due to the lack of good antibodies for Dja1, we were unable to achieve a conclusion whether endogenous Dja1 is on the Golgi by immunofluorescence microscopy (not shown).

Since cytosolic proteins such as Dja1 may be too abundant in the cytosol to present a clear enrichment on the Golgi, we then tested whether Dja1 binds Golgi membranes using an *in vitro* Golgi recruitment assay. Purified rat liver Golgi (RLG) membranes were incubated with interphase or mitotic cytosol, or sequentially treated with mitotic cytosol followed by interphase cytosol to mimic the change in the cell cycle (Figure 5.3C). The membrane bound proteins were analyzed by Western blotting. As a Golgi protein, CHC was found on purified RLG and after cytosol incubations. Hsc70 and its co-chaperon Dja1 were not found on the purified RLG, but can be recruited to the Golgi membrane from interphase cytosol. Similarly, MENA and SHIP2

were recruited to the membrane from both interphase and mitotic cytosol. These results indicated that GRASP65 binding proteins can be recruited to the Golgi and play a role there.

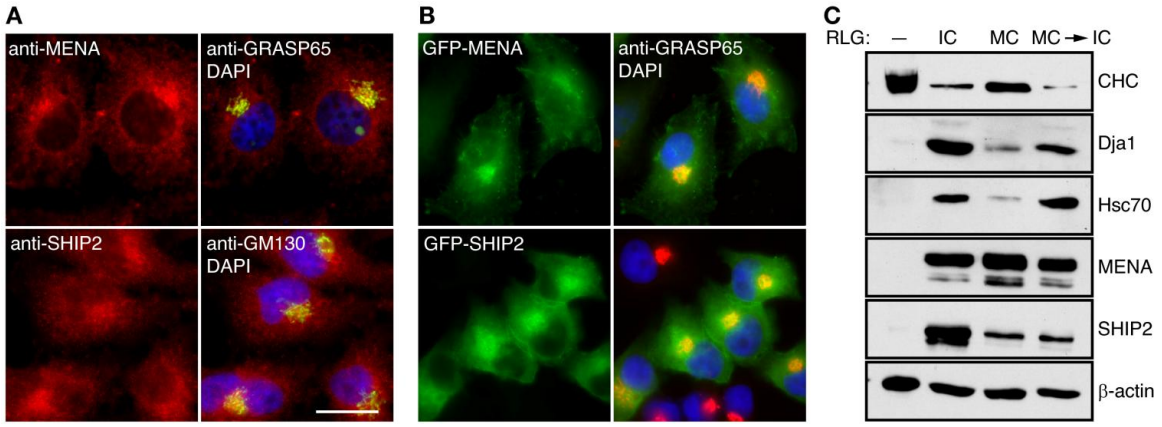

Figure 5.3. CHC, Dja1, MENA and SHIP2 can be recruited to the Golgi membrane.
(A) Endogenous MENA and SHIP2 partially localize to the Golgi. HeLa cells were immunostained with indicated antibodies. Scare bar, 20 μm. **(B)** Exogenous MENA and SHIP2 are concentrated on the Golgi. HeLa cells expressing indicated GFP-tagged constructs were fixed and stained with indicated Golgi marker. Scare bar, 20 μm. **(C)** Purified rat liver Golgi membranes with no treatment (–), incubated with interphase cytosol (IC), mitotic cytosol (MC), or subsequently incubated with mitotic cytosol and then interphase cytosol (MC→IC), were analyzed by SDS-PAGE and western blotting for indicated proteins.

CHC, Dja1, MENA and SHIP2 are required for Golgi ribbon integrity

We then asked whether the four candidates play a role in maintaining Golgi structure in the cells. We depleted CHC, Dja1, MENA or SHIP2 from cells by RNA interfernce (RNAi) and examined Golgi morphology by immunofluorescence and electron microscopy (EM) (Figure 5.4). All four proteins were effectively knocked down after 96 hrs siRNA transfection (Figure 5.4, A-D, L-O). Under fluorescence microscope, depletion of CHC, Dja1, MENA and SHIP2 all led to Golgi fragmentation, with GRASP65 (Figure 5.4, A & C) or GM130 (Figure 5.4, B & D) as Golgi maker. In control siRNA transfected cells, only 9.0 ± 0.2% of the cells had fragmented Golgi. Conversely, in CHC, Dja1, MENA and SHIP2 depleted cells, the percentage of cells with fragmented Golgi increased significantly to 68.2 ± 6.0%, 92.3 ± 1.4%, 78.2 ± 1.5% and 72.9 ± 0.6%, respectively (Figure 5.4J).

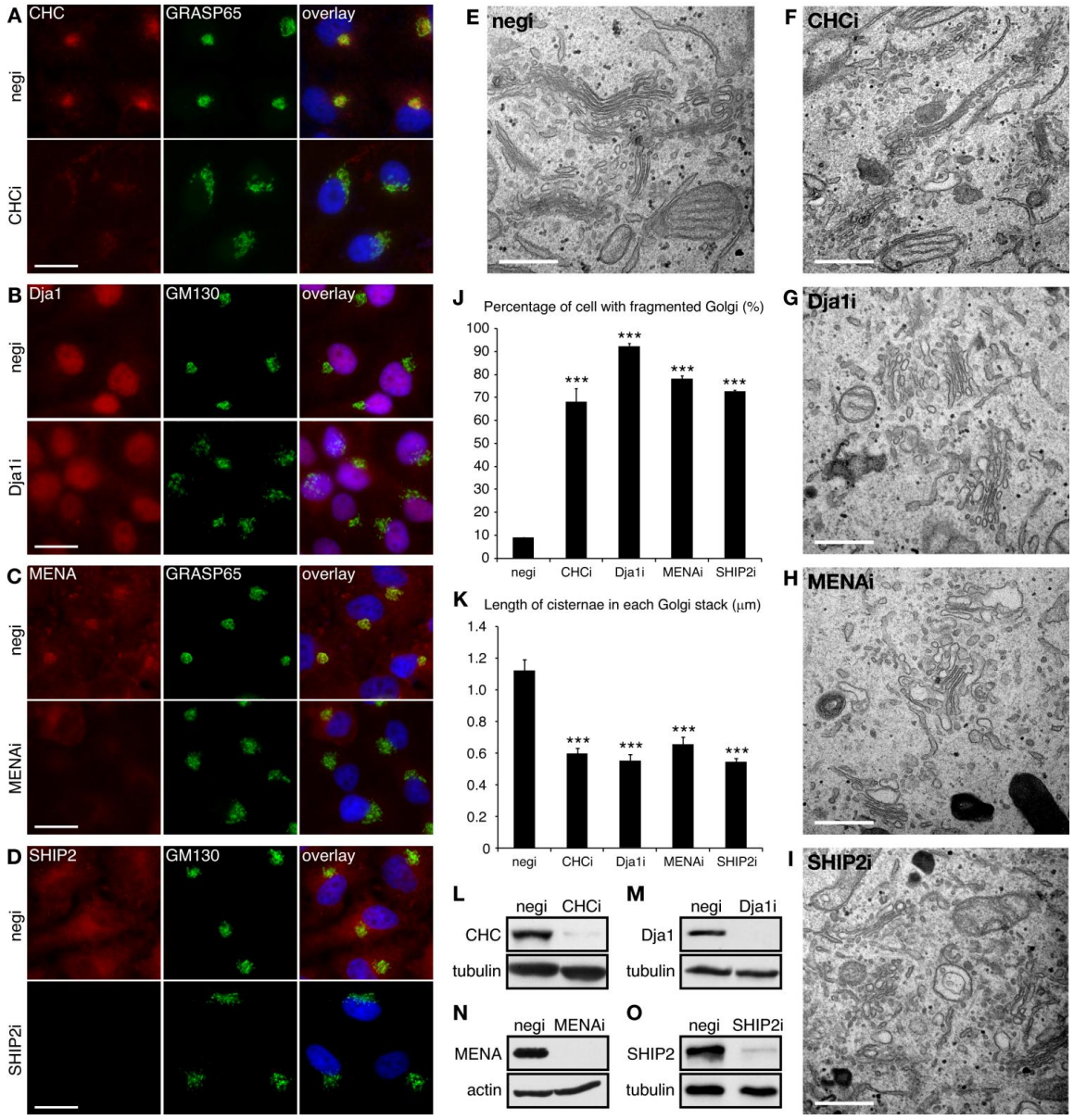

Figure 5.4. Knock down of CHC, Dja1, MENA or SHIP2 leads to Golgi fragmentation.
(A-D) HeLa cells transfected with control or indicated siRNA were fixed 96 h after transfection, immunostained by indicated antibodies. Note the fragmented Golgi in the knock down cells. Scale bar, 20 μm. **(E-I)** HeLa cells transfected with indicated siRNA were fixed and processed for EM. Note that the Golgi stacks in CHC, Dja1, MENA and SHIP2 depleted cells were disconnected, shorter in length and more vesiculated. Scale bar, 500 nm. **(J)** Quantification of percentage of cells with fragmented Golgi among 300 siRNA transfected cells for each set of experiments. Statistical significance was assessed by comparison to the negative siRNA transfection. P-value was determined by Student's t-test; ***, $p<0.001$. **(K)** Quantification of average length of Golgi stacks in 20 siRNA transfected cells. Statistical significance was assessed by comparison to the negative siRNA transfection. P-value was determined by Student's t-test; ***, $p<0.001$. **(L-O)** Western blot illustrating that the indicated protein was depleted from the cell. Actin or tubulin was used as loading control.

We then examined Golgi morphology in the knockdown cells more closely by EM. In control siRNA-transfected cells, the Golgi appeared as well-organized stacks that were linked

laterally into a ribbon. However, in cells with CHC, Dja1, MENA or SHIP2 depleted, the lateral linkage of Golgi ribbon was disrupted, with each Golgi stack shorter in length and decorated with many local vesicles (Figure 5.4E-I). Quantification of the EM images showed that the average length of each Golgi stack notably reduced from 1.23 ± 0.08 μm as in control siRNA transfected cells to 0.66 ± 0.04, 0.60 ± 0.04, 0.72 ± 0.05, and 0.59 ± 0.02 μm in CHC, Dja1, MENA and SHIP2 depleted cells, respectively (Figure 5.4K). These results suggested that these GRASP65 binding proteins participate in Golgi structure organization.

CHC, Dja1, MENA and SHIP2 enhance GRASP65 oligomerization

Since interphase cytosol greatly enhanced GRASP65 oligomerization as shown in the bead aggregation assay (Figure 5.1A). We then asked whether the identified cytosolic GRASP65-interacting proteins contribute to this activity. To test this possibility, CHC or MENA was immuno-depleted from interphase cytosol, which resulted in significant reduction of CHC or MENA level from the cytosol (Figure 5.5A). The immuno-depleted cytosol was then used to incubate GRASP65 coated beads in the bead aggregation assay. Depletion of CHC or MENA had notably decreased the activity of interphase cytosol in enhancing GRASP65-coated beads aggregation (40.5 ± 2.5% and 33.9 ± 2.4% of the beads in aggregation, respectively) compared to control IgG depleted cytosol (84.2 ± 3.9% of the beads in aggregation) (Figure 5.5 B-D, H). Due to incomplete immuno-precipitation abilities of the antibodies, SHIP2 or Dja1 in the interphase cytosol was immuno-blocked by polyclonal antibodies against them. The pre-treated cytosol was then used in the bead aggregation reactions. Inhibition of SHIP2 or Dja1 led to reduced of the aggregation efficiency of GRASP65 coated beads (48.6 ± 2.1% and 43.5 ± 2.5%, respectively), in comparison with control IgG pre-treated cytosol (80.1 ± 1.9%) (Figure 5.5 E-G, I). These

results confirmed that CHC, Dja1, MENA and SHIP2 enhance GRASP65 bead aggregation, possibly by enhancing or stabilizing GRASP65 oligomerization, or cross-link GRASP65 oligomers.

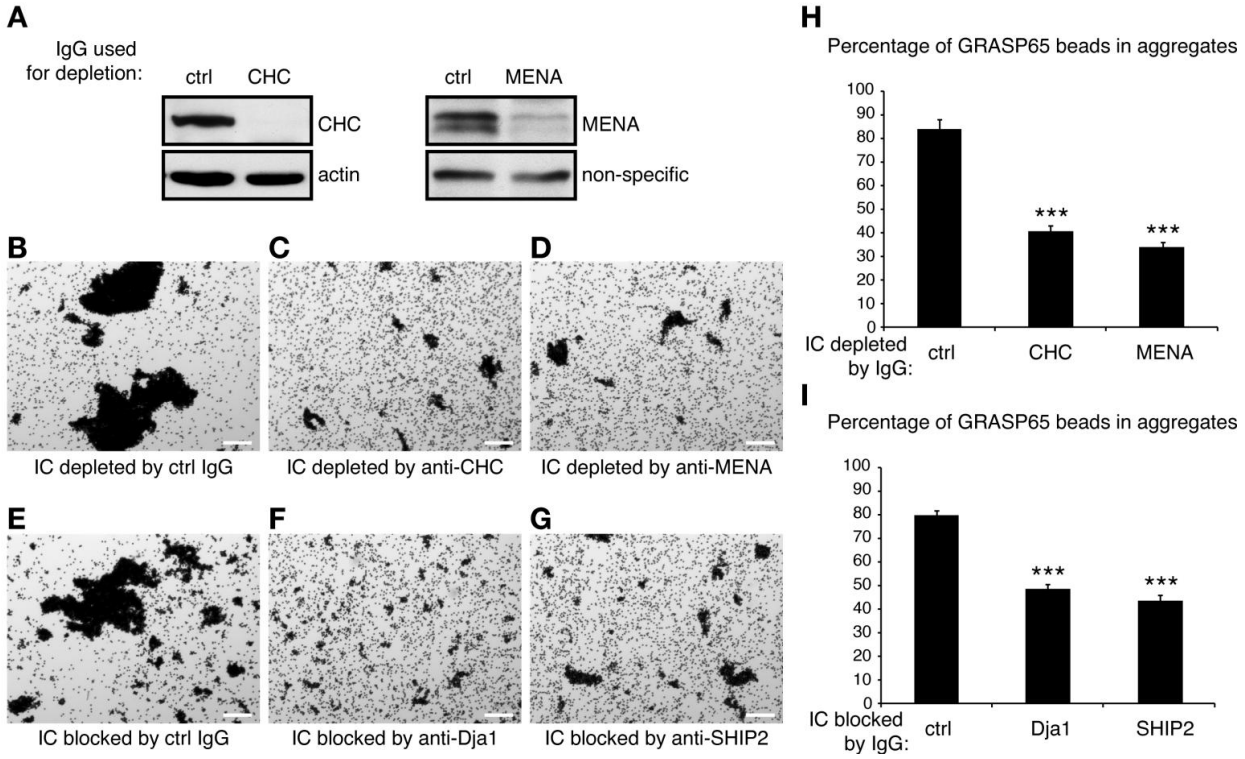

Figure 5.5. CHC, Dja1, MENA and SHIP2 enhance GRASP65 coated beads aggregation.
(A) Immuno-depletion of CHC or MENA from interphase cytosol. Interphase cytosol immuno-depleted by indicated IgG was analyzed by Western blot for indicated proteins. **(B-D)** GRASP65 coated Dynal M-500 beads were incubated with interphase cytosol that was immuno-depleted by indicated antibodies. Note that the GRASP65 coated beads incubated with interphase cytosol depleted by control IgG form large aggregates, while the beads incubated with CHC or MENA-depleted cytosol only form small aggregates. Scale bar, 100 μm. **(E-G)** GRASP65 coated Dynal M-500 beads were incubated with interphase cytosol that was pre-immunoinhibited by indicated antibodies. GRASP65 beads incubated with anti-Dja1 or anti-SHIP2 formed less aggregates comparing to the ones incubated with interphase cytosol incubated with control IgG. Scale bar, 100 μm. **(H)** Quantification of percentage of beads aggregation in B-D. Statistical significance was assessed by comparison to the interphase cytosol depleted by control IgG. P-value was determined by Student's t-test; ***, $p<0.001$. **(I)** Quantification of E-G. Statistical significance was assessed by comparison to the interphase cytosol pre-incubated with control IgG. P-value was determined by Student's t-test; ***, $p<0.001$.

CHC, Dja1, MENA and SHIP2 enhance post-mitotic Golgi reassembly

Depletion of GRASP65-interacting proteins led to Golgi fragmentation in HeLa cells. It is possible that the depletion of these proteins impaired Golgi post-mitotic reassembly, therefore left the Golgi remaining fragmented during interphase. To test this possibility, the function of GRASP65-interacting proteins in post-mitotic Golgi reassembly was examined in an *in vitro* Golgi disassembly/reassembly assay. Purified Golgi stacks were first disassembled into vesicles and short tubular structures (referred to as mitotic Golgi fragments, or MGFs) by treatment with mitotic cytosol (Figure 5.6C). These MGFs were re-isolated and further incubated with interphase cytosol with GRASP65-interacting proteins immuno-depleted (for CHC or MENA), or immuno-inhibited (for Dja1 and SHIP2). When MGFs were incubated with interphase cytosol that were depleted or pre-blocked by control IgG, long and stacked Golgi cisternae were reassembled (Figure 5.6, D & G). However, immuno-depletion of CHC or MENA, or immuno-inhibition of Dja1 or SHIP2, significantly reduced Golgi reassembly, leaving a great amount of vesicles not fused (Figure 5.6, E-F, H-I). Further quantification results confirmed that the relative Golgi membrane fusion efficiency was reduced to 47.1 ± 4.2, 56.4 ± 4.5, 35.1 ± 7.1, 32.7 ± 5.6%, when CHC, Dja1, MENA or SHIP2 were depleted or inhibited, respectively (Figure 5.6 A-B).

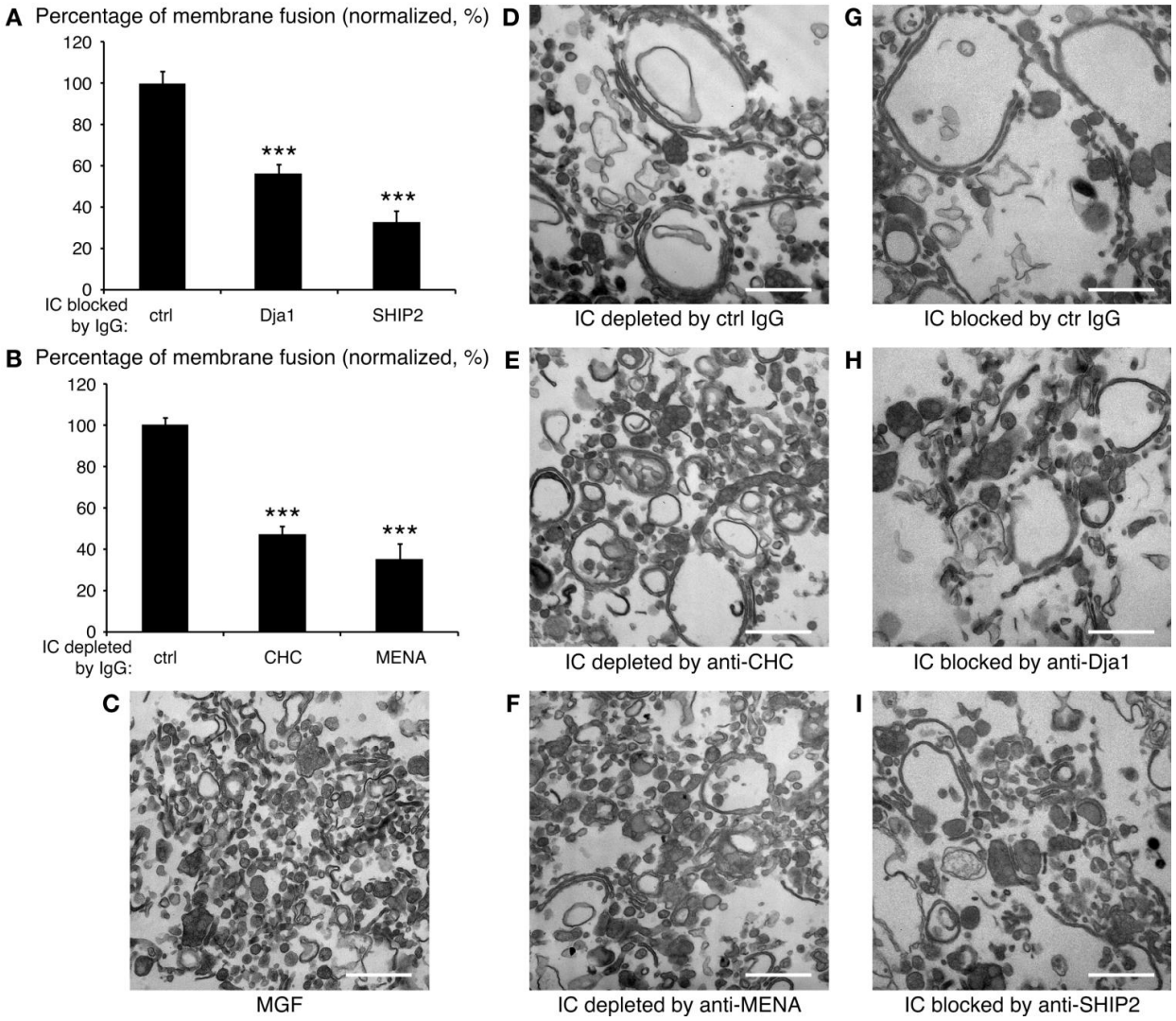

Figure 5.6. CHC, Dja1, MENA and SHIP2 are required for post-mitotic Golgi reassembly.
(A) Quantification of relative Golgi membrane fusion rate in the *in vitro* reassembly assay using interphase cytosol that was immuno-depleted by indicated antibodies. Golgi fusion by the control interphase cytosol was normalized to 100%. Statistical significance was assessed by the comparison to the interphase cytosol depleted by control IgG. P-value was determined by Student's t-test; ***, $p<0.001$. **(B)** Quantification of relative Golgi membrane fusion in the in vitro reassembly assay using interphase cytosol that was immuno-inhibited by indicated antibodies. Golgi fusion by the control was normalized to 100%. Statistical significance was assessed by comparison to the interphase cytosol inhibited by control IgG. P-value was determined by Student's t-test; ***, $p<0.001$. **(C)** EM image of mitotic Golgi fragments. Purified rat liver Golgi stacks were disassembled by incubation with mitotic cytosol. Note that the Golgi stacks were disassembled into vesicles and few single cisternae. Scale bar, 500 nm. **(D-F)** Mitotic Golgi fragments reassembled by interphase immuno-depleted by indicated antibodies. **(G-I)** Mitotic Golgi fragments reassembled by interphase cytosol immuno-inhibited by indicated antibodies.

Discussion

In this study we have identified and characterized several cytosolic proteins that interact with the Golgi matrix protein GRASP65 and function in Golgi structural organization. We validated the binding of CHC, Dja1, MENA and SHIP2 with GRASP65, especially confirmed the direct interaction of CHC and Dja1 with GRASP65 in the pull-down assay using purified proteins. We also showed for the first time that MENA and SHIP2 partially localized on the Golgi, while Dja1 together with Hsc70 could be recruited to the Golgi membranes when purified Golgi membranes were incubated with interphase cytosol. Depletion of CHC, Dja1, MENA or SHIP2 from cells led to Golgi fragmentation, with Golgi mini-stacks unlinked and vesiculated. GRASP65-interacting proteins activity was required to enhance GRASP65 bead aggregation, suggesting that they may stabilize or cross-link GRASP65 oligomers. Finally, inhibition of CHC, Dja1, MENA and SHIP2 reduced post-Golgi reassembly *in vitro*.

Among the four GRASP65-interacting proteins we characterized, CHC is the only one shown by previous studies to be involved in Golgi reassembly during cell division [157, 158]. CHC is best characterized as a membrane coat protein that mediates endocytosis and trafficking between TGN and endosomes. In addition, clathrin has several other functions in the cell. On endosomes, flat clathrin pits mediate sorting of degradative proteins into microdomains of endosomes [163, 164]. Clathrin also participates in a complex comprised of the microtubule-binding proteins TACC3 and ch-TOG [165], which localizes to kinetochore microtubule and centrosomes and contributes to their stability during mitosis [165-168]. Furthermore, clathrin is also found in lamellipodia, associated with the Scar/Wave complex, and is required for Rac-dependent lamellipodia formation [169]. In this study, we found that CHC directly interacts with

GRASP65, facilitates its oligomerization and Golgi ribbon integrity. GRASP65 has been suggested playing a role functioning in Golgi ribbon linkage. We speculate that CHC triskelia cross-link GRASP65 oligomers on the *cis*-Golgi, therefore connect Golgi mini-stacks as a ribbon, similarly to the function of CHC triskelia in cross-linking TACC3/ch-TOG complex and bridging microtubules of the kinetochore fibers [170]. Our finding indentified a new localization of clathrin in the cell and provided molecular explanations to the previous finding that clathrin functions in Golgi reassembly.

Little is known about Dja1 (DNAJA1), except that it is a co-chaperone of Hsc70 that mediates cytosolic protein folding. Due to its molecular weight (40kD), it is also referred to as Hsp40 family protein [162]. Several other J-domain proteins are known to function with Hsc70 and directc clathrin vesicle uncoating. One of the best characterized J-domain proteins is auxilin (DNAJC6) [171]. The nerve-specific auxilin and its ubiquitous expressed homologue GAK (cyclin G associated kinase, or DNAJC26) function with Hsc70 not only to uncoat clathrin coated vesicles but also to regulate the rebinding of clathrin to the membrane [171]. Another J-domain protein, RME-8 (DNAJC13), regulates clathrin uncoating in endosome-to-Golgi retrograde transport which is mediated by the endosomal clathrin and retromer [172]. Similarly to these J-domain proteins, it is possible that Dja1 together with Hsc70 regulate CHC function on the *cis*-Golgi. Dja1 directly interacts with GRASP65. Also, it is recruited to the Golgi membrane under interphase condition with Hsc70. Therefore, Dja1 and Hsc70 may associate with clathrin triskelia through GRASP65 and regulate CHC function in cross-linking GRASP65 and maintaining Golgi integrity.

MENA is the mammalian homolog of *Drosophila* enabled (Ena), which belongs to the Ena/VASP family that directly enhance actin filament elongation by interacting with the barbed end of actin filament and recruiting monomeric actin for polymerization [173]. The function of MENA has been determined in filopodia and lamellipodia formation [174-176]. In this study we showed that MENA also localizes on the Golgi membranes, facilitates GRASP65 oligomerization and is required for Golgi ribbon integrity. MENA may regulate Golgi mini-stack linkage by promoting the formation of local short actin filaments. So far, how actin regulates Golgi structure is still unclear. Treating the cells with either actin filament disrupting drug or stabilizing drug both lead to Golgi condensation, however the mechanisms remain unknown [78]. There are indications that actin cytoskeleton is required for Golgi integrity. For example, in *Drosophila* S2 cells, actin depolymerization induces the scission of neighboring Golgi stacks at late G2 phase, which is mediated by the inactivation of actin nucleation promoting factors WAVE/Scar/Abi [80]. One more indication that actin is required for Golgi integrity came from the study of another actin nucleation factor, WHAMM, which is an Arp2/3 activator on the Golgi. WHAMM-depletion led to reduced F-actin level in the Golgi region and dispersed Golgi mini-stacksg [177]. MENA may be the third actin nucleation promoting factor that regulates Golgi ribbon connection. It probably promotes the formation of actin filament that cross-links GRASP65 oligomers from the neighboring stacks.

SHIP2 is originally known as a phosphoinositidylinositol 3,4,5 trisphosphate (PtdIns(3,4,5)P_3) 5-phosphatase which dephosphorylates PI(3,4,5)P_3 to generate PI(4,5)P_2. Later researches indicate that SHIP2 can also use PI(4,5)P_2 as a substrate and generate PI(4)P [178]. SHIP2 is found concentrated in the clathrin coated pits on plasma membrane and negatively

regulates clathrin coated vesicle formation by controlling $PI(4,5)P_2$ level. Other than its kinase activity, SHIP2 is also a docking protein for cytoskeletonal proteins, focal adhesion proteins, adaptors, scaffold proteins and other phosphatases [161]. For example, SHIP2 binds filamin and regulates the formation of submembranous actin filaments [179]. It directly binds and recruits RhoA to the cell edges, thus regulates lamellipodia protrusions, as well as cell polarity and migration [180]. A similar inositol 5-phosphatase which is better known is OCRL1, whose mutation results in Lowe syndrome. OCRL1 catalyzes the formation PI(4)P from $PI(4,5)P_2$ similar to SHIP2. OCRL1 localizes on plasma membrane, clathrin coated vesicles and especially enriched on the Golgi complex. It is incorporated into clathrin coated pits by interacting with clathrin and clathrin adaptors, thus regulates clathrin mediated trafficking between endosomes and TGN, as well as between endosomes and plasma membrane [181]. It also modulates the local actin filament density by controlling $PI(4,5)P_2$ level [182]. Similar to OCRL1, SHIP2 is also found recruited onto the Golgi membrane in this study. It is required for Golgi integrity and enhances GRASP65 oligomerization. Therefore, we speculate that SHIP2 links Golgi mini-stacks via GRASP65 oligomers, through either CHC triskelia or actin filaments.

In conclusion, we have identified CHC, Dja1, MENA and SHIP2 that interact with GRASP65 and function in Golgi assembly. It is possible that these proteins cross-link GRASP65 (e.g. through clathrin triskelia or short actin filaments) from the rim of neighboring Golgi stacks and link the stacks into a ribbon. The molecular mechanisms underlying the function of each protein requires further investigation.

Materials and Methods

Reagents, plasmids, antibodies and siRNA

All reagents were purchased from Sigma-Aldrich, Roche or Calbiochem, unless otherwise stated. The following antibodies were used: monoclonal antibodies against GM130 (Transduction Laboratories), clathrin heavy chain (X22 [183], and TD.1, gifts from Hong Chen, OMRF), MENA (gift from Frank Gertler, MIT), Hsc70 (gift from Xunqun Chen, Wayne State University), α-tubulin (Developmental Studies Hybridoma Bank University of Iowa) and β-actin (AC-15, Sigma); polyclonal antibodies against human GRASP65 (gift from Joachim Seemann, UT Southwestern), Dja1 (gift from Jason C. Young, McGill University) and SHIP2 (gift from Stuart J. Decker, University of Michigan).

His-tagged and MBP-tagged GRASP65 were prepared as described previously [14]. cDNA constructs used in this study include GFP-tagged CHC (Frances Brodsky, UCSF), GFP-tagged SHIP2 (Christina A. Mitchell, Monash University). GFP-tagged MENA cDNA was excised from a construct of pMSCV-EGFP-MENA (gift from Frank B. Gertler, MIT) and re-ligated into the pcDNA pcDNA™3.1(-)/myc-His vector.

Control siRNA (SilencerÂ® Select Negative Control #1 siRNA) was purchased from Applied Biosystem. CHC, Dja1, MENA, and SHIP2 specific siRNAs were synthesized by Sigma. The sequences of sense chain were UAAUCCAAUUCGAAGACCAA for CHC17 [184, 185], GGACAUACAGCUCGUUGAA(TT) for Dja1 [186], GCCAUUCCUAAAGGGUUGAAGUACA for MENA [159], and UCAUGGUGUGACCGGAUUC(TT) for SHIP2 [160].

Ammonium sulfate precipitation

Interphase cytosol purified from HeLa S3 cells [8, 133] was first precipitated with indicated concentration (percentage saturation) of ammonium sulfate. After centrifugation, the ammonium sulfate concentration in the supernant was further increased to another concentration. The precipitants were collected by centrifugation, dissolved and dialyzed into KHM buffer (20 mM Hepes-KOH, pH 7.0, 0.2 M sucrose, 60 mM KCl, 5 mM $Mg(OAc)_2$, 2 mM ATP, 1 mM GTP, 1 mM glutathione and protease inhibitors). The dissolved proteins were used for SDS-PAGE and in other assays.

Velocity gradient

Protein samples were loaded onto a 15-35% glycerol gradient, then centrifuged in a VT165 rotor, at 65 000 rpm for 80 min. After centrifugation, the gradient was fractionated from the top to the bottom into 12 fractions. Proteins from each fraction were concentrated for further analysis.

Identification of GRASP65-interacting proteins and in vitro binding assay

Interphase cytosol was diluted and fractionated with 15-30% ammonium sulfate precipitation. Proteins in the pellet were dissolved and dialyzed into KHM buffer. Dissolved proteins were incubated with BSA or His-GRASP65 pre-coupled Cyanogen bromide-activated (CNBr) beads in the presence of an ATP-regenerating system (10 mM creatine phosphate, 1 mM ATP, 20 μg/ml creatine kinase and 20 ng/ml cytochalasin B) in KHM buffer at 4ºC overnight. The beads were washed extensively. Bound proteins were boiled in SDS buffer followed by analysis by SDS-PAGE and Western blotting. For protein identification, specific bands in the

GRASP65 lane but not in the BSA lane were excised and analyzed by mass spectrometry (University of Michigan, Proteomics & Peptide Synthesis Core).

To test whether CHC and Dja1 directly binds GRASP65, purified CHC or His-tagged Dja1 full length proteins were incubated with BSA or MBP-GRASP65 coupled to CNBr beads (pre-blocked with BSA) in the presence of an ATP-regenerating system in KHM buffer at 4ºC overnight. The beads were washed extensively and then analyzed by SDS-PAGE and immunoblotting for CHC and Dja1.

Preparation of recombinant proteins

His-tagged (in pET30a, Novagen) and MBP-tagged (in pMAL-2CX, NEB) GRASP65 were expressed and purified on nickel (Qiagen) or amylase (NEB) agarose as previously described [14]. Purified full length CHC was a gift from Dr. Frances Brodsky (UCSF). His-tagged Dja1 was expressed in BL21(DE3)Gold bacteria and purified on nickel (Qiagen) agarose.

In vitro Golgi recruitment assay

Golgi membranes were purified from rat liver [16]. Interphase (IC) and mitotic (MC) cytosols were prepared from HeLa S3 cells [8, 133]. Purified Golgi membranes (20 μg) were mixed with 2 mg of interphase in KHM buffer or mitotic cytosol in MEB buffer (50 mM Tris-HCl, pH 7.4, 0.2 M sucrose, 50 mM KCl, 20 mM β-glycerophosphate, 15 mM EGTA, 10 mM $MgCl_2$, 2 mM ATP, 1 mM GTP, 1 mM glutathione and protease inhibitors) in a final volume of 200 μl. After 60 min incubation at 37°C, Golgi membranes were isolated by centrifugation (135,000 g for 30 min in a TLA55 rotor) through a 0.4 M sucrose cushion in KHM buffer onto a

6-µl 2 M sucrose cushion and soluble proteins that did not bind to the Golgi membranes were removed (same method used in other steps and experiments). For the sequential treatments, Golgi membranes were first incubated with mitotic cytosol for 20 min, re-isolated, resuspended and mixed with 2 mg of interphase cytosol and incubated at 37°C for 60 min. The membranes were reisolated, suspended in KHM buffer and analyzed by SDS-PAGE and Western blotting.

Cell culture and microscopy

HeLa cells were routinely cultured in DMEM supplemented with 10% donor bovine serum (Gibco/Invitrogen), 2 mM L-glutamine, penicillin (100 U/ml), and streptomycin (100 µg/ml). For knock down experiments, HeLa cells were transfected using Lipofectamine RNAiMAX (Invitrogen) following the manufacturer's instructions. Assays were performed 96 h after transfection unless otherwise stated. For expression of GFP-tagged proteins, HeLa cells were transfected with indicated constructs using Lipofectamine 2000 (Invitrogen), fixed and analyzed by immunofluorescence microscopy 16h after transfection.

Immunofluorescence microscopy and the electron microscopy are performed as previously described [8, 18]. Images were taken with a Zeiss Observer Z1 epifluorescence microscope with a 63X oil lens. In interphase cells, fragmented Golgi was defined as disconnected or scattered dots. To quantify the percentage of cells with fragmented Golgi, more than 300 cells transfected with control or target specific siRNAs were counted, and the results are presented as mean ± SEM (n=3).

For EM analysis, Golgi stacks were identified using morphological criteria and quantified using standard stereological techniques [8, 18]. Golgi stack images were captured at 11,000x magnification. Interphase cells were defined as profiles that contained an intact nuclear envelope. The longest cisterna was measured as the cisternal length of a Golgi stack using the ruler function in Photoshop CS3. At least 20 cells were quantified in each experiment, and the results represent at least three independent experiments. Statistical significance was assessed by Student's t-test.

Immuno-depletion and immuno-inhibition of GRASP65-binding proteins in interphase cytosol

Interphase cytosol prepared from HeLa S3 cells was incubated with unspecific control mouse IgG, anti-CHC IgG or anti-MENA IgG and protein-G agarose at 4ºC overnight. The beads were pelleted and the supernatant analyzed by immunoblotting for CHC or MENA. Equal amount of cytosol immuno-depleted by control IgG, anti-CHC or anti-MENA IgG was used in bead aggregation assay and Golgi disassembly and reassembly assay described below.

For immuno-inhibition of the cytosol, interphase cytosol was pre-incubated with unspecific control rabbit IgG, anti-SHIP2 or anti-Dja1 IgG at 4ºC for 30 min. Equal amount of cytosol pre-incubated with control IgG, anti-SHIP2 or anti-Dja1 IgG was used in bead aggregation assay and Golgi disassembly and reassembly assay described below.

Bead aggregation assay

Bead aggregation assay were performed as previously described [8, 14, 18]. For quantification of the aggregation efficiency, 10-20 random phase contrast digital images of each

reaction were captured by Zeiss Observer Z1 epifluorescence microscope with a 10X lens. Images were analyzed with the MATLAB7.4 software to determine the surface area of objects, which was used to calculate the number of beads in the clusters. Aggregates were defined as those with ≥ 6 beads. Only those beads on the surface were counted; therefore, the number of beads in large aggregates was underestimated. Results were expressed as the mean ± SEM from one representative experiment out of 3 independent experiments; statistical significance was assessed by student's t-test.

Golgi disassembly and reassembly assay and quantification

The Golgi disassembly assay was performed as described previously [8]. Briefly, purified Golgi membranes (20 μg) were mixed with 2 mg of mitotic cytosol, 1 mM GTP and an ATP-regenerating system in MEB buffer in a final volume of 200 μl. After incubation for 60 min at 37°C, mitotic Golgi fragments (MGF) were isolated and soluble proteins were removed by centrifugation (135,000 g for 30 min in a TLA55 rotor) through a 0.4 M sucrose cushion in KHM buffer onto a 6-μl 2 M sucrose cushion. The membranes were resuspended in KHM buffer, either fixed or processed for EM [8], or used in reassembly reactions. For Golgi reassembly, 20 μg of mitotic Golgi fragments were resuspended in KHM buffer, mixed with 400 μg interphase cytosol either immuno-depleted or immuno-inhibited as described above in the presence of an ATP regeneration system in a final volume of 30 μl in KHM buffer and incubated at 37°C for 60 min. The membranes were pelleted by centrifugation, and processed for EM.

To quantify the reassembly of Golgi, EM images of Golgi membranes were captured at 11000x magnification. The percentage of membranes in cisternae or in vesicles was determined

by the intersection method [8, 128]. All experiments were repeated at least 3 times; statistical significance was assessed by Student's t-test.

Acknowledgement

We thank Frances Brodsky (UCSF), Hong Chen (OMRF), Yuxin Mao (Cornell), Stuart J. Decker (University of Michigan) Christina A. Mitchell (Monash University), Frank B. Gertler (MIT), and Jason C. Young (McGill University) for antibodies and plasmids. We thank other members of the Wang Lab for suggestions and reagents. This work was supported by grants from NIH (GM087364) and American Cancer Society (RGS-09-278-01-CSM) to Y. Wang. D. Tang was supported by the Rackham Predoctoral Fellowship from the University Michigan and granted a Chinese Government Award for Outstanding Self-financed Students Abroad by China Scholarship Council. The authors declare no conflicts of interest.

Abbreviations

BSA, bovine serum albumin; GFP, enhanced green fluorescent protein; EM, electron microscopy; GRASP65, Golgi reassembly stacking protein of 65 kDa; GRASP55, Golgi reassembly stacking protein of 55 kDa; CHC, clathrin heavy chain; Dja1, DnaJA1/dj2/HSDJ/hdj2; Hsc70, heat shock cognate 70K protein; MENA, mammalian enabled (Ena); SHIP2, SH2-containing inositol phosphatase 2; INPPL1, inositol polyphosphate phosphatase-like 1; IC, interphase cytosol; MC, mitotic cytosol; PBS, phosphate-buffered saline; siRNA, small interference RNA; CNBr, cyanogens bromide

Chapter 6 . Clathrin directly binds GRASP65 providing glue for Golgi ribbon integrity

Abstract

Reassembly of the Golgi following fragmentation in mitosis requires clathrin. Here we establish the molecular basis for this phenomenon. The *cis*-Golgi stacking factor GRASP65 is directly bound by the clathrin N-terminal domain and thereby clathrin crosslinking promotes Golgi fragment assembly in vitro. In cells, Golgi ribbon connectivity after disassembly required only a truncated, trimeric form of clathrin, demonstrating that clathrin acts in this capacity as molecular glue, not by vesicle formation. Golgi clathrin is not preferentially derived from spindle-associated clathrin, which is rapidly exchanging, but STORM imaging identified a candidate pool of crosslinking clathrin in the *cis*-Golgi. Acute inactivation of clathrin in interphase generated Golgi fragments indicating that Golgi ribbons are labile and clathrin maintains their integrity. Clathrin depletion also eliminated Golgi-derived microtubules leading to loss of Golgi polarization. Thus, a non-conventional role for clathrin in promoting GRASP65 oligomerization, independent of its mitotic or vesicle-forming functions, is required for sustaining Golgi ribbon architecture and polarization.

Introduction

Mammalian cells display a unique Golgi architecture comprising stacks of tightly aligned flat cisternal membranes through which secreted proteins traffic for sequential exposure to processing enzymes. Golgi stacks are laterally connected into cisternal ribbons. Although the exact morphology and mechanisms of traffic through the interphase Golgi are debated [187, 188], it is clear that lateral Golgi connectivity contributes to optimal cargo processing in the secretory pathway [155].

In the late G2 phase of mitosis the Golgi architecture is disassembled. First, Golgi ribbons are dissolved, generating individual stacks that are distributed throughout the cell. In prophase and prometaphase, the dispersed Golgi stacks are further disassembled into tubulovesicular structures that are equally distributed into the emerging daughter cells [4]. Subsequent Golgi reformation is initiated in telophase with fusion of Golgi vesicles to generate small Golgi cisternae that stack into ministacks. The ministacks then move towards each other and to the cell center to form characteristic Golgi "twins" during cytokinesis, before assuming the final interphase morphology comprised of stacked pericentriolar ribbons [189-191]. Golgi formation has not been fully characterized but it has been shown to involve membrane fusion machinery and microtubules, as well as Golgi tethering and stacking factors including golgins and the GRASP proteins. The homologues GRASP55 and GRASP65 mediate Golgi stack and ribbon formation via homo-oligomerization, with GRASP65 operating in the *cis*-Golgi and GRASP55 in the medial and *trans*-Golgi cisternae [13, 155, 190]. Importantly, while GRASP65's ability to homo-oligomerize has been demonstrated [16, 192], this activity is promoted by cytosolic components that remain elusive [14, 16]. Furthermore, some Golgi ribbon formation factors are

spindle-associated in mitosis and thereby actively distributed to emerging daughter cells [193]. These factors are also yet to be defined, as GRASP proteins are not spindle-associated.

Among the proteins suggested to support Golgi biogenesis is clathrin [190] because clathrin depletion by RNAi was shown to prevent Golgi reassembly after fragmentation in mitosis or by nocodazole treatment [157, 158]. The major clathrin isoform, consisting of clathrin heavy chain CHC17 with bound clathrin light chains (CLCs), is best understood as a membrane coat component that mediates vesicle formation at the plasma membrane, endosomes and the TGN. The CHC17 subunits trimerize to form a soluble triskelion, the building block of polyhedral clathrin coats that capture cargo via adaptor molecules [194, 195]. CHC17 clathrin also participates in a complex comprising the microtubule-binding proteins TACC3 and ch-TOG [165]. The clathrin-TACC3-ch-TOG complex is mitotic spindle-associated and required for kinetochore microtubule stability [166, 167]. The complex also localizes to centrosomes and contributes to centrosome integrity during early mitosis [168]. These particular cell cycle functions of clathrin are independent of clathrin's membrane traffic function. Both spindle-associated [190] and membrane-bound forms of clathrin have been suggested to support Golgi biogenesis [158].

Here we define the origin and required properties of the clathrin involved in Golgi morphogenesis, and its mechanism of action. Using live cell imaging, we observe that spindle-associated clathrin is rapidly exchanging and is not preferentially recruited to the post-mitotic Golgi. Instead, clathrin laterally interconnects Golgi fragments through a crosslinking, but non-trafficking function via directly binding and promoting oligomerization of GRASP65. Golgi

fragmentation occurs within two hours of acute clathrin inactivation in interphase, suggesting Golgi ribbon connections are labile and maintained by clathrin. As a consequence of this role, clathrin also regulates Golgi-derived microtubule formation by promoting Golgi integrity. This trafficking-independent contribution to Golgi architecture represents an unconventional function for clathrin, taking advantage of its unique trimerization ability.

Results

Loss of Golgi Ribbon Connectivity Upon Clathrin Depletion

The involvement of clathrin in Golgi reformation after mitosis and drug-induced fragmentation has been indicated by RNAi-mediated depletion experiments. In the absence of clathrin the Golgi does not reform properly in either circumstance. Rather, the Golgi was reported as having a range of altered morphologies in interphase after treatment of NRK cells with siRNA targeting clathrin for 72-96 h [157, 158]. Phenotypes included persistent fragmentation but also a more tightly clustered appearance. In interphase HeLa cells depleted of clathrin for 96 h, we observed a phenotype of persistent Golgi fragmentation without the tight clustering, possibly reflecting a cell type difference (Figure 6.S1). To better characterize Golgi disruption in HeLa cells following clathrin depletion, we analyzed post-mitotic Golgi reformation using an unbiased quantitative approach. Golgi twin formation during cytokinesis was analyzed by measuring the average angle between the GM130 or GS27 signals and the axis of division from the center of the cells (Figure 6.1A, B). As expected, Golgi reformation was morphologically abnormal in cells depleted of clathrin for 72 h. Golgi twins did not properly form and fragments staining for GM130 or GS27 were scattered throughout the cell, as indicated by a wider angle of distribution compared to the division access. To further characterize and quantify the Golgi fragmentation phenotype, we analyzed cells after clathrin depletion for 96 h by electron microscopy. In CHC17-depleted interphase cells, we observed that the lateral linkage of Golgi ribbons was disorganized and the length of cisternae in each Golgi stack significantly shorter than in control-treated interphase cells (Figure 6.1C-E). These short Golgi stacks were also characterized by more local vesicles. To assess loss of Golgi connectivity upon clathrin depletion, we examined diffusion of the resident Golgi enzyme, galactosyl-transferase

(GalT) by fluorescence recovery after photobleaching (FRAP) in cells transiently expressing GalT-GFP (Figure 6.1F-H). In cells treated with non-silencing (control) siRNA, photobleached GalT-GFP in intact Golgi ribbons was rapidly replaced by diffusion of fluorescent GalT, leading to quick recovery in FRAP experiments. In clathrin-depleted cells little fluorescence recovery was observed after photobleaching, consistent with nearby stacks not being laterally connected to one another, thereby preventing diffusion. Notably, the reduced cisternae length and inhibition of intra-Golgi diffusion were observed for interphase Golgi, indicating the connectivity defect from clathrin depletion persists following disrupted reassembly.

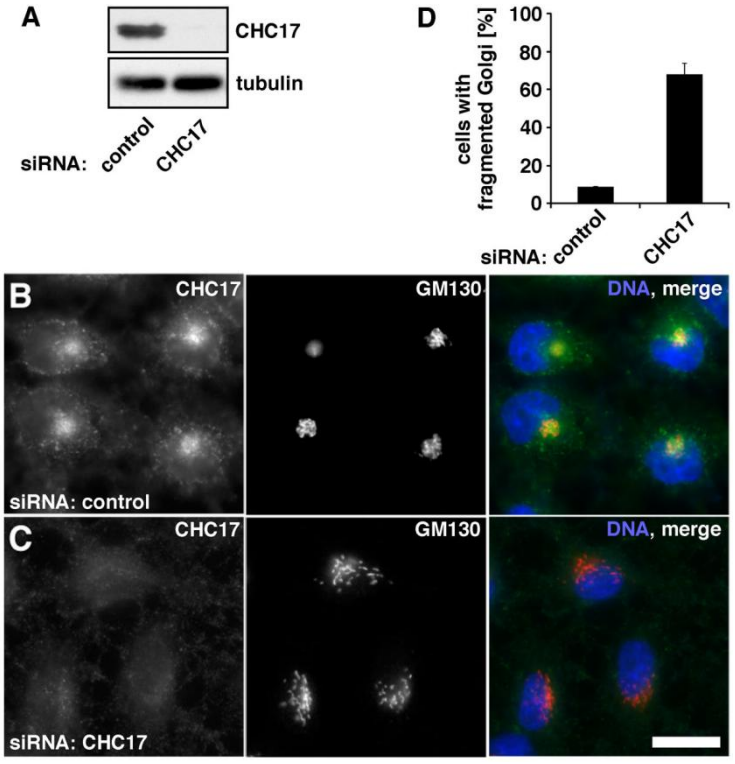

Figure 6.S1: Golgi Dispersion Upon Prolonged Clathrin Depletion.
(A) HeLa cells treated with control or siRNA targeting CHC17 were lysed and analyzed by immunoblotting for CHC17 protein. **(B-C)** HeLa cells treated with (B) control siRNA or (C) siRNA targeting CHC17 for 96h were stained for CHC17 (green), GM130 (red) and DNA (DAPI, blue). Bar, 20μm. **(D)** The number of cells with fragmented Golgi were scored manually and plotted. Significance was assessed using Student's t-test.

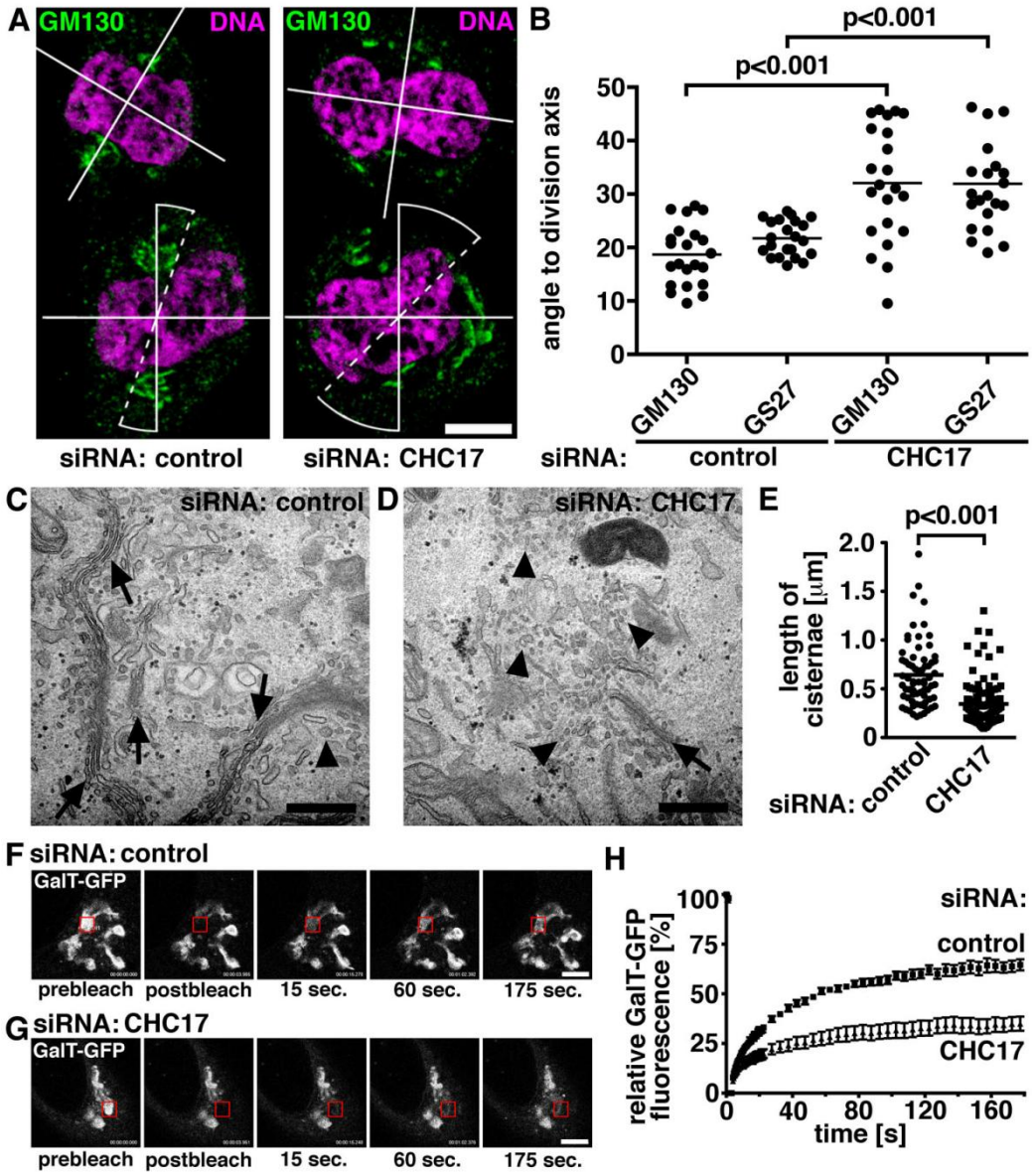

Figure 6.1: Clathrin Requirement for Normal Golgi Morphology and Stack Connectivity.
(A) HeLa cells treated with control or siRNA targeting CHC17 were stained for GM130 (green) and DNA (TO-PRO, magenta). Cells in cytokinesis were identified by Golgi twin formation and the presence of an adjacent daughter cell with Golgi twins. A solid crosshair was overlaid to mark the cell center along the vertical axis of division from the neighboring cell. The average angle of the Golgi signal, measured from the center relative to the division axis, is indicated by dashed line. Bar, 5μm. **(B)** HeLa cells were processed as in (A) and stained for GM130 (*cis*-Golgi marker) and GS27 (*medial*-Golgi marker). Average angles of Golgi staining to division axis are plotted for siRNA treatments. **(C, D)** HeLa cells treated with (C) control or (D) siRNA targeting CHC17 were processed for electron microscopy and imaged. The Golgi region was identified by characteristic stacked cisternal membranes (arrows) and surrounding vesicles (arrowheads). Note that the Golgi ribbon is disorganized in CHC17 depleted cells, the Golgi stacks are shorter and more vesiculated compared to control siRNA treated cells. Bars, 500nm. **(E)** Cisternae length was measured in cells processed as in (C, D) and plotted. **(F, G)** GalT-GFP was transfected into HeLa cells treated with control (F) or siRNA targeting CHC17 (G) and imaged live. Regions marked by red square were photobleached and recovery imaged for three minutes. **(H)** Fluorescent intensity plots of GalT-GFP signal as in (F, G) are plotted. Bar, 5μm. Significance was assessed using Student's t-test.

Rapid Exchange of Spindle Clathrin Without Enrichment in the Golgi

Golgi reformation after mitosis has been shown to require two activities [193]. We addressed whether clathrin accounts for either. The first activity comes from at least one unknown Golgi ribbon formation factor that is present in the Golgi/TGN in interphase and on the spindle in mitosis. Segregation of this unknown factor with the spindle into the two daughter cells is essential for Golgi ribbon formation [193]. Clathrin is a good candidate for this factor given its reported presence on the spindle and implication in Golgi reassembly [158, 190] (Figure 6.1). To address its potential recruitment from the spindle, we first used super-resolution Stochastic Optical Reconstruction Microscopy (STORM) [196] to visualize the forms of clathrin in mitotic cells. We observed a large, diffuse cytoplasmic pool of clathrin mixed with vesicle-like clathrin structures, as well as a strong clathrin signal decorating spindle microtubules (Figure 6.2A). Consistent with its participation in a microtubule-binding complex [167], the spindle clathrin signal cluster was much smaller in size than typical for vesicles (Figure 6.2A). We then generated cells expressing Dendra2-CLC to mark spindle clathrin with a photo-convertible fluorescent tag and tested whether it is first present on the spindle in mitosis and then in the Golgi of daughter cells, fulfilling the criteria of a spindle-associated Golgi formation factor. The fate of the photoconverted mitotic spindle-associated CLC pool (emitting red fluorescence in contrast to non-spindle associated CLC emitting green fluorescence signal) was followed in a pulse chase experiment (Figure 6.2 B & C). During the observation time, spindle-associated CLC mixed with previously non-spindle-associated CLC and after 2 hours complete overlap between both pools was seen throughout the cell such that their distribution was indistinguishable. Note that CLC is a stable subunit of clathrin [195], so this represents whole clathrin mixing. This prompted us to investigate clathrin turnover on the mitotic spindle. We varied the experimental

setup to increase the frequency of detection (at a cost of increased photobleaching) and photoconverted CLC on one of the two halves of the mitotic spindle (Figure 6.2 D & E). The spindle-associated clathrin dissociated rapidly to the cytosol with similar kinetics to clathrin turnover at other cellular locations in interphase (Figure 6.S2). Photoconverted CLC from one half of the spindle was recruited to the other half within 90 seconds. This indicates that spindle-derived clathrin is not distinguishable from total clathrin during late stages of cell division and argues against clathrin as a spindle-associated factor required in subsequent Golgi formation.

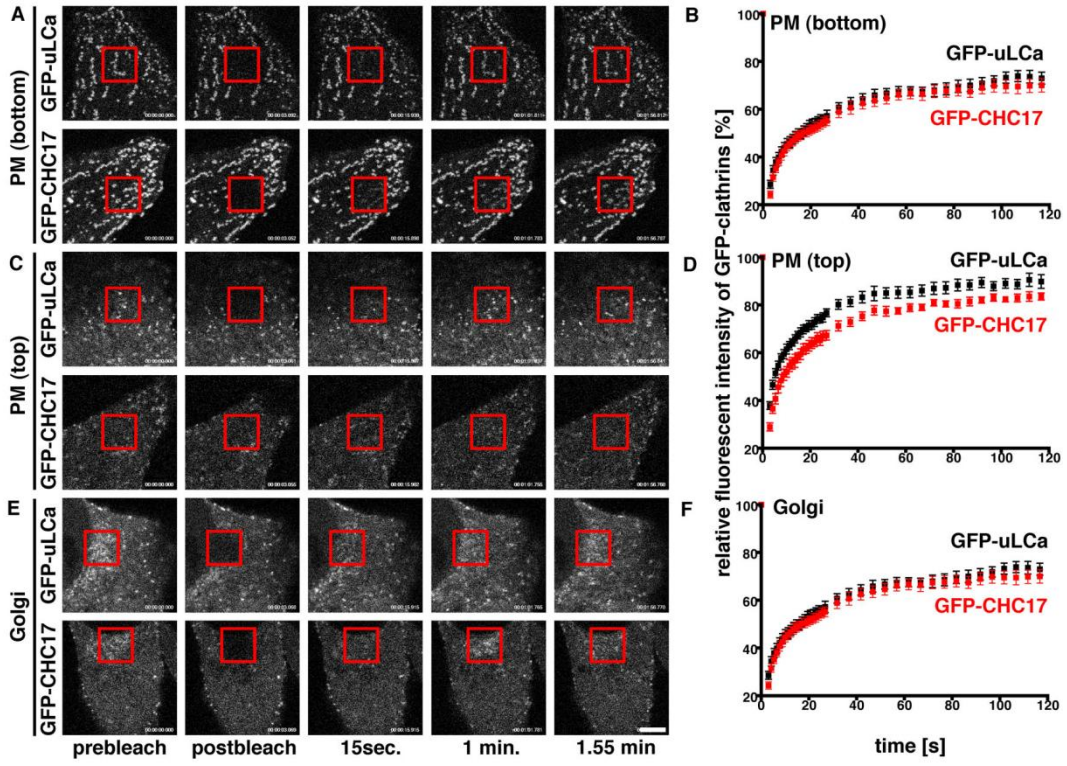

Figure 6.S2: Clathrin Turnover at Various Cellular Membranes

(A-F) Cells were transfected with either GFP-uLCa (A, C, E, upper panels) or GFP-CHC17 (A, C, E, lower panels) and subjected to FRAP analysis in the indicated areas. Quantifications of recovered fluorescence are shown in B, D, F. The focal plane was set on the plasma membrane near the coverslip (PM bottom, A, B), the media-facing plasma membrane (PM top, C, D) or the Golgi (Golgi, E, F). Bar, 5µm.

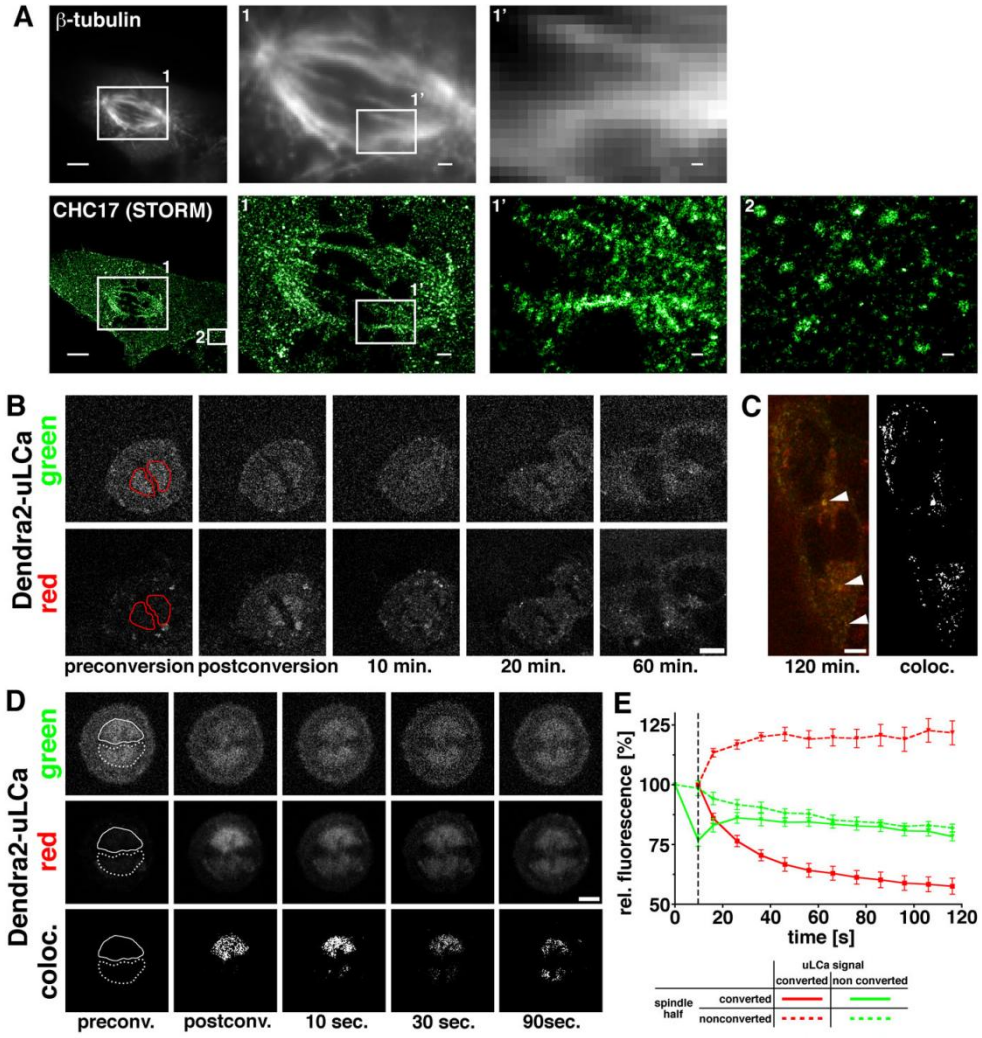

Figure 6.2: Rapid Turnover and Uniform Dispersion of Spindle-Associated Clathrin

(A) Fixed RPE1 cells were stained for microtubules (β-tubulin, gray, conventional resolution) and CHC17 (green, STORM resolution). Clathrin can be seen on the spindle along microtubules and in vesicle form (boxes 1, 1' and compare image from cell adjacent to mitotic cell, box 2). Bars, 5μm, 1μm (1), 200nm (1', 2). **(B, C)** A HeLa cell expressing Dendra2-uLCa was photoconverted in the indicated area containing the mitotic spindle. Green (non-converted, upper panel in (B)) and red (converted, lower panel in (B)) Dendra2-uLCa signal was followed throughout cytokinesis. Note mixing of spindle associated and cytosolic clathrin pools. Left panel in (C) shows overlay of non-converted (green) and converted (red) Dendra2-uLCa. Areas of extensive colocalization are marked by arrowheads. Right panel in (C) shows overall colocalization of Dendra2-CLC pools throughout the cell. Bars, 5μm. **(D)** A HeLa cell expressing Dendra2-uLCa was photoconverted in the area indicated by the solid line containing one mitotic spindle. Green (non-converted, upper panel) and red (converted, middle panel) signals were collected at high frequency for 2 minutes. Colocalizing green and red signal is indicated in the lower panel. Note rapid mixing of photoconverted with non-converted protein pools with proteins from one spindle concentrating on the other indicating rapid exchange. Bar, 5μm. **(E)** Plots of experiments as in (D). Non-converted, green signal from converted spindle (solid green line) and non-converted spindle (dashed green line) was normalized to prebleach levels (T = 0sec.). Converted red signal from converted spindle (solid red line) and non-converted spindle (dashed red line) was normalized to postbleach levels indicated by black dashed line 8 sec. into the measurements. Significance was assessed using Student's t-test.

Clathrin Requirement for Interphase Golgi Connectivity

The RNAi experiments implicating clathrin in Golgi reformation require depletion over the course of at least 2 cell cycles. During this period continuous loss of clathrin could compound membrane traffic defects that indirectly affect Golgi reassembly. To investigate a direct involvement of clathrin in post-mitotic Golgi reassembly, we tested its function in an in vitro Golgi reassembly assay that measures the regrowth of Golgi cisternae from fragments produced by mitotic disassembly [8] (Figure 6.3A-D). When mixed with interphase cytosol depleted by non-specific control IgG, Golgi membranes readily reassembled. In contrast cytosol depleted by clathrin-specific IgG was significantly reduced in its ability to support Golgi membrane reassembly. Efficient clathrin depletion from interphase cytosol was confirmed by immunoblotting (Figure 6.S3). We also assessed whether interphase Golgi structure in cells was affected after acute clathrin inactivation, which can be achieved within 2 hours. This was possible using a cell line expressing CLC subunits tagged with a SNAP sequence that can be chemically crosslinked by the membrane-permeable compound BG-GLA-BG [168]. Rapid clathrin inactivation caused Golgi ribbon disintegration, similar to the defect in Golgi appearance observed in cells depleted of clathrin by RNAi (Figure 6.3E, F compared to Figure 6.S1C). Additionally, intra-Golgi diffusion, measured by recovery of photobleached GalT-GFP, was impaired after acute clathrin inactivation (Figure 6.3G, H). Thus, clathrin's role in Golgi assembly is not confined to cell cycle recovery, but clathrin also contributes to maintenance of connections between Golgi ribbons in interphase.

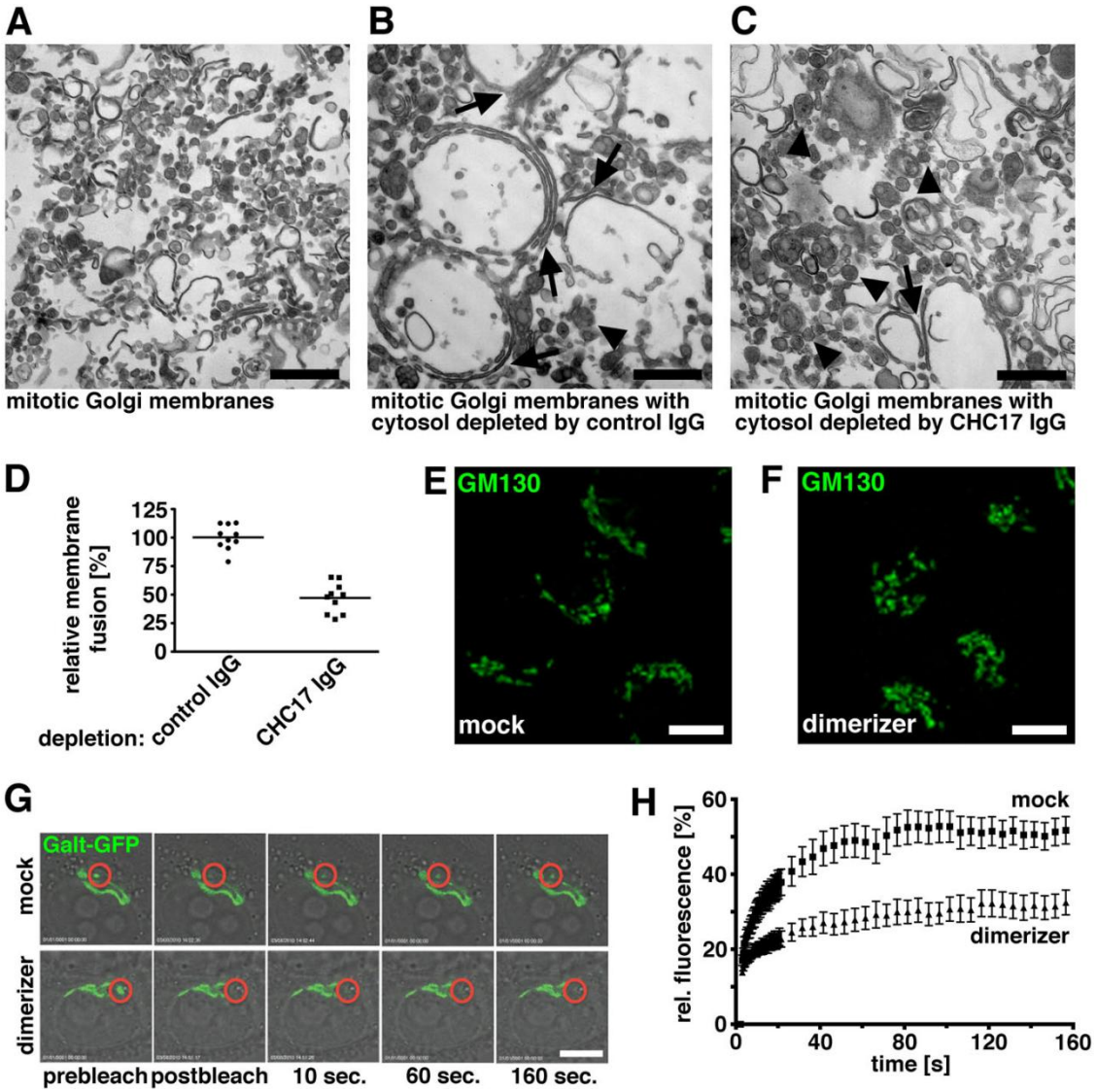

Figure 6.3: Golgi Ribbon Formation By Clathrin

(A-D) Purified rat liver Golgi membranes (see methods) were disassembled by treatment with mitotic cytosol (A), then isolated and further incubated with interphase cytosol depleted by (B) non-specific control IgG or (C) anti-CHC17 IgG. Membranes were processed for electron microscopy and imaged. Relative membrane fusion was calculated and plotted in (D). Note strong cisternae formation (arrows) in (B) in comparison to remaining vesicles (arrowheads) in (C). **(E, F)** HeLa cells stably expressing SNAP-uLCa were rapidly inactivated for clathrin function using a chemical dimerizer (BG-GLA-BG, F) or mock-treated (DMSO, E) 2 hours after inactivation cells were processed for immunofluorescence using anti-GM130 and imaged. Bars, 5μm. **(G)** HeLa cells stably expressing SNAP-uLCa were transfected with GalT-GFP and clathrin was rapidly inactivated using a chemical dimerizer (BG-GLA-BG) or mock-treated. 2 hours after inactivation cells were subjected to FRAP assay. Bar, 5μm. **(H)** Fluorescent intensity plots of GalT-GFP signal as in (G) are plotted. Significance was assessed using Student's t-test.

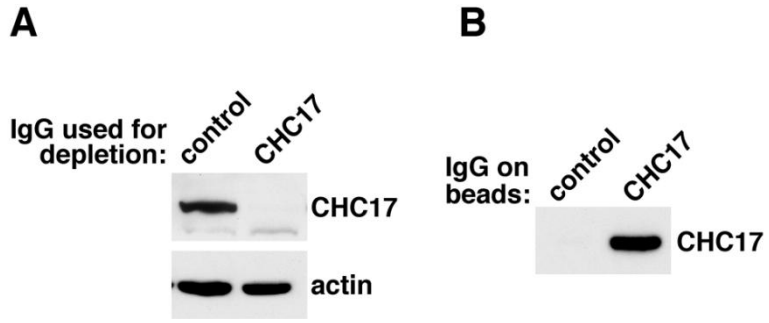

Figure 6.S3: Efficient Removal of CHC17 from Cytosol by Immunodepletion
Cytosol harvested from cells in interphase was exposed to beads with either control IgG or anti-CHC17 antibody. The exposed cytosol (A) and bead-bound protein (B) were analyzed by immunoblotting for the presence of CHC17 to confirm depletion from cytosol.

Clathrin as Glue for GRASP65-Mediated Golgi Ribbon Formation

It has long been established that clathrin is not involved in trafficking cargo within the Golgi [197], raising the question of how clathrin exerts its function on Golgi ribbon formation. In an effort to visualize clathrin at the Golgi we disassembled the Golgi using nocodazole and washed out the drug for 5 min to produce *cis*-to-*trans* ministacks. This allowed for detailed analysis of Golgi clathrin using STORM (Figure 6.4A). Opposite to the clathrin-rich TGN side of the ministacks (arrows in Figure 6.4A) we observed linear clathrin labeling immediately adjacent to the *cis*-Golgi marker GM130 (arrowheads in Figure 6.4A). This resembles a minor site of Golgi clathrin localization previously observed in this area using immuno-electron microscopy [198].

Cis-Golgi ribbon formation involves the protein GRASP65 [13] and GRASP65 depletion leads to *cis*-, medial and *trans*-Golgi ribbon disintegration comparable to that seen upon clathrin depletion [15, 17, 199]. Therefore we addressed whether there might be a connection between GRASP65 and clathrin by testing for their interaction. First, recombinantly-expressed GRASP65 immobilized on beads was exposed to cytosolic proteins prepared from interphase or mitotic cells (Figure 6.4B). CHC17 clathrin heavy chain from both cytosol preparations was

captured by GRASP65 beads. Interestingly, recombinantly-expressed GRASP55, the GRASP65 homologue, did not bind clathrin. To establish whether the GRASP65-clathrin binding is direct, we tested recombinant clathrin and clathrin fragments for their ability to bind to immobilized GRASP65. Full-length clathrin (aa1-1675), as well as fragments containing aa1-1074 and aa1-545, bound to GRASP65 (Figure 6.4C). In contrast fragments comprising distal (aa 565-1074) and proximal leg (1074-1521) segments or the Hub fragment (aa 1074-1675) did not show specific interaction with GRASP65 compared to BSA immobilized on beads (Figure 6.4D). This data establishes that clathrin directly binds to GRASP65 specifically via the N-terminal domain (aa 1-545). Since clathrin is not needed for vesicular Golgi transport, we addressed whether clathrin might function in a complex with GRASP65 independent of its transport activity. To this end, we tested whether loss of Golgi connectivity in clathrin-depleted cells could be rescued using a mutant clathrin that functions at the spindle, but does not perform in membrane traffic pathways (CHC17-stunted; aa1-544, 1431-1675) [200]. This protein is trimerized and has the clathrin terminal domain but is missing most of the triskelion leg. Golgi connectivity was assessed by FRAP analysis of transiently expressed GalT in cells depleted of clathrin expressing RNAi-resistant full-length CHC17 or CHC17-stunted fused to Apple fluorescent protein (Figure 6.4E,F). Full length CHC17 rescued Golgi-connectivity in the absence of endogenous CHC17, while empty vector alone (Apple) did not. Notably, CHC17-stunted was able to largely restore Golgi ribbon formation when expressed in a clathrin-depleted background. This indicates that trimerized soluble clathrin is sufficient to restore Golgi integrity, independent of clathrin's ability to form vesicle coats.

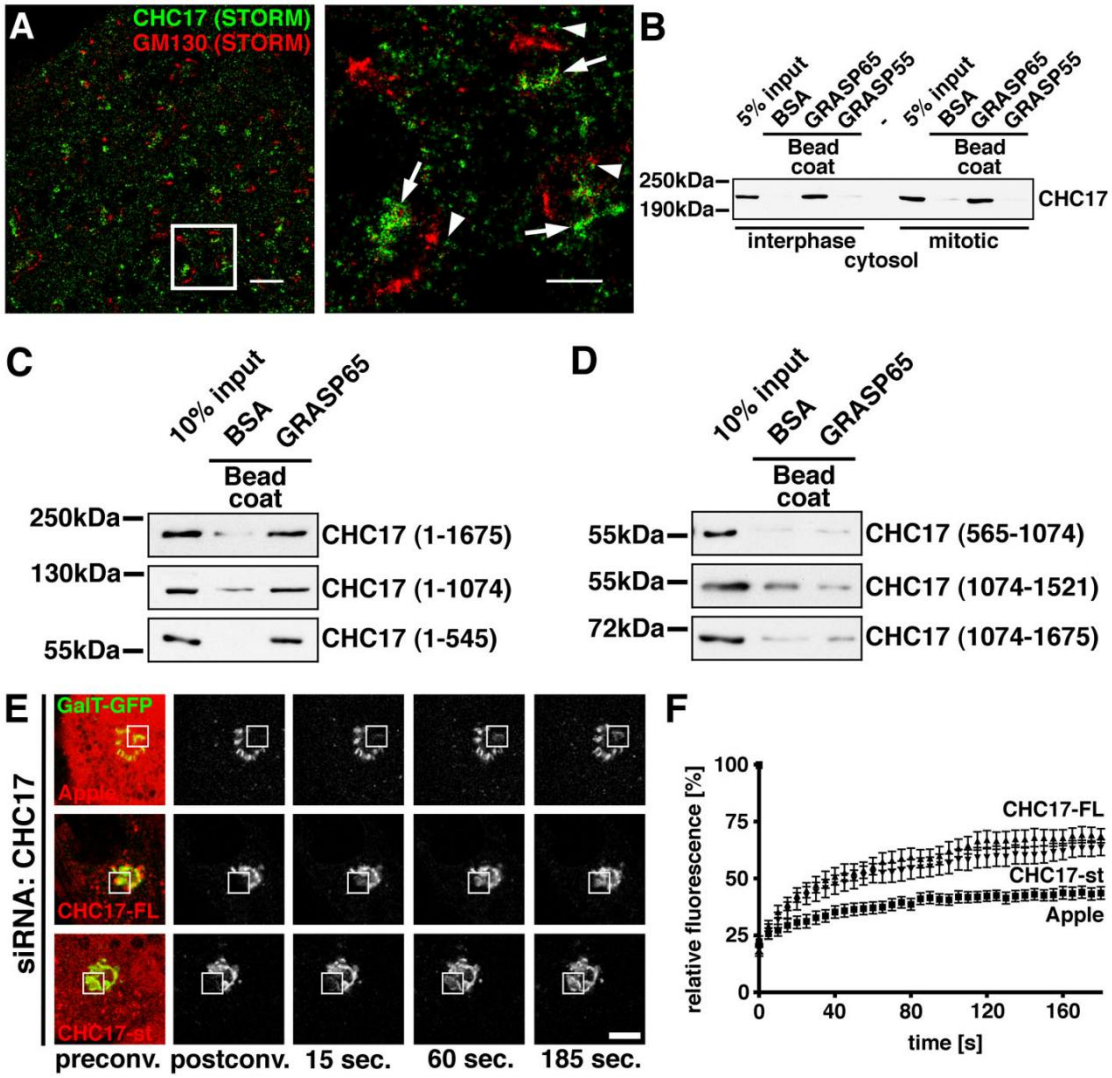

Figure 6.4: Direct binding of the N-terminal Domain of Clathrin to GRASP65 and Promotion of Golgi Connectivity by Crosslinking.

(A) RPE1 cells, treated with nocodazole for 2 hours and recovered for 5 min, were fixed and stained for CHC17 (red, STORM) and GM130 (green, STORM). Reforming ministacks show cisternal architecture including GM130 on cis-cisternae and a large pool of clathrin at the TGN (arrows). A small clathrin pool is also associated with cis-cisternae (arrowheads). Bars, 3μm, 1μm (box). (B) Beads coated with BSA or purified GRASP65 and GRASP55 were incubated with proteins enriched by ammonium sulfate cut (15-30%) from interphase or mitotic cytosol, washed and analyzed by western blotting for CHC17 binding. Molecular mass indicated in kilodaltons (kDa). (C, D) Beads coated with BSA or recombinant GRASP65 were incubated with recombinant clathrin fragments (amino acid (aa) residues indicated). Molecular mass indicated in kilodaltons (kDa). (C) GRASP65-binding clathrin fragments including full-length protein (1-1675) and the N-terminal domain (1-545). (D) Non-binding clathrin fragments. (E, F) GalT-GFP and siRNA targeting CHC17 along with Apple empty vector (upper panel), Apple-CHC17-full-length (FL, siRNA-resistant, middle panel) or Apple-CHC17-stunted (ST, 1-544,1431-1675; siRNA-resistant, lower panel) were transfected into RPE1 and imaged live. Regions marked by red square were photobleached and recovery was imaged for three minutes. Pre-bleach images show overlay of GalT-GFP and Apple constructs to demonstrate localizations. Subsequent images are GalT-GFP signal only to visualize fluorescence recovery. Bar, 5μm. (F) Fluorescent intensity plots of GalT-GFP signal from (E) are plotted. Significance was assessed using Student's t-test.

GRASP65 contributes to Golgi stack and ribbon formation by homo-oligomerization [14, 199]. GRASP65 homo-oligomerization can be mimicked in vitro by aggregation of GRASP65-coated beads and is greatly enhanced in the presence of cytosol (Figure 6.5A), as previously shown [14]. When clathrin was depleted from cytosol using specific IgG less aggregation was observed than mediated by cytosol exposed to control IgG (Figure 6.5A-C), indicating that clathrin promotes GRASP65-mediated crosslinking of beads. To determine whether clathrin is sufficient to enhance GRASP65 oligomerization, we incubated GRASP65-coated beads with recombinantly-expressed full-length clathrin as well as the trimerized Hub fragment (1074-1675) missing the N-terminal domain (Figure 6.5D-G). Full-length clathrin but not Hub promoted bead aggregation. This confirms that clathrin promotes clustering of GRASP65-associated structures and, together with the cell-based rescue experiments (Figure 6.4E), indicates that clathrin acts as molecular glue for GRASP65-decorated Golgi fragments.

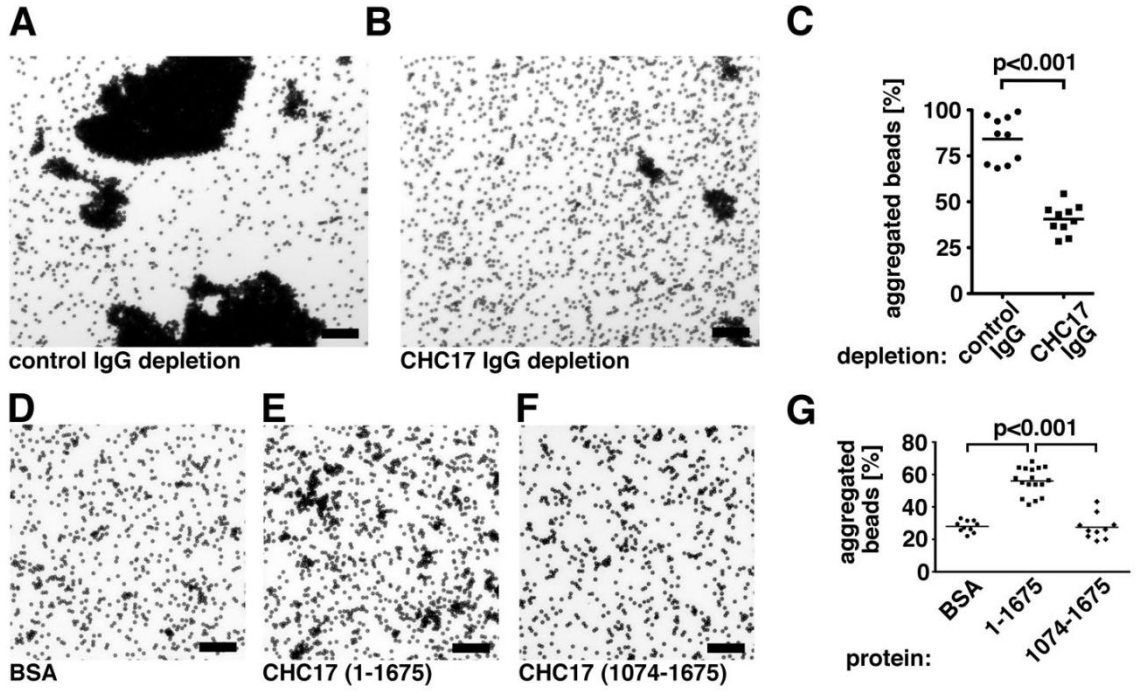

Figure 6.5: Homotypic GRASP65 Oligomerization Enhanced by Clathrin
(A-C) GRASP65-coated beads were incubated with interphase cytosol depleted by (A) non-specific control IgG or (B) anti-CHC17 IgG. Beads were imaged by light microscopy and aggregated beads were scored and plotted as a percentage of total (C) Bars, 50μm. **(D-G)** GRASP65-coated beads were incubated with purified BSA (D),

recombinant full-length CHC17 (1-1675) (E) or a CHC17 fragment lacking the GRASP65-binding terminal domain (F) and imaged and quantified (G) as in (A-C). Bars, 50μm. Significance was assessed using Student's t-test.

Clathrin-dependent Ribbon Formation Needed for Golgi-derived Microtubules and Polarization

The data presented here indicate that clathrin maintains Golgi ribbon integrity through binding and crosslinking GRASP65-decorated *cis*-Golgi fragments. Our analysis of spindle-associated clathrin however, suggests that clathrin is not the spindle-derived Golgi formation factor defined by the studies of Wei and Seamann, which also define microtubules as a second factor needed for Golgi formation [193]. Because clathrin participates in a microtubule-interacting complex during mitosis [165], we addressed the possibility that clathrin might also influence Golgi formation through an effect on microtubules. To test for microtubule function in clathrin-depleted cells, we first disrupted microtubules by nocodazole treatment of clathrin-depleted or non-silenced cells expressing GalT-GFP. As previously reported, nocodazole treatment caused fragmentation of the Golgi in both [157]. We then followed Golgi reformation by live imaging after drug washout (Figure 6.6A, B). Both control and clathrin-depleted cells clustered their Golgi fragments, although clathrin-depleted cells showed slightly delayed and incomplete clustering (arrows in Figure 6.6A, B). In clathrin-depleted cells, individual Golgi fragments frequently escaped the bulk of Golgi membranes only to rejoin the remaining Golgi fragments shortly after (see arrowheads 1 and 2 in Figure 6.4B and high resolution image series). This suggests that some functional microtubules were still present after clathrin depletion and explains the static phenotypes observed in interphase cells after clathrin depletion, which showed varying degrees of Golgi fragment clustering [157] (Figure 6.1), compared to no fragment clustering after nocodazole treatment.

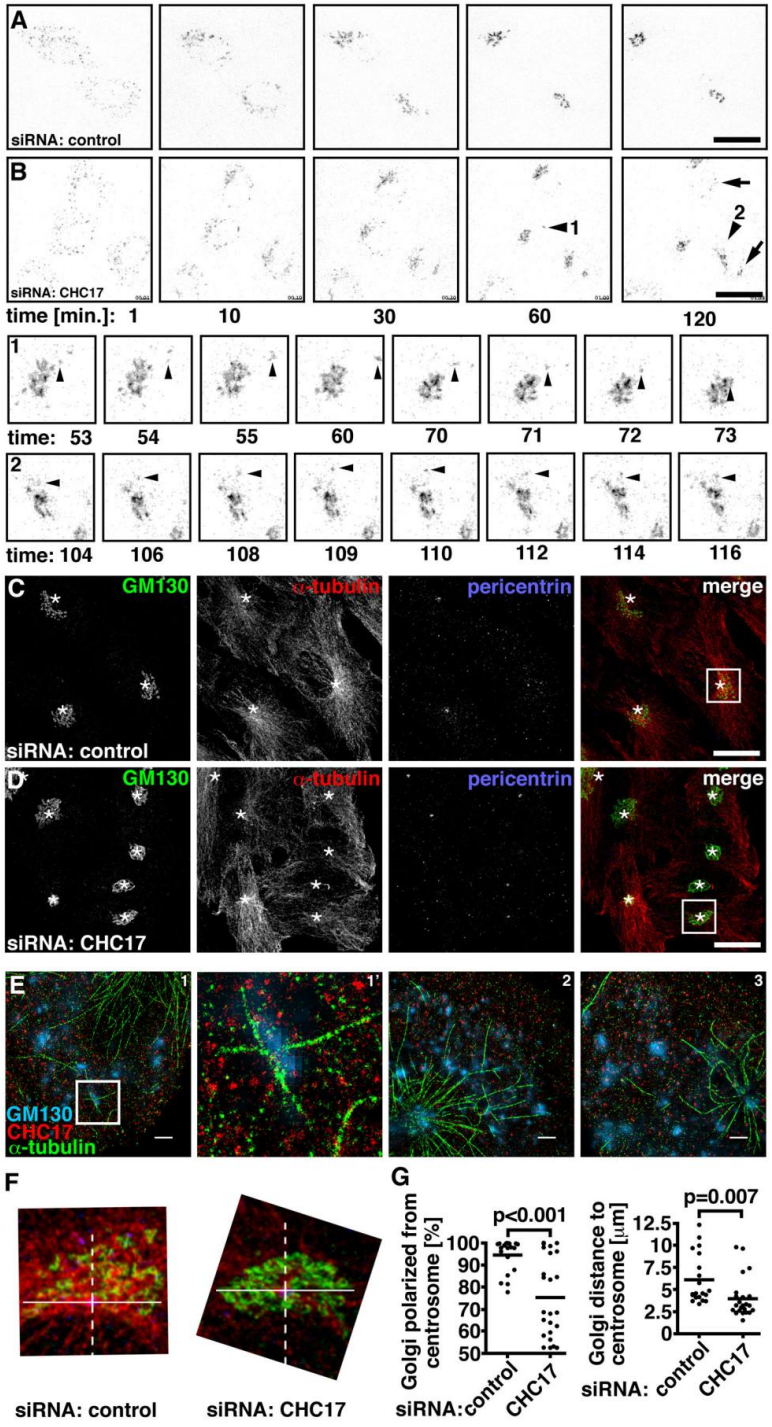

Figure 6.6: Loss of Golgi-derived Microtubules and Centrosomal Concentration of Golgi Fragments Upon Clathrin Depletion.

(A, B) RPE1 cells transfected with GalT-GFP and (A) control or (B) siRNA targeting CHC17 were treated with nocodazole for 2 hours and imaged for 2 hours after nocodazole washout. Note slower recovery of Golgi morphology in clathrin-depleted cells as well as Golgi fragments (marked by arrows) not joining the main Golgi. Also, Golgi fragments frequently escaped the bulk of Golgi signal but were rapidly recaptured (see arrowheads 1, 2 and corresponding high resolution series). Bars, 20μm. **(C, D)** Fixed RPE1 cells treated with (C) control or (D) siRNA targeting CHC17 were stained for Golgi (GM130, green), microtubules (α-tubulin, red) and centrosomes

(pericentrin, blue). Pericentrin-labeled centrosomes are indicated by asterisks in the GM130, α-tubulin and merged images. Boxes described in F. Bars, 20μm. **(E)** RPE1 cells, treated with nocodazole for 2 hours and recovered for 5 min, were fixed and stained for microtubules (α-tubulin, green, STORM), CHC17 (red, STORM) and the Golgi (GM130, blue, conventional). Three examples are shown. Low-magnification field of (1) is shown left and blow-up of box shown right (1'). Bars, 2μm. **(F)** Boxed areas of (C) and (D) were overlaid with crosshairs centered on the centrosome and the image was rotated to maximize the polarity of the GM130 signal relative to the crosshairs, then the fluorescence above the centrosome center was quantified. **(G)** Golgi polarization and position relative to centrosomes was measured in cells as in (C, D and F). Percentages of Golgi polarization in individual cells (percent of total Golgi signal offset from centrosome) and average distances of Golgi fragments from the centrosome are plotted. Significance was assessed using Student's t-test.

There are two subpopulations of microtubules that have been implicated in Golgi reformation, Golgi-derived and centrosome-derived [66, 70]. Centrosomal microtubules are needed for clustering and Golgi-derived microtubules are needed for ribbon formation [70]. The phenotype of our live cell images indicates centrosomal microtubules were still functional since fragments were able to cluster. However, Golgi-derived microtubules were apparently impaired, since ribbons did not reform and Golgi fragments persisted. Preferential loss of Golgi-derived microtubules from clathrin-depleted cells was confirmed by labeling microtubules. Compared to cells treated with non-silencing siRNA, which displayed a network of microtubules overlaying the Golgi ribbons stained with GM130, clathrin-depleted cells lacked microtubules overlaying clusters of GM130-labeled fragments. Microtubules emanating from the pericentrin-labeled centrosome were still observed in cells treated with either non-silencing or clathrin-targeting siRNA (Figure 6.6C, D). To determine whether a stabilizing association between clathrin and Golgi-derived microtubules might explain their loss upon clathrin depletion, we used STORM microscopy. Interphase cells were treated with nocodazole followed by washout of the drug and 5 minutes recovery time to allow for microtubule formation. Costaining for clathrin and microtubules in the vicinity of Golgi fragments (labeled for GM130) that were distant from the centrosome did not reveal any colocalization between clathrin and newly emerging Golgi microtubules (Figure 6.6E). Furthermore, clathrin was not aligned along microtubules, as

observed by STORM for spindle clathrin (Figure 6.2). In clathrin-depleted cells, turnover of remaining cellular microtubules, as measured by FRAP, was only slightly delayed compared to turnover of non-Golgi-associated microtubules in cell treated with non-silencing siRNA (Figure 6.S4A-E). These observations are consistent with biochemical evidence that clathrin participates in a microtubule-stabilizing complex only during mitosis [165].

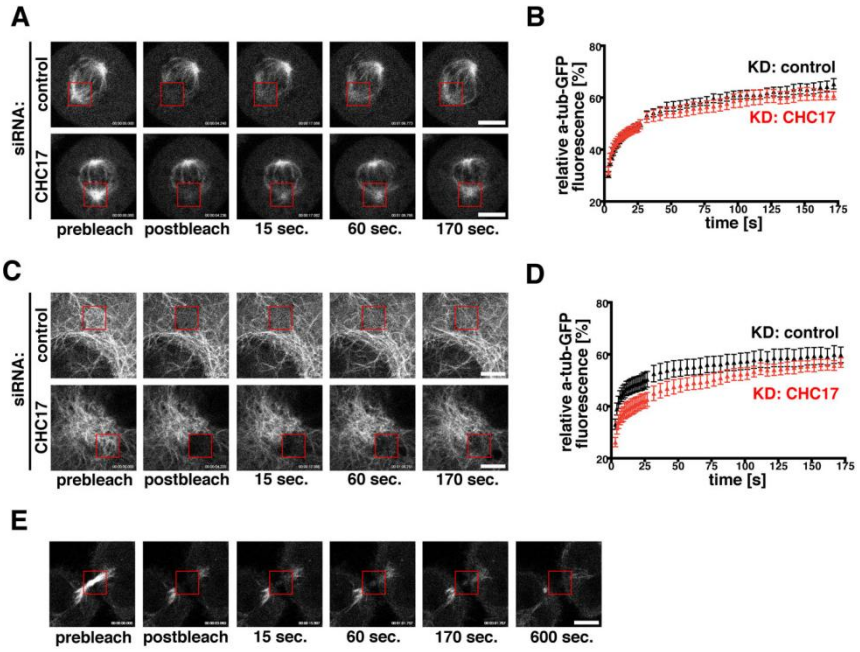

Figure 6.S4: α-Tubulin Turnover at the Mitotic Spindle and the Golgi
(A-D): HeLa cells stably expressing α-tubulin-GFP were treated with either control siRNA or CHC17-specific siRNA, as indicated, and imaged in a live microscopy setup. Regions representing the mitotic spindle (A) or the Golgi (C) marked by red squares were photobleached with a short, high intensity laser pulse and imaged for three minutes. (B, D) Fluorescent intensity plots of α-tubulin-GFP signal from (A) and (C) are plotted. (E) HeLa cells stably expressing α-tubulin-GFP were photobleached in areas marked by the red square corresponding to the midbody and fluorescence recovery recorded. Note the complete absence of microtubule nucleation in the midbody, contrasting with spindle- and Golgi-associated microtubules. Bars, 5μm.

To further characterize the impaired microtubule function in cells lacking clathrin, we analyzed the position of clustered Golgi fragments relative to the centrosome. A normal Golgi is always polarized to the non-nuclear side of the centrosome and is offset from the centrosome. The centrosome in clathrin-depleted and control cells was labeled with pericentrin and the positions of GM130-labeled fragments were measured for proximity and polarization relative to

the centrosome (Figure 6.6F, G). We observed a loss of Golgi polarization (percent of GM130 signal offset from the centrosome) and decreased distance of Golgi fragments to the centrosome in cells depleted of clathrin when compared to control-treated cells. Closer apposition to the centrosome is consistent with a reduction in space constraints upon loss of Golgi connectivity, possibly accounting for the "tight Golgi" phenotype produced by clathrin depletion described by Radelescu et al (2007). Loss of Golgi polarization is consistent with loss of Golgi-derived microtubules. We conclude that these phenotypes following clathrin depletion result from a failure to form Golgi-derived microtubules due to persistence of Golgi fragmentation in clathrin's absence and lack of ribbon formation.

Discussion

In this study we describe an unexpected role for clathrin as a Golgi ribbon formation factor. This function is independent from clathrin-mediated vesicle formation. We demonstrate that the N-terminal domain of clathrin directly binds the Golgi-stacking factor GRASP65 and that this crosslinking activity is needed for reformation of Golgi ribbons from ministacks generated during mitosis or by nocodazole treatment, in vitro and in situ. Furthermore, upon acute inactivation of clathrin in interphase, Golgi ribbon continuity is lost, indicating a role for clathrin in maintaining the lateral integrity of Golgi ribbons, which apparently undergo continuous dissociation and reassociation. We also show that spindle-associated clathrin is rapidly exchanging and does not preferentially associate with the Golgi as a proposed spindle-associated Golgi formation factor [158, 190, 193]. By STORM imaging we observe a pool of clathrin adjacent to the cis-Golgi where GRASP65 operates, consistent with the biochemical function we define. Lastly, we observe loss of Golgi-derived microtubules upon clathrin depletion, mapping clathrin-mediated ribbon formation upstream of nucleation of these important microtubules and demonstrating their specific role in Golgi polarization. Together these observations resolve several outstanding issues regarding the molecular mechanism of Golgi formation. First, the debated functions of GRASP65 in stack formation and in ribbon formation can be segregated, with the latter being dependent on crosslinking by clathrin. Second, the role and source of clathrin in promoting and maintaining Golgi integrity are defined, and ribbon formation is shown to be a dynamic process with implications for intra-Golgi cargo transport. Third, the need for ribbon integrity to generate the Golgi-derived microtubules required for polarization is established.

The integrity of the mammalian Golgi apparatus depends on two membrane apposition processes. One results in formation of unfused, but organized membrane stacks segregating *cis*, medial and *trans* processing enzymes. The second involves the formation of lateral contacts between the stacks and their fusion into ribbons. GRASP65 is localized to the *cis*-Golgi and its homologue, GRASP55 is localized to the medial and *trans*-Golgi regions. Both GRASP proteins are required for stacking and lateral integrity [13, 16, 85, 155]. To facilitate stacking, GRASP65 initially homo-dimerizes via its membrane-proximal domain and then forms higher order oligomers between stacks. We propose that clathrin is not necessary for this stacking action but that clathrin-mediated crosslinking at the edges of ministacks enhances lateral interaction to appose membranes for subsequent fusion into ribbons. This clathrin-mediated enhancement could be dependent or independent of higher order GRASP65 homo-oligomerization. Assays defining the need for GRASP65 in ribbon formation have been performed either in the presence of cytosol or in a cellular context [16, 192]. Here we show that clathrin is a necessary and sufficient factor from cytosol needed for GRASP65 to perform this function. GRASP65 also interacts in a complex with the tethering factor GM130 [192, 199] and this interaction is also needed for ribbon formation. Consistent with models proposed by others [155, 192] GM130, through interactions with the golgin family members p115 and giantin acting as tethering factors, is likely to mediate long range capture vesicles for integration into GRASP65-coated cisternae and ministacks [4]. We propose that when the latter are sufficiently close, trimeric clathrin stabilizes *cis*-cisternal juxtaposition by crosslinking GRASP65 so that the cis-face of adjacent ministacks are close enough to fuse into ribbons, probably requiring additional fusion mediators (see model in Figure 6.7). Another feature of ribbon formation that emerges from our study is that, without clathrin, ribbons are labile. This suggests that the clathrin-GRASP65 meshwork

serves as ribbon glue that could potentially regulate lateral cisternal fusion. One of the proposed mechanisms for cargo transport through the Golgi (cisternal progenitor model) suggests that ribbons potentially form between two different types of cisternae, thereby changing cargo environment and effectively moving it forward [201], a cross between cisternal maturation [202, 203] and instant access to all processing enzymes [188]. Glueing and unglueing of labile lateral connections by clathrin is consistent with all three proposed mechanisms of intra-Golgi transport. Although GRASP55 does not bind clathrin, liberation of GRASP65-cisterna from a clathrin-glued ribbon could free up a *cis*-cisterna to form a ribbon with a medial cisterna via other crosslinkers, of which there are many in the Golgi.

We observe that disruption of *cis*-Golgi ribbons by loss of clathrin also disrupts *trans*-Golgi ribbons, as demonstrated by loss of GalT mobility. Thus the glueing function of clathrin on the *cis*-side of the Golgi must lay the foundation for ribbon formation throughout the stack by maintaining the juxtaposition of ministacks. We further observe that Golgi-derived microtubules do not form when the Golgi is disrupted by clathrin depletion. However, clathrin does not decorate Golgi-derived microtubules, as we observed for spindle microtubules in STORM. The latter interaction is a function of clathrin's mitotically regulated participation in a complex with the microtubule-binding proteins TACC3 and ch-TOG [165]. Thus, a role in interphase microtubule stability would not be expected, consistent with our findings. Therefore, clathrin's role in lateral Golgi integrity cannot be ascribed to a loss of Golgi-derived microtubule stability. The converse seems to be the case and we propose that Golgi-derived microtubules cannot form if Golgi architecture is disrupted by loss of clathrin function at the *cis*-Golgi. We suggest that this could simply be due to loss of the glueing function we identify here and the need for an

organized Golgi structure for microtubule nucleation (see model in Figure 6.7). Though we cannot rule out that clathrin plays an additional role in membrane traffic pathways that contribute to nucleation of Golgi-derived microtubules, disruption of clathrin-mediated Golgi traffic by knockout of the μ1A subunit of the AP1 adaptor does not affect Golgi architecture [204]. Notably our data further establish a role for Golgi-derived microtubules in Golgi polarization and demonstrate that centrosomal microtubules are not sufficient, in agreement with the work of Kaverina and colleagues [70]. Loss of Golgi polarization upon clathrin depletion likely contributes to the documented additional clathrin-depletion phenotype of migration inhibition [205].

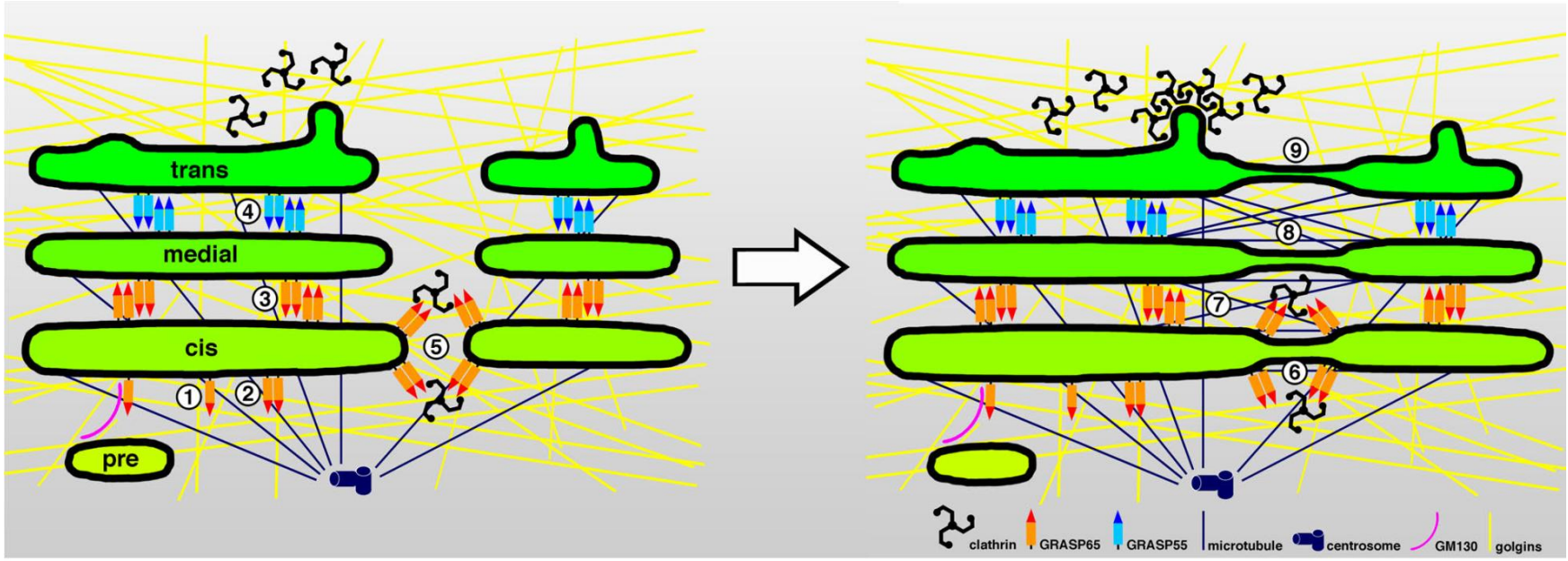

Figure 6.7: Model for role of the clathrin-GRASP65 interaction in Golgi formation
Steps 1-4: GRASP65 forms dimers which homo-oligomerize and stabilize *cis*-medial stacking while GRASP55 dimer homo-oligomerization stabilizes medial and *trans*-stacking to form ministacks. Centrosome-derived microtubules contribute to Golgi fragment and ministack clustering. **Steps 5 and 6:** Clathrin triskelia glue GRASP65 into a meshwork that facilitates and maintains transient *cis*-Golgi ribbon formation. **Steps 7-9:** The foundation of *cis*-Golgi ribbon formation promotes Golgi-derived microtubule formation and ultimately leads to medial and trans-Golgi ribbon formation. GM130 interaction with GRASP65 and golgins captures pre-Golgi fragments to support fusion of cis-Golgi membranes. In their conventional function, polymerized clathrin triskelia form lattices to coat transport vesicles and tubules for membrane traffic at the *trans*-Golgi network. Golgi stack and ribbon formation occurs in a matrix of tethering golgins that contribute to stabilizing Golgi superstructure.

Clathrin's function in Golgi ribbon formation can be reconstituted with a trimeric version of clathrin with short legs that is non-functional for vesicle formation. While exploiting clathrin's three-fold symmetry, this glueing activity represents a significant expansion of clathrin's functionality beyond membrane coating and its participation in a mitotic complex with TACC3 and ch-TOG. In the latter function, clathrin crosslinking stabilizes spindle microtubules and centrosomes [168, 206], but in the case of crosslinking GRASP65, clathrin contributes to the formation of Golgi ribbons, as well as stabilizing them. Similarly to the clathrin-TACC3-ch-TOG complex, clathrin's interaction with GRASP65 might be regulated to coordinate with the cell cycle. Here we show that GRASP65 binds clathrin from protein fractions prepared from either interphase or mitotic cytosol and that clathrin from interphase cytosol can crosslink mitotically generated Golgi ministacks in vitro. However, both of these assays could bypass modifications that regulate clathrin function at the *cis*-Golgi in situ.

All of clathrin's activities – membrane coating, spindle microtubule and centrosome stabilization, as well as Golgi glueing described here – depend on the special three-legged structure of the clathrin triskelion. The most evolutionarily conserved clathrin function as a membrane coat makes use of clathrin's ability to self-assemble into a lattice and this function is conserved in all eukaryotes in which clathrin has been characterized [195]. Golgi ribbons are unique to vertebrates, perhaps reflecting the need for a more efficient secretory pathway in complex organisms. Likewise, spindle clathrin is not a feature of all eukaryotes [165]. Notably, clathrin's functions in microtubule stabilization and facilitating Golgi ribbon formation only require trimerization of clathrin's versatile protein-interacting N-terminal domain [207] and clathrin is used to crosslink other proteins in these instances. Thus, the evolutionarily younger

clathrin functions seem to derive from selection of convenient terminal domain variants that confer a moonlighting function on the clathrin triskelion.

In conclusion, this study defines a function for clathrin in Golgi ribbon formation by directly binding GRASP65 and thereby glueing and facilitating lateral fusion of Golgi membranes. This represents a previously un-described moonlighting function of clathrin in Golgi integrity, which is required for formation of Golgi-derived microtubules and consequent Golgi polarization and positioning.

Materials and Methods

Plasmids, antibodies and siRNA

His-tagged CHC17 fragments (aa1-1074 in pET23d, aa1074-1521 in pET15b, aa1-545, 564-1074, and 1074-1675 in pET21a) as well as GFP-uLCa, GFP-CHC17, Dendra2-uLCa, SNAP-uLCa, Apple-CHC17 and Apple-CHC17-stunted (1-544, 1431-1675) were cloned using standard methods and some previously described [208, 209]. The CHC17 full-length cDNA was cloned into the baculovirus transfer vector pAcSG2 (BD Biosciences) and expressed in Hi5 cells with the baculovirus expression system (Expression Systems).

Antibodies used were monoclonal anti-CHC17 X22 [183], monoclonal anti-GM130 (BD Biosciences), rabbit polyclonal anti-GM130 (Santa Cruz), rabbit polyclonal anti-GS27 (gift from Regis Kelly, UCSF)), goat polyclonal anti-pericentrin (Santa Cruz), anti-α-tubulin (Sigma), anti-β-tubulin (Cytoskeleton).

Control and CHC17 specific siRNAs were synthesized by QIAGEN. DNA sequences targeted were AATTCTCCGAACGTGTCACGT for non-targeting control and AAGCAATGAGCTGTTTGAAGA for CHC17 [210-212].

Cell culture

HeLa and RPE1 cells were grown in DMEM supplemented with 10% FBS, 50U/ml penicillin and 50 mg/ml streptomycin. HeLa cells stably expressing Dendra2-uLCa and SNAP-uLCa were generated by selection using 500-1000 mg/ml G418 (Sigma).

Cells were transfected with 5 nM siRNA using HiPerfect (Qiagen) and expression plasmids using Lipofectamine 2000 (Invitrogen) according to manufacturer's instructions. Cells were treated with siRNA for 72 hours with expression plasmids transfection after 48 hours.

Preparation of recombinant proteins

His-tagged CHC17 fragments were expressed in BL21-CodonPlus(DE3)RILP bacteria and purified on nickel beads (Qiagen). His-tagged (in pET30a from Novagen) and MBP-tagged (in pMAL-2CX from NEB) GRASP65 were expressed in BL21(DE3)Gold bacteria and purified on amylase (NEB) or nickel (Qiagen) agarose [14]. Purification of CHC17 expressed in Hi5 cells was by self-assembly from cell lysate based on a published protocol [213].

CHC17 depletion from cytosol

Interphase cytosol prepared from HeLa cells [8, 133] was incubated with non-specific control IgG or anti-CHC17 IgG (X22) and protein-G agarose beads at 4ºC overnight. The beads were pelleted and supernatant analyzed by immunoblotting for CHC17. Equal amount of cytosol immunodepleted by control IgG or anti-CHC17 IgG was used in the bead aggregation assay and Golgi disassembly and reassembly assay described below.

In vitro binding assays

To test for CHC17 - GRASP65 interaction, proteins were concentrated from interphase or mitotic cytosol by a sequential 15-30% ammonium sulfate precipitation. Precipitated proteins were dissolved and dialyzed into KHM buffer (20 mM Hepes-KOH, pH 7.0, 0.2 M sucrose, 60 mM KCl, 5 mM Mg(OAc)2, 2 mM ATP, 1 mM GTP, 1 mM glutathione and protease inhibitors,

for interphase cytosol) or MEB buffer (50 mM Tris-HCl, pH 7.4, 0.2 M sucrose, 50 mM KCl, 20 mM β-glycerophosphate, 15 mM EGTA, 10 mM MgCl2, 2 mM ATP, 1 mM GTP, 1 mM glutathione and protease inhibitors, for mitotic cytosol), then incubated with BSA or His-GRASP65 pre-coupled cyanogen bromide-activated beads (CNBr agarose, Sigma-Aldrich) in the presence of an ATP-regenerating system (10 mM creatine phosphate, 1 mM ATP, 20 μg/ml creatine kinase and 20 ng/ml cytochalasin B) at 4ºC overnight. After washing, bound proteins were analyzed by immunoblotting.

To test whether CHC17 directly binds GRASP65 and to determine the binding site, purified CHC17 full length protein or fragments were incubated with BSA or MBP-GRASP65 pre-coupled to cyanogen bromide-activated (CNBr) beads (pre-blocked with BSA), in the presence of ATP-regenerating system in KHM buffer at 4ºC overnight. The beads were washed extensively and then analyzed by SDS-PAGE and immunoblotting for CHC17.

Bead aggregation assay

Bead aggregation assays were performed as previously described [8, 14, 18]. For quantification of the aggregation efficiency, 10-20 random phase contrast digital images of each reaction were captured by Zeiss Observer Z1 epifluorescence microscope with a 10X lens. Images were analyzed with the MATLAB7.4 software to determine the surface area of objects, which was used to calculate the number of beads in the clusters. Aggregates were defined as those with ≥ 6 beads. Only visible surface beads were counted; therefore, the number of beads in large aggregates was underestimated. Results were expressed as the mean ± SEM from 3 independent experiments; statistical significance was assessed by Student's t-test.

Golgi disassembly and reassembly assay and quantification

Golgi membranes were purified from rat liver [16]. Interphase (IC) and mitotic (MC) cytosols were prepared from HeLa S3 cells [8, 133]. The Golgi disassembly assay was performed as described previously [8]. Briefly, purified Golgi membranes (20 μg) were mixed with 2 mg of mitotic cytosol, 1 mM GTP and an ATP-regenerating system in MEB buffer in a final volume of 200 μl. After incubation for 60 min at 37°C, mitotic Golgi fragments (MGF) were isolated and soluble proteins were removed by centrifugation (135,000 g for 30 min in a TLA55 rotor) through a 0.4 M sucrose cushion in KHM buffer onto a 6-μl 2 M sucrose cushion. The membranes were resuspended in KHM buffer, either fixed and processed for EM [8], or used in reassembly reactions. For Golgi reassembly, 20 μg of mitotic Golgi fragments were resuspended in KHM buffer, mixed with 400 μg interphase cytosol immunodepleted using either non-specific IgG or anti-CHC17 IgG as described above in the presence of an ATP regeneration system in a final volume of 30 μl in KHM buffer and incubated at 37°C for 60 min. The membranes were pelleted by centrifugation, and processed for EM.

To quantify the reassembly of Golgi, EM images of Golgi membranes were captured at 11000x magnification. The percentage of membranes in cisternae or in vesicles was determined by the intersection method [8, 128]. Cisternae were defined as long membrane profiles with a length greater than four times of their width, and the latter did not exceed 60 nm. Normal cisternae ranged from 20-30 nm in width and were longer than 200 nm. Stacks were defined as two or more cisternae that were separated by no more than 15 nm and overlapped in parallel by more than 50% of their length. All experiments were repeated at least 3 times; statistical significance was assessed by Student's t-test.

Electron microscopy

For EM analysis, Golgi stacks and clusters were identified using morphological criteria and quantified using standard stereological techniques [8, 18]. Golgi stack images were captured at 11000x magnification. Interphase cells were defined as profiles that contained an intact nuclear envelope. The longest cisterna was measured as the cisternal length of a Golgi stack using the ruler function in Photoshop CS3. At least 20 cells were quantified in each experiment, and the results represent at least three independent experiments. Statistical significance was assessed by Student's t-test.

Immunofluorescence and image analysis

For fixed cell analysis, cells grown on coverslips were washed in warm PBS, fixed in warm PFA (3.7% in PBS, 10 min), then washed (2x, 5 min, PBS), permeabilized (4 min, 3% BSA, 0.5% Triton X-100 in PBS), and blocked in blocking solution (3% BSA in PBS, 30 min). Antibody labeling was performed by inversion of coverslips on 20 μl blocking solution with primary or secondary antibodies (1–5 μg/ml), DAPI, or TO-PRO3 on parafilm and washing with PBS. Samples were mounted in the Prolong Antifade kit (Invitrogen).

Measurements of Golgi angles to division axis were performed on fixed cells. Cells in cytokinesis were identified by Golgi twin formation, slightly condensed DNA and neighbouring corresponding daughter cell. A solid crosshair was overlaid to mark the cell center along the vertical axis of division from the neighboring cell. Golgi signal for individual cells was

thresholded and angles for every pixel containing Golgi labeling were calculated from the center relative to the division axis. The average angle of the Golgi signal per cell is shown.

Golgi distances from centrosomes were measured as above with the average distance of Golgi labeled pixels to pericentrin staining being shown.

Colocalization of green and red Dendra2 signal was plotted using NIH Image J's colocalization highlighter plugin.

Polarization of the Golgi from centrosomes was measured by applying a crosshair through pericentrin staining and rotating Golgi labeling around the centrosome such that the maximal difference between the areas separated by the horizontal line was achieved. The percentage of Golgi labeling on the side containing more labeling is shown. Therefore, complete loss of polarization results in a percentage of 50 while complete segregation of labeling to one side, corresponding to maximum polarization would lead to a value of 100.

Live cell imaging

Live imaging was carried out at 37°C in 5% CO_2 on a Leica SP5 or a Zeiss LSM 510 confocal microscopes. GFP and green Dendra2 were excited by 488nm lasers and emissions were collected from 495-550nm (Leica SP5) as well as a BP500-550 (Zeiss LSM 510). Apple and red Dendra2 were excited by 543 or 561nm lasers and emissions were collected from 555-650nm (Leica SP5) as well as a LP575 (Zeiss LSM 510). Imaging was performed using 63x, NA=1.4 objectives using low level excitation to reduce photobleaching.

For FRAP analysis GFP was photobleached in the indicated regions using 80-100% laser power for 10-15 iterations. Fluorescence in regions of interests was measured using Leica and Zeiss software respectively and analyzed in Microsoft Excel and GraphPad Prism software. Photoconversion of Dendra2 was achieved with a 405nm laser at 15-30% output for 5-10 iterations. Analysis was as for FRAP experiments.

Rapid inactivation experiments were performed in HeLa clone 3.3 that stably expresses SNAP-uLCa by addition of 10 μM benzylguanine-glutaric acid-benzylguanine (BG-GLA-BG) crosslinking dimerizer for two hours, a condition shown to functionally inactivate the CHC17 in these cells by crosslinking associated SNAP-uLCa (Foraker et al, 2012).

STORM imaging

Sample preparation for STORM imaging was similar to that described above for immunofluorescent labeling, except for two steps: the fixation was done using 3% PFA + 0.1% glutaraldehyde, followed by treatment of 1% sodium borohydride, and the sample was post-fixed with PFA + glutaraldehyde after the second washing step. Secondary antibodies were labeled with a mixture of two fluorophores, either Alexa Fluor 405 and Alexa Fluor 647, or Cy3 and Alexa Fluor 647. This use of activator / reporter dye pairs allows two-color STORM measurement [214].

Acquisition of STORM images was performed on a home-built super-resolution microscope described previously [215]. Briefly, the microscope was based on an inverted

fluorescence microscope (Nikon Ti-E) with an oil immersion objective (100x Plan Apo VC NA 1.4, Nikon). Four excitation/activation lasers (642 nm, Stradus 642, Vortran; 561 nm, Sapphire 561-200-CW, Coherent; 488 nm, Stradus 488, Vortran; 405 nm, Stradus 405, Vortran) were combined and sent into the microscope through a home-built epi/TRIF illuminator that can adjust the incident angle of the excitation laser beam at the sample. The on/off state and the power of the three diode lasers (642, 488 and 405 nm) were directly controlled by the computer, whereas the 561 nm laser beam was controlled through an acoustic optical modulator (Crystal Technology). A quad-band dichroic mirror (zt405/488/561/640rpc, Chroma) and a bandpass filter (ET705/70m, Chroma) were used for fluorescence detection in STORM. A different bandpass filter (ET525/50m, Chroma) was used for conventional fluorescence imaging of GFP. The images were recorded by and EMCCD camera (Ixon+ DU897E-CS0-BV, Andor). A cylindrical lens (f = 700 mm, Thorlabs) was inserted between the image plane of the microscope side-port and the microscope body to create the astigmatism for three-dimensional STORM (Huang et al., 2008). The instrument was controlled through custom software written in Python and Visual Basic, whereas image analysis was done with the same software (written in Visual C++) as in previous publications [216]. Crosstalk in the two-color STORM images was subtracted for figure display [217].

Acknowledgement

We thank Hong Chen (OMRF), Pietro De Camilli,(Yale) Yuxin Mao (Cornell), Regis Kelly (UCSF) and Keith Mostov (UCSF) for antibodies and plasmids. We thank Hebao Yuan and other members of the Wang Lab for suggestions and reagents. This work was supported by NIH grant GM038093 to F. M. Brodsky, NIH grant GM087364 and American Cancer Society grant (RGS-09-278-01-CSM) to Y. Wang, and NIH grant 2R01 AI073922 to E. Adams. D. Tang was supported by the Rackham Predoctoral Fellowship from the University Michigan and granted by the Chinese Government Award for Outstanding Self-financed Students Abroad by China Scholarship Council. B. Chhun and B. Huang were supported by the UCSF Program for Breakthrough Biomedical Research and the Searle Scholars Program. Laboratory experiments were performed by C.E., D.T., L.V., Y.S., S.M., A.F., B.C. and E.A. with equal and primary contributions from C.E. and D.T. Expression of full length CHC17 in insect cells was developed by E.A. and Y.S. STORM imaging was done in the laboratory of B.H. by C.E., L.V. and B.C. Data analysis was performed by C.E., D.T., B.H., Y.W. and F.B. The manuscript was written by C.E., D.T., Y.W. and F.B. with input from B.H. The contributions of the Brodsky and Wang laboratories were equal. The authors declare no conflicts of interest.

Abbreviations

GRASP65, Golgi reassembly stacking protein, 65kDa; CHC17, clathrin heavy chain, isoform 1 encoded by the gene on chromosome 17; CLC, clathrin light chain; STORM, stochastic optical reconstruction microscopy; RNAi, RNA interference; siRNA, small interference RNA; NRK, normal rat kidney; GalT, galactose-1-phosphate uridylyltransferase; TGN, *trans*-Golgi network; IC, interphase cytosol; MC, mitotic cytosol.

Chapter 7 . Conclusion

The Golgi apparatus is the central conduit of the secretary pathway. Proteins and lipids that are newly synthesized in the ER are transported to the *cis*-side of the Golgi apparatus by COPII vesicles and then through the stacked Golgi membranes. In the Golgi, the proteins receive a series of modifications such as glycosylation, phosphorylation and sulfation. At the *trans*-side of the Golgi apparatus, the proteins are sorted to their destinations including plasma membrane, endosomal/lysosomal system, and secretary granules by different transport carriers. These functions require proper structure formation of the Golgi. In mammalian cells, the Golgi complex exhibits a very unique structure. It consists of dozens of stacks of flattened membrane cisternae with the stacks laterally linked into a ribbon [218]. Despite its important function, little is known about how and why the Golgi forms this unique structure.

During cell division, the biogenesis of the Golgi apparatus occurs through a highly dynamic disassembly and reassembly process which facilitates the inheritance of this organelle and also allows the cell cycle progression [2, 10]. Mitotic disassembly of the Golgi complex can be dissected into three steps: (1) Golgi ribbon breaking down into stacks; (2) cisternae unstacking; and (3) cisternae vesiculation. Conversely, post-mitotic reassembly includes (1) vesicle fusion into cisternae; (2) cisternae stacking; and (3) ribbon formation. However, the factors that regulate these processes have not been thoroughly studied. Therefore, my research attempts to provide

new information for better understanding these three processes in Golgi inheritance during cell division: (1) unstacking and re-stacking, (2) cisternae vesiculation and regrowth, and (3) ribbon formation.

GRASP65 regulates Golgi stacking and unstacking

Golgi stacks are the basic structural and functional units of the Golgi. In chapter II and III, I studied the function and mechanism of GRASP65 (Golgi Re Assembly Stacking Protein, 65kD) in regulating Golgi stack formation. GRASP65 is one of the only two known proteins directly involved in Golgi stacking; the other one, GRASP55, is a homolog of GRASP65 [12, 13]. These proteins function as a glue that sticks Golgi cisternae into stacks. The initial studies identified GRASP65 as a Golgi stacking factor because inhibiting its function by adding anti-GRASP65 antibodies in the in vitro Golgi reassembly assay or microinjection of GRASP65 antibodies into mitotic cells both abolished Golgi stack reformation [13, 14]. However, other studies involving RNA interference in cells [15, 49-51] or with other model organisms [88, 89, 102, 109, 110, 219-222] raised controversial results and suggested other functions for GRASP65, which include linking Golgi stacks into a ribbon, maintaining spindle stability, unconventional secretion and cell cycle regulation [22, 23, 223]. To address this controversy, I optimized the experimental condition to knockdown GRASP65 and analyzed the structural change of Golgi stacks by systematic electron microscopy. I found that although the overall Golgi morphology under light microscopy is not obviously altered upon GRASP65 deletion, under the electron microscopy the number of cisternae in each Golgi stack significantly reduced to 4.0 ± 0.1 from 5.9 ± 0.2 in control siRNA transfected cells. This effect was rescued by the expression of a siRNA-resistant

GFP-tagged rat GRASP65 construct in the knock down cells. These results confirmed that GRASP65 plays essential roles in Golgi cisternal stacking.

I also studied the mechanism of GRASP65 in mediating Golgi stacking. Based on previous *in vitro* biochemical experiments, it has been proposed that GRASP65 stacks Golgi cisternae by forming *trans*-oligomers from adjacent cisternal membranes. Phosphorylation of this protein abolishes its oligomerization and allows cisternae separation during mitosis. The N-terminal half of the protein, the GRASP65 domain, is required for both GRASP65 homo-dimerization and *trans*-oligomerzation. And the C-terminal SPR domain contains multiple phosphorylation sites and regulates the oligomerization state of the N-terminal half [18]. To understand the mechanism of Golgi stacking, I further narrowed the oligomerzation domain of GRASP65. The GRASP domain contains two PDZ domains that are known to be capable of interacting with proteins. I found that the first PDZ domain of GRASP65, aa 1-112, is both necessary and sufficient for GRASP65 oligomerization. This first PDZ domain lacks the GM130 binding site that is located in the second PDZ domain, is still localized onto the Golgi membrane. This result argues against the previous speculation that GRASP65 is targeted to the Golgi through interacting with GM130. To examine the hypothesis that phosphorylation of the C-terminal SPR domain of GRASP65 regulates GRASP65 de-oligomerization and Golgi unstacking, I expressed several non-phosphorylatable mutant of GRASP65 in the cells and looked for the change in Golgi morphology in interphase and mitosis. I found that expressing these phospho-deficient mutants enhanced Golgi stacking during interphase and inhibited Golgi disassembly during mitosis, therefore confirmed the observation from the *in vitro* assays that GRASP65 phosphorylation is required for Golgi unstacking.

I also inhibited Golgi disassembly during mitosis by expressing GRASP65 phospho-deficient mutants and thereby studied the significance of mitotic Golgi disassembly. Expression of GRASP65 phospho-deficient mutants did not impair the equal partitioning of Golgi membranes into the two daughter cells. Instead, inhibition of Golgi disassemble at the onset of mitosis delayed mitotic entry of the cells and decreased cell proliferation rates, suggesting that the Golgi disassembly during mitosis is required for cell cycle progression [17].

GRASP65 contains at least eight phosphorylation sites [19]. I further examined the mitotic kinases that phosphorylate these sites, the tempo relationship and the impacts on Golgi disassembly of their phosphorylation. Using phospho-specific mouse monoclonal antibodies that are either raised in our lab or human single chain antibodies selected from a phage display library in collaboration with Dr. Franck Perez's lab in France [94], I was able to follow the phosphorylation of three phosphorylation sites on GRASP65: T220/T224, S277 and S376. First, I found that the mitotic kinase that phosphorylates all the three sites is cdc2, while plk enhances their phosphorylation. S277 is also phosphorylated by MEK/ERK upon growth factor stimulation in interphase, which is consistent with previous reports [19, 91].

To determine the tempo relationship of GRASP65 phosphorylation at different sites and with cell cycle progression, I co-stained cells with GRASP65 phospho-specific antibodies with anti-phospho-Histone H3 to estimate the mitotic stage of the cell, or with three sets of two different phospho-specific antibodies. I found that S277 is phosphorylated the earliest in G2 phase and is de-phosphorylated the latest during cytokinesis. S376 is phosphorylated later than

S277 in late G2 phase, but earlier than T220/T224 which is phosphorylated at prophase. S376 is de-phosphorylated earlier than T220/T224, both in cytokinesis earlier than S277 de-phosphorylation.

Also, from prometaphase to anaphase, antibodies against the phosphorylated-T220/T224 of GRASP65 stained the Golgi haze containing the mitotic Golgi vesicles, not only the Golgi remnants, suggesting that the phosphorylation of T220/T224 is most critical for Golgi vesiculation. To verify this assumption, I constructed and expressed GRASP65 mutants that are mutated at T220/T224 (S216A/S217A/T220A/T224A), S277 (S277A) or S376A (S367A/S376A). Unlike the S277A or S367A/S376A mutant, expression of the S216A/S217A/T220A/T224A mutant significantly inhibited Golgi disassembly under both fluorescence microscopy and electron microscopy. These results suggested that S216/S217/T220/T224- phosphorylation site is most important for Golgi disassemble, perhaps because that this cluster is in closest proximity to the GRASP domain, therefore is critical for GRASP65 de-oligomerization.

The Golgi ubiquitin ligase HACE1 regulates Golgi cisternae regrowth during cell division

After the initial Golgi ribbon breaking down at the onset of mitosis, unstacking and vesiculation take place at almost the same time to disassemble the Golgi apparatus completely into thousands of vesicles. Vesicle budding and scission in this process require COPI coat and active Arf1 [7]. After mitosis, two AAA ATPases, p97/VCP and NSF, mediate the membrane fusion for Golgi reassembly [32]. It is also found that mono-ubiquitination of Golgi membrane protein(s) during mitosis is required for targeting p97/p47 to the Golgi membranes before fusion

[35]. The deubiquitinating enzyme VCIP135 removes the ubiquitin tag which allows p97/p47 mediated fusion to take place [36]. In chapter IV, my colleagues and I characterized the newly found ubiquitin E3 ligase HACE1 as the ligase in this process [38, 148], which regulates mono-ubiquitination of Golgi proteins in mitosis.

First of all we determined that HACE1 partially localizes to the Golgi membranes by interacting with Golgi Rabs, especially Rab1. Knocking down HACE1 in cells or overexpressing an inactive mutant of HACE1 led to Golgi fragmentation. Using live-cell imaging, we found that the fragmented phenotype of Golgi in HACE1-knockdown cells was due to a defect of post-mitotic-Golgi reassembly. Furthermore, in the *in vitro* Golgi disassembly and reassembly assay, inhibition of HACE1 activity highly affected post-mitotic Golgi membrane fusion. It is worth to notice that although HACE1 is not required for Golgi disassembly, it needs to be active during disassembly to allow Golgi reassembly. These result confirmed the hypothesis that mono-ubiquitin is added to Golgi membrane during mitosis, later serves as a receptor for the p97/p47/VCIP135 complex at the end of mitosis for membrane fusion. Currently, the ubiquitinated substrate(s) on Golgi membrane has not been identified. Future work should be emphasized on finding the substrate.

Identification of GRASP65 interacting proteins that maintain Golgi ribbon integrity

How the Golgi stacks laterally connect to form a ribbon is so far not well understood, but involves a number of proteins including the microtubule and actin cytoskeleton, as well as several golgins [43, 49-51, 63, 80, 130, 224-226]. Golgi stacks are brought to the cell center by dynein along centrosome-derived microtubules, and linked with each other via Golgi-derived

microtubules [70, 77]. The function of actin cytoskeleton on Golgi organization is unclear, but it has been suggested that actin filaments connect Golgi stacks into pairs based on the study in *Drosophila* S2 cells [80]. Depletion of many golgins leads to Golgi fragmentation [1]. Golgi ribbon integrity relies on their ability to tether membrane and facilitate continuous membrane input [1], interacting with microtubules and centrosome to bring the Golgi stacks together [58, 66, 67, 70, 72, 227], as well as direct tethering of the membrane from neighboring stacks (e.g. GMAP210 and GRASPs) [49, 61]. The Golgi stacking factor GRASPs have been proposed to play roles in maintaining ribbon integrity, as depletion of either GRASP65 or GRASP55 led to Golgi fragmentation. It was suggested that GRASPs form trans-oligomers from rims of Golgi stacks similarly to their function in stacking the cisternae, which is also regulated by mitotic phosphorylation. However, the gaps between the stacks in the ribbon are relatively larger and more heterogeneous (10s to 100s nm) compared to those between the cisternae in the stack, it is also possible that GRASPs are cross-linked by other proteins to connect Golgi stacks. In chapter V and VI I attempted to identify GRASP65 binding proteins that play this role.

The idea that cytosolic proteins crosslink GRASP65 came from the observation that GRASP65 coated bead form large aggregates when incubated with interphase cytosol compared to the ones incubated with buffer. This result indicated the existence of cytosolic factors that enhance or stabilize GRASP65 oligomerization. Using affinity chromatography and mass spectrometry, we found 23 cytosolic proteins that bind to GRASP65 either directly or indirectly. I further selected the ones which showed strong binding with GRASP65 and affected Golgi organization when depleted in cells for further characterization, including clathrin heavy chain (CHC) [157, 165], a J-domain heat shock protein Dja1 [162], actin nucleation promoting factor

MENA [159], and inositol 5-phoaphatase and scaffold protein SHIP2 [160, 161]. All of them can be co-purified with GRASP65 from cytosol, while CHC and Dja1 showed direct interaction with GRASP65 *in vitro*. MENA and SHIP2 have been found for the first time localized on the Golgi complex in cells, and Dja1 can also be recruited to the Golgi membrane *in vitro*. Depletion of any of the four proteins led to Golgi fragmentation. Furthermore, inhibiting these four GRASP65-interacting proteins in interphase cytosol largely decreased GRASP65 coated beads aggregation efficiency, and reduced post-mitotic Golgi reassembly in the *in vitro* Golgi disassembly and reassembly assay. These results suggest the possibility that CHC, Dja1, MENA and SHIP2 directly or indirectly crosslink GRASP65 oligomers which is required for Golgi biogenesis.

In collaboration with Dr. Frances Brodsky's lab, we further characterized the function and mechanism of clathrin in GRASP65 oligomer crosslinking and Golgi formation. Using STORM microscopy, we were able to detect a pool of clathrin at cis-side of the Golgi, localized next to GM130, which further supports our finding that GRASP65 directly interacts with CHC and recruits it to cis-Golgi. I also mapped the domain of CHC which interacts with GRASP65 to the N-terminal domain of CHC (aa1-545). We then determined whether clathrin functions in a complex with GRASP65 independent of its function in transport using a CHC mutant which trimerizes and has the terminal domain but is missing the most part of the triskelion leg therefore does not form the clathrin coat. This mutant rescued the Golgi fragmentation caused by endogenous CHC depletion, therefore suggested that binding to GRASP65 and trimerization are enough for CHC to maintain Golgi integrity. I further tested whether clathrin triskelions are sufficient to crosslink GRASP65. Indeed, purified CHC triskelions enhanced GRASP65 coated

beads to form aggregates, while the triskelion without the N-terminal binding domain had no effect. Based on these results, we propose that clathrin triskelions crosslink GRASP65 from the rim of Golgi stacks, assists GRASP65 in connecting Golgi stacks into a ribbon.

References

1 Mironov, A.A. and Beznoussenko, G.V. (2011) Molecular mechanisms responsible for formation of Golgi ribbon. *Histol Histopathol* 26, 117-133

2 Barr, F.A. (2004) Golgi inheritance: shaken but not stirred. *J Cell Biol* 164, 955-958

3 Altan-Bonnet, N., *et al.* (2006) Golgi Inheritance in Mammalian Cells Is Mediated through Endoplasmic Reticulum Export Activities. *Mol Biol Cell* 17, 990-1005

4 Wang, Y. and Seemann, J. (2011) Golgi biogenesis. *Cold Spring Harb Perspect Biol* 3, a005330

5 Yang, J.S., *et al.* (2005) A role for BARS at the fission step of COPI vesicle formation from Golgi membrane. *Embo J* 24, 4133-4143

6 Wang, Y. (2008) Golgi: Methods for Preparation. *Encyclopedia of Life Sciences*

7 Tang, D., *et al.* (2008) Molecular mechanism of mitotic Golgi disassembly and reassembly revealed by a defined reconstitution assay. *J Biol Chem* 283, 6085-6094

8 Tang, D., *et al.* (2010) Reconstitution of the cell cycle-regulated Golgi disassembly and reassembly in a cell-free system. *Nat Protoc* 5, 758-772

9 Wang, Y. (2008) Golgi apparatus inheritance. In *The Golgi apparatus. State of the art 110 years after Camillo Golgi's discovery* (Mironov, A., *et al.*, eds), pp. 580-607, Springer

10 Shorter, J. and Warren, G. (2002) Golgi architecture and inheritance. *Annu Rev Cell Dev Biol* 18, 379-420

11 Satoh, A., *et al.* (2003) Golgin-84 is a rab1 binding partner involved in Golgi structure. *Traffic* 4, 153-161

12 Shorter, J., *et al.* (1999) GRASP55, a second mammalian GRASP protein involved in the stacking of Golgi cisternae in a cell-free system. *Embo J* 18, 4949-4960

13 Barr, F.A., *et al.* (1997) GRASP65, a protein involved in the stacking of Golgi cisternae. *Cell* 91, 253-262

14 Wang, Y., *et al.* (2003) A direct role for GRASP65 as a mitotically regulated Golgi stacking factor. *Embo J* 22, 3279-3290

15 Sutterlin, C., *et al.* (2005) The Golgi-associated protein GRASP65 regulates spindle dynamics and is essential for cell division. *Mol Biol Cell* 16, 3211-3222

16 Xiang, Y. and Wang, Y. (2010) GRASP55 and GRASP65 play complementary and essential roles in Golgi cisternal stacking. *J Cell Biol* 188, 237-251

17 Tang, D., *et al.* (2010) The Role of GRASP65 in Golgi Cisternal Stacking and Cell Cycle Progression. *Traffic* 11, 827-842

18 Wang, Y., *et al.* (2005) Mapping the functional domains of the Golgi stacking factor GRASP65. *J Biol Chem* 280, 4921-4928

19 Preisinger, C., *et al.* (2005) Plk1 docking to GRASP65 phosphorylated by Cdk1 suggests a mechanism for Golgi checkpoint signalling. *Embo J* 24, 753-765

20 Tang, D., *et al.* (2012) Sequential phosphorylation of GRASP65 during mitotic Golgi disassembly. *Biol Open* 1, 1204-1214

21 Bisel, B., *et al.* (2008) ERK regulates Golgi and centrosome orientation towards the leading edge through GRASP65. *J Cell Biol* 182, 837-843

22 Vinke, F.P., *et al.* (2011) The multiple facets of the Golgi reassembly stacking proteins. *Biochem J* 433, 423-433

23 Giuliani, F., *et al.* (2011) Unconventional secretion: a stress on GRASP. *Curr Opin Cell Biol* 23, 498-504

24 Sengupta, D. and Linstedt, A.D. (2010) Mitotic inhibition of GRASP65 organelle tethering involves Polo-like kinase 1 (PLK1) phosphorylation proximate to an internal PDZ ligand. *J Biol Chem* 285, 39994-40003

25 Truschel, S.T., *et al.* (2012) Allosteric regulation of GRASP-dependent Golgi membrane tethering by mitotic phosphorylation. *J Biol Chem*

26 Wang, Y., *et al.* (2008) Golgi Cisternal Unstacking Stimulates COPI Vesicle Budding and Protein Transport. *PLoS ONE* 3, e1647

27 Popoff, V., *et al.* (2011) COPI budding within the Golgi stack. *Cold Spring Harb Perspect Biol* 3, a005231

28 Xiang, Y., *et al.* (2007) Active ADP-ribosylation factor-1 (ARF1) is required for mitotic Golgi fragmentation. *J Biol Chem* 282, 21829-21837

29 Lowe, M. and Barr, F.A. (2007) Inheritance and biogenesis of organelles in the secretory pathway. *Nat Rev Mol Cell Biol* 8, 429-439

30 Seemann, J., *et al.* (2002) Partitioning of the matrix fraction of the Golgi apparatus during mitosis in animal cells. *Science* 295, 848-851

31 Puri, S., *et al.* (2004) Dispersal of Golgi matrix proteins during mitotic Golgi disassembly. *Journal of cell science* 117, 451-456

32 Meyer, H.H. (2005) Golgi reassembly after mitosis: the AAA family meets the ubiquitin family. *Biochim Biophys Acta* 1744, 481-492

33 Dalal, S., *et al.* (2004) Distinct Roles for the AAA ATPases NSF and p97 in the Secretory Pathway. *Mol Biol Cell* 15, 637-648

34 Uchiyama, K., *et al.* (2006) p37 is a p97 adaptor required for Golgi and ER biogenesis in interphase and at the end of mitosis. *Dev Cell* 11, 803-816

35 Meyer, H.H., *et al.* (2002) Direct binding of ubiquitin conjugates by the mammalian p97 adaptor complexes, p47 and Ufd1-Npl4. *Embo J* 21, 5645-5652

36 Wang, Y., *et al.* (2004) VCIP135 acts as a deubiquitinating enzyme during p97-p47-mediated reassembly of mitotic Golgi fragments. *J Cell Biol* 164, 973-978

37 Tang, D., *et al.* (2011) The ubiquitin ligase HACE1 regulates Golgi membrane dynamics during the cell cycle. *Nature Communications* 2, 501

38 Zhang, L., *et al.* (2007) The E3 ligase HACE1 is a critical chromosome 6q21 tumor suppressor involved in multiple cancers. *Nat Med* 13, 1060-1069

39 Totsukawa, G., *et al.* (2011) VCIP135 deubiquitinase and its binding protein, WAC, in p97ATPase-mediated membrane fusion. *Embo J* 30, 3581-3593

40 Muller, J.M., *et al.* (2002) Sequential SNARE disassembly and GATE-16-GOS-28 complex assembly mediated by distinct NSF activities drives Golgi membrane fusion. *J Cell Biol* 157, 1161-1173

41 Diao, A., *et al.* (2008) Coordination of golgin tethering and SNARE assembly: GM130 binds syntaxin 5 in a p115-regulated manner. *J Biol Chem* 283, 6957-6967

42 Nakamura, N. (2010) Emerging new roles of GM130, a cis-Golgi matrix protein, in higher order cell functions. *J Pharmacol Sci* 112, 255-264

43 Diao, A., *et al.* (2003) The coiled-coil membrane protein golgin-84 is a novel rab effector required for Golgi ribbon formation. *J Cell Biol* 160, 201-212

44 Sohda, M., *et al.* (2010) Interaction of Golgin-84 with the COG complex mediates the intra-Golgi retrograde transport. *Traffic* 11, 1552-1566

45 Colanzi, A. and Corda, D. (2007) Mitosis controls the Golgi and the Golgi controls mitosis. *Curr Opin Cell Biol* 19, 386-393

46 Feinstein, T.N. and Linstedt, A.D. (2007) Mitogen-activated protein kinase kinase 1-dependent Golgi unlinking occurs in G2 phase and promotes the G2/M cell cycle transition. *Mol Biol Cell* 18, 594-604

47 Wei, J.H. and Seemann, J. (2010) Unraveling the Golgi ribbon. *Traffic* 11, 1391-1400

48 Traub, L.M. (2005) Common principles in clathrin-mediated sorting at the Golgi and the plasma membrane. *Biochim Biophys Acta* 1744, 415-437

49 Puthenveedu, M.A., *et al.* (2006) GM130 and GRASP65-dependent lateral cisternal fusion allows uniform Golgi-enzyme distribution. *Nat Cell Biol* 8, 238-248

50 Duran, J.M., *et al.* (2008) The Role of GRASP55 in Golgi Fragmentation and Entry of Cells into Mitosis. *Mol Biol Cell* 19, 2579-2587

51 Feinstein, T.N. and Linstedt, A.D. (2008) GRASP55 Regulates Golgi Ribbon Formation. *Mol Biol Cell* 19, 2696-2707

52 Corda, D., *et al.* (2006) The multiple activities of CtBP/BARS proteins: the Golgi view. *Trends Cell Biol*

53 Colanzi, A., *et al.* (2007) The Golgi mitotic checkpoint is controlled by BARS-dependent fission of the Golgi ribbon into separate stacks in G2. *Embo J* 26, 2465-2476

54 Sinka, R., *et al.* (2008) Golgi coiled-coil proteins contain multiple binding sites for Rab family G proteins. *J Cell Biol* 183, 607-615

55 Munro, S. (2011) The golgin coiled-coil proteins of the Golgi apparatus. *Cold Spring Harb Perspect Biol* 3

56 Matteis, M., *et al.* (2008) The Golgi ribbon and the function of the Golgins. In *The Golgi Apparatus* (Mironov, A. and Pavelka, M., eds), pp. 223-246, Springer Vienna

57 Marra, P., *et al.* (2007) The biogenesis of the Golgi ribbon: the roles of membrane input from the ER and of GM130. *Mol Biol Cell* 18, 1595-1608

58 Rios, R.M., *et al.* (2004) GMAP-210 recruits gamma-tubulin complexes to cis-Golgi membranes and is required for Golgi ribbon formation. *Cell* 118, 323-335

59 Drin, G., *et al.* (2007) A general amphipathic alpha-helical motif for sensing membrane curvature. *Nat Struct Mol Biol* 14, 138-146

60 Drin, G., *et al.* (2008) Asymmetric tethering of flat and curved lipid membranes by a golgin. *Science* 320, 670-673

61 Cardenas, J., *et al.* (2009) Golgi localisation of GMAP210 requires two distinct cis-membrane binding mechanisms. *BMC Biol* 7, 56

62 Pernet-Gallay, K., *et al.* (2002) The overexpression of GMAP-210 blocks anterograde and retrograde transport between the ER and the Golgi apparatus. *Traffic* 3, 822-832

63 Yadav, S., *et al.* (2012) Golgin160 recruits the dynein motor to position the Golgi apparatus. *Dev Cell* 23, 153-165

64 Houghton, F.J., *et al.* (2009) The localization of the Golgin GCC185 is independent of Rab6A/A' and Arl1. *Cell* 138, 787-794

65 Luke, M.R., *et al.* (2003) GRIP domain-mediated targeting of two new coiled-coil proteins, GCC88 and GCC185, to subcompartments of the trans-Golgi network. *J Biol Chem* 278, 4216-4226

66 Efimov, A., *et al.* (2007) Asymmetric CLASP-dependent nucleation of noncentrosomal microtubules at the trans-Golgi network. *Dev Cell* 12, 917-930

67 Lin, Y.C., *et al.* (2011) ARL4A acts with GCC185 to modulate Golgi complex organization. *Journal of cell science* 124, 4014-4026

68 Brownhill, K., *et al.* (2009) Molecular motors and the Golgi complex: Staying put and moving through. *Semin Cell Dev Biol*

69 Shima, D.T., *et al.* (1998) An ordered inheritance strategy for the Golgi apparatus: visualization of mitotic disassembly reveals a role for the mitotic spindle. *J Cell Biol* 141, 955-966

70 Miller, P.M., *et al.* (2009) Golgi-derived CLASP-dependent microtubules control Golgi organization and polarized trafficking in motile cells. *Nat Cell Biol* 11, 1069-1080

71 Chabin-Brion, K., *et al.* (2001) The Golgi complex is a microtubule-organizing organelle. *Mol Biol Cell* 12, 2047-2060

72 Rivero, S., *et al.* (2009) Microtubule nucleation at the cis-side of the Golgi apparatus requires AKAP450 and GM130. *EMBO J* 28, 1016-1028

73 Jiang, S., *et al.* (2006) Capacity of the Golgi Apparatus for Cargo Transport Prior to Complete Assembly. *Mol Biol Cell*

74 Kasap, M., *et al.* (2004) Dynamic Nucleation of Golgi Apparatus Assembly from the Endoplasmic Reticulum in Interphase HeLa Cells. *Traffic* 5, 595-605

75 Hoppeler-Lebel, A., *et al.* (2007) Centrosomal CAP350 protein stabilises microtubules associated with the Golgi complex. *Journal of cell science* 120, 3299-3308

76 Walenta, J.H., *et al.* (2001) The Golgi-associated hook3 protein is a member of a novel family of microtubule-binding proteins. *J Cell Biol* 152, 923-934

77 Vinogradova, T., *et al.* (2012) Concerted effort of centrosomal and Golgi-derived microtubules is required for proper Golgi complex assembly but not for maintenance. *Mol Biol Cell* 23, 820-833

78 Egea, G., *et al.* (2006) Actin dynamics at the Golgi complex in mammalian cells. *Curr Opin Cell Biol*

79 Lanzetti, L. (2007) Actin in membrane trafficking. *Curr Opin Cell Biol* 19, 453-458

80 Kondylis, V., *et al.* (2007) The Golgi Comprises a Paired Stack that Is Separated at G2 by Modulation of the Actin Cytoskeleton through Abi and Scar/WAVE. *Dev Cell* 12, 901-915

81 Hu, Z., *et al.* (2007) The study of Golgi apparatus in Alzheimer's disease. *Neurochem Res* 32, 1265-1277

82 Ungar, D. (2009) Golgi linked protein glycosylation and associated diseases. *Semin Cell Dev Biol* 20, 762-769

83 Ladinsky, M.S., *et al.* (1999) Golgi structure in three dimensions: functional insights from the normal rat kidney cell. *J Cell Biol* 144, 1135-1149

84 Lucocq, J.M. and Warren, G. (1987) Fragmentation and partitioning of the Golgi apparatus during mitosis in HeLa cells. *Embo J* 6, 3239-3246

85 Sengupta, D., *et al.* (2009) Organelle tethering by a homotypic PDZ interaction underlies formation of the Golgi membrane network. *J Cell Biol* 186, 41-55

86 Lane, J.D., *et al.* (2002) Caspase-mediated cleavage of the stacking protein GRASP65 is required for Golgi fragmentation during apoptosis. *J Cell Biol* 156, 495-509

87 Pfeffer, S.R. (2001) Constructing a Golgi complex. *J Cell Biol* 155, 873-875.

88 Behnia, R., *et al.* (2007) The yeast orthologue of GRASP65 forms a complex with a coiled-coil protein that contributes to ER to Golgi traffic. *J Cell Biol* 176, 255-261

89 Kondylis, V., *et al.* (2005) dGRASP localization and function in the early exocytic pathway in Drosophila S2 cells. *Mol Biol Cell* 16, 4061-4072

90 Sutterlin, C., *et al.* (2002) Fragmentation and dispersal of the pericentriolar Golgi complex is required for entry into mitosis in mammalian cells. *Cell* 109, 359-369

91 Yoshimura, S., *et al.* (2005) Convergence of cell cycle regulation and growth factor signals on GRASP65. *J Biol Chem* 280, 23048-23056

92 Kaplan, W., *et al.* (1997) Conformational stability of pGEX-expressed Schistosoma japonicum glutathione S-transferase: a detoxification enzyme and fusion-protein affinity tag. *Protein Sci* 6, 399-406

93 Heusser, K., *et al.* (2006) Scavenging of 14-3-3 proteins reveals their involvement in the cell-surface transport of ATP-sensitive K+ channels. *Journal of cell science* 119, 4353-4363

94 Vielemeyer, O., *et al.* (2009) Direct Selection of Monoclonal Phosphospecific Antibodies without Prior Phosphoamino Acid Mapping. *J Biol Chem* 284, 20791-20795

95 Warren, G. (1993) Membrane partitioning during cell division. *Annu Rev Biochem* 62, 323-348

96 Shima, D.T., *et al.* (1997) Partitioning of the Golgi apparatus during mitosis in living HeLa cells. *J Cell Biol* 137, 1211-1228

97 Uchiyama, K., *et al.* (2003) The localization and phosphorylation of p47 are important for Golgi disassembly-assembly during the cell cycle. *J Cell Biol* 161, 1067-1079

98 Seemann, J., *et al.* (2000) The role of the tethering proteins p115 and GM130 in transport through the Golgi apparatus in vivo. *Mol Biol Cell* 11, 635-645

99 Moyer, B.D., *et al.* (2001) Rab1 Interaction with a GM130 Effector Complex Regulates COPII Vesicle cis-Golgi Tethering. *Traffic* 2, 268-276

100 Weide, T., *et al.* (2001) The Golgi matrix protein GM130: a specific interacting partner of the small GTPase rab1b. *EMBO Rep* 2, 336-341

101 Alvarez, C., *et al.* (2001) The p115-interactive Proteins GM130 and Giantin Participate in Endoplasmic Reticulum-Golgi Traffic. *J Biol Chem* 276, 2693-2700.

102 D'Angelo, G., *et al.* (2009) GRASP65 and GRASP55 sequentially promote the transport of C-terminal valine bearing cargoes to and through the golgi complex. *J Biol Chem* 284, 34849-34860

103 Barr, F.A., *et al.* (1998) Mapping the interaction between GRASP65 and GM130, components of a protein complex involved in the stacking of Golgi cisternae. *Embo J* 17, 3258-3268

104 Yoshimura, S.I., *et al.* (2001) Direct targeting of cis-Golgi matrix proteins to the Golgi apparatus. *Journal of cell science* 114, 4105-4115

105 Wittig, I., *et al.* (2006) Blue native PAGE. *Nat Protoc* 1, 418-428

106 Lucocq, J.M., *et al.* (1989) Mitotic Golgi fragments in HeLa cells and their role in the reassembly pathway. *J Cell Biol* 109, 463-474

107 Schwartz, M., *et al.* (2009) Impaired replication stress response in cells from immunodeficiency patients carrying Cernunnos/XLF mutations. *PLoS One* 4, e4516

108 Xiang, Y. and Wang, Y. (2011) New components of the Golgi matrix. *Cell Tissue Res* 344, 365-379

109 Gee, H.Y., *et al.* (2011) Rescue of DeltaF508-CFTR Trafficking via a GRASP-Dependent Unconventional Secretion Pathway. *Cell* 146, 746-760

110 Kinseth, M.A., *et al.* (2007) The Golgi-associated protein GRASP is required for unconventional protein secretion during development. *Cell* 130, 524-534

111 Kuo, A., *et al.* (2000) Transmembrane transforming growth factor-alpha tethers to the PDZ domain-containing, Golgi membrane-associated protein p59/GRASP55. *Embo J* 19, 6427-6439

112 Truschel, S.T., *et al.* (2011) Structure of the membrane-tethering GRASP domain reveals a unique PDZ ligand interaction that mediates Golgi biogenesis. *J Biol Chem* 286, 20125-20129

113 Lin, C.Y., *et al.* (2000) Peripheral Golgi protein GRASP65 is a target of mitotic polo-like kinase (Plk) and Cdc2. *Proc Natl Acad Sci U S A* 97, 12589-12594

114 Sutterlin, C., *et al.* (2001) Polo-like kinase is required for the fragmentation of pericentriolar Golgi stacks during mitosis. *Proc Natl Acad Sci U S A* 98, 9128-9132

115 Jesch, S.A., *et al.* (2001) Mitotic phosphorylation of Golgi reassembly stacking protein 55 by mitogen-activated protein kinase ERK2. *Mol Biol Cell* 12, 1811-1817

116 Miesch, C., *et al.* (2000) Radiative transfer solution for rugged and heterogeneous scene observations. *Appl Opt* 39, 6830-6846

117 Abarca, M.L., *et al.* (2000) [Mycotoxin producing fungi]. *Rev Iberoam Micol* 17, S63-68

118 Colanzi, A., *et al.* (2000) A specific activation of the mitogen-activated protein kinase kinase 1 (MEK1) is required for Golgi fragmentation during mitosis. *J Cell Biol* 149, 331-339

119 Gaietta, G.M., *et al.* (2006) Golgi twins in late mitosis revealed by genetically encoded tags for live cell imaging and correlated electron microscopy. *Proc Natl Acad Sci U S A* 103, 17777-17782

120 Wang, Y., *et al.* (2006) Purification of Rat Liver Golgi Stacks. In *Cell Biology: A Laboratory Handbook, 3rd Edition* (Celis, J., ed), pp. 33-39, Elsevier Science (USA)

121 Chen, X., *et al.* (2010) Quantitative proteomics analysis of cell cycle regulated Golgi disassembly and reassembly. *J Biol Chem* 285, 7197-7207

122 Cabrelli, C., *et al.* (2000) A constructive algorithm to solve "convex recursive deletion" (CoRD) classification problems via two-layer perceptron networks. *IEEE Trans Neural Netw* 11, 811-816

123 Husain, E. and Cabral, D. (2000) Febrile illness in a toddler: the diagnostic clue lays skin deep. *Can J Infect Dis* 11, 16-17

124 Menager, L., *et al.* (2000) Diode laser extended cavity for broad-range fast ramping. *Opt Lett* 25, 1246-1248

125 Moskwa, B., *et al.* (2000) [Some aspects of the immune response of Polish Wrzosowka sheep against gastrointestinal nematodes infection]. *Wiad Parazytol* 46, 141-148

126 Saparrat, M.C., *et al.* (2000) Extracellular ABTS-oxidizing activity of autochthonous fungal strains from Argentina in solid medium. *Rev Iberoam Micol* 17, 64-68

127 Check, E. (2002) Cell biology: will the real Golgi please stand up. *Nature* 416, 780-781

128 Misteli, T. and Warren, G. (1994) COP-coated vesicles are involved in the mitotic fragmentation of Golgi stacks in a cell-free system. *J Cell Biol* 125, 269-282

129 Rabouille, C., *et al.* (1995) Reassembly of Golgi stacks from mitotic Golgi fragments in a cell-free system. *J Cell Biol* 129, 605-618

130 Lowe, M., *et al.* (1998) Cdc2 kinase directly phosphorylates the cis-Golgi matrix protein GM130 and is required for Golgi fragmentation in mitosis. *Cell* 94, 783-793

131 Acharya, U., *et al.* (1995) The formation of Golgi stacks from vesiculated Golgi membranes requires two distinct fusion events. *Cell* 82, 895-904

132 Rabouille, C., *et al.* (1998) Syntaxin 5 is a common component of the NSF- and p97-mediated reassembly pathways of Golgi cisternae from mitotic Golgi fragments in vitro. *Cell* 92, 603-610

133 Rabouille, C., *et al.* (1995) An NSF-like ATPase, p97, and NSF mediate cisternal regrowth from mitotic Golgi fragments. *Cell* 82, 905-914

134 Kondo, H., *et al.* (1997) p47 is a cofactor for p97-mediated membrane fusion. *Nature* 388, 75-78

135 Meyer, H.H., *et al.* (1998) The p47 co-factor regulates the ATPase activity of the membrane fusion protein, p97. *FEBS Lett* 437, 255-257

136 Meyer, H.H., *et al.* (2000) A complex of mammalian ufd1 and npl4 links the AAA-ATPase, p97, to ubiquitin and nuclear transport pathways. *Embo J* 19, 2181-2192

137 Sagiv, Y., *et al.* (2000) GATE-16, a membrane transport modulator, interacts with NSF and the Golgi v-SNARE GOS-28. *Embo J* 19, 1494-1504

138 Zerial, M. and McBride, H. (2001) Rab proteins as membrane organizers. *Nat Rev Mol Cell Biol* 2, 107-117

139 Christoforidis, S. and Zerial, M. (2000) Purification and identification of novel Rab effectors using affinity chromatography. *Methods* 20, 403-410

140 Anglesio, M.S., *et al.* (2004) Differential expression of a novel ankyrin containing E3 ubiquitin-protein ligase, Hace1, in sporadic Wilms' tumor versus normal kidney. *Hum Mol Genet* 13, 2061-2074

141 Allan, B.B., *et al.* (2000) Rab1 recruitment of p115 into a cis-SNARE complex: programming budding COPII vesicles for fusion. *Science* 289, 444-448

142 de Wit, H., *et al.* (2001) Rab4 regulates formation of synaptic-like microvesicles from early endosomes in PC12 cells. *Mol Biol Cell* 12, 3703-3715

143 White, J., *et al.* (2001) Spatial partitioning of secretory cargo from Golgi resident proteins in live cells. *BMC Cell Biol* 2, 19

144 Rabouille, C., *et al.* (1995) Mapping the distribution of Golgi enzymes involved in the construction of complex oligosaccharides. *Journal of cell science* 108, 1617-1627

145 Xu, Y., *et al.* (2002) GS15 forms a SNARE complex with syntaxin 5, GS28, and Ykt6 and is implicated in traffic in the early cisternae of the Golgi apparatus. *Mol Biol Cell* 13, 3493-3507

146 Tang, B.L., *et al.* (1995) Segregation of ERGIC53 and the mammalian KDEL receptor upon exit from the 15 degrees C compartment. *Eur J Cell Biol* 68, 398-410

147 Wilson, B.S., *et al.* (1994) A Rab1 mutant affecting guanine nucleotide exchange promotes disassembly of the Golgi apparatus. *J Cell Biol* 125, 557-571

148 Hibi, K., *et al.* (2008) Aberrant methylation of the HACE1 gene is frequently detected in advanced colorectal cancer. *Anticancer Res* 28, 1581-1584

149 Diaz-Corrales, F.J., *et al.* (2004) Rotenone induces disassembly of the Golgi apparatus in the rat dopaminergic neuroblastoma B65 cell line. *Neurosci Lett* 354, 59-63

150 Yoshimura, M., *et al.* (1996) Aberrant glycosylation of E-cadherin enhances cell-cell binding to suppress metastasis. *J Biol Chem* 271, 13811-13815

151 Roberts, J.D., *et al.* (1998) The role of protein glycosylation inhibitors in the prevention of metastasis and therapy of cancer. *Cancer Detect Prev* 22, 455-462

152 Krishnan, V., *et al.* (2005) Altered melanoma cell surface glycosylation mediates organ specific adhesion and metastasis via lectin receptors on the lung vascular endothelium. *Clin Exp Metastasis* 22, 11-24

153 Dong, X.P., *et al.* (2008) The type IV mucolipidosis-associated protein TRPML1 is an endolysosomal iron release channel. *Nature* 455, 992-996

154 Wang, Y., *et al.* (2005) Purification of Rat Liver Golgi Stacks. In *Cell Biology: A Laboratory Handbook, 3rd Edition* (Celis, J., ed), pp. 33-39, Elsevier Science (USA)

155 Lowe, M. (2011) Structural organization of the Golgi apparatus. *Curr Opin Cell Biol* 23, 85-93

156 Cluett, E.B. and Brown, W.J. (1992) Adhesion of Golgi cisternae by proteinaceous interactions: intercisternal bridges as putative adhesive structures. *Journal of cell science* 103, 773-784

157 Radulescu, A.E., *et al.* (2007) A role for clathrin in reassembly of the Golgi apparatus. *Mol Biol Cell* 18, 94-105

158 Radulescu, A.E. and Shields, D. (2012) Clathrin is required for postmitotic Golgi reassembly. *FASEB J* 26, 129-136

159 Higashi, M., *et al.* (2009) Human Mena associates with Rac1 small GTPase in glioblastoma cell lines. *PLoS ONE* 4, e4765

160 Prasad, N.K. and Decker, S.J. (2005) SH2-containing 5'-inositol phosphatase, SHIP2, regulates cytoskeleton organization and ligand-dependent down-regulation of the epidermal growth factor receptor. *J Biol Chem* 280, 13129-13136

161 Erneux, C., *et al.* (2011) SHIP2 multiple functions: a balance between a negative control of PtdIns(3,4,5)P(3) level, a positive control of PtdIns(3,4)P(2) production, and intrinsic docking properties. *J Cell Biochem* 112, 2203-2209

162 Tzankov, S., *et al.* (2008) Functional divergence between co-chaperones of Hsc70. *J Biol Chem* 283, 27100-27109

163 Raiborg, C., *et al.* (2002) Hrs sorts ubiquitinated proteins into clathrin-coated microdomains of early endosomes. *Nat Cell Biol* 4, 394-398

164 Raiborg, C., *et al.* (2006) Flat clathrin coats on endosomes mediate degradative protein sorting by scaffolding Hrs in dynamic microdomains. *Journal of cell science* 119, 2414-2424

165 Royle, S.J. (2012) The role of clathrin in mitotic spindle organisation. *Journal of cell science* 125, 19-28

166 Okamoto, C.T., *et al.* (2000) Clathrin in mitotic spindles. *Am J Physiol Cell Physiol* 279, C369-374

167 Royle, S.J., *et al.* (2005) Clathrin is required for the function of the mitotic spindle. *Nature* 434, 1152-1157

168 Foraker, A.B., *et al.* (2012) Clathrin promotes centrosome integrity in early mitosis through stabilization of centrosomal ch-TOG. *J Cell Biol* 198, 591-605

169 Gautier, J.J., *et al.* (2011) Clathrin is required for Scar/Wave-mediated lamellipodium formation. *Journal of cell science* 124, 3414-3427

170 Booth, D.G., *et al.* (2011) A TACC3/ch-TOG/clathrin complex stabilises kinetochore fibres by inter-microtubule bridging. *Embo J* 30, 906-919

171 Eisenberg, E. and Greene, L.E. (2007) Multiple roles of auxilin and hsc70 in clathrin-mediated endocytosis. *Traffic* 8, 640-646

172 Shi, A., *et al.* (2009) Regulation of endosomal clathrin and retromer-mediated endosome to Golgi retrograde transport by the J-domain protein RME-8. *Embo J* 28, 3290-3302

173 Breitsprecher, D., *et al.* (2011) Molecular mechanism of Ena/VASP-mediated actin-filament elongation. *Embo J* 30, 456-467

174 Rottner, K., *et al.* (1999) VASP dynamics during lamellipodia protrusion. *Nat Cell Biol* 1, 321-322

175 Bear, J.E., *et al.* (2002) Antagonism between Ena/VASP proteins and actin filament capping regulates fibroblast motility. *Cell* 109, 509-521

176 Applewhite, D.A., *et al.* (2007) Ena/VASP proteins have an anti-capping independent function in filopodia formation. *Mol Biol Cell* 18, 2579-2591

177 Campellone, K.G., *et al.* (2008) WHAMM is an Arp2/3 complex activator that binds microtubules and functions in ER to Golgi transport. *Cell* 134, 148-161

178 Nakatsu, F., *et al.* (2010) The inositol 5-phosphatase SHIP2 regulates endocytic clathrin-coated pit dynamics. *J Cell Biol* 190, 307-315

179 Dyson, J.M., *et al.* (2001) The SH2-containing inositol polyphosphate 5-phosphatase, SHIP-2, binds filamin and regulates submembraneous actin. *J Cell Biol* 155, 1065-1079

180 Kato, K., *et al.* (2012) The inositol 5-phosphatase SHIP2 is an effector of RhoA and is involved in cell polarity and migration. *Mol Biol Cell* 23, 2593-2604

181 Choudhury, R.R., *et al.* (2005) Phosphoinositides and membrane traffic at the trans-Golgi network. *Biochem Soc Symp*, 31-38

182 Vicinanza, M., *et al.* (2011) OCRL controls trafficking through early endosomes via PtdIns4,5P(2)-dependent regulation of endosomal actin. *Embo J* 30, 4970-4985

183 Brodsky, F.M. (1985) Clathrin structure characterized with monoclonal antibodies. I. Analysis of multiple antigenic sites. *J. Cell Biol.* 101, 2047-2054

184 Motley, A., *et al.* (2003) Clathrin-mediated endocytosis in AP-2-depleted cells. *J Cell Biol* 162, 909-918

185 Lin, C.H., *et al.* (2010) Clathrin heavy chain mediates TACC3 targeting to mitotic spindles to ensure spindle stability. *J Cell Biol* 189, 1097-1105

186 Walker, V.E., *et al.* (2010) Hsp40 chaperones promote degradation of the HERG potassium channel. *J Biol Chem* 285, 3319-3329

187 Emr, S., *et al.* (2009) Journeys through the Golgi--taking stock in a new era. *J Cell Biol* 187, 449-453

188 Patterson, G.H., *et al.* (2008) Transport through the Golgi apparatus by rapid partitioning within a two-phase membrane system. *Cell* 133, 1055-1067

189 Gaietta, G.M., *et al.* (2006) Golgi twins in late mitosis revealed by genetically encoded tags for live cell imaging and correlated electron microscopy. *Proc. Natl. Acad. Sci. U.S.A* 103, 17777-17782

190 Sutterlin, C. and Colanzi, A. (2010) The Golgi and the centrosome: building a functional partnership. *J Cell Biol* 188, 621-628

191 Wei, J.H. and Seemann, J. (2009) Spindle-dependent partitioning of the Golgi ribbon. *Commun Integr Biol* 2, 406-407

192 Bachert, C. and Linstedt, A.D. (2010) Dual anchoring of the GRASP membrane tether promotes trans pairing. *J Biol Chem* 285, 16294-16301

193 Wei, J.H. and Seemann, J. (2009) The mitotic spindle mediates inheritance of the Golgi ribbon structure. *J Cell Biol* 184, 391-397

194 Ungewickell, E.J. and Hinrichsen, L. (2007) Endocytosis: clathrin-mediated membrane budding. *Curr. Opin. Cell Biol.* 19, 417-425

195 Brodsky, F.M. (2012) Diversity of Clathrin Function: New Tricks for an Old Protein. *Annu Rev Cell Dev Biol*

196 Bates, M., *et al.* (2007) Multicolor super-resolution imaging with photo-switchable fluorescent probes. *Science* 317, 1749-1753

197 Malhotra, V., *et al.* (1989) Purification of a novel class of coated vesicles mediating biosynthetic protein transport through the Golgi stack. *Cell* 58, 329-336

198 Orci, L., *et al.* (1985) Clathrin-immunoreactive sites in the Golgi apparatus are concentrated at the trans pole in polypeptide hormone-secreting cells. *Proc Natl Acad Sci U S A* 82, 5385-5389

199 Puthenveedu, M.A., *et al.* (2006) GM130 and GRASP65-dependent lateral cisternal fusion allows uniform Golgi-enzyme distribution. *Nat. Cell Biol.* 8, 238-248

200 Royle, S.J. and Lagnado, L. (2006) Trimerisation is important for the function of clathrin at the mitotic spindle. *J. Cell Sci.* 119, 4071-4078

201 Pfeffer, S.R. (2010) How the Golgi works: a cisternal progenitor model. *Proc Natl Acad Sci U S A* 107, 19614-19618

202 Pelham, H.R. and Rothman, J.E. (2000) The debate about transport in the Golgi--two sides of the same coin? *Cell* 102, 713-719

203 Losev, E., *et al.* (2006) Golgi maturation visualized in living yeast. *Nature* 441, 1002-1006

204 Meyer, C., *et al.* (2000) mu1A-adaptin-deficient mice: lethality, loss of AP-1 binding and rerouting of mannose 6-phosphate receptors. *EMBO J.*. 19, 2193-2203

205 Ezratty, E.J., *et al.* (2009) Clathrin mediates integrin endocytosis for focal adhesion disassembly in migrating cells. *J Cell Biol* 187, 733-747

206 Cheeseman, L.P., *et al.* (2012) Aurora A kinase activity is required for localization of TACC3/ch-TOG/clathrin inter-microtubule bridges. *Commun Integr Biol* 4, 409-412

207 Lemmon, S.K. and Traub, L.M. (2012) Getting in Touch with the Clathrin Terminal Domain. *Traffic*

208 Knuehl, C., *et al.* (2006) Novel binding sites on clathrin and adaptors regulate distinct aspects of coat assembly. *Traffic* 7, 1688-1700

209 Liu, S.H., *et al.* (1995) Regulation of clathrin assembly and trimerization defined using recombinant triskelion hubs. *Cell* 83, 257-267

210 Vassilopoulos, S., *et al.* (2009) A role for the CHC22 clathrin heavy-chain isoform in human glucose metabolism. *Science* 324, 1192-1196

211 Esk, C., *et al.* (2010) The clathrin heavy chain isoform CHC22 functions in a novel endosomal sorting step. *J Cell Biol* 188, 131-144

212 Huang, F., *et al.* (2004) Analysis of clathrin-mediated endocytosis of epidermal growth factor receptor by RNA interference. *J. Biol. Chem.* 279, 16657-16661

213 Rapoport, I., *et al.* (2008) A motif in the clathrin heavy chain required for the hsc70/auxilin uncoating reaction. *Mol Biol Cell* 19, 405-413

214 Bates, M., *et al.* (2008) Super-resolution microscopy by nanoscale localization of photo-switchable fluorescent probes. *Curr Opin Chem Biol* 12, 505-514

215 Beaudoin, G.M., 3rd, *et al.* (2012) Afadin, a Ras/Rap effector that controls cadherin function, promotes spine and excitatory synapse density in the hippocampus. *J Neurosci* 32, 99-110

216 Huang, B., *et al.* (2008) Three-dimensional super-resolution imaging by stochastic optical reconstruction microscopy. *Science* 319, 810-813

217 Dani, A., *et al.* (2010) Superresolution imaging of chemical synapses in the brain. *Neuron* 68, 843-856

218 Warren, G. and Malhotra, V. (1998) The organisation of the Golgi apparatus. *Curr Opin Cell Biol* 10, 493-498

219 Schotman, H., *et al.* (2008) dGRASP-mediated noncanonical integrin secretion is required for Drosophila epithelial remodeling. *Dev Cell* 14, 171-182

220 Cabral, M., *et al.* (2010) Unconventional secretion of AcbA in Dictyostelium discoideum through a vesicular intermediate. *Eukaryot Cell* 9, 1009-1017

221 Duran, J.M., *et al.* (2010) Unconventional secretion of Acb1 is mediated by autophagosomes. *J Cell Biol* 188, 527-536

222 Levi, S.K., *et al.* (2010) The yeast GRASP Grh1 colocalizes with COPII and is dispensable for organizing the secretory pathway. *Traffic* 11, 1168-1179

223 Ramirez, I.B. and Lowe, M. (2009) Golgins and GRASPs: holding the Golgi together. *Semin Cell Dev Biol* 20, 770-779

224 Nakamura, N., *et al.* (1997) The vesicle docking protein p115 binds GM130, a cis-Golgi matrix protein, in a mitotically regulated manner. *Cell* 89, 445-455

225 Lowe, M., *et al.* (2000) The mitotic phosphorylation cycle of the cis-Golgi matrix protein GM130. *J Cell Biol* 149, 341-356

226 Thyberg, J. and Moskalewski, S. (1999) Role of microtubules in the organization of the Golgi complex. *Exp Cell Res* 246, 263-279

227 Infante, C., *et al.* (1999) GMAP-210, A cis-Golgi network-associated protein, is a minus end microtubule-binding protein. *J Cell Biol* 145, 83-98